

***THE SEPARATION OF RECOMBINANT
PROTEINS BY METAL-CHELATING
MAGNETIC AFFINITY SUPPORTS***

BY

SUSAN MARY O'BRIEN

**A Thesis Submitted to The University of London
for the Degree of Doctor of Philosophy**

**DEPARTMENT OF CHEMICAL AND BIOCHEMICAL
ENGINEERING**

UNIVERSITY COLLEGE LONDON

ProQuest Number: 10106894

All rights reserved

INFORMATION TO ALL USERS

The quality of this reproduction is dependent upon the quality of the copy submitted.

In the unlikely event that the author did not send a complete manuscript and there are missing pages, these will be noted. Also, if material had to be removed, a note will indicate the deletion.



ProQuest 10106894

Published by ProQuest LLC(2016). Copyright of the Dissertation is held by the Author.

All rights reserved.

This work is protected against unauthorized copying under Title 17, United States Code.
Microform Edition © ProQuest LLC.

ProQuest LLC
789 East Eisenhower Parkway
P.O. Box 1346
Ann Arbor, MI 48106-1346

Dedication

To my mother, Jennie O'Brien (1935-1981), who always told me to aim high and ^{who} would have been very proud of me.

Acknowledgements

I would like to thank the following people:

Dr. Owen Thomas for his infectious enthusiasm, his unfailing interest, and for all the advice and help he has given me.

My supervisor, Professor Peter Dunnill, for his guidance and motivating encouragement.

Jim Pierce for his helpful discussions.

Rhona Sloane for the recombinant lysozyme construct.

Pawendeep Pannu for her expertise on high gradient magnetic separation.

Billy Doyle and Stuart Pope for their technical assistance.

A special thanks to Andy Greenwood for letting me kidnap his computer.

And finally, I'd like to thank the numerous people, both past and present, who have made the last few years so enjoyable, I am grateful to them all.

Abstract

The introduction of selective protein adsorption early in the downstream process has the potential to reduce the overall number of steps and increase efficiency and yield. However, the conventional format of a packed column of porous adsorbent is unsuitable for processing particulate containing feed streams as the matrix becomes clogged with trapped solids. There is evidence that non-porous supports are less prone to fouling and are easier to clean (Munro et al. 1977; Halling and Dunnill, 1979) and are therefore potentially more useful in protein purification from fouling feedstreams.

This work describes the preparation, characterisation and use of non-porous magnetic metal chelator adsorbents for the selective recovery of native (haem protein family) and recombinant metal-binding proteins from crude liquors. Non-porous, micron-sized (0.5-1.5 μm), magnetic iron oxide particles were functionalised with metal chelating iminodiacetic acid (IDA) ligands to produce a high capacity pseudoaffinity support. In magnetic affinity adsorption the covalently bound chelating ligand binds to its target protein in solution and the resulting complex is removed from suspension by the application of a magnetic field. The interaction is carried out in free solution and introduction at the start of the purification process renders pre-treatment steps such as clarification and concentration unnecessary and in doing so reduces costs and increases yield.

The coating and derivatisation methods resulted in supports with a high level of substitution and low non-specific binding while retaining a high effective surface area for target ^{protein} capture ($\sim 100 \text{ m}^2/\text{g}$). Supports were optimised with respect to ligand density (60 $\mu\text{moles Cu}^{2+}/\text{g}$), specific protein binding capacity (200 mg/g), and absence of non-specific binding. Selectivity and interaction strength of magnetic chelator particles were assessed using a set of native proteins with known behaviour towards immobilised metal chelates. A recombinant bacteriophage T4 lysozyme carrying a polyhistidine tail at its C-terminus was purified in a single step to 94% purity from crude *E. coli* cell extract using IDA- Cu^{2+} magnetic chelator supports. By comparison, single step purification by Cu^{2+} -charged IDA agarose supports achieved only 81% purity. Magnetic separation resulted in an overall yield of 82% which corresponded to a purification factor of 4.5.

Table of Contents

Title Page	1
Dedication	2
Acknowledgements	3
Abstract	4
Table of Contents	5
List of Figures	14
List of Tables	17
CHAPTER 1 INTRODUCTION	
1.1 Protein Purification Strategy	18
1.1.1 Process design	19
1.1.2 Process selection	20
1.1.3 Solid-liquid separation	21
1.1.3.1 Centrifugation	21
1.1.3.2 Filtration	22
1.1.4 Cell disruption	23
1.1.4.1 Mechanical disruption	24
1.1.4.2 Nonmechanical disruption	25
1.1.5 Primary separation operations	26
1.1.5.1 Ultrafiltration and diafiltration	26
1.1.5.2 Precipitation	27
1.1.5.3 Extraction	27
1.1.6 Chromatography	27
1.1.6.1 Ion exchange chromatography	27
1.1.6.2 Hydrophobic interaction chromatography	28
1.1.6.3 Affinity chromatography	28
1.1.6.4 Gel filtration chromatography	29
1.2 Affinity Separation	29
1.2.1 Affinity matrices	30
1.2.1.1 Chromatographic based matrices	30
1.2.1.2 Non-chromatographic based matrices	31
1.2.1.3 Non-porous matrices	32
1.2.2 Activation and coupling chemistry	32
1.2.2.1 Spacer molecules	34
1.2.2.2 Choice of ligand	34
1.2.3 High affinity ligands	34
1.2.3.1 Immunoaffinity ligands	34
1.2.3.2 Receptor ligands	35

1.2.3.3 Avidin/streptavidin-biotin complexes	35
1.2.4 General affinity ligands	35
1.2.4.1 Chelated metal ions	35
1.2.4.2 Textile and biomimetic triazine dyes	35
1.2.4.3 Amino acid based ligands	36
1.2.4.4 Nucleotide-based ligands and coenzymes	36
1.2.4.5 Carbohydrate-binding ligands	36
1.2.4.6 Protein ligands	37
1.2.4.7 Protease inhibitors	37
1.2.5 Affinity separation techniques	37
1.2.5.1 Affinity precipitation	37
1.2.5.2 Affinity partitioning	38
1.2.5.3 Affinity cross-flow filtration	38
1.2.5.4 Affinity separation using reversed micelles	38
1.2.5.5 Liquid affinity perfluorocarbon supports	39
1.2.5.6 Affinity water-soluble nonionic surfactants	39
1.3 Immobilised Metal Chelate Affinity	39
1.3.1 Mechanism of metal affinity separation	40
1.3.1.4 Adsorption and elution	40
1.3.2 Choice of metal ion	41
1.3.3 Metal chelating ligands	42
1.3.4 Protein-metal interaction	44
1.3.4.1 Amino acids	44
1.3.4.2 Spatial distribution	45
1.3.4.3 Other factors	45
1.4 Pre-derivatised Recombinant Proteins: an aid to recovery	46
1.4.1 Recovery of fusion proteins	47
1.4.1.1 Ion-exchange tails	47
1.4.1.2 Hydrophobic and covalent tails	48
1.4.1.3 Affinity tails	48
1.4.2 Specific cleavage methods	50
1.4.3 Solubility of gene fusion product	50
1.4.4 Localization of fusion proteins	51
1.4.5 Metal chelating purification handle	52
1.5 Magnetic Particle Supports	55
1.5.1 Performance criteria of magnetic supports	56
1.5.2 Non-porous supports	57

1.5.2.1 Advantages of non-porous supports	58
1.5.3 Ferrofluids	59
1.5.3.1 Superparamagnetism	60
1.5.4 Porous supports	61
1.5.5 Pellicular supports	62
1.5.6 Magnetic particle behaviour	62
1.5.7 Commercially available magnetic particles	63
1.6 Magnetic Separation Technology	64
1.6.1 Magnetic properties of materials	64
1.6.1.1 Diamagnetism	65
1.6.1.2 Paramagnetism	65
1.6.1.3 Ferromagnetism	65
1.6.2 Principles of magnetic separation	65
1.6.3 High gradient magnetic separation	66
1.6.3.1 Factors affecting separation	68
1.6.4 High gradient magnetic filters	69
1.6.5 Magnetic collection and separation devices	70
1.6.5.1 Permanent magnets	70
1.6.5.2 Electromagnets	70
1.6.5.3 Superconducting magnets	71
1.6.5.4 Open field gradients	72
1.6.5.5 Magnetically stabilised fluidised beds	73
1.7 Aims	74
CHAPTER 2 MATERIALS AND METHODS	76
2.1 Materials	76
2.1.1 Microorganisms	76
2.1.2 Culture media	76
2.1.3 Chemicals	77
2.1.4 Proteins	77
2.2 Magnetic Support Particle Preparation	77
2.2.1 Preparation of iron oxide particles	77
2.2.2 Silane coating	78
2.2.3 Polyglutaraldehyde grafting	78
2.2.3.1 BioMag® particles	78
2.2.3.2 In-house particles	79
2.2.4. Reduction of surface carbonyl groups	79
2.2.5. Alkoxide hydrolysis	80

2.2.6. Epoxide activation	80
2.2.6.1 BioMag® particles	80
2.2.6.2 In-house particles	80
2.2.7. Iminodiacetic acid coupling	81
2.2.7.1 BioMag® particles	81
2.2.7.2 In-house particles	81
2.2.8. Metal ion charging	82
2.2.8.1 BioMag® particles	82
2.2.8.2 In-house particles	82
2.3 Magnetic Support Particle Characterisation	82
2.3.1 Determination of amine group density	82
2.3.1.1 TNBS assay	83
2.3.1.2 SPDP assay	83
2.3.2 Determination of epoxide group density	83
2.3.3 Determination of ligand group density	84
2.3.4 Quantitative support measurement	84
2.3.5 Measurement of pH stability	85
2.3.5.1 Potassium thiocyanate test	85
2.3.5.2 Effect of successive coating and coupling chemistries	85
2.4 Magnetic Particle Performance Analysis	85
2.4.1 Experiment to optimise ligand density	86
2.4.1.1 Effect of varying oxirane concentration	86
2.4.1.2 Effect of varying IDA concentration	86
2.4.2 Adsorption-desorption studies of native metal-binding proteins by magnetic chelator supports	86
2.4.3 Experiment to compare protein adsorption-desorption profiles of magnetic chelator and chelating Sepharose 6B supports	87
2.4.4 Determination of adsorption isotherms for native metal-binding proteins on magnetic chelator supports	88
2.4.5 Experiment to investigate the effect of magnetic support recycle for re-use	88
2.4.6 Recovery of recombinant metal-binding protein expressed in <i>E. coli</i>	89
2.4.6.1 Extracellular histidine-tailed single chain antibody fragment from culture medium	89

2.4.6.2	Intracellular histidine-tailed T4 lysozyme from crude cell extract	90
2.4.7	Recovery of native and recombinant metal-binding proteins from crude <i>E.coli</i> homogenate	90
2.4.7.1	Recovery of haemoglobin from solution spiked with whole cells and media.	90
2.4.7.2	Recovery of recombinant T4 lysozyme from crude extract in the presence of cells and cell debris	91
2.4.8	Magnetic particle separation technology using a high gradient magnetic separation device	92
2.5	Fermentation	93
2.5.1	<i>E. coli</i> HB101 expressing ZZ-his fusion protein	93
2.5.1.1	Shake flask cultivation	93
2.5.2	<i>E. coli</i> XL1-blue expressing histidine-tailed single chain antibody fragment	94
2.5.2.1	Shake flask cultivation	94
2.5.3	<i>E. coli</i> JM107 expressing histidine-tailed T4 lysozyme	94
2.5.3.1	Shake flask cultivation	95
2.5.3.1	Pilot scale cultivation	95
2.5.4	<i>E. coli</i> JM83 expressing α -amylase	95
2.5.5	Analytical methods	96
2.5.5.1	Optical cell density	96
2.5.5.2	Dry cell weight	96
2.5.5.3	Cell count and plasmid stability	96
2.5.6	Cell disruption	96
2.5.6.1	Osmotic shock	96
2.5.6.2	Osmotic shock with lysozyme	97
2.5.6.3	Sonication	97
2.5.6.4	Homogenisation	97
2.5.7	Concentration	98
2.5.7.1	Sucrose dehydration	98
2.6	Column Affinity Chromatography	98
2.6.1	Immobilised metal affinity chromatography	98
2.6.1.1	Chelating Sepharose 6B	98
2.6.1.2	HiTrap™ chelating column	99
2.6.2	IgG affinity chromatography	99

2.6.3 Antigen (mucin) affinity chromatography	100
2.6.3.1 Coupling of mucin to Sepharose	100
2.6.3.2 Purification on mucin-Sepharose	100
2.6.4 Gel filtration	101
2.7 Protein Analysis	101
2.7.1 Determination of protein concentration	101
2.7.2 Enzyme assays	102
2.7.2.1 Lysozyme assay	102
2.7.2.2 α -Amylase assay	102
2.7.3 Preparation of samples for electrophoresis	102
2.7.3.1 Trichloroacetic acid precipitation	102
2.7.3.2 Sample preparation	103
2.7.4 Polyacrylamide gel electrophoresis	103
2.7.4.1 Preparation of denaturing gels	104
2.7.4.2 Loading and running gels	105
2.7.4.3 Gel staining and destaining	105
2.7.4.4 Gel documentation	106
2.7.5 Western blotting	107
2.7.5.1 Horizontal semi-dry electroblotting	107
2.7.5.2 Immunodetection of immobilised protein	108

CHAPTER 3

MAGNETIC SUPPORT DEVELOPMENT AND CHARACTERISATION

3.1 Aim	110
3.2 Introduction	110
3.3 Choice of Preparative Route	113
3.3.1 Comparison of preparative routes	115
3.3.2 Preparative route evaluation	118
3.4 Adsorption Profiles of Haem Proteins on Magnetic Chelator Supports Charged with Various Metal Ions	119
3.5 Support Characterisation	121
3.5.1 pH stability	121
3.5.1.1 Effect of successive coating and coupling chemistries on corrosion resistance	123
3.5.2 Functional group density	124
3.5.2.1 Primary amino group determination	124
3.5.3 Magnetic support recycle for re-use	125

3.5.3.1 Particle aggregation	128
3.6 Comparison of Magnetic Chelator Supports with Chelating Sepharose 6B	129
3.7 Separation of Native Metal-binding Proteins	131
3.8 Adsorption Isotherms	133
3.9 Desorption of Haem Proteins	138
3.10 Optimisation of Supports	139
3.11 Effect of Ligand Density on Protein Binding	143
3.11.1 Effect of ligand density on non-specific binding	146
3.11.2 Comparison with commercial supports	146
3.12 Conclusions	147

CHAPTER 4 SEPARATION OF PREDERIVATISED METAL-BINDING PROTEINS

4.1 Aim	149
4.2 Screening of Prederivatised Recombinant Proteins by IMAC	149
4.2.1 ZZ Histidine fusion protein	149
4.2.2 Histidine-tailed single chain antibody fragment	152
4.2.3 Histidine-tailed T4 lysozyme	154
4.3 Recovery of Histidine-tailed T4 Lysozyme	154
4.3.1 Recovery from <i>E.coli</i> cell extract	154
4.3.2 Recovery from <i>E.coli</i> cell homogenate	159
4.3.2.1 Process optimisation	159
4.3.2.2 Recovery of recombinant T4 lysozyme	161
4.4 High Gradient Magnetic Affinity Separation	164
4.4.1 Introduction	164
4.4.2 High gradient magnetic affinity separation of T4 lysozyme-his from <i>E. coli</i> cell homogenate	165
4.9 Conclusions	166

CHAPTER 5 FERMENTATION AND EXPRESSION OF RECOMBINANT T4 LYSOZYME

5.1 Aim	168
5.2 Introduction	168
5.3 <i>E. coli</i> Fermentation on Nutrient Broth	168
5.3.1 Shake flask cultivation	168

5.3.2 Bioreactor cultivation	169
5.3.2.1 14 L fermentation	170
5.3.2.2 42 L fermentation	172
5.3.2.3 Discussion	176
5.4 Optimisation of Cell Growth and Recombinant Protein Production	177
5.4.1 Introduction	177
5.4.2 Effect of media composition and temperature	177
5.4.2.1 Discussion	182
5.4.3 Effect of induction conditions and IPTG concentration	183
5.4.3.1 Discussion	187
5.5 <i>E. coli</i> Fermentation on High Biomass Medium	188
5.5.1 Bioreactor cultivation	188
5.5.2 High pressure homogenisation	195
5.6 Conclusions	197
CHAPTER 6	
PERIPLASMIC LYSIS BY T4 LYSOZYME-HIS	
6.1 Aim	200
6.2 Introduction	200
6.3 Expression and Purification of T4 Lysozyme-his	201
6.4 Periplasmic Lysis	203
6.5 Post-lysis Recovery of T4 lysozyme-his	208
6.6 Conclusion	211
CHAPTER 7	
CONCLUSIONS AND FUTURE WORK	
7.1 Conclusions	212
7.2 Future Work	214
Bibliography	235

Figures

- Figure 1.1 Principle of establishing a high gradient magnetic field
(a) Steel strand in the external magnetic field.
(b) Magnetic field generated by steel strand
(c) Sum of (a) and (b).
- Figure 1.2 External high gradient magnetic field devices.
- Figure 3.1 Scheme for preparation of non-porous magnetic chelator supports.
- Figure 3.2 Effect of pH on the destruction of amine terminated iron oxide magnetic particles.
- Figure 3.3 The effect of magnetic support preparation process coating and coupling reactions on the acid corrosion resistance of the iron oxide core particles exposed to 1 M HCL (pH 0).
- Figure 3.4 Effect of recycle, over 3 successive cycles, on magnetic support integrity.
- Figure 3.5 Effect of 'preparation', 'testing' and 'regeneration' phases (i.e., buffer composition) on Fe ion liberation (% total w/w) per unit volume (mL).
- Figure 3.6 Effect of support recycle over 3 successive cycles on immobilised Cu^{2+} (ligand) density and protein binding capacity.
- Figure 3.7 Comparison of elution pattern of *C. krusei* cytochrome *c* from chelating magnetic and chelating Sepharose 6B supports.
- Figure 3.8 Resolution of cytochromes *c* on IDA- Cu^{2+} -charged Chelating Sepharose column.
- Figure 3.9 Scatchard plots of tuna cytochrome *c*, horse cytochrome *c*, *C. krusei* cytochrome *c* and bovine haemoglobin equilibrium binding data.
- Figure 3.10 Equilibrium binding isotherms for native proteins on IDA- Cu^{2+} magnetic chelator supports.
- Figure 3.11 Batch desorption of haem proteins from 'loaded' Cu^{2+} -charged magnetic chelator supports.
- Figure 3.12 Effect of 1,4-butanediol diglycidyl ether concentration on surface oxirane density, ligand density and specific protein binding capacity.
- Figure 3.13 Effect of IDA concentration on the immobilised Cu^{2+} (ligand) density and protein binding capacity of charged magnetic chelator supports.
- Figure 3.14 Relationship between $Q^* \text{Cu}$, the ' Cu^{2+} specific' binding capacity and the immobilised Cu^{2+} ligand density for magnetic chelator supports.
- Figure 3.15 Effect of IDA ligand density on the binding of haem proteins to magnetic chelators supports.
- Figure 4.1 Immobilised metal affinity chromatography of recombinant ZZ-His4 fusion protein on a Zn^{2+} -IDA Sepharose 6B column.

- Figure 4.2 Recovery of ZZ-His4 by Zn²⁺-IDA Sepharose 6B IMAC.
- Figure 4.3 Western blot of batch binding of ScFv_{hinge(his)5} with magnetic chelator supports.
- Figure 4.4 (a) Direct recovery of recombinant T4 lysozyme from crude *E. coli* cell extracts on magnetic chelator supports.
- Figure 4.4 (b) Graphic reproduction of SDS-PAGE analysis showing the recovery of recombinant T4 lysozyme-his from crude *E. coli* cell-free extract.
- Figure 4.5 The effect of various suspension concentrations of cells / media and buffer composition on the the adsorption efficiency of Cu²⁺-charged magnetic chelator supports for bovine haemoglobin.
- Figure 4.6 Magnetic affinity recovery of recombinant T4 lysozyme-his from (a) crude extract in the presence of cells and (b) clarified extract with the cells and cell debris removed, at two different biomass concentrations.
- Figure 4.7 Recovery of recombinant T4 lysozyme from crude *E. coli* cell homogenate on Cu²⁺-charged magnetic chelator supports. SDS-PAGE of unbound and bound (desorbed) samples.
- Figure 4.8 Recovery of recombinant T4 lysozyme from clarified (cell free) *E. coli* cell homogenate on Cu²⁺-charged magnetic chelator supports. SDS-PAGE of unbound and bound (desorbed) samples.
- Figure 5.1 Shake flask fermentation of *E. coli* pQR752 producing recombinant T4 lysozyme (T4 lysozyme-his).
- Figure 5.2 14 L *E. coli* pQR 752 fermentation on Nutrient Broth media.
- Figure 5.3 Cellular distribution of T4 lysozyme-his following a 14 L fermentation.
- Figure 5.4 42 L *E. coli* pQR 752 fermentation on Nutrient Broth media.
- Figure 5.5 Distribution of T4 lysozyme-his following a 42 L fermentation.
- Figure 5.6 Off-line measurements of 42 L *E. coli* pQR752 fermentation grown on nutrient broth.
- Figure 5.7 Growth curves of *E. coli* pQR752 grown on two different complex media types and at two different temperatures - not induced.
- Figure 5.8 Growth curves of *E. coli* pQR752 producing T4 lysozyme-his grown on two different complex media types and at two different temperatures.
- Figure 5.9 Activity of intracellular T4 lysozyme-his produced by *E. coli* pQ752 grown on High Biomass Medium.
- Figure 5.10 Growth curves of *E. coli* pQR752, IPTG induced at mid-log and late-log phase of growth.
- Figure 5.11 Lysozyme activity (intracellular) as a result of mid-log phase IPTG induction of *E. coli* pQR752 producing T4 lysozyme-his.

- Figure 5.12 Lysozyme activity (extracellular) as a result of mid-log phase IPTG induction of *E. coli* pQR752 producing T4 lysozyme-his.
- Figure 5.13 Lysozyme activity (intracellular) as a result of late log phase IPTG induction of *E. coli* pQR752 producing T4 lysozyme-his.
- Figure 5.14 7L *E. coli* pQR752 fermentation on High Biomass Medium at 28°C. Not induced.
- Figure 5.15 Cellular distribution of T4 lysozyme-his following 7 L fermentation on High Biomass Media.
- Figure 5.16 Growth of 7 L *E. coli* pQR752 fermentation (induced) on High Biomass Medium at 28°C.
- Figure 5.17 7L *E. coli* pQR752 fermentation on High Biomass Medium at 28°C. Culture induced.
- Figure 5.18 T4 lysozyme-his released by high pressure homogenisation of *E. coli* pQR752 cells (23 hr old).
- Figure 5.19 Specific activity of T4 lysozyme-his released by high pressure homogenisation.
- Figure 6.1 Immobilised metal affinity chromatographic recovery of recombinant T4 lysozyme on a Cu²⁺-charged HiTrap™ column.
- Figure 6.2 Release of α-amylase (activity Units/mL culture) from the periplasm by 0.23, 1.50 and 2.57 mg T4 lysozyme-his in lysis buffer at three increasing dry cell weight concentrations.
- Figure 6.3 T4 lysozyme-his recovered (%) from lysed cell supernatant at increasing dry cell weight, at constant T4 lysozyme-his input concentration (0.23 mg).
- Figure 6.4 Schematic representation of the effect of ionic strength and pH on the electrostatic interaction between lysozyme and *M. lysodeikticus* cells (Muraki et al., 1988). The symbols + and - denote positive and negative charge respectively.
- Figure 6.5 Chromatogram of IMAC-Zn²⁺ post-lysis recovery and purification of T4 lysozyme-his from released periplasmic protein.
- Figure 6.6 SDS-polyacrylamide gel showing post-lysis recovery of T4 lysozyme-his by IMAC-Zn²⁺.

Tables

- Table 2.1 Solutions spiked with *E.coli* cells, cell debris and media components.
- Table 2.2 Gel formulations for discontinuous SDS-PAGE.
- Table 2.3 SDS-polyacrylamide gel stock solutions.
- Table 2.4 Western Blot stock solutions.
- Table 3.1 Properties of selected proteins.
- Table 3.2 Comparison of routes for the preparation of magnetic chelator particles.
- Table 3.3 Effect of metal ion species on binding of native 'his' proteins on magnetic chelator supports.
- Table 3.4 Comparison of batch binding capacities of chelating magnetic and Sepharose 6B supports.
- Table 3.5 Langmuir binding parameters for native proteins to magnetic chelator supports.
- Table 4.1 Recovery of recombinant T4 lysozyme from crude *E. coli* cell extract by Cu²⁺-charged magnetic chelator supports.
- Table 4.2 Recovery of recombinant T4 lysozyme from *E. coli* extracts - comparison of magnetic purification with a two-step conventional chromatographic procedure.
- Table 4.3 Composition of solutions used to test the effect of cells, media components and buffer on the adsorption efficiency of magnetic chelator supports for bovine haemoglobin.
- Table 5.1 Effect of media and temperature on growth of *E. coli* JM107 pQR752.
- Table 5.2 Effect of enriched culture media and temperature reduction on biomass, cell integrity and T4 lysozyme-his productivity.
- Table 6.1 Purification of recombinant T4 lysozyme on Cu²⁺-charged Chelating Sepharose HP.
- Table 6.2 Recovery of recombinant T4 lysozyme-his from the cell-free lysis supernatant and from subsequent high pH and ionic strength phosphate buffer washes.
- Table 6.3 Post-lysis recovery of recombinant T4 lysozyme-his from the released periplasmic protein.

CHAPTER 1 INTRODUCTION

1.1 Protein Purification Strategy

The importance of proteins to the world community and economy cannot be overestimated, whether as food, antibiotics, therapeutics, subunit vaccines or industrial and diagnostic enzymes. In addition many recombinant proteins are currently available as drugs, for example, insulin, interferon, hepatitis B vaccine, tissue plasminogen activator and human growth hormone. Therefore, cost effective production and purification of proteins is one of the major concerns of the biotechnology industry. But manufacturing must keep pace with the development of these products and their movement into the marketplace. To manufacture many of these proteins, one must have a process that operates on a large scale, producing large quantities economically. Bioseparation processes have a significant impact on the economics of producing proteins and often accounts for ~ 50-80% of total costs (Gupta and Mattiasson, 1994; Labrou and Clonis, 1994). The expected market for downstream processing equipment was ~\$2.5 billion in 1995 (Spalding, 1991). Protein products range from human therapeutics (high cost and ultra-purity) to animal growth hormones of medium cost and high purity to industrial enzymes where the cost is low and purity is not so critical. In order to develop a cost effective purification strategy it is essential to define the product's end use, the amount required and the final purity requirements. The goal of a purification strategy is to obtain a maximum yield of protein with maximum purity, cost effectively. Product is lost at each stage and so the key to cutting processing costs is to limit the number of steps in the overall process, and to get more out of each step. The ideal process should have no more than two or three steps with 90% recovery in each, so the total recovery stays above 80% (Spalding, 1991).

The uncompromising standards for protein quality which relate to use and are based on FDA guidelines, provide further challenges to the scale up of protein purification and are achieved as a result of rigorous quality control of manufacturing practices (cGMP). Thus biological molecules isolated from natural sources, or expressed from recombinant DNA systems, must be shown to have acceptably low levels of biologically active contaminants such as DNA, viruses, pyrogen and 'leachates' from the separation media. Not surprisingly, therefore, the development of gentle, but effective, purification processes which yield fully active pharmaceutical proteins presents major challenges to the process engineer.

1.1.1 Process design

The downstream process may be defined as a series of steps that when followed results in a purified protein product. Process design and scale-up may be divided into three distinct steps: selection of unit operations, optimisation of operating parameters at the small scale and finally, increase of equipment size while maintaining the same operating parameters. An important consideration in the design of a purification process is the market volume and the ultimate scale of production. Consideration of this at the outset ensures avoidance of unit operations that are difficult or expensive to operate on a large scale. The design of a scaled-down process as the starting point for process design allows feasibility studies and optimisation of each unit operation (Smith, 1968; Bisio, 1985).

Alternatively, according to Taguchi (1986), the design of a process to manufacture a product consists of three overlapping stages: system design, operation design, and parameter design. The integration of upstream and downstream operations during the design stage may result in a product with lower cost and higher quality. Skillful improvement of the upstream fermentation process through selection of high-producing organisms, high-growth media and optimal operating conditions may produce a thousand-fold increase in production (Wheelwright, 1991). There are four factors in the upstream operation that affect the downstream operation: namely, the volume of material delivered, the amount of impurities relative to the product, the nature of the impurities and the phases present.

Another method by which the downstream purification may be greatly helped by upstream activities is the purposeful alteration of the protein to include a region that aids recovery. This may be through fusion of an affinity tail, as described by Uhlén (1988), where the protein is recovered by affinity chromatography or it may be via the incorporation of multiple charges, such as the polyarginine tail described by Smith et al. (1984) with purification by ion exchange chromatography.

In addition to defining the design goals, one must collect the necessary background data on the target protein to aid design development, i.e., chemical and physical data such as solubility, pH, size, shape, net charge and distribution of charge, density, adsorption isotherms and detergent binding (Ratafia and Keenan, 1986). Knowledge of the major contaminants and the presence of different phases and physical characteristics of the product, such as thermal stability, isoelectric point and hydrophobicity, also aid in developing the design process (Wheelwright, 1987).

1.1.2 Process selection

The requirements at each stage of purification must be balanced against one another. Thus, in the early stages, capacity and low cost are important whilst at the later stages high resolution is important. Successful process selection and its optimisation relies on the design of an optimal sequence of processing events with maximal yield and minimal number of steps. Protein purification techniques should be simple, easily scalable, have maximum throughput, low cost and be non-inactivating.

Downstream processing may be divided into two stages; primary recovery stages and high resolution stages (Datar, 1986). The objective of the primary recovery stage is to obtain a well clarified supernatant which is suitable for high resolution stages. For extracellular proteins, the primary recovery stages involve the removal of cells from spent medium. For intracellular proteins the primary recovery stages include (a) recovery of cells (b) disruption of cells to release target proteins and (c) removal of cell debris.

Sequential separation processes should be chosen based on different physio-chemical properties. Conditions should be chosen that will exploit the greatest differences in the properties of the product and the background impurities. Separation of the most plentiful impurities at the earliest possible stage should lead to the greatest concentration in terms of mass or volume. Thus the product stream may be handled more quickly and conveniently. When process volumes are large, the operation used should be physically appropriate. Adsorption-desorption processes such as affinity chromatography rather than gradient elution from ion exchange columns are much more suitable for bulk processing.

The stages of downstream processing are generally depicted as recovery, low-resolution purification and high resolution purification. The recovery stage starts with the spent medium and ends with the aqueous solution containing the protein product or a dried and formulated product. If the product is secreted as a soluble species the recovery step consists solely of a concentration step to remove excess liquid. However, product proteins may be insoluble (inclusion bodies) and/or they may be located inside the cell mass. A procedure is therefore required to break the cells, separate out the debris and recover the protein product either from the supernatant or from the cellular debris by extraction with detergents or otherwise. Once a soluble concentrate is obtained, purification consists of steps that increasingly remove impurities and increase the relative concentration or purity of the product.

In practice two approaches to protein purification exist. One approach utilises a series of "traditional " methods in a concerted way to achieve the desired goal (purity, yield, cost, scalability) and is more commonly the tested and reliable approach taken. The first step should be of a non-specific type, one that has a low resolution such as precipitation. This should be followed by high resolution steps such as ion exchange chromatography. This in turn should be followed by a step such as gel filtration (Belter et al., 1988; Bonnerjea et al., 1986; Ostlund, 1986; Scawen et al., 1980; Werner and Berthold., 1988; Wheelwright, 1987).

However, extensive processing eventually carries the cost of a low yield as well as high capital and operational costs. It is desirable to reduce the total number of steps by combining some of them. The second approach is to use a highly specific method such as affinity separation early on to achieve the required purification in a single step. This appealing approach necessitates a high resolution affinity method that is also economical and scalable.

1.1.3 Solid-liquid separation

Solid-liquid separation is used at several stages during a protein isolation process to remove particulate matter (e.g. cells, organelles, debris or precipitated macromolecules) from the surrounding fluid. In the case of microbial production, this may be accomplished with either cross-flow filtration (Gabler, 1985) or centrifugation (Axelsson, 1985). Both methods employ few interfaces capable of denaturing proteins, and are readily scalable in the lower and middle ranges of production volumes (Kelley and Hatton, 1991). For the very largest volumes employed in industrial enzyme fermentations, rotary vacuum filtration is more common (Belter, 1985).

1.1.3.1 Centrifugation

Centrifugation takes advantage of the differences in density between the solid and liquid. The density gradient is amplified through the application of centrifugal force by rotating the solid-liquid mixture at high speed. The rate of particle sedimentation is defined by the balance between the centrifugal force, the Brownian diffusional force and the kinetic drag of the fluid (Ambler, 1952). Continuous centrifuges are necessary to handle large volumes but they are less efficient than laboratory centrifuges because of the lower g forces and residence times used. Centrifuges are classified by their internal structures, which have been developed to handle somewhat differing suspensions leading to different methods of solids discharge. A tubular bowl centrifuge (Sharples) rotates around the axis of the bowl and the inside wall becomes covered with precipitate. The centrifuge is

optimised by monitoring the supernatant for clarity and adjusting the flow input for effective separation over a reasonable time period. The precipitate in the bowl cannot be removed without stopping the centrifuge. The disc-type centrifuge (Alfa-Laval) has an infinite capacity for solids in that they may be discharged without stopping the centrifuge for cleaning. The advantage of this type of centrifuge is its low labour involvement, but the solids obtained tend to have a higher liquid content than those from the tubular bowl centrifuge (Lee, 1989). Industrial centrifuges, such as the disc stack for use with microbial solutions are generally continuous flow through design and can achieve flowrates greater than 1000 L/hr (Mannweiler and Hoare, 1992). One of the major factors that affects centrifuge capacity and running costs is particle size. The design of centrifuges with faster rotational speed ensures shorter cell residence time but is not suitable for shear sensitive cells. The limitations of centrifuge operation include the generation of heat, aerosols and noise, in addition to the high cost and clumsiness of operation.

1.1.3.2 Filtration

Filtration is used at several stages of downstream processing. Separation is based on relative size. It involves the physical retention of the particles behind a filter medium with passage of the process fluid through the filter medium. The process can be so designed that the product of interest is found in either the filtrate or the retentate. The most widely used types of membrane separations are microfiltration and ultrafiltration, microfiltration being used for the clarification of fermentation broths and cell homogenates and ultrafiltration to concentrate dilute protein solutions, and/or to place a protein in a suitable solution for subsequent purification or stabilisation. Filtration can be divided into two subcategories: dead-end filtration (feed stream flows perpendicular to the filter surface) and tangential flow filtration (feed stream flows parallel to the filter and the filtrate diffuses across it).

1.1.3.2.1 Dead-end filtration

The two most commonly used large scale dead-end filtration systems are 'continuous rotary vacuum drum filter' and 'plate and frame filter press'. Filtrate is drawn into the rotary vacuum drum, covered by a filter medium, by an internal vacuum. As the partially submerged drum rotates, it is coated with the solids that are in turn removed by a scraper. The filter press is a batch type filter, although liquid flow through the press is continuous, solids accumulate and the filter must be dismantled to remove them. The press can be precoated with filter aid (e.g., diatomaceous earth) which can also be added to the mixture to be filtered to assist efficient operation and to prevent biomass from blocking the filter.

1.1.3.2.2 *Cross-flow microfiltration*

Microfiltration membranes used in the separation of cells from fermentation broths or cell debris from cell homogenates have a pore size of typically 0.1-0.2 μm . The process is usually performed at low transmembrane pressure. The major advance in cross-flow microfiltration (or tangential flow filtration) over the conventional dead-end filtration is that the high shear across the membrane surface limits blinding by suspended solids. No aerosols are produced and the process is well suited to containment (Kroner et al., 1984). The filter designs include flat sheet (plate and frame or spiral configurations), hollow fiber, tubular and rotating filter units (Mackay and Salusbury, 1988).

Problems encountered with membrane processes include membrane fouling and concentration polarization. Membrane fouling is a decline in flux (volume of permeate per unit membrane surface area per unit time) with time under constant operating conditions. Fouling is an irreversible and time-dependent process caused when a membrane adsorbs, or its pores are plugged by some components in the feed solution, thus lowering the flux. Concentration polarization is due to the build-up of rejected feed components on the membrane surface as a result of convective flow of solutes towards the membrane under the applied pressure gradient. Flux is lowered due to the additional hydrodynamic resistance of the polarized layer and the associated boundary layer (Patel et al., 1987).

Ultrafiltration is a separation process using membranes with pore sizes ranging from 2 to 50 nm. Membranes used for the separation of proteins or polysaccharides are classified by their molecular weight cut-off and range from 5 to 500 kDa. The process is usually performed at intermediate transmembrane pressure (1-10 bar). The main fouling of the membrane is caused by adsorption and gel layer formation of proteins and polysaccharides.

The approaches currently used in industrial applications to improve membrane performance are careful selection of the membrane materials and the use of relatively high cross-flow velocities both to increase the shear rate and, subsequently to transfer material away from the membrane surface (Dekker and Moom, 1995).

1.1.4 Cell disruption

Product recovery often requires cell disruption. The product within the cell may be soluble or insoluble (protein aggregates called inclusion bodies). Traditionally, mechanical, chemical and biological disruption techniques have been used to disrupt cells

at the bench level (Kula et al., 1990; Fish and Lilly, 1984). Mechanical processes such as high pressure homogenisation or high speed bead mills are well recognised as the methods of choice for the large scale disruption of microbial cells in the recovery of intracellular products (Engler, 1985; Chisti and Moo-Young, 1986; Kula and Schütte, 1987).

The methods of cell disruption may generally be divided into two subcategories: mechanical and non-mechanical methods.

1.1.4.1 Mechanical disruption

1.1.4.1.1 Sonication

One of the most widely used laboratory disruption methods is sonication. Ultrasonic disintegration generally operates at frequencies of 15 to 25 kHz, with cell disruption resulting from cavitation effects. Disruption is caused by shear stresses developed by viscous dissipative eddies arising from shock waves produced by imploding cavitation bubbles (Doulah, 1977). This method can cause degradation of enzymes (Coakley et al., 1974) and it is not suitable for large-scale processing because of difficulties in providing adequate cooling and high power input (Lilly and Dunnill, 1969).

1.1.4.1.2 High-pressure homogenisation

Homogenisation is at present the most widely used large-scale disruption technique. The APV Gaulin high-pressure homogeniser employs a positive displacement pump to pass the cell suspension through an adjustable, restricted orifice discharge valve with an opening in the range 20-100 μm . Gram negative bacteria are easily ruptured by two passes through this device (Lee, 1989). The Constant Systems Ltd. high pressure disrupter, which has proven containment capability (Bennett, 1991) can operate over a greater pressure range up to 40 kpsi. The breakage of gram positive cells such as micrococci, streptococci, yeast and lactobacilli are more difficult. Breakage of high cell concentrations or the disruption of cells at the stationary phase of growth requires multiple passes or continuous recycling of the suspension (Charm and Matteo, 1971). The operational parameters which influence the cell disruption in a high pressure homogeniser include operating pressure, design of the valve unit, cell density and temperature. In general, it is desirable to operate at higher pressures in order to achieve a higher efficiency for the single passage (Chisti and Moo-Young, 1986; Kula and Schütte, 1987).

Any improvements to the optimisation of recombinant product release has been via supplementation of existing equipment with chemical or enzymatic pretreatments. Harrison et al. (1991) showed that pretreatments with detergents, pH shock, EDTA and

enzymes, enhanced disruption, especially for release of non-soluble intracellular products.

1.1.4.1.3 High-speed bead milling

Glass bead milling is more efficient than high pressure homogenisation in the case of more resistant cells (Darbyshire, 1981) and is also particularly useful for the disruption of highly filamentous micro-organisms. Mechanical grinders consist of a cylindrical chamber, containing cells in liquid suspension, and grinding media, such as glass beads, with a turning shaft. Agitation at a high rate results in disruption from impact and shear force applied against the cell wall by the grinding media. The efficiency of disruption is affected by the concentration of cells, the optimum varying between 30-60% cells wet weight (Bjurstrom, 1985). The major parameters of concern for scale-up are the grinding media and the shaft speed, or peripheral velocity. Uniformly sized grinding media (0.1 mm diameter for bacteria and 0.5 mm diameter for yeast) are preferred for consistent results. As in homogenisation, heat is generated and this is countered by use of a cooling jacket.

Large scale disruption by high pressure homogenisation and high speed bead milling has its drawbacks. These processes are energy intensive in nature. The dissipation of the energy expended as heat demands costly and efficient cooling plants to prevent product deterioration. The micronisation of the cell debris (Schütte et al., 1983) and the gelatinous nature of the homogenate (Naglak et al., 1989) can hinder subsequent solid-liquid separations by conventional processes such as centrifugation and filtration. In addition there is a tendency to generate foams by degassing or by the inclusion of air and shear at gas-liquid interfaces (Fish and Lilly, 1984). The largest available homogenisers can handle up to 6000 litres per hour.

1.1.4.2 Nonmechanical disruption

The high shear forces of mechanical disruption may denature the target protein which then must be separated from a complex mixture of contaminants. Alternative nonmechanical disruption methods include enzyme lysis, chemical lysis (acid/alkali or detergents), heat treatment and freezing and thawing. Some of these techniques are of limited usefulness, particularly when biologically active materials are being prepared.

1.1.4.2.1 Enzymatic lysis

An advantage of enzymatic lysis is the specific enzyme action and the mild conditions under which lysis occurs. However, the application of enzyme lysis requires selection of an appropriate enzyme and determination of reaction conditions (Engler, 1979).

Combinations of lytic enzymes have been shown to be effective (Knorr et al., 1979). Enzymatic lysis of gram positive bacteria was studied using a crude enzyme preparation consisting of supernatant of *Cytophaga sp.* (LeCorre et al., 1985). The only lytic enzyme available on a commercial scale for the disruption of cells is lysozyme. Although cell wall lysis of gram negative bacteria (e.g., *E. coli*) by lysozyme has advantages over other nonmechanical methods, of specificity, better control of pH and temperature, and lower capital investment, the major disadvantage is the relatively high cost and therefore this is not presently an economical method for large-scale applications (Kula and Schütte, 1987).

1.1.4.2.2 Osmotic shock

Cells are allowed to equilibrate briefly in a medium of high osmotic pressure, (e.g., 1 M sucrose). When the medium is suddenly diluted, water enters the cells rapidly increasing the hydrostatic pressure which causes disruption. This method is good only for very fragile organisms or when the cell wall is first weakened by enzyme treatment or by inhibition of cell wall synthesis (Hughes et al., 1971).

Physical treatments, such as freezing and thawing in repeated cycles, and heating and drying, have been used successfully but yields tend to be low and denaturation is likely to occur.

1.1.5 Primary separation operations

At large scale it is essential that the protein be concentrated at an early stage in the purification process in order to lower the process volume to make it more manageable and to ensure a minimum protein concentration required for subsequent purification.

1.1.5.1 Ultrafiltration and diafiltration

Ultrafiltration (see also section 1.1.3.2) is widely used to concentrate (dehydrate) protein solutions. The pores of the membrane are small enough (0.2 μm -200 nm) to prohibit the passage of proteins through the membrane while not prohibiting the passage of salt ions, buffers and water. 'Concentration polarization' which is the build-up of proteins on the surface of the membrane rapidly reduces the rate of flow dramatically. This is controlled at scale by a cross-flow system. Ultrafiltration has been used successfully with shear-sensitive products (Trudel et al., 1983). Another application of ultrafiltration is diafiltration which is an exchange of buffers, similar to dialysis but capable of handling large volumes rapidly. Problems associated with ultrafiltration include protein

flocculation, causing unexpected blockages, non-specific protein binding to filters and denaturation.

1.1.5.2 Precipitation

Precipitation can be used to concentrate protein with an associated degree of purification. Precipitation occurs when the solubility of the protein in solution is reduced to some critical value by increasing the concentration of salt or some other material such as polyethylene glycol (salting out), by decreasing the salt concentration (salting in), by the addition of organic solvents or by adjusting pH or temperature (Bell et al., 1983).

1.1.5.3 Extraction

Aqueous two phase partitioning exploits the varying distribution of proteins between two immiscible water-based phases. Aqueous two phase systems made from PEG and dextran or salt are finding increased utility in large-scale protein purification. Unlike non-polar solvents, they show low interfacial surface tensions and dielectric constants and hence do not denature proteins (Andrews and Asenjo, 1989). Two phase partitioning can be used to separate proteins from cell debris, to purify proteins or to concentrate proteins.

1.1.6 Chromatography

Chromatographic methods dominate downstream processing. It has been estimated that in the \$2 billion global market for downstream equipment, liquid chromatography along with membrane separations account for around 90% (Spalding, 1991). Chromatography is a separation method in which the different components in a sample migrate through a column at different rates. There are two mechanisms for chromatography: adsorption, in which the sample molecules are adsorbed onto the chromatographic medium through binding (either noncovalent in the case of ion exchange and hydrophobic interaction or covalent in the case of thiophilic affinity chromatography) and nonadsorption (such as gel filtration chromatography).

1.1.6.1 Ion exchange chromatography

Ion exchange is the most commonly practised chromatographic method of protein purification. It is easy to use and scale-up, with wide applicability and low cost in comparison with other separation methods. Proteins bind to the ion-exchange resin by electrostatic forces between the protein's surface charges (mainly) and the close clusters of charged groups on the exchangers. The electrically charged species, such as carboxyl or quaternary ammonium groups, are balanced by counter ions e.g. metal ions or chloride

ions, which the protein displaces on binding (Hutchens, 1989). Elution with fractionation and/or concentration is achieved with an aqueous solution of higher ionic strength, or by changing the charge of the protein or by displacement with another protein or similar multivalent polymer (Torres et al., 1984).

1.1.6.2 Hydrophobic interaction chromatography

Hydrophobic interaction chromatography (HIC) and reversed phase chromatography (RPC) are separations based on the attraction between hydrophobic groups on the protein and a hydrophobic matrix. In HIC the sample is applied under conditions of high salt concentration and eluted under conditions of low salt concentration. In RPC the sample is applied in an aqueous buffer and eluted in an organic buffer. The matrix in RPC is more highly hydrophobic than in HIC (Fausnaugh et al., 1984). The mechanism of interaction has been described as the result of the balance of van der Waals, electrostatic and hydrophobic forces (Srinivasan and Ruckenstein, 1980). The matrix may consist of a hydrophobic polymer such as styrene cross-linked with divinylbenzene, or it may be a hydrophilic polymer such as agarose with a hydrocarbon chain attached to provide hydrophobicity.

HIC is applicable to most proteins and particularly to unstable proteins as it may be performed in the presence of high concentrations of ammonium sulphate, a condition that favours protein stability. However the degree of separation is often lower than a comparable ion exchange or affinity chromatography operation. RPC is most effective with small proteins. A major problem encountered in the use of HIC and RPC is the harsh conditions which are frequently required to elute proteins. This can increase the likelihood of protein denaturation which is also caused by protein interaction with the high density of alkyl groups attached to the packing of the stationary organic phase (Osterman, 1986). RPC provides a high resolution technique for the purification of peptides and proteins where retention in the native state is not essential e.g., hormones.

1.1.6.3 Affinity chromatography

Affinity chromatography relies on a specific interaction between the product protein and the solid phase to effect a separation from contaminants in the feed. This specific reaction allows hundred to thousand-fold purifications within a single step. Affinity chromatography can also concentrate very dilute solutions (Knight, 1989) and it can stabilise the protein once it is bound to the column (Hones, 1985). Packed-bed affinity chromatography typically comprises of a porous hydrophilic agarose-derived support matrix, bridged by a spacer molecule to the functional group, the affinity ligand (see section 1.2). Affinity ligands may be high or general affinity and bio- or pseudo-specific.

Affinity chromatography is usually classified according to ligand type. In immunoaffinity chromatography molecular recognition between a monoclonal antibody and its antigen occurs through the formation of a non-covalently bonded immunological complex. The antigen-antibody interaction is the basis of immunoaffinity chromatography. The specific interaction is very strong and too tight binding to immunoadsorbents is often a problem (Scopes, 1993). Monoclonal or polyclonal antibodies may be used. This method has been used for the purification of biomolecules such as interferons of various origins (Novick et al., 1983), interleukin-2 (Robb et al., 1983), blood clotting factors (Katzman et al., 1981), and membrane antigens (Hermann and Mescher, 1979). Affinity chromatography is discussed further in section 2.1.

1.1.6.4 Gel filtration chromatography

Gel filtration chromatography is a process for the separation of molecules on the basis of size. The molecules of the sample which are small enough to diffuse an appreciable distance into the matrix will be retarded in their passage through the chromatography column; thus the retardation results in a separation in space and time between large and small molecules (Fischer, 1980). The applications for gel filtration chromatography include buffer exchange, desalting, separation of product from contaminants of different size, determination of molecular weight of a particle or molecule.

1.2 Affinity Separation

The first affinity purification of an enzyme was made by Starkenstein in 1910, who purified amylase on insoluble starch. Affinity chromatography was established as a practical technique during the 1970's (Dean et al., 1985). It comprises of a reversible, specific interaction between a solid phase bound group (ligand) and the substance to be separated. This ensures the advantage of a high degree of purification and offers an attractive way to reduce the number of separation steps in a protein purification. Rather than relying on relatively small differences between the product and the contaminants that lead to purifications of only fewfold improvement, affinity reactions allow hundred to thousand fold purifications within a single step (Wheelwright, 1991).

The bioaffinity ligand may be a small molecule such as a pseudosubstrate, an inhibitor, an allosteric effector or a macromolecule such as a hormone receptor or antibody. The binding mechanisms include hydrophobic or hydrophilic interactions, as well as biospecific and electrostatic interactions. Elution may be non-selective (change of pH, ionic strength, temperature, polarity, increase in salt concentration) or biospecific (using substances such as cofactors and inhibitors).

The term "affinity" in affinity separations is frequently used in the broader sense to mean attraction. It is often used to describe processes that do not involve biospecific interactions. There are two classes of affinity adsorbents; biospecific adsorbents, which are truly specific in that they bind little other than proteins that have binding sites for the immobilised ligand and pseudo-specific (or general) adsorbents, which, although showing specificity for certain classes of proteins, bind many others also. So, separation on adsorbents such as dyes, immobilised metals and mixed-function ligands which do not necessarily interact at natural ligand binding sites are still classed as affinity interactions. Affinity adsorbents are usually synthesized by covalently attaching a ligand to a suitable matrix. However, there are some ready made insoluble materials that mimic substrates or are actual substrates, e.g., starch (for amylases and glycogen-metabolising enzymes).

The construction of an affinity adsorbent for the purification of a particular protein involves three major factors:

- (i) Choice of a suitable ligand.
- (ii) Selection of a support matrix and spacer.
- (iii) Attachment of the ligand to a support matrix.

1.2.1 Affinity matrices

An affinity ligand is immobilised to a solid support or matrix via one or more covalent bonds. The effectiveness of the immobilised ligand can be markedly dependent on the structure of the matrix (Fowell and Chase, 1986). Typically matrix supports for affinity chromatography should be hydrophilic but insoluble in water, macroporous but rigid, easily chemically modified but stable, resistant to microorganisms and in possession of a large surface area but inert to non-specific adsorption.

1.2.1.1 *Chromatographic based matrices*

Support materials suitable for affinity chromatography applications are expected to consist of macroporous hydrophilic, beaded particles, usually bearing free hydroxyl groups for ligand attachment. Various types of beaded supports are used in affinity separation, for example, natural polymers (e.g. agarose, dextran and cellulose), synthetic polymers (e.g., perfluorocarbons, polyacrylamide, polyacryloyltrihydroxymethylacrylamide, polyhydroxyethylmethacrylate, plastics and latex), inorganics (e.g., silica, controlled pore glass, and titania) and composite materials (e.g., silica-polysaccharides, polyacrylamide-agarose, and core-shell graft composites). A recent development in porous matrix design is perfusion chromatography, where the pores are wide enough to allow convective flow through the particles. Smaller diffusive pores along the

throughpore channels of the particles provide high adsorption area. The binding capacity of perfusive media is therefore limited by the fact that binding sites must be confined to the pore wall surface or a surface coating (Afeyan, 1990).

Although affinity chromatography remains the most favored and widely used affinity technology there are problems associated with its use and application. Porous particles in a packed column are prone to fouling and diffusional limitations which have an adverse effect on throughput and ligand usage. Non-porous silica (Krause et al., 1991) quartz (Wikstrom and Larssen, 1987) and agarose (Hjereter and Li, 1990) matrices, used in high performance affinity chromatography, circumvent the problems of mass transfer and compression, but because of the high cost this technique is confined to small scale analytical applications.

Large scale application of affinity chromatography at an early stage in the purification process is limited by the porous, compressible nature of the matrices commonly used. The need to pre-clarify/partially purify the target protein prior to column loading and the high cost of the packing material severely undermines the potency of chromatography as an affinity technique at large scale.

1.2.1.2 Non-chromatographic based matrices

Non-chromatographic affinity technologies include continuous affinity recycle extraction, aqueous two-phase affinity partitioning, membrane affinity filtration, affinity cross-flow ultrafiltration, reversible soluble affinity polymers, liquid affinity perfluorocarbon emulsions and affinity precipitation. In the case of continuous affinity recycle extraction, although the mode of solid/liquid interaction might differ from a packed bed configuration, the support matrices generally remain porous in character. Aqueous two-phase affinity partitioning, reversible soluble affinity polymers, liquid affinity perfluorocarbon emulsions and affinity precipitation purification are performed in a single liquid phase with no need for solid support matrices.

In membrane affinity filtration and affinity cross flow filtration a ligand is immobilised to a hollow-fibre microporous membrane (Iwata et al., 1991; Spalding, 1991). In affinity cross-flow filtration the membrane must have pores large enough to allow passage of all unwanted substances as well as the target protein, but not the affinity ligand (Luong et al., 1987). Membrane configurations other than hollow fibres used in biomolecule separation include membrane discs and modules of flat membrane sheets bearing immobilised ligands (Briefs and Kula, 1992; Champluvier and Kula, 1992). However

these technologies are mainly designed for large to medium scale operation (Spalding, 1991) and membrane affinity filtration is frequently compromised by the cost factor.

1.2.1.3 Non-porous matrices

A serious limitation of commercial porous supports is their propensity to become 'plugged' with debris and the difficulty in washing away such contaminating substances (Eveleigh, 1978; Munro et al., 1977; Halling and Dunnill, 1979a, 1980). There is evidence that non-porous support particles are less prone to fouling and are easier to clean, and are therefore potentially more useful in purifications from dirty feed streams (Munro et al., 1977; Halling and Dunnill, 1979a, 1980). Munro et al. (1977) investigated fouling of a non-porous magnetic support and demonstrated that stirring in chilled whole milk for 48 hours caused only a slight fall in the activity of nickel-chymotrypsin, while a cellulose support was seriously fouled under these conditions.

In addition, diffusional limitation effects are minimised and mass transfer rates improved. In a study by Halling and Dunnill (1979a) diffusional limitation effects were shown at a minimum for Ni-chymotrypsin non-porous supports. This contrasts with a porous support with immobilised chymotrypsin which shows severe diffusional limitations (Halwachs et al., 1973; Kay and Lilly, 1970). For a truly non-porous support only external diffusion of reactants will occur (Halling and Dunnill, 1980).

Conventional supports are typically porous in nature so as to provide a maximum effective surface area for ligand attachment and adsorption to take place. In order to obtain a comparable surface area to macroporous particles of ~100 μm size, the particle dimensions for a non-porous support would have to be in the order of 0.1-1 μm (Groman and Wilchek, 1987). Probably the only feasible method for recovery of such small particles in the presence of biological debris of similar size is by magnetic separation (see sections 1.5 and 1.6). The use of magnetic separation for affinity purification eliminates the need for centrifuges, columns, pumps or filters. But it is of greatest advantage when the purification involves solutions of marginally soluble materials that clog columns or foul filters. Magnetic affinity chromatography can even be performed in the presence of particulates such as cells or cell debris resulting from cell lysis (Menz et al., 1986)

1.2.2 Activation and coupling chemistry

Successful affinity chromatography requires that the ligand remain active after it is coupled to the matrix. The ligand is bound to the matrix in two steps: The matrix is first

activated; then the ligand reacts with the activated matrix. If a spacer is used, it may be attached to the matrix and the ligand attached to it, or the spacer may be attached first to the ligand and the ligand-spacer complex attached to the matrix. The major support activation methods are listed as follows:

(i) *Cyanogen Bromide*. Cyanogen bromide (CNBr) reacts with hydroxyls in agarose and other polysaccharide matrices to produce a reactive support which can subsequently be derivatised with spacer molecules or ligands containing primary amines (Kohn and Wilchek, 1982). With this method slow hydrolysis occurs at extremes of pH resulting in leakage of ligand and the HCN produced during coupling is extremely toxic. In spite of this and mainly for historical reasons, CNBr activation is one of the most widely used processes in the preparation of affinity adsorbents.

(ii) *Epoxide groups*. Epoxy activation introduces an epoxy group as an active electrophile. There are two reagents; one is epichlorohydrin which results in a three-carbon propane 2-ol spacer arm after reaction with the ligand (Pepper, 1992). The other is 1,4-butanediol diglycidyl ether (a bisoxirane) which results in a 12-atom spacer (Sundberg and Porath, 1974). They react rapidly with primary amine and sulfhydryl groups and more slowly with hydroxyls to yield derivatives which possess a long chain reactive oxirane (which can act as a spacer arm). Oxirane coupled ligands are extremely stable.

(iii) *Carbonyldiimidazole*. Polysaccharide matrices may be activated using carbonylating agents such as N,N' carbonyldiimidazole (CDI) under anhydrous conditions to give reactive imidazole carbonate derivatives (Bethell et al., 1979). These in turn will react with ligands containing primary amino groups at alkaline pH to give stable carbonate derivatives. CDI is non-toxic, gives high levels of activation and does not introduce ion-exchange groups into the matrix.

(iv) *Sulphonyl chloride*. Organic sulphonyl halides react with matrix hydroxyl groups to form sulphonyl esters. Nucleophiles will readily displace the sulphonate enabling efficient and rapid coupling. Activation using *p*-toluene sulphonyl (tosyl) chloride (Nilsson and Mosbach, 1980), or trifluoroethyl sulphonyl (tresyl) chloride, which is more reactive (Nilsson and Mosbach, 1981), is carried out in organic solvents and the resulting matrix is stable for extended periods.

1.2.2.1 Spacer molecules

A spacer molecule serves to move the ligand off the surface of the solid support, making it more accessible to the protein and overcoming the steric hindrance between the product and the ligand caused by the matrix. (Lowe, 1979; Lowe and Dean, 1974; Turkova, 1978). The length of the spacer arm is crucial and must be determined empirically. Hydrocarbon chains of from five to ten carbons are frequently used. It was thought desirable to reduce or eliminate the hydrophobic nature of the spacer arm and eliminate nonspecific binding interactions. In fact the hydrophobic interactions were shown to be a necessary part of binding to the adsorbent (O'Carra et al., 1974; Lowe, 1977) and that even weak nonspecific interactions are sufficient to add to the specific ones to create quite strong binding overall (Scopes, 1993).

1.2.2.2 Choice of ligand

Attributes to consider when choosing a ligand for protein purification are specificity, stability and reversibility, size, and affinity. The affinity ligand may be distinguished into two categories: high affinity ligands with dissociation constant (k_d) values ranging from 10^{-7} up to 10^{-15} M, and general affinity ligands - ligands of a broader spectrum of interaction and selectivity with k_d values typically 10^{-4} to 10^{-6} M (Labrou and Clonis, 1994). Affinity ligands may also be classified as biospecific or pseudospecific. Biospecific ligands as their name suggests are biological in nature and they bind little other than the proteins that they have binding sites for. Although pseudospecific ligands show specificity for certain classes of proteins, they bind many others also.

1.2.3 High affinity ligands

1.2.3.1 Immunoaffinity ligands

Immunoaffinity ligands work on the basis of the ability of antibodies to distinguish between very similar antigens. The interaction is highly specific and reversible. Numerous procedures have been developed to couple antibodies to solid supports (O'Shannessy, 1990; Ernst-Cabrera and Wilchek, 1988). In general antibodies are cross-linked by either random coupling or selective oligosaccharide directed immobilisation to the matrix. The technique may be used either with polyclonals or monoclonals (MAb), although the latter are often preferred. Random coupling through the amino acid side chains is often accompanied by a partial or complete loss of antigen binding capacity owing to a reduced efficiency of antibody-antigen interactions (Schneider et al., 1982).

Antibodies as a class of proteins are particularly resistant to proteolytic attack and are cleaved quite selectively by only a limited number of enzymes (Hill et al., 1989).

However in affinity chromatography there are drawbacks and care must be taken in the choice of ligands. Antibodies are not a practical choice because of high cost, low binding capacity upon immobilisation, ligand leaching problems and fairly poor selectivity for closely related molecules. Antibodies have very high binding constants for their antigens and excessively strong binding is often a major problem. Nevertheless they were used industrially in the early years of the biotech industry. However in practice, affinity adsorbents created with naturally occurring biological ligands tend to be expensive to produce since the ligands themselves are chemically and biologically labile and are difficult to immobilise in high yield with retention of activity (Lowe et al., 1990; McLoughlin and Lowe, 1988). However the exploitation of 'pseudo-' or 'biomimetic' ligands, in place of their natural counterparts as ligands for chromatography, offers the prospect of circumventing many of these difficulties.

1.2.3.2 Receptor ligands

Receptors and receptor-binding substances are highly specific affinity systems. Thus, employment of receptor adsorbents is an effective high-affinity method for isolating receptor-binding molecules. Recombinant interleukin-2 (rIL-2) is purified to homogeneity from mammalian and microbial sources on its immobilised receptor (Weber and Bailon, 1990) as are estrogen receptors from cytosols of rat uteri and human fibroid uterine tissue (Bhattachacharjee and Ali, 1992).

1.2.3.3 Avidin/streptavidin-biotin complexes

High affinity systems are based on the avidin/streptavidin-biotin complexes (Bayer and Wilchek, 1990; Desarnaud et al., 1992). Biotin is a vitamin and avidin (streptavidin is the bacterial analogue to avidin) is a glycoprotein of egg-white, which together form a strong complex of K_d value of approx. 10^{-15} M. Among several applications of the biotin/avidin system, one is the purification of solid-phase synthesized peptides. Biotinylated methionine as the terminal amino acid is finally purified on an avidin affinity column (Bayer and Wilchek, 1990).

1.2.4 General affinity ligands

1.2.4.1 Chelated metal ions

See section 1.3.3.

1.2.4.2 Textile and biomimetic triazine dyes

The commonest class of 'biomimetic' ligand is the reactive textile dyes which originate from the serendipitous discovery that the dye component of blue dextran, Cibacron blue

F3G-A, bound to pyruvate kinase during gel filtration (Haekel et al., 1968). It is now generally accepted that most enzymes that bind a purine nucleotide will show an affinity for Cibacron Blue F3Ga. It also binds human serum albumin, fibroblast interferon and lipoproteins. The advantages of using textile dyes are manifold. They are inexpensive, commodity chemicals, readily coupled to a variety of support matrices via their reactive groups and resistant to biological and chemical degradation. Immobilised dye adsorbents display high capacities for their complementary protein and thus have considerable scale-up potential. However in practice blue dye is not nearly as specific as was first thought; moreover, it is estimated that that as many as 50% of enzymes are nucleotide binding. The selectivity of these affinity ligands can be improved by designing and synthesizing dyestuffs which mimic the structure and binding of natural biological ligands more sympathetically (Lowe et al., 1986).

Since the discovery of the interaction of Cibacron blue with various enzymes there has been a considerable expansion in the application of other reactive dyes to protein purification. Dye ligand chromatography has become more popular because the ligands are inexpensive, easy to couple to matrices and extremely stable. Numerous examples of protein purification using dye-ligands have been published (Lowe et al., 1984). However it is not possible to predict if a particular protein will bind to a given dye column. This disadvantage necessitates systematic screening to identify suitable adsorbents from a collection. Furthermore ligand leaching is a concern because of the relationship of the polycyclic dyes to carcinogens.

1.2.4.3 Amino acid based ligands

Amino acid sequences encoded in the antisense strand of DNA are called 'antisense peptides' and are used as affinity ligands of appreciable selectivity against the corresponding 'sense peptides' (Chaiken, 1992) or 'sense' region of proteins (Scapol et al., 1992).

1.2.4.4 Nucleotide-based ligands and coenzymes

Immobilised nucleotides and nucleotide coenzymes find application in enzyme purification (Clonis and Lowe, 1980). However they are expensive, tend to be unstable and have low binding capacity.

1.2.4.5 Carbohydrate-binding ligands

Lectins and boronates exhibit affinity against the carbohydrate moiety of target molecules and are therefore used in affinity purifications. The affinity of lectins for specific carbohydrate moieties has made them particularly useful for the purification of distinct

groups of glycoproteins. For example, many receptors bind to wheatgerm agglutinin (WGA) whereas cytokines and other growth factors bind preferentially to concanavalin A (ConA) or lentil lectin (LCA).

Lectins will bind both naturally occurring glycoproteins (soluble and membrane bound) and those produced by recombinant DNA techniques. A large number of lectins are available commercially but in order to find the appropriate lectin it is necessary to screen a range of lectins for binding of the glycoprotein.

1.2.4.6 Protein ligands

Protein A is a very stable ligand which binds specifically to the Fc region of immunoglobulins from various species. Binding is enhanced at high pH (8-9) and high salt concentrations (3 M) (Kruger et al., 1988). Protein G complements Protein A by binding immunoglobulins that the latter fails to bind. Binding is usually carried out in physiological buffers and elution requires 0.1M glycine-HCl pH 2.5.

1.2.4.7 Protease inhibitors

An approach to the isolation of proteases by affinity chromatography exploits the specific inhibitory action of the naturally occurring protein inhibitors. They form stable complexes with the corresponding proteases at neutral pH but are dissociable at low pH values. Soybean trypsin inhibitor-Sepharose has been successfully employed for the purification of several proteases from activated bovine pancreatic juice.

1.2.5 Affinity separation techniques

Affinity chromatography is the most widely used affinity technique at large scale. However it is not without its drawbacks and problems. There are several non-chromatographic approaches being developed which aim to offer a superior alternative to chromatographic technologies.

1.2.5.1 Affinity precipitation

Separation occurs when complexes formed between target protein and water-soluble macroligand precipitate out of the solution. The nature of the macroligands may be homo-bifunctional (two identical ligand molecules attached by a spacer molecule) or hetero-bifunctional (protein binding ligand attached to a function that causes precipitation) (Chen, 1990). For the former an empirically determined ligand concentration must be determined to optimise precipitation, and in most cases only multimeric proteins may be separated as the macroligand needs multiple binding sites in the same protein. The length

of the spacer molecule is critical and can vary with the application (Larson and Mosbach, 1979; Mosbach, 1983). Van Dam et al. (1989) utilised bis-chelates of Cu(II) for selective precipitation. The Cu(II) binds the metal coordinating (histidine) residues on protein surfaces.

1.2.5.2 Affinity partitioning

Proteins can be partitioned between two water rich phases (two polymers or a polymer and a salt) and the selectivity of partitioning may be influenced by a suitable affinity ligand for the target protein (Johansson and Tjerneld, 1989). Metal affinity partitioning of proteins in Cu(II)-PEG/dextran aqueous two phase systems has been described (Suh and Arnold, 1990). Although easy to scale up (Buckmann et al., 1987) the cost of synthesizing ligand-polymer is the major operating cost in this system and an efficient ligand recycle scheme is essential to make this process competitive. The capacity for processing crude protein mixtures is limited by the solubility of the protein together with their effects on the viscosity of the phases (Chen, 1990). The method exhibits low to medium purifying potential, therefore it may not be a good choice for therapeutic proteins or diagnostic enzymes (Johansson, 1987).

1.2.5.3 Affinity cross-flow filtration

This method combines biospecific affinity interaction with the scalability of membrane separation such as cross-flow ultra-filtration (Herak and Merrill, 1989). The high molecular weight carrier with immobilised ligand - target protein complex is retained by the membrane. The macroligands can be either water-insoluble particles or water soluble high molecular weight polymers. Binding capacities are limited by the size of the ligand carriers and low yields as a result of enzyme denaturation are due to prolonged filtration, the limiting factor being the filtration rate (Ling and Mattiasson, 1989).

1.2.5.4 Affinity separation using reversed micelles

Reversed micelles are surrounded by surfactant molecules in an organic solvent. They consist of an inner core of water and are capable of solubilising hydrophilic species, including enzymes, in otherwise inhospitable organic environments (Woll et al., 1989). Protein partitioning between the two phases can be manipulated and depends on the relative volumes of the two phases, polar solvent, ionic strength, pH, and the presence of biologically active surfactants (Hatton, 1989). The biospecificity of the protein is exploited in the reversed micellar recovery of bioproducts from the aqueous feed solution through inclusion of an affinity ligand detergent in the extractant phase formulation.

1.2.5.5 Liquid affinity perfluorocarbon supports

Liquid fluorocarbon supports (Breillatt and Eveleigh, 1987; Bodeker and Lenhoff, 1989) have the high specificity and avidity of solid supports and the mechanical advantages of liquid-liquid systems which makes them particularly useful for large-scale operations. The supports are chemically and biologically inert, they exhibit negligible non-specific binding and they can be recovered easily by sedimentation. However there are no large scale studies which indicate their recovery efficiency. The affinity ligand C.I. Reactive Blue 2 may be immobilised via polyvinyl alcohol conjugated to perfluorooctanoyl chloride (Stewart et al., 1990). Stability is a problem through droplet evaporation and coalescence and emulsion creaming (Stewart et al., 1990).

1.2.5.6 Affinity water-soluble nonionic surfactants

Affinity surfactants are produced by the covalent attachment of specific ligands for various enzymes to a class of water-soluble nonionic surfactants like the ethoxylated fatty alcohols and the corresponding ethoxylated fatty acids (Guzman et al., 1989). They are capable of binding reversibly to reverse-phase packing materials normally used in high performance liquid chromatography (HPLC). These packing materials can withstand high pressure and severe sterilization methods.

1.3 Immobilised Metal Chelate Affinity

Bioseparations based on metal recognition is an appealing concept. Proteins with surface accessible histidine (imidazole group) and cysteine (thiol group) amino acid residues were known to form stable complexes with zinc and copper ions in nearly neutral aqueous solutions as far back as 1948 (Hearon, 1948). Porath was the first (Porath et al., 1975) to apply this idea to test whether cross-linked agarose with covalently attached chelating ligands and loaded with metal ions could act as a selective adsorbent for histidine and cysteine-containing peptides and proteins. It worked and he called it immobilised metal affinity chromatography (IMAC). The potential presented was quickly recognised of stable, inexpensive chelated metals which effectively mimic biospecific interactions and provide selective ligands for protein binding. Applications of IMAC range from purification of recombinant human growth hormone (Maisano et al., 1989) and tissue plasminogen activator (Furlong et al., 1988) to purification of wheat α -amylases (Zawistowska et al., 1988), glycoproteins (Corradini et al., 1988) and the separation of cells (Botros and Vijayalakshui, 1989).

Metal affinity separation has a number of advantages over biospecific affinity separation. The small chelates are stable under a wide range of solvent conditions and temperatures

which suggests that they may be recyclable with negligible loss in performance. High metal loadings can be achieved with metal affinity separations which therefore implies high protein capacities. Product may be eluted under mild conditions and ligand regeneration may be achieved with relative ease and finally, but highly significantly, metal chelates are inexpensive. In addition, metal chelate ligands are suited to the fractionation of hydrophobic proteins which may require the use of neutral detergents (Choquet and Sprott, 1991).

Considerable progress has been made in understanding the molecular basis for the selectivity of metal affinity separations. Immobilised metal affinity technology has been transferred from packed bed chromatographic operation to aqueous two phase partitioning (Schustollar et al., 1992; Suh and Arnold, 1990; Wuenschell et al., 1991), electrophoresis (Goubran-Botros et al., 1992), precipitation (Van Dam et al., 1989; Suh et al., 1990), membranes (Iwata et al., 1991), immobilisation of enzymes (Coulet et al., 1981) and cell separation (Goubran-Botros, 1989). The most potent use of immobilised metal affinity is the separation of specifically tailored recombinant proteins (Janknecht et al., 1991; Loetscher et al., 1992; Berthold et al., 1992) at large scale (Zawistowska et al., 1992).

1.3.1 Mechanism of metal affinity separation

1.3.1.4 Adsorption and elution

Adsorption of a protein to a chelating metal has to be performed at alkaline pH at which the electron donor grouping(s) on the protein surface is at least partially unprotonated. Deprotonation of the aquoligands occurs with concomitant lowering of the charge. An efficient separation is achieved by employing a pH gradient (Lönnerdal et al., 1977; Edy et al., 1977; Lebreton, 1977; Torres et al., 1979; Bollin and Sulkowski, 1981). Proteins bind metal ions mainly via amino acid residues which have electron donating side chains. Unlike ion-exchange chromatography, adsorption can take place at high concentrations of NaCl. In fact, the adsorption capacity and the degree of selectivity under such circumstances seem to increase as the salt concentration in the equilibration buffer is increased (Porath and Olin, 1983; Hemden and Porath, 1985). Charge controlled attraction forces (ion exchange or ionic adsorption) predominate at low ionic strength, whereas the adsorption at very high salt concentration may be due to a frontier orbital controlled electron transfer, which, together with the desolvation energy, results in the formation of the coordinate bonded adsorption complex.

Elution can be performed by either (i) protonation, (ii) ligand exchange or (iii) chelate annihilation.

(i) Protonation of an electron donor grouping(s) on the protein surface is effected by lowering the pH by either a gradient or step method which results in protein displacement. This elution method must not compromise metal chelate stability. This is a problem with IDA-Zn²⁺ and IDA-Co²⁺ where leaching of the latter is visible at pH 5. The protein must not irreversibly lose its activity upon decrease of pH and neither should isoelectric precipitation of protein take place.

(ii) Proteins can be eluted from metal chelate complexes at near neutral pH by competing electron donor solutes, eg. imidazole, histidine, histamine or glycine gradient. However, because imidazole forms a fairly stable complex with metal chelates the column has to be first saturated and equilibrated. The cost of the competing agent and the possible necessity of removing it from the purified protein make this method unsuitable for large scale applications.

(iii) The metal-chelate can be destroyed at low pH by a mild chelating agent (e.g., histidine) or a strong chelating agent (e.g., EDTA) resulting in the elution of all bound protein. Protein recovery is achievable by this method but with little purification (unless the protein of interest is the only one still bound) and at the risk of inactivation. The use of this protocol can be recommended only in cases where other attempts at recovery have failed.

Elution by decreasing the salt concentration or changing to a different salt during the chromatography run (Gentz et al., 1988) may be run in conjunction with other methods or alone (Porath, 1987).

1.3.2 Choice of metal ion

The affinity of proteins for transition metal ions provides the basis for their purification by metal chelate affinity separations. The ligands most often used in IMAC are first row transition metal ions (Ni²⁺, Cu²⁺ and Co²⁺) and Zn²⁺, chelated in the majority of cases by iminodiacetic acid (IDA). The apparent affinity of a protein for a metal chelate depends strongly on the metal ion involved in coordination. Both protein retention (Yip et al., 1989; Hemden et al., 1989) and stability constants for complexation with imidazole (Sundberg and Malin, 1974), follow the order Cu²⁺ > Ni²⁺ > Zn²⁺ ~ Co²⁺. The affinity of imidazole for Cu²⁺ is fifteen times that for Ni²⁺ whose affinity in turn is more than three

times that for Zn^{2+} and Co^{2+} . The side chains of histidine dominate protein binding to chelated metal ions (Sulkowski, 1989). The histidine imidazole nitrogen coordinates metals in the unprotonated state, and studies have demonstrated the linear dependence of apparent metal affinity on histidine content (Suh and Arnold, 1990).

The metal ion is immobilised (usually chelated) on a support which may be a solid matrix or a liquid carrier. All ions are highly solvated in an aqueous solution as a result of the coordination of water molecules (Chaberek and Martell, 1959). The metal ion can be considered as a Lewis acid (electron-pair acceptor) and the water molecule as a Lewis base (electron pair donor). The water molecules can be replaced by a stronger base to form a metal complex. The incoming protein binds to the metal ion(s) via electron donor grouping(s) resident on its molecular surface. A donor atom (N,S,O) with a free electron pair in coordination with a metal ion (Me^{2+}) is called a monodentate ligand. Two or more atoms in one ligand constitute a polydentate ligand and coordination of such with a metal ion results in a metal chelate.

The usefulness of IMAC can depend on the metal chelated to the affinity matrix. In the separation of a soluble F420-reducing hydrogenase from its membrane bound form, Ni^{2+} and Zn^{2+} chelates were equally effective but Cu^{2+} chelate inactivated the enzyme and Co^{2+} or Fe^{2+} chelates failed to bind the enzyme (Choquet and Sprott, 1991).

Andersson et al. (1991) found that of several serum albumins studied, all were retained on a column with IDA- Cu^{2+} , all but one with IDA- Ni^{2+} and there was no interaction with IDA- Zn^{2+} and IDA- Co^{2+} . This non-interaction is thought to occur because the high affinity binding site of an albumin molecule is capable of scavenging Zn^{2+} and Co^{2+} ions from their immobilised chelates. Similar metal ion transfer phenomena have been observed for carboxy peptidase A (Muszynska et al., 1986) and transferrins (Sulkowski, 1988).

1.3.3 Metal chelating ligands

The nature and density of the chelating ligand appears to influence the selectivity and capacity obtained as well as the quantitative and qualitative aspects of the adsorption process. An ideal chelate resin for the purification of biopolymers must on the one hand strongly complex the metal ions and on the other must permit reasonable interactions between the metal ions and proteins. The nucleophilicity of the atoms (N,O,S) participating in coordination to metals is of primary importance. However, there are other contributory factors: steric fit or hindrance, entropic gain resulting from

disorganisation of some hydration water and coulombic interactions (Hemden and Porath, 1985).

Bidentate chelators afford too weak a binding of the metals, therefore unwanted leakage of metal ion would be high (Porath and Olin, 1983). Iminodiacetic acid (IDA) and tris (carboxymethyl)ethylenediamine (TED) chelators belong to the ligand group of chelones, (i.e. carboxymethylated amines). IDA is the most commonly used chelating ligand for the immobilisation of metal ions (Porath et al., 1975; Porath and Olin, 1983). IDA is a tridentate chelator which binds metal ions through its nitrogen atom and two carboxylate oxygens. IDA-bound metal ion coordinates the ϵ or δ nitrogen of a surface accessible histidine. The small size and hydrophilic nature of IDA, as well as the overall neutral charge of the complex with divalent ions, minimise secondary interactions between metal chelate and protein (Arnold, 1991).

The coupling of TED results in stronger retention of metal ion and weaker retention of protein and more steric hindrance to proximal contact than is experienced with IDA. When chelated by the tridentate IDA resin, Cu^{2+} has one coordination site free for interactions with biopolymers where as Ni^{2+} has three such sites. However, Ni^{2+} is not bound tightly enough and may be released from the adsorbent during chromatography. The pentadentate TED resin binds metal ions having a coordination number of six very strongly, but again only one coordination site remains for biopolymer interaction.

A quadridentate chelate former, nitrilotriacetic acid (NTA), was claimed by Hochuli et al., (1987) to be superior to the known IDA adsorbent. It was thought to be especially suitable for metal ions with coordination numbers of six, since two valencies remain for the reversible binding of biopolymers. Hochuli found that the Ni^{2+} -NTA adsorbent is selective for proteins and peptides which have as a structural element neighbouring histidines on the surface. He also suggested that Ni^{2+} -NTA adsorbent is more stable than Ni^{2+} -IDA adsorbent since the latter Ni^{2+} is only weakly bound and is often washed out even upon loading with the protein mixture. However no difference in the selectivity of a histidine tagged antibody fragment was found on Ni^{2+} -NTA as compared to Zn^{2+} -IDA (Skerra et al., 1991). It has been suggested that NTA is useful mainly for binding (high affinity) proteins that have a tendency to scavenge the metal (Arnold, 1991). Ni^{2+} -NTA adsorbent was used in the purification of a soluble human interferon V receptor expressed in *E. coli* and containing an auxiliary amino acid sequence of six sequential histidine residues (Fountoulakis et al., 1990) and vaccinia virus expression of proteins fused to an amino-terminal tag of six-histidines were affinity purified by Ni^{2+} -NTA chromatography (Janknecht et al., 1991).

Another seldom employed chelating ligand is dipicolylamine (DPA), a tridentate ligand, like IDA. DPA possesses three nitrogen atoms for coordination whereas IDA has only one. The π electrons and heteroaromatic nitrogen should affect the affinity character of a DPA matrix. The bulkiness of the pyridyl groups will, because of steric hindrance, only allow one of the three possible metal coordination sites to bind water or solutes (Porath and Hansen, 1991).

1.3.4 Protein-metal interaction

1.3.4.1 Amino acids

Amino acids form stable chelates with metal ions (Gurd and Wilcox, 1956). Both amino and carboxyl groups of an amino acid participate in the formation of a chelate. Some amino acids such as cysteine, histidine and arginine bind through electron donor atoms in their side chains. Peptides containing histidine residues form more stable coordination compounds with metal ions due to participation of imidazole side-chains in chelation. Although free cysteines can potentially bind chelated metals, in practice they are rarely available in the appropriate reduced state. An accessible N-terminus may also contribute to retention but only weakly at neutral pH (Arnold, 1991). Amino acids with aromatic side chains such as tryptophan, phenylalanine, and tyrosine will contribute to apparent metal affinity only if they are near accessible histidines (Leporati, 1986).

Individual histidyl residues vary in their affinities for immobilised metal ions. Variations in metal affinity can be attributed to differences in the histidyl pKa's and steric accessibilities of the imidazole nitrogens. An average binding constant from the interaction of a single protein histidyl with Cu^{2+} -IDA is $K_a = 4.5 \times 10^3 \text{ M}^{-1}$. However experiments performed with Cu^{2+} -IDA derivatised polyethylene glycol in PEG/dextran two phase systems have demonstrated the linear dependence of apparent metal affinity on histidine content (Suh et al., 1990).

It appears that the presence of a single histidine residue on the surface of a protein is sufficient for the retention of the latter on IDA- Cu^{2+} at neutral pH, and multipoint attachment to IDA- Cu^{2+} (two/three histidines) results in a strong retention. (Sulkowski, 1985; Andersson and Sulkowski, 1992; Hemden et al., 1989). Ni^{2+} -IDA appears to retain proteins via their surface accessible histidines in a manner similar to Cu^{2+} -IDA but at much lower binding strengths. The binding of a protein to an IDA- Ni^{2+} column seems to require more than one histidine residue.

1.3.4.2 *Spatial distribution*

The spatial distribution of histidines on the protein surface may influence apparent metal-binding affinities. Two histidines brought into close proximity as a result of protein folding will result in stronger binding to the chelated metals (Sulkowski, 1989). A favorable entropic contribution to the binding free energy appears only when protein donating groups are interconnected with a considerable degree of rigidity (Suh et al., 1991).

A His-X₃-His motif, inserted at the N-terminal α -helix of a cytochrome *c* variant, complexes Cu²⁺ that is bound to IDA-PEG 24 times higher than does a single histidine (Todd et al., 1991). Conformational changes are known to accompany protein adsorption (Sandwick and Schray, 1988) and the potential flexibility of the α -helix carrying the metal-binding may reflect the strength of binding. His-X₃-His high affinity, α -helical motif, occurs naturally in the metalloproteins thermolysin (Holmes and Matthews, 1982) and "zinc finger" DNA binding proteins (Berg, 1988). In the His-X₃-His orientation the ϵ -nitrogens of the imidazole groups from both histidines can coordinate a single metal.

Study of binding affinities of His-X₃-His and His-X₂-His variants for metal ions found a very large drop in the copper binding affinity for His-X₂-His (Suh et al., 1991) which is corroborated by His-X₂-His occurring naturally in an α -helix of myoglobin exhibiting no chelate effect for Cu²⁺ binding (Suh and Arnold, 1990). However, it has been suggested that natural His-X₂-His sites in α -helices can bind strongly to immobilised Zn²⁺ and Cu²⁺ (Sulkowski, 1985).

1.3.4.3 *Other factors*

High concentrations of anti-chaotropic salts promote the retention of proteins on IMA adsorbents by a mechanism that is similar to that operating in hydrophobic interaction chromatography (Porath and Olin, 1983). Sodium chloride enhanced the retention more than did other salts (Hemden and Porath, 1985). The following order has been suggested for the relative contribution to protein adsorption i.e., phosphates > sulfates > acetates > chlorides > nitrates > thiocyanates (Porath, 1987). Sulkowski showed that high salt concentration enhanced the retention of acidic proteins and decreased that of basic proteins (Sulkowski, 1987). There are other desirable features to high salt concentrations in IMA buffers - proteins in general are stabilised by high salt concentrations and protein aggregation is retarded by the presence of salt (Torres et al., 1979).

A study by Hutchens and Yip (1991) showed the differential effects of temperature and urea on protein interactions with surface immobilised metal ions. Alterations in temperature had little or no effect on the immobilised Cu^{2+} binding capacity of either protein tested. Temperature effects on the interaction affinity, however, were protein dependent and varied considerably. For example the affinity of lysozyme for immobilised Cu^{2+} ions was significantly decreased with increased temperature (0°C - 37°C).

It is interesting to note that at a pH above 8, the α -amino terminal has an affinity for immobilised Cu^{2+} ions that is similar in strength to the affinity of histidine. Immobilised Ni, Zn, and Co ions displayed little or no attraction for the terminal α -amino group (Andersson and Sulkowski, 1992).

1.4 Pre-derivatised Recombinant Proteins: an aid to recovery

The major disadvantage with any affinity purification technique is that each method will be applicable only for the protein or the group of proteins for which it has been developed. Recombinant DNA techniques have been utilised to make affinity purification techniques general for the purification of an expressed protein from cloned genes. The concept is based on the fusion of the gene encoding the protein of interest to a gene fragment encoding a peptide, "the handle", with a strong affinity to a ligand.

In recent years the growth of a large biotechnology industry has provided the means for obtaining large quantities of recombinant proteins. Proteins produced in tiny quantities by their host cell can now be produced in high yield systems. In addition to the benefit of an unlimited supply of a product, precise genetic manipulations can be used to introduce desired protein properties that can be exploited for purification purposes. This is achieved by introducing adjacent to the structural gene for the desired protein product, a DNA sequence that codes for a specific polypeptide tail. Such tails can be inserted at the N- or C-terminal of the product protein, in some instances at both terminals, yielding a so-called fusion protein. If necessary, the additional peptide sequence can be removed either chemically or enzymatically after the purification to generate the desired protein sequence.

Fusion proteins are specifically designed to facilitate secretion and for purification of the target proteins. Foreign proteins are often rapidly degraded by most proteases, and this may sometimes be avoided by a gene fusion strategy, as has been demonstrated for a large number of small peptides (Marston, 1986). General and efficient purification

schemes may be obtained which allow rapid recovery of gene products (Uhlén et al., 1983; Germino and Bastia, 1984). The proteins can be localised to different compartments of the host cell (e.g., periplasm, cell wall, culture medium) through specific peptides fused to the protein (Marston, 1986; Nilsson and Abrahmsen, 1990).

The first examples of recombinant proteins with purification handles were reported by Sassenfeld and Brewer (1984). One of the earliest examples cited was the fusion of somatostatin to β -galactosidase with subsequent chemical cleavage of the fusion with cyanogen bromide at the joining methionine. Stabilisation of the product, as in this case, can still be an important factor, but it has been superseded in recent years by the attractive concept of using fusions to endow the product with specific properties which can be exploited for purification.

1.4.1 Recovery of fusion proteins

Genetic modifications for facilitated protein purification can be designed to take advantage of affinity, ion-exchange, hydrophobic, metal-chelate and covalent separations. The protocols for recovery of fusion proteins take account of the same considerations given to native proteins, namely intracellular versus extracellular, and soluble versus insoluble.

1.4.1.1 *Ion-exchange tails*

Sassenfeld and Brewer (1984) demonstrated a two-step ion-exchange purification of a recombinant human urogastrone with a C-terminal polyarginine fusion. In the first step, a substantial purification was obtained due to the unusual basicity of the polyarginine fused protein. Arginine is the most basic amino acid, therefore, at acid pH a polyarginine fused protein should bind strongly to a cation exchanger. Furthermore, since most bacterial proteins are acidic, they should bind weakly or not at all under these conditions. Further purification was achieved after removing polyarginine using carboxypeptidase B .

A single step purification may be possible using a ligand that selectively binds polyarginine. The binding of polyarginine to dyes (Itzhaki, 1972) and polyanions (Mita et al., 1978) has been described using ion-exchange.

In a similar manner, an N-terminal Ala-Glu tail has been added to recombinant human growth hormone (hGH), which allows its separation on an anion-exchanger. This tail can be removed by the enzyme dipeptidylaminopeptidase which removes dipeptides except when the second residue is proline as is the case in native hGH (Dalboge et al., 1987).

1.4.1.2 Hydrophobic and covalent tails

β -galactosidase tailed at the N-terminus with eleven phenylalanine residues was retained on Phenyl Superose (Pharmacia), significantly more so than native β -galactosidase or the bulk of the unwanted cellular proteins (Persson et al., 1988). A possible disadvantage is that many proteases from crude cell extracts bind well to hydrophobic matrices. The activity of the enzyme was almost unaffected by the presence of the polyphenylalanine tail so its removal was not necessary for use. Similarly, galactokinase tailed with four cysteine residues bound rapidly and specifically to Thiopropyl Sepharose (Pharmacia) and it could be used without removal of the tail (Persson et al., 1988).

1.4.1.3 Affinity tails

1.4.1.3.1 β -Galactosidase

One of the first of the larger proteins used as a fusion to aid the purification of protein products was the enzyme β -galactosidase. Numerous fusions have been prepared including β -endorphin (Shine et al., 1980), lysozyme, gal-repressor (Ullman, 1984) the replication initiator protein of plasmid R6K (Germino and Bastia, 1984), and erythropoietin (Nielson et al., 1988). C-terminal fusions to β -galactosidase normally yield insoluble inclusion bodies while most fusion proteins obtained after N-terminal fusions are soluble and allow affinity purification with substrate analogues as ligands. Fusions to β -galactosidase are thought to stabilise the recombinant protein by protecting against proteolysis, in addition to facilitating purification by affinity chromatography on immobilised *p*-aminophenyl- β -D-thiogalactoside. However the large size of the enzyme reduces the attractiveness of the system, as even high expression levels give rather low yields of the desired product. In addition it is not possible to obtain secretion using β -galactosidase as the fusion partner.

1.4.1.3.2 Chloramphenicol acetyl transferase (CAT)

This enzyme has been used as a fusion tail for the purification of recombinant human atrial natriuretic factor (ANF) (Knott et al., 1988; Dykes et al., 1988). The fusion protein was purified by affinity chromatography on immobilised *p*-aminochloramphenicol. However, problems with enzymic cleavage gave low yields or unwanted cleavage of product.

1.4.1.3.3 Protein A

Fusions to Protein A cloned from *Staphylococcus aureus* have been used to purify recombinant human insulin-like growth factor I (IGFI), expressed either in *S. aureus* or in *E. coli* (Moks et al., 1987). Protein A binds to the constant region of immunoglobulins, thus, protein A fusion proteins can be readily purified by affinity

chromatography on immobilised immunoglobulin G (IgG) by adsorption at neutral pH followed by elution at low pH. This system was the first to be used on a large scale for the purification of recombinant human IGF-I from 1000 L cultures of *E. coli* (Moks et al., 1987). However, the protein ligands might be susceptible to degradation by bacterial proteases in the extracts.

A synthetic IgG-binding domain of staphylococcal Protein A, designated Z, and in dimer form ZZ, has been demonstrated by Nilsson et al. (1987) as the optimal gene fusion partner in terms of maximal binding and efficient secretion. This fusion partner has been used extensively for the production of recombinant proteins, such as growth factors, receptors, enzymes and synthetic peptides (Nilsson and Abrahmsen, 1990).

1.4.1.3.4 *Dual affinity gene-fusion*

Dual affinity fusion is when the gene of interest, X, is fused between two heterologous domains, A and B, with specific affinity for two different ligands (Hammarberg et al., 1989). The advantage is that a full-length protein can be selectively recovered by two subsequent affinity purification steps. The dual fusion technique involves the fusion of two protein ligands, e.g., the SpA derived IgG-binding ligand ZZ and the albumin binding fraction of streptococcal protein G, to the ends of a proteolytically sensitive molecule. It was shown that such fusions reduced the proteolysis of IGF-II to a considerable extent. The fact that a split in the product leads to loss of at least one of the two affinities (IgG or albumin) means that only un-cleaved products are obtained after serial affinity chromatography based on these ligands.

1.4.1.3.5 *FLAG peptide tail*

A short (eight residue), hydrophilic, antigenic peptide (the FLAG peptide) was introduced by Hopp et al. (1988). The hydrophilic nature of the peptide should minimise complexing with the adjoining protein structure and maximise availability for interaction with the immobilised ligand. A monoclonal antibody was raised to the N-terminal end of the peptide sequence. Fusion to the target protein e.g., interleukin or granulocyte-macrophage colony stimulating factor resulted in a single-step immunopurification on the immobilised mAb. The peptides removal is facilitated by the action of enterokinase and the unwanted sequence (highly negative) was separated by ion-exchange chromatography.

1.4.2 Specific cleavage methods

One of the major requirements in designing fusion proteins is that, in most cases, the purification tail must be removed before the protein can be used, particularly when the protein is a therapeutic agent. A variety of techniques are available, both chemical and enzymatic. If the protein lacks natural methionine residues, cleavage with cyanogen bromide can be used to remove the tail. β -galactosidase fusions with insulin A and B chains were so cleaved at a methionine residue linking the two polypeptides (Goeddel et al., 1979). This was possible because human insulin does not contain a methionine residue. If the protein lacks tryptophan, then oxidative cleavage with a reagent like BNPS-skatole can be used (Knott et al., 1988). Both of these methods require the use of very low pH and can cause unwanted side reactions. Cleavage with hydroxylamine at an asparagine-glycine peptide bond can be carried out at pH 9.0 and is less liable to cause problems. Enzymic methods can be performed under mild conditions and enzymes can often be immobilised to reduce processing costs and avoid contamination. For C-terminal tails an exopeptidase can be used. Carboxypeptidase B, which is specific for basic amino acids is used to cleave polyarginine tails and carboxypeptidase A, which cannot cleave basic residues but can cleave, for example, a histidine tail providing the protein has a basic or proline amino acid at the C-terminus, can be applied. β -endorphin was released from a β -gal fusion using trypsin (which cleaves at the carboxyl side of arginine and lysine residues (Shine et al., 1988). This was possible because β -endorphin has no arginine residue and its lysine residues were chemically protected from enzymatic cleavage.

Specific chemical or enzymatic cleavage of the affinity tag for the protein of interest may be successful in several instances but often there are limitations of poor cleavage yields or unwanted cleavage that occurs within the desired protein sequence. The optimal procedure for removal of the affinity tag must be determined on a case-by-case basis, after analysis of the amino acid sequence of the protein of interest (Hochuli, 1990).

1.4.3 Solubility of gene fusion product

A major consideration of relevance for expression of gene fusions is whether the fusion product should be produced in soluble or insoluble (inclusion body) form. Both methods have advantages and disadvantages, depending on the nature and final use of the gene product.

Inclusion bodies appear within the cell as microcrystalline granules or amorphous aggregates (Hammond et al., 1991). Their formation depends on the solubility of the fusion protein, the protein synthesis rate, and the growth conditions (Marston, 1986). Inclusion bodies can protect the protein from proteolysis and they can be separated by differential centrifugation with relatively high (often > 50%) levels of purification obtained. However the product is recovered in a non-active form and must be dissolved and renatured to obtain a biologically active protein. A large number of recombinant proteins produced as fusion proteins in *E. coli* have been obtained as inclusion bodies, e.g., somatostatin (Itakura et al., 1977), insulin A and B chain (Goeddel et al., 1979), β -endorphin (Shine et al., 1980) and human growth hormone (Szoka et al., 1986).

The alternative expression strategy is to produce the fusion protein in a soluble form. This approach has the great advantage that a product with full biological activity can be obtained directly without renaturation. In addition, this allows the introduction of soluble "affinity handles" as fusion partners, thus facilitating the recovery of recombinant protein. However the soluble recombinant protein must be stable in the heterologous host.

1.4.4 Localization of fusion proteins

Localization of the gene fusion product is another important consideration. Fusion proteins may be expressed intracellularly to the periplasm (directed by one of a number of signal peptides) or extracellularly to the medium. Secretion outside the cytoplasm has been shown to enhance disulphide bond formation, e.g., human insulin like growth factor I (IGF-I) (Moks et al., 1987) and human IGF-II (Hammarberg et al., 1989). Secretion of proteins to the periplasm can also protect protein from degradation e.g., the half-life of pro-insulin located in the periplasm was 10-fold longer than when located in the cytoplasm (Talmadge and Gilbert, 1982). Since the periplasm of *E. coli* only contains approximately 4% of the cellular proteins, it is obvious that a large degree of purification can be achieved by secretion of the recombinant gene product followed by selective release of the periplasmic content. However secretion strategies do not work for all proteins. Earlier secretion systems gave low yields and the use of strong promoters has led to cell lysis or accumulation of the gene product intracellularly (Hsiung et al., 1986). Expression levels corresponding to 30% of total cell protein have been achieved as a result of a better understanding of the secretion mechanism and the necessary growth conditions (Tahahara et al., 1986). More recently systems have been developed for the extracellular production of *E. coli* proteins (Moks et al., 1987).

1.4.5 Metal chelating purification handle

The affinity of certain surface amino acid residues, predominately histidine, for first row transition metal ions, provides the basis for metal chelate separation of proteins (see Section 1.3). Histidine is a relatively rare amino acid, accounting for only about 2% of the amino acids in globular proteins (Klapper, 1977) and only about half are exposed on the protein surface. If a high affinity for chelated metals is conferred on a specific protein by the incorporation of one or more histidine residues at its C or N termini, it becomes unique and thereby easily isolated from its contaminants. In contrast to previously discussed purification handles, metal chelating histidine tails are small and the materials for immobilised metal affinity (IMA) separation are readily available, stable and inexpensive.

A specific chelating peptide with a high affinity for immobilised metal ions can be used to purify a recombinant protein by extending the gene sequence of the recombinant protein to code for the entire amino acids in the chelating peptide sequence. The resulting fusion protein can be purified by IMA separations. Polyhistidine extensions of varying lengths have been utilised for immobilised metal affinity chromatography (IMAC) purifications (Lilius et al., 1991; Gentz et al., 1988; LeGrice et al., 1991). Protein expression levels may be altered by the addition of polyhistidine tails (Skerra et al., 1991). In the production of a polyhistidine-extended galactose dehydrogenase (Galdh-(His)₅) from *E. coli* cell extracts, the authors noted that a 2-fold increase in production could be effected by including histidine in Luria broth (Lilius et al., 1991).

Smith and coworkers (1987) were first to suggest that certain small histidine-containing peptides can be attached to proteins as purification handles for metal-affinity separations. They showed that the peptides His-Trp, His-Tyr-NH₂ and His-Gly-His had unusually high affinities for Co²⁺, Ni²⁺ and Cu²⁺ immobilised on iminodiacetic acid (IDA)-derivatised Sephadex G-25 compared to other histidine, lysine and aspartic acid containing peptides and also that peptides with the formula His-X bound Cu²⁺ strongly and most bound Ni²⁺ to a lesser extent.

The high affinity of a small dipeptide could be transferred to the NH₂ terminus of a protein that had no affinity for immobilised metal ions, thus enabling its subsequent purification. A leutenising hormone-releasing hormone (LHRH) which contains the chelating peptide, His-Trp, on the NH₂ terminus had a higher affinity for a Ni²⁺ IMAC column than an unmodified LHRH.

Hochuli et al. (1988) described the affinity purification of two polyhistidine fusion proteins containing two and six adjacent histidines, (His)₂ and (His)₆, at both the C- and N-termini of mouse dihydrofolate reductase on a nitrilotriacetic acid (NTA)- Ni²⁺ column. Increasing binding strength was mirrored by the increasing number of histidine residues. The efficiency of the polyhistidine peptide is dependent on the solvent system used during chromatography. The (His)₆ tag bound more strongly than the (His)₂ tag and elution of the product was difficult under physiological buffering conditions but highly successful in 6 M guanidine hydrochloride (which is appropriate for the purification of proteins which are formed in inclusion bodies). On the other hand the (His)₂ tag did not bind in 6 M guanidine hydrochloride but worked perfectly in physiological buffers. The C-terminal chelating peptide could be removed using limited digestion with carboxypeptidase A.

A number of HIV viral proteins have been purified by IMAC including Rev, Tat, and reverse transcriptase with a (His)₆ chelating peptide sequence attached to the NH₂-terminus (Cochrane et al., 1989; Gentz et al., 1989; LeGrice and Leitch, 1990). The presence of the chelating peptide did not interfere with the biological activity of these proteins; therefore, the fusion proteins were used directly. A single chain antibody Fv fragment containing a five-histidine tail at the C-terminus was purified from *E. coli* homogenates and periplasmic fractions on Zn²⁺-IDA (Skerra et al., 1991). The polyhistidine sequence did not alter the fragment's hapten affinity, nor did it have any negative effect on the export of the recombinant protein to the periplasm.

Ljungquist et al. (1989) synthesized a series of histidine fusion proteins. An affinity linker Ala-His-Gly-His-Arg-Pro was polymerised at gene level to two, four and eight copies and fused to the 3' end of a structural gene encoding a two-domain protein A molecule, ZZ, and to the 5' end of a gene encoding β-galactosidase. Fusion proteins of both types, with zero or two copies of the linker showed little or no binding to immobilised Zn²⁺, while a relatively strong interaction was observed for the fusions based on four or eight copies of the linker. This suggests that the Zn²⁺ interaction of histidines is relatively weak and that multivalent binding is needed to achieve efficient recovery of the recombinant protein. Zn²⁺ has been shown to have a low binding affinity for native proteins (Sulkowski, 1985). This makes the system suitable for applications in which low background binding of non-recombinant proteins is desired.

Angiotensin 1, a decapeptide containing a His-X₂-His sequence was used as an affinity tail for a one-step IMAC purification on Zn²⁺-IDA columns (Beitle and Attai, 1993). This peptide was shown to exhibit strong metal binding properties (Sulkowski, 1982;

Hutchens and Yip, 1990; Yip et al., 1989). In general, proximal metal-binding residues are necessary for a protein to display an affinity toward Zn^{2+} -IDA (Hemden et al., 1989).

The composition and conformation of a protein, in particular the proximity and surface exposure of histidine residues, dictate the affinity a protein may have toward a given metal chelated to a stationary phase (Sulkowski, 1985). Both Suh et al. (1991) and Todd et al. (1991) engineered synthetic metal binding sites consisting of two solvent exposed histidines separated by a single turn of an α -helix (His- X_3 -His variants) on to the surface, and the N-terminus respectively, of a protein. In this orientation the ϵ nitrogens of the imidazole groups from both histidines can co-ordinate a single metal. This motif forms part of the metal co-ordination sites in a number of metalloproteins, including 'zinc-finger' proteins (Berg, 1988; Parraga et al., 1988) and thermolysin (Holmes and Mathews, 1982). The affinities of the His- X_3 -His sites for Cu^{2+} dramatically increased the proteins' retention on a metal affinity column compared to proteins containing independent histidines. Incorporation of the His- X_3 -His site into a potentially flexible N-terminal region yielded a synthetic metal binding protein whose affinity for metal ions was sensitive to environmental conditions which affect helix structure or stability. The affinity of the synthetic metal-binding cytochrome *c* for Cu^{2+} -IDA-PEG (Todd et al., 1991) increased with pH from 5.5 to 8.0. However above pH 8.0 the copper binding affinity of the His- X_3 -His cytochrome *c* decreased rapidly. The helicity of short peptides in solution depends on the temperature, pH, ionic strength and replacements in the amino acid sequence (Finkelstein et al., 1991).

The use of immobilised metal affinity separation with chelating fusion proteins has several advantages. The technique can handle either soluble or insoluble recombinant proteins. Supernatants of lysed cells can be applied directly to an IMA system column with or without using salt concentrations. Denaturants, such as detergents, urea, guanidine hydrochloride, and organic solvents, can be used in the IMAC chromatographic separation when the expression product is insoluble. The bound proteins can be eluted with a pH gradient or with increasing concentrations of a displacing ligand, such as imidazole, in cases in which the protein of interest cannot tolerate a low pH. IMA supports are also resistant to microbial contamination because of the high metal content. One of the major advantages of chelating fusion proteins peptides is their small size. The efficiency of expression is optimal because the purification handle is tiny compared to that of most fusion proteins whose purification handle is large or larger than the protein of interest. Another advantage of small size means that affinity purification can be achieved without interference with the biological activity of the

protein which then eliminates the need to remove the chelating peptide (except for *in vivo* use).

1.5 Magnetic Particle Supports

The potential for using magnetizable solid phases in protein purification has been recognised (Whitesides et al., 1983; Janson, 1982; Groman and Wilchek, 1987), but relatively little has been reported on the application of this approach. The inherent advantage of magnetic particle preparations is their ease of recovery by application of a magnetic field which eliminates the usual centrifugation and column chromatography steps. Thus, when used as affinity supports, their easy retrieval from liquors containing colloids or undissolved solids would be of great practical value (Munro et al., 1977; Horisberger, 1976; Chaplin and Kennedy, 1976).

Much of the pioneering work on magnetic supports for immobilised enzymes (Robinson et al., 1973) and their application as bioaffinity adsorbents (Dunnill and Lilly, 1974) was carried out in our laboratories some 20 years ago. However, the majority of published work on magnetic supports since then concerns their use with immobilised enzymes and in cell sorting applications at analytical scale (Larsson and Mosbach, 1979; Birnbaum and Larsson, 1982; Tsung-Thing and Jian-Jone, 1987). More recently this technology has gained popularity in the field of immunodiagnosics (Selisker et al., 1995) and the range of applications also includes radioimmunoassays, ELISA, cell depletion, chemiluminescent immunoassays and DNA probes.

Conventional column chromatography can be very effective in purifying proteins but the approach is not very versatile. It requires clarified sample, free from cellular and other debris, to avoid the porous packed bed matrix becoming clogged with trapped solids. A relatively large sample volume is required that is further diluted during the elution process and the technique is slow and difficult to automate. Magnetic supports for protein purification offer several advantages when compared to non-magnetic systems. Besides allowing separation of the support from the suspended solids in the process medium, the ease and power of magnetic collection permits the use of very small particles. In addition, this allows the use of non-porous particles while still retaining a reasonable specific surface area for protein adsorption.

A wide variety of enzymes have been immobilised on magnetic supports. These include α -chymotrypsin, β -galactosidase (Robinson et al., 1973), trypsin, invertase (van Leemputten and Horisberger, 1974), adenylate kinase and horseradish peroxidase (Pollak

et al., 1980). Enzymes have been adsorbed to magnetite with glutaraldehyde (van Leenputten and Horrisberger, 1974) bound to macromolecule-coated magnetite (Molday and Machenzie, 1982) and embedded jointly with magnetite to macromolecules (Sada et al., 1981). In these studies the average particle sizes were 300-700 nm, 40-50 nm and 10-100 μm respectively - particle size dictates how quickly the particles can be recovered from aqueous solution. Enzymes immobilised on magnetic matrices can be readily recovered for reuse from a suspended-solids mixture by the application of a magnetic field (Dekker, 1990). β -galactosidase immobilised onto magnetic particles retained up to 25-27 % of its original activity upon immobilisation but it appears that the magnetic matrix did not affect the immobilised enzymes' properties or impede hydrolysis performance.

A magnetic PEG-lipase conjugate was prepared which can be dispersed in organic solvents and in aqueous solution (Inada et al., 1988). The conjugate catalyses ester synthesis in organic solvents and can be readily recovered by magnetic force without loss of enzymic activity.

1.5.1 Performance criteria of magnetic supports

The most commonly used procedure for the synthesis of magnetic particles for use in biological systems has been to coat (or embed) a magnetic particle with(in) a polymer matrix containing functional groups permitting the covalent coupling of proteins. The criteria for evaluating the performance of magnetic particles are similar to those for conventional supports - the number of reactive groups on the surface to which protein can be covalently attached, the surface area, the ability of the particles to permit adsorption with retention of biological activity, defined and reproducible surface characteristics, the absence of non-specific adsorption effects and the uniformity of particle size. Other properties required for magnetic supports are unique. Magnetic susceptibility, which allows simple and speedy removal from a dilute suspension by the application of a magnetic field. Very small particles are often desirable to (a) improve transport characteristics, (b) provide a large surface area for protein adsorption and (c) to ensure the advantages of superparamagnetism (section 1.5.3): efficient aggregation and collection in the presence of a magnetic field, but uniform stable suspension in its absence.

The variety of supports that have been used are classified initially as porous or non-porous. This distinction is made on the basis of the location of the immobilised

molecules: if these are found on the interior of the support particles, the matrix must be porous to reactants.

1.5.2 Non-porous supports

A review by Halling and Dunnill (1980) concluded that non-porous magnetic particles seem more resistant to fouling, diffusional limitations and attrition than porous supports. Chymotrypsin immobilised to non-porous magnetic supports was not fouled significantly by either whole milk or clarified yeast homogenate (Munro et al., 1977). Fouled conventional porous supports are very difficult to clean. In addition the problem of diffusion of reactants through unstirred liquid in the pores can be avoided with non-porous supports. Attrition damage can also be minimised due to the solid core of non-porous supports.

Non-porous supports require smaller particles than porous supports in order to provide a large area of catalytic surface. A variety of magnetic materials have been used in the preparation of non-porous supports, including iron, cobalt nickel and their oxides (Halling and Dunnill, 1979a) as well as alumina or silica admixtures with stainless steel (Siever and Gernand, 1983). The methods used (apart from direct adsorption) to prepare non-porous magnetic supports have included silane coupling agents, particularly 3-aminopropyltriethoxysilane (APS), which have been used to attach an organic functional group to the surface of a magnetic particle, the desired biochemical can then be reacted with this group by standard methods (van Leemputten and Horisberger, 1974; Halling and Dunnill, 1979a). Biological polymers have been adsorbed to the support surface, sometimes by cross-linking with glutaraldehyde (van Leemputten and Horisberger, 1974; Gelf and Boudrant, 1974). Organic polymer beads have been prepared with magnetic particles encapsulated in them, with the biological molecule subsequently coupled by conventional means. Finally polymers have been deposited as thin cross-linked layers over the particle surface, then reacted with the species to be immobilised (Chaplin and Kennedy, 1976; Kronick et al., 1978)).

Some recently developed manufacturing methods include silanisation of crushed magnetite (Sambamurthy and Vijaya, 1987) and synthetic magnetite (Matsunaga and Kamiya, 1987). Magnetite particles have also been covered with a stable non-porous layer of a zeolite-like material or activated carbon (Al-Hassan et al., 1991). Particles made by coprecipitation of dicarboxypolyethylene glycol with $\text{Fe}^{3+}/\text{Fe}^{2+}$ ions at basic pH have been reported successful for lipase immobilisation (Tamaura et al., 1986). However, these particles of around 100 nm in diameter require a very high field for separation and

because of extensive derivatisation reactions, may well be subjected to stability problems (Yokoi et al., 1990). Polyethyleneimine-coated magnetite, crosslinked with glutaraldehyde and derivatized with adipic dihydrazide were used to immobilise enzymes (Pieters and Bardeletti, 1992).

1.5.2.1 Advantages of non-porous supports

1.5.2.1.1 Less fouling

Non-porous supports are less prone to fouling than conventional porous supports in a packed bed configuration, whose support pores and column voids become clogged with foulants which are difficult to remove. Fouling of a non-porous support was first investigated by Munro et al. (1977). They showed only a slight fall in activity of nickel-chymotrypsin stirred over 48 hrs in chilled milk compared to a porous cellulose support which was seriously fouled under the same conditions. Halling and Dunnill (1979b) demonstrated only a small fall in activity of ferrite lactase catalysts which could be attributed to fouling, and the foul that did accumulate was easily removed.

1.5.2.1.2 Better mass transfer

In a study by Halling and Dunnill (1979a) diffusional limitation effects were shown at a minimum for Ni-chymotrypsin non-porous supports. This contrasts with a porous support with immobilised chymotrypsin which shows severe diffusional limitations (Halwachs et al., 1973; Kay and Lilly, 1970). For a truly non-porous support only external diffusion of reactants will occur (Halling and Dunnill, 1980). The behaviour of mass transfer coefficients (per unit surface area) is undoubtedly such that mass transfer rates/unit catalyst weight will continue to increase with decreasing particle size. Both the small size and high density of non-porous magnetic supports will make external mass transfer better than with conventional supports.

1.5.2.1.3 Less attrition

Substantial attrition^{damage} has been demonstrated with conventional porous supports due to their soft and compressible nature in a packed bed (Regan et al., 1974). Attrition is usually less for smaller particles of any type (Ahuja, 1976) and small, non-porous particles with a solid iron core should be mechanically stronger and more resistant to damage. Magnetic particles can be stirred magnetically to minimise physical damage due to mechanical stirring. Magnetic mixing has been demonstrated for immobilised urease in a batch enzyme reactor (Sada et al., 1980) and also for immobilised antibodies in immunoassays (Nye et al., 1976). Munro et al. (1977) observed some attrition of rock magnetite and of a large ferrite particle, which both appeared to consist of much smaller particles in a loose aggregate. Attrition could be more of a problem with the weaker

organic polymer matrix of encapsulated supports, but was not observed with nylon beads as large as 100 μm containing sub-micron magnetite particles.

1.5.2.1.4 Particle size

For an affinity support, the capacity for specific protein adsorption depends on the specific surface area available for attachment. The specific surface area of a non-porous support is $3 / \rho r$, where ρ is the solid density and r is the radius for a spherical particle, or an equivalent radius for a textured surface. For any truly non-porous particle r will be close to the particle dimensions. A magnetic material will generally have $\rho > 3 \text{ g/cm}^3$ so it must have $r < 1 \mu\text{m}$ to give a specific surface area $> 1 \text{ m}^2/\text{g}$, the range found with conventional porous supports (Halling and Dunnill, 1980). However, it is not necessary for magnetic supports to have site densities quite as high as with conventional supports, on a weight basis (Munro et al., 1977). Though their high density results in a reduced specific surface area it also permits a higher loading of catalyst or adsorbent in a reactor on a weight / unit volume basis. As a result, the denser support can give a similar weight of immobilised molecules per unit reactor volume (the crucial ratio) even though the amount is less on the basis of unit support weight.

The most commonly used commercially available non-porous magnetic supports are the precipitated magnetite polymeric beads which are obtainable in the micron size range (section 1.5.7). Al-Hassan et al. (1991) covered magnetite particles with a stable non-porous layer of a zeolite-like material (1.6-2.0 mm diameter) or with activated carbon (1.2-1.6 mm diameter) which were used to immobilise yeast cells.

1.5.3 Ferrofluids

Ferrofluids, first described by Elmore in 1938, are defined as a liquid comprising a colloidal dispersion of finely divided magnetic particles of subdomain size, usually 50-500 \AA , in a carrier liquid and a surfactant material, in which particles remain substantially uniformly dispersed throughout the liquid carrier even in the presence of magnetic fields up to about 0.5 Tesla. They have the thermodynamic properties of solutions (Kaiser and Miskolczy, 1970). Ferrofluids are composed of magnetite crystal and they are typically coated with surfactant to keep them from interacting. Ferrofluids comprising magnetic particles with a mean diameter in solution less than about 0.03 μm can be kept in solution by thermal agitation and therefore do not spontaneously settle. However, the magnetic field and magnetic field gradient required to remove such particles from solution are so great as to be impractical for applications requiring separation of the magnetic particles from surrounding media, especially at process scale. However, there

have been many analytical scale applications using ferrofluids. Extremely fine ferrite particles (10-20 nm), coated with biological ligands, asialoglycopeptides (ASGP), were used to isolate endocytic vesicles (Sato et al., 1986). Submicron encapsulated supports have been prepared by emulsion polymerisation techniques (Molday et al., 1977) but there is a danger of permanent aggregation of the micron sized particles by the encapsulating polymer (Halling and Dunnill, 1979a). Polymers already substituted with biological molecules were 'post-magnetised' with a ferrofluid suspension which had the effect of reducing binding capacity by 50% (Mosbach and Andersson, 1977). Sugimoto et al. (1992) produced colloidal monodisperse hematite particles of different shapes; pseudocubic (1.65 μm in mean edge length), platelet (1.9 μm in diameter) and spindle (0.43 μm length, 0.13 μm width) formed from highly condensed ferric hydroxide gel through a kind of phase transformation referred to as the gel-sol method.

1.5.3.1 Superparamagnetism

Ferromagnetic materials (iron oxides with crystal size greater than about 500 Å) in general become permanently magnetised in response to magnetic fields. Materials termed 'superparamagnetic' experience a force in a magnetic field gradient, but do not become permanently magnetized. Crystals of magnetic iron oxides may be either ferromagnetic or superparamagnetic, depending on the size of the crystals. Superparamagnetic oxides of iron generally result when the crystal is less than about 300 Å (0.03 μm) in diameter; larger crystals generally have a ferromagnetic character. A 0.03 μm diameter particle is the minimum volume element capable of retaining a permanent magnetic dipole (Bean and Livingston, 1959). Crystals this size or less become magnetic dipoles when placed in a magnetic field (where efficient and speedy aggregation and collection takes place) but lose their magnetism when the field is turned off. Hence, particles composed of individual crystals or groups of crystals can be readily and stably resuspended after the application of a magnetic field.

Following initial exposure to a magnetic field, ferromagnetic particles tend to aggregate between the permanently magnetised particles (Robinson et al., 1973; Hersh and Yaverbaum, 1975). If a significant amount of aggregation occurs in a reactor then much of the advantage of a non-porous support will be lost; it will tend to behave as a porous support of larger particle size suffering diffusional and fouling problems (Halling and Dunnill, 1980). Magnetic particle manufacture carried out by Sato et al. (1986) and Dekker (1990) results in particles of irregular shape and size due to the aggregation of the synthetic magnetic crystals of about 500 nm in diameter during the coating step, which occurred despite ultrasonic treatment and high speed stirring. Particle size ranged

from 5-20 μm . Sada et al. (1981) reported residual magnetism in polyacrylamide / magnetic beads which caused bead agglomeration.

Superparamagnetic particles retain no permanent magnetic dipole and accordingly are not attracted to each other following removal of the magnetic field (Whitesides et al., 1983). Therefore problems associated with particle clumping, i.e. entrapment and production of high background recoveries of unwanted materials, are eliminated. In addition, because the superparamagnetic particles have no magnetic memory and so do not aggregate, they may be used more than once. Superparamagnetic particles (3 nm) used for the isolation of cells were precipitated from a mixture of ferrous and ferric ions in the presence of dextran (Kronick and Gilpin, 1986).

1.5.4 Porous supports

In the main, porous magnetic supports are conventional supports that have been made magnetically responsive by the incorporation of suitable sub-particles (Robinson et al., 1973). The same characteristics are desirable as for non-porous supports. A small size is not essential because of the pore surface area, but may be required if a magnetic support is used to improve mass transfer. Magnetically susceptible porous supports described in the literature include magnetite distributed in cross-linked polysaccharide beads (Burns et al., 1985; Lochmuller and Wigman, 1987), and cross-linked mixtures of protein and magnetic particles (Gelf and Boudrant, 1974).

Highly rigid dried spheres of low porosity made from alginate solution containing magnetite particles have been developed as supports for enzyme immobilisation and chromatographic applications (Burns et al., 1985). The beads have a high density of 2.2 g/mL and a narrow size distribution. The low porosity is compensated for by a high degree of micro-roughness which provides a large exposed surface area for enzyme and ligand binding. Some buffers cause dissolution of the beads but this was overcome by cross-linking them with Tyzor-TE. However, the flexibility of calcium alginate / magnetite beads is limited because Ca^{2+} ions must always be present in the process stream to prevent the support from decomposing. The presence of such added calcium as well as fixed negative charges in the polymer chain can interfere with the process (Goetz et al., 1991).

Lochmuller and Wigman (1987) developed a uniform spherical magnetic carrageenan-gel particle (suitable for enzyme immobilisation). The particles are made using an aerosol jet technique with the incorporation of a magnetite pigment in the sol-phase before gelation.

The recovery and specific activity values of enzyme obtained using magnetisable agarose beads and magnetic field separation were significantly greater than those for enzyme purified by centrifugation and conventional dye ligand chromatography (Ennis and Wisdom, 1991). The direct application of the beads to the crude homogenate of porcine muscle allowed LDH to be extracted at maximum (100%) yield and at a higher specific activity than that obtained by centrifugation on conventional dye ligand chromatography (50%).

Hirschbein and Whitesides (1982) rendered derivatised agarose beads magnetisable by treating them with a colloidal suspension of magnetite and found their performance compared favourably with a more conventional technique using polyacrylamide immobilised on a glass fibre cloth as solid phase. The ion-exchange kinetics of magnetite-coated porous ion-exchange particles were slightly retarded as a result of the coating (Nixon et al., 1992).

1.5.5 Pellicular supports

The pellicular bead was first described by Horvath and Lipsky in 1967. These are hybrid supports of porous and non-porous supports. The concept involves an impermeable core coated with a thin porous active layer containing the enzyme or affinity ligand. It has improved transport characteristics over totally porous supports and it is also less susceptible to diffusion limitations (Goetz et al., 1991).

A magnetic pellicular silica bead was prepared by electrostatically depositing alternating layers of colloidal silica and cationic polymer onto macroscopic nickel core particles. The polymer was then burned out and the silica partially sintered to yield a porous shell of $\geq 100 \mu\text{m}$ diameter and $5\text{-}80 \text{ m}^2 / \text{g}$ of surface area (Goetz et al., 1991). The support was designed for use in magnetically stabilised fluidised bed applications.

1.5.6 Magnetic particle behaviour

The magnetic separation of particles can be considered to be based on forces corresponding to those of gravity or moderate centrifugation (Whitesides et al., 1983). The size and density of the magnetic particle will determine how long it will remain suspended in a magnetic field. A commercial particle, BioMag[®] (PerSeptive Biosystems, Inc.) has a size distribution $0.5\text{-}1.5 \mu\text{m}$ and less than 10% settles in 30 minutes under most circumstances, compared to a magnetic agarose mixture which is $60\text{-}140 \mu\text{m}$ in diameter (~ 100 times bigger) and greater than 90% settles under the same conditions

(Menz et al., 1986). Minimal settling under gravity is desirable to avoid the need for constant stirring or magnetic mixing.

The magnetic force on a highly magnetic particle in a slurry is a strong function of the particle shape and the concentration density of the magnetic particles in the suspension. An expression was derived (Eyssa and Boom, 1976) for the coagulation forces between magnetised particles as a function of magnetic moment, size and concentration.

A method of rheomagnetic measurement was developed to study the orientation of magnetic particles in suspension (Karis and Jhon, 1991). By induction measurement the rotary diffusion coefficient is obtained which contains information about a floc size and shape (Jhon and Karis, 1989). Hence the state of flocculation and agglomeration may be characterised.

1.5.7 Commercially available magnetic particles

The number of applications of biomagnetic separations have grown rapidly in recent years to include cell separation, immunoassays, ELISA, latex agglutination, blood cell stimulation, chemiluminescent assays, DNA probes/PCR, magnetic resonance imaging contrast agents, microcarriers in cell culture, cell tags, blood flow markers and more. Although magnetics are hailed as appealing due to their scalability, efficiency, simplicity, mild conditions, ease of automation and low cost, their application to date at preparative and process scale is rare. This is most probably due to the high cost, small scale analytical applications favoured by commercial interest.

The most successful firms producing beads for magnetic separations tend to specialise in some aspect of bead technology. Bang's (Bangs Laboratories, Inc., Carmel, IN, U.S.A.) product line is based on 1 nm to 20 nm ferrite crystals dispersed in polymerised styrene/divinylbenzene to diameters in the 0.7 micron to 1.3 micron range. Dynal, Inc., (Oslo, Norway) produce uniformly smooth beads of polystyrene-coated ferrite. They are available in different sizes depending on the application i.e. protein, cellular and organelle isolation. CPC, Inc. (Lincoln Park, NJ, U.S.A.) offer magnetic porous glass superparamagnetic particles which comprise iron oxide-impregnated borosilicate glass containing 500 nm pores (surface area 60 m²/g solid phase). Immunicon Corp. (Huntington Valley, PA, U.S.A.) produces biomagnetic ferrofluids for immunodiagnostics, cellular diagnostics and therapeutics and molecular diagnostics. Hydrophilic polymer coated magnetite ferrofluids are produced in various sizes, again, depending on the application. A superparamagnetic iron-oxide, surface-functionalised

with primary amino groups (BioMag[®], PerSeptive Biosystems, Framingham, MA, U.S.A.) of particle size 0.5 to 1.5 μm was chosen for use in this research project to develop a magnetic immobilised metal chelating affinity support (section 3.1). Other commercially available magnetic particles include: iron oxide coated with poly-1,3-diaminobenzene which is activated by diazotization (Enzacryl FEO-M, Aldrich Chemical Co., Milwaukee, WI), polyacrylamide-agarose coated ferric oxide activated by cyanogen bromide or glutaraldehyde (Magnogel, LKB Instruments, Inc, Gaithersburg, MD, U.S.A.) and ferric oxide particles coated with polyacrylamide gel containing N-hydroxy-succinimide active esters.

1.6 Magnetic Separation Technology

A magnetic separation system has two primary components, a magnetisable particle or bead which acts as a solid phase for capture of the material of interest and a magnet which provides the force to move the particle. Magnetism has been used as a practical tool for achieving physical separation of materials since the days of Thomas Edison (Dyer et al., 1929). Magnetic microparticulate supports can be easily and gently separated by the simple application of a magnetic field which facilitates their manufacture and their handling in the reaction phase. Potentially, they can be selectively recovered from a crude cell homogenate containing both suspended particles and fouling materials thus eliminating the several stages of pre-treatment normally necessary. The power and efficiency of magnetic separation can be seen in comparison with gravitational and centrifugal methods (Ennis and Wisdom, 1991) and its utilisation can reduce the capital and operational costs of the whole process.

1.6.1 Magnetic properties of materials

The magnetic method separates materials on the basis of differences in their magnetic properties. Substances placed in a magnetic field acquire a magnetic moment. The ratio of the magnetic moment per unit volume to the magnetic field strength, H , is known as the susceptibility, χ , and substances are classed as diamagnetic, paramagnetic or ferromagnetic according to the nature of their susceptibility. Superparamagnetism is dealt with in section 1.5.3.1.

1.6.1.1 Diamagnetism

In diamagnetic substances the magnetism is in the opposite direction to the applied field so that χ is negative. Diamagnetic substances such as water, sugars, lipids and most proteins are weakly repelled from regions of high magnetic fields and are commonly

regarded as magnetically unresponsive. Therefore diamagnetism is not commonly used as a positive basis for separation particularly as paramagnetic and ferromagnetic effects overwhelm any diamagnetic effects that would be observed.

1.6.1.2 Paramagnetism

Paramagnetism results from the independent behavior of unpaired electron spins in an external magnetic field. The induced field reinforces the applied field. The force on the particle is proportional both to the strength of the magnetic field and to that of the field gradient. Typical paramagnetic materials include the organic free radicals, O₂ and transition metal complexes (including many proteins containing iron, copper, vanadium, nickel and other metals).

1.6.1.3 Ferromagnetism

Ferromagnetic substances are distinguished by very large (positive) values of χ , which are not independent of the field strength. In addition, they may possess a magnetic moment, even in the absence of an applied field, as in a permanent magnet. Ferromagnetism results from the cooperative interaction and alignment of electronic spins. It is observed only in solids (metals and metal oxides) in which the structure of the solid permits strong interaction between electrons on different atoms. Ferromagnetic materials have three distinguishing properties: First, they have very high magnetic susceptibilities compared to paramagnetic materials. Second, their response to large magnetic fields is finite; i.e., in sufficiently strong applied magnetic fields their induced magnetism reaches a maximum. Third, they show magnetic hysteresis i.e., after the removal of an applied magnetic field, their spins remain aligned and they exhibit residual magnetism. Ferromagnetic substances may be broadly divided into two classes: (1) magnetically soft materials which have high permeability and are easily magnetized and demagnetized (e.g., used in electromagnetic machinery and transformers) and (2) magnetically hard materials which have a relatively low permeability and are difficult to magnetize or demagnetize (e.g., used in permanent magnets).

1.6.2 Principles of magnetic separation

A magnetically isotropic material in a perfectly uniform magnetic field experiences no net force and a magnetic field gradient is necessary to effect its movement. The relationship between properties of the particle, the magnetic field, and the force on the particle is described by the equation (Kolm et al., 1975; Hirschbein et al., 1982):

$$F_x = V\chi_v H \delta H / \delta x$$

Here F_x is the force on the particle in the direction x , V is the volume of the particle (assumed to be spherical), χ_v is its magnetic susceptibility per unit volume, H is the strength of the magnetic field and $(\delta H/\delta x)$ is the magnetic field gradient. The equation indicates qualitatively that the force on a particle is proportional to χ_v , H , V and $\delta H/\delta x$. For a permanent magnet the gradient is most intense at the magnetic poles.

The above equation implies firstly that the magnetic field gradient can be maximised and manipulated to achieve the most rapid movement of a particle in a particular magnetic field, H . Secondly, the force a particle experiences is related to its volume. Thus, large particles move most rapidly in a given magnetic environment while small particles move most inefficiently. However, small particles have the largest surface area and slowest settling rates, two advantageous properties for magnetic affinity supports. Particles between 0.6 μm and 2.0 μm appear well suited to affinity separations because they are large enough to be manipulated by the magnetic fields produced by permanent, hand held magnets, while small enough to have a high capacity for protein (Menz et al., 1986).

However, the above equation makes no allowance for particle shape or for interactions between magnetic particles. It has been shown that the magnetic force on a highly magnetic particle in a slurry is a strong function of the particle shape and the concentration density of the magnetic particles in the suspension (Hirschbein et al., 1982).

1.6.3 High gradient magnetic separation

High gradient magnetic separation (HGMS) (Kolm et al., 1975), a relatively new concept in industrial separation technology, uses the magnetic traction force to capture magnetic particles upon a magnetised fiber filtration matrix. HGMS technology was initially developed around the abilities of high field strength to polarize weakly magnetic materials (Jones, 1960) and of non-uniform or gradient magnetic fields to develop magnetic forces in dipolar materials (Frantz, 1937).

The application of HGMS is indicated for highly dilute, high capacity process streams that are to be filtered with a high removal efficiency. HGMS uses magnetic fields as high as 8 T (Tesla) (compared to 0.5 T for rotating drum magnetic separators) (Munro et al., 1981). Current applications of HGMS in the process industry include clay beneficiation (Lawver and Hopstock, 1974) and the filtration of nuclear reactant coolant (Liu, 1979). Other demonstrated uses for HGMS are in the desulphurisation of coal (Petrakis et al., 1981), the purification of drinking water (Kolm et al., 1975), the treatment of municipal

sewage (deLatour, 1973; Allen et al., 1976), and the removal of actinoids from contaminated waste streams (Gerber and Biss, 1982). In the realm of biotechnology, HGMS has been used to remove viruses (Bitton and Mitchell, 1974), bacteria (Harland et al., 1976), yeast (Dauer and Dunlop, 1991), algae (deLatour, 1974) and red tide plankton from waste streams (Korinobu and Uchiyama, 1982).

Magnetic separation technology has also been applied to cell sorting. Magnetic separations are ideal for preparative cell sorting and can be used in conjunction with fluorescent-activated cell sorting (FACS) which excels in analytical cell sorting. The majority of examples so far have been with monoclonal antibodies directed to cell surface antigens (Margel et al., 1979). Other applications have been in the separation of lymphocytes (Molday et al., 1977) and macrophages. Future work will probably include sorting subcellular organelles, bacteria and viruses (Vaccaro, 1990).

The simplest design for high gradient separation is to place magnetic stainless steel wool into a tube which is then placed between the poles of a magnet. The separating tube is loosely packed with fine strands (about 50 μm diameter) of filamentary magnetic material such as stainless steel wool. The gradient field produced around the fibre is a result of the superposition of the external field and of the field induced on the fibre. The direction of the field lines of the induced field are opposite to those of the external field. Hence, a gradient field is established around the fibres forcing magnetic materials to the sides of the fibres facing the magnetic poles. These gradients attract and hold the magnetic particles while the external field is on. A high voidage matrix also provides a large volume for trapping magnetic particles. The liquid containing the magnetic particles is pumped through the magnetised ferromagnetic matrix. The particles are attracted to the matrix and so are removed from the liquid. The collected particles can be released by removing the external field. Any residual magnetism in the steel wool retains particles only weakly and can be overcome by vibrating the matrix.

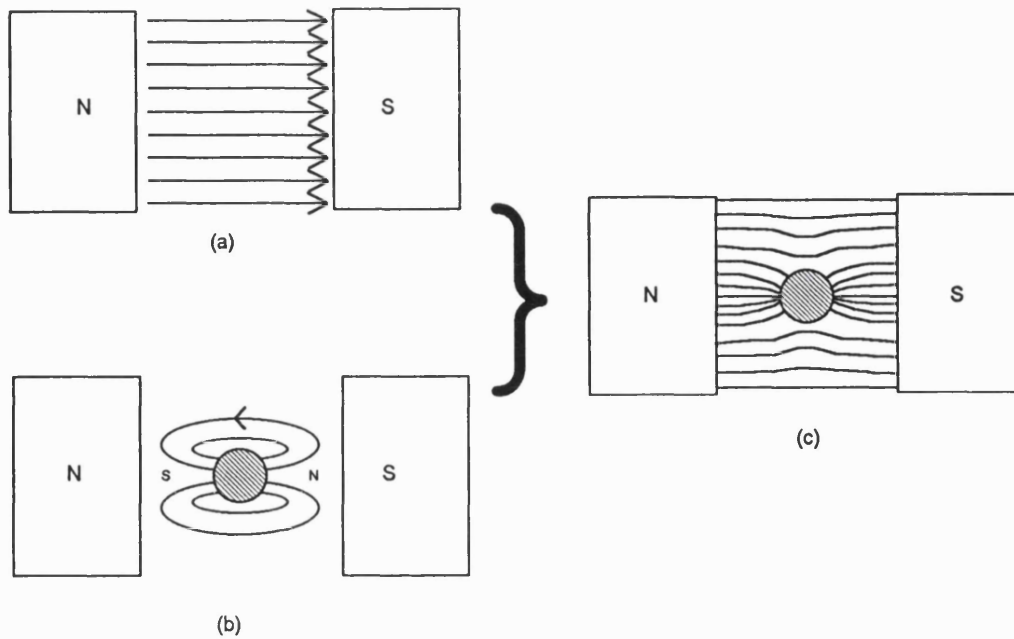


Figure 1.1 Principle of establishing a high gradient magnetic field.

(a) Steel strand in the external magnetic field.

(b) Magnetic field generated by steel strand.

(c) Sum of (a) and (b).

1.6.3.1 Factors affecting separation

Advantages of HGMS include automatic operation, small space requirements, simple maintenance, low energy consumption and easy uncostly scalability (Obertruffer and Wechsler, 1980). The efficiency of separation is related to various operating parameters such as matrix packing density, matrix strand size, flow velocity and field intensity (Setchell, 1985). The study of high gradient magnetic separation has developed along two distinct, but interrelated lines. Firstly, the study of bulk filters and their applications, and secondly, the investigation theoretically, and experimentally, of the capture and buildup of particles on single magnetised wires. The trajectory model of Watson (1973) and the empirical impact-capture model of Oder (1976) both predict that the probability of particle capture by a given segment of wire is dependent on the ratio of the magnitudes of the magnetic and the viscous forces on the particle, evaluated at the surface of the wire. However, recent work by Svoboda (1994) has shown that the presence of an external magnetic force enhances the probability of collision only in a single collector HGMS system, whereas in a real matrix, the efficiency of collision is determined mainly by the mechanical 'non-magnetic' mechanisms of collision. According to Svoboda (1994), the parameters, as understood in the single-particle, single-collector

approach lead to misinterpretation when applied to the multiple-collector matrix. They showed that practically every particle of a reasonable size, suspended in a fluid passing through the matrix, has a probability approaching unity of colliding with the matrix, in the absence of magnetic traction force, provided certain conditions concerning flow velocity, matrix length and porosity, and collector size are met (Svoboda and Ross, 1989).

1.6.4 High gradient magnetic filters

It is impossible to generate high magnetic field gradients over large volumes (> several cm), thus it is difficult to collect magnetic materials from large volumes of solution using only externally applied fields (Whitesides et al., 1983). The use of ferritic stainless steel wools in combination with intense magnetic fields is the practical key to the success of HGMS. Since the ferritic stainless steel wools are strongly magnetic and have a large surface to volume ratio, high separation efficiency can be achieved even with very open and porous separator beds. This means that very high process throughputs can be utilised to improve process economics without fears of high pressure drop or filter plugging when processing well dispersed micron size materials (Oder, 1976).

A typical HGMS column is filled to 2-4% of its volume with ferromagnetic stainless steel wool of average diameter 50 μm . Polyvinylpyrrolidone was used to coat fibres to prevent non-specific adsorption (Sato et al., 1986) and Miltenyi coated the surface with plastic by immersion into laque to avoid corrosion (Miltenyi, 1990). The column can be characterised by the product of length and packing density, termed trapping coefficient, (f), and the surface of the matrix. The surface of the matrix gives an estimate for the binding capacity of a column. A secondary magnet is induced in the steel wire when it is placed in a uniform magnetic field. The induced magnet sets up its own magnetic circuit of field lines vectored from North to South pole which are opposite in direction to those of the external field. This generates large field line differences around the wire resulting in huge magnetic gradients.

Stainless steel wool is the most commonly used magnetic matrix material. Riley and Watson (1976) suggested using a paramagnetic matrix to collect ferromagnetic particles in order to overcome problems of matrix blocking as a result of residual magnetism at zero field. Many of the requirements for good matrix performance (high void volume, short mean free path) are the same for good dimester performance (Lannicelli, 1976).

Leitermann et al. (1984) showed that a HGMS filter can be used effectively to remove micron-sized, strongly magnetic particles from a liquid flowing through the filter at high velocities. They also found that the longitudinal configuration of parallel nickel wires (125 μm diameter) shows the largest buildup of particles, closely followed by the transverse arrangements and the parallel wires in the axial configuration, while the longitudinal grid has the smallest buildup at a given time. Also noted was that an increase of the magnetic field had hardly any effect for all concentrations and flow velocities used in the experiment. A two dimensional theoretical model for the capture of ultra-fine particles on a HGMS collector was developed which suggested that the particles retained at the downstream side of the wire were supplied by forces of diffusion and not by fluid flow (Davies and Gerber, 1990).

1.6.5 Magnetic collection and separation devices

1.6.5.1 *Permanent magnets*

Strong, high gradient magnetic fields are produced by rare earth permanent magnets. Yoked rare earth bar magnets have been shown to generate an external field in the intervening gap of about 0.8 T (Liberti, 1991). Materials used are given as follows with increasing flux densities (up to 1.2 T): Barium ferrite < platinum-cobalt < samarium-cobalt < alnico 5. While the alloys are brittle, they can be shaped for use in separators which require no electricity, have no moving parts and can be located anywhere in the laboratory (Vaccaro, 1990).

For most laboratory scale and some production scale biotechnological applications, the lower magnetic fields produced by permanent magnets are sufficient (Menz et al., 1986). Miltenyi (1990) has shown that cells labelled immunologically with magnetic particles (diameter $\geq 0.5 \mu\text{m}$) can be easily separated from unlabelled cells by a simple permanent magnet.

The fundamental drawback of permanent magnets is that they are not suitable for large scale applications (Groman et al., 1985).

1.6.5.2 *Electromagnets*

When fields of greater magnitude or adjustable fields are required an electromagnet is used. HGMS electromagnetic devices are capable of generating magnetic fields as high as 12 T (Tesla). Of these, iron bound solenoids are thought to provide the most economical magnetic fields.

Iron and other magnetic materials saturate at 1-2 T. But flux densities above 3 T can be achieved using flat conductors which distribute a non-uniform current. It has been shown that higher efficiency is obtained if the current density is not uniform but falls off inversely with the radius (Bitter, 1936). The solenoid is constructed of a number of such discs mounted one above the other with a hole in the middle through which cooling water can be forced. This low resistance design ($\sim 0.01 \Omega$) can achieve flux densities of 10 T (Bitter, 1940).

An improvement on the electromagnet design which makes better use of the iron, positions the magnetising coil at the centre surrounded by soft iron (Bitter, 1936). With iron bound solenoid devices, the field strength inside the coil increases indefinitely with increasing current and does not reach a saturation value as it does with conventional electromagnets.

The ultimate performance of an electromagnet is limited by the rate at which heat generated in the conductors can be removed and by the mechanical strength of the material, which must withstand enormous magnetic forces. Electromagnets are more suited economically to large scale applications, their major disadvantage being their high power requirement. However, electromagnetic HGMS is widely believed to be the most economical design for magnetising the working volume up to field strengths of 2 T (Oder, 1976).

1.6.5.3 Superconducting magnets

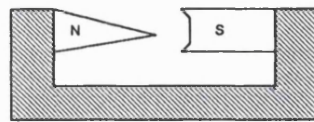
Below its transition temperature a superconductive material offers zero resistance to the flow of electric current, provided that any magnetic field present does not exceed the critical field above which normal resistivity is restored (Bleany and Bleany, 1989). Hence, superconducting coils below their transition temperature can produce very high magnetic fields with little or no power requirement. The critical field is 0.1 T or less for most Type I superconductors, but in a number of Type II superconductors it lies between 5 T and 20 T. The discovery of materials such as niobium and the alloys niobium-titanium (NbTi), niobium-tin (Nb₃Sn), niobium-zirconium (NbZr), and vanadium-gallium (V₃Ga) has made it possible to construct superconductive magnets, which can be energized by small laboratory power supplies (Bleaney and Bleaney, 1989).

However, superconducting magnets in either batch or cyclic separators encounter serious mechanical complications if canisters must be moved in and out of magnetic fields. In addition, savings in low electrical consumption compared to electromagnets are often offset by compressor power for cryostats (Lannicelli et al., 1976).

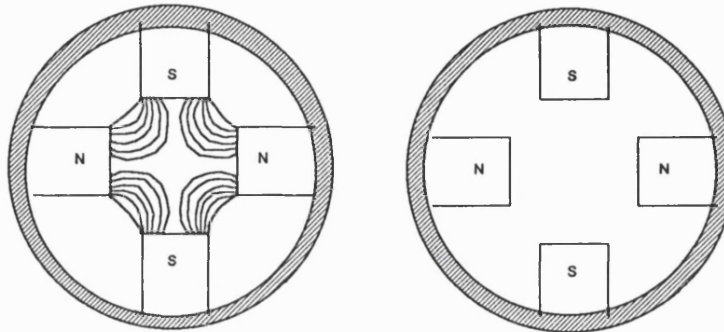
1.6.5.4 Open field gradients

HGMS devices have been developed which generate field gradients, termed open field gradients, which do not make use of metal collectors and internally generated gradients. Open field gradients exist at the corners of magnetic pole pieces or can be achieved between poles of a magnet by shaping pole pieces appropriately. For example, when a flat pole piece is opposed by a triangular shaped pole, the field lines converge to the apex of the latter and thus a gradient of flux lines is created. Such fields have been used to collect labelled cells to the sides of a vessel (Kronick, 1980; Molday and MacKenzie, 1982). Their use is limited as only relatively small field gradients can be generated.

The concept of open field gradients has been extended to the use of quadrupole (2N fields) for separating ferrofluids. Quadrupoles or multipole arrangements, are unlimited as to the gradient which can be established. In a typical quadrupole arrangement the North and South poles oppose each other. The field is zero at the midpoint between two like poles. By appropriate pole piece design and placement, radial gradient fields can be established. The gradient is determined by one half the gap diameter and the field strength at the pole faces. Since the field and field gradient is zero at the centre of such arrangements, magnetic material at the centre will feel no force. By placing a cylindrical vessel in the quadrupole, magnetic particles collect on the inner radius of the cylinder. Liberti (1991) has reported that experiments done with gradients generated by quadrupole fields produced results equivalent in discrimination to those done with the wire loops or internally generated gradient devices.



(a) Pole Piece Design, Corners of Magnets



(b) Typical pole configuration in quadrupole magnet

(c) Radial gradient flux density created by quadrupole magnetic arrangement

Figure 1.2 External high gradient magnetic field devices.

1.6.5.5 Magnetically stabilised fluidised beds

The magnetically stabilised fluidised bed (MSFB) is a fluidised bed loaded with magnetically susceptible particles which are stabilised against flow perturbations by the application of a uniform external magnetic field. The MSFB offers an attractive combination of the best feature of both packed and fluidised beds for biochemical processing. Coupled with its ability to process large volumes of fermentation broth continuously, in some cases without prior filtration, the MSFB chromatograph offers a continuous, low-pressure alternative to conventional packed bed processes (Goetz et al., 1991). Axial dispersion in this system under appropriate operating procedures is similar to that in packed beds (Goetz and Graves, 1991).

MSFB technology has been applied to affinity chromatography separations (Burns and Graves, 1985; Burns and Graves, 1988), plant cell culture (Bramble, 1989), and immobilised enzyme reactions (Gelf and Boudrant, 1974) and has been shown capable of particle filtration from both liquid (Terranova and Burns, 1989; Riley, 1987) and gas streams (Albert and Tien, 1985).

1.7 Aims

The introduction of selective protein adsorption at an early stage in the downstream process has the potential to reduce the overall number of processing steps and increase efficiency and yield. Traditional affinity supports and ligands require highly clarified liquors and are therefore generally employed during the later stages of purification. The conventional operating format for preparative separations is a packed column of adsorbent. Commercial porous adsorbents are prone to severe fouling which is difficult to remove (Eveleigh, 1978; Halling and Dunnill, 1979a, 1979b, 1980; Munro et al., 1977). Fouling leads not only to reduced adsorbent efficiency but also to an increase in pressure drop across the bed and compression and deformation of the non-rigid adsorbents. Downstream processes must usually contain one or two steps for the removal of particulates, such as centrifugation and/or filtration. These techniques, not without their own operational drawbacks, can, by their introduction, result in a considerable reduction in the product yield. The time taken to remove particulates by these methods can also result in further losses through denaturation. The use of a technology whereby clarification, concentration and purification could be replaced by a single processing step would be both technically and economically valuable and the development of such is the main aim of this project.

There is evidence that non-porous supports are less prone to fouling than conventional porous supports and are easier to clean (Munro et al., 1977; Halling and Dunnill, 1979a) and are therefore potentially more useful in protein purification from fouling feedstreams. However, in order to obtain a comparable surface area to typical macro-porous particles of 100 μm size, the dimensions for a non-porous support have to be of the order of 0.1-1.5 μm . Probably the only feasible method for recovery of such small particles in the presence of biological debris of similar size is magnetic separation. This work aims to design and develop a stable non-porous, sub-micron magnetic affinity support that has good mass transfer characteristics, is resistant to attrition damage, has a low settling velocity, can be rapidly removed from suspension by the application of a magnetic field and has no magnetic memory.

Biospecific affinity ligands (e.g., antibodies, lectins) are equally unsuitable for use in feed streams containing fouling materials as conventional porous matrices. They are expensive, yield low capacities on immobilisation and are labile to sanitizing agents used to regenerate the adsorbent. As ligands for affinity separations, pseudoaffinity chelated metal ions offer many advantages over classical biological affinity types. They are small molecules, inexpensive, chemically and physically stable, and can be easily coupled to

matrices at high density resulting in high capacity adsorbents (Arnold, 1991; Jones, 1991). This work aims to functionalise non-porous, sub-micron magnetic supports with immobilised metal affinity chelating ligands to produce a high capacity magnetic affinity adsorbent.

Immobilised metal affinity separation occurs when certain amino acid side-chains of protein, primarily histidine, are able to co-ordinately bind first series transition metal and zinc ions which are immobilised on an adsorbent via attached chelating agents (Porath et al., 1975). Characterisation and optimisation of metal chelating magnetic supports will be carried out by testing them with a range of native proteins bearing variable numbers of surface accessible histidine residues. Adsorbent stability, ligand density, protein capacity, strength of interaction, adsorption and elution conditions, and ease of process scale-up will be investigated.

Dramatic enhancements in binding interactions between target proteins and immobilised metal ions have been demonstrated recently through the introduction by recombinant techniques of high affinity metal binding motifs (Arnold, 1991; Suh et al, 1991; Todd et al., 1991) and particularly histidine rich tails (Arnold, 1991; Hochuli et al., 1988; Ljungquist et al., 1988; Smith et al., 1988; Vosters et al., 1992) into a protein of interest. In recent collaborative work with the Department of Biochemistry and Molecular Biology, UCL, we described the engineering, expression and purification of a recombinant metal-binding T4 phage lysozyme fusion protein useful for repeated lysis of *E. coli* and possibly other Gram negative cells (Sloane et al., submitted). This work sets out to characterise the separation and purification of recombinant polyhistidine-tailed metal binding proteins by magnetic chelator supports in the presence of crude cell extract and cell homogenate.

Cell culturing conditions for *E. coli* producing recombinant T4 lysozyme will be optimised in order to improve productivity and recovery of T4 lysozyme. Currently 50% of T4 lysozyme is found to leak to the medium at 3 hours following induction (Sloane, personal communication). Following optimisation, fermentation will be scaled up to pilot scale. The performance of recombinant histidine-tailed T4 lysozyme as a lytic enzyme in the selective disruption of *E. coli* cells by periplasmic lysis will be investigated with particular emphasis on the enzyme's ease of recovery by immobilised metal affinity separation and its subsequent re-use.

CHAPTER 2 MATERIALS AND METHODS

2.1 Materials

2.1.1 Microorganisms

E. coli K12 JM107 pQR752 (ampicillin resistant) encoding for a cysteine-free bacteriophage T4 lysozyme, genetically modified to carry a poly-histidine tail sequence, His-Gln-(His)₃, at its C-terminus and *E. coli* K12 JM83 containing the plasmid pQR187 (kanamycin resistant) which encodes for *Streptomyces thermoviolaceus* CUB74 α -amylase, were kindly provided by R. P. Sloane and C. French respectively, Department of Biochemistry and Molecular Biology, University College London. *E. coli* HB101 pEZZT his4 (kanamycin resistant) encoding for a two-domain protein A molecule, ZZ, fused to an affinity peptide containing 4 copies of a His-X-His sequence, was received as a gift from M. Uhlén, Royal Institute of Technology, Stockholm, Sweden. *E. coli* XL1 blue cells expressing a recombinant penta-histidine tailed single chain antibody fragment incorporating a hinge region (ScFv hinge(his)₅) was kindly provided by S. Martin of this department (courtesy of Celltech, Slough, U.K.). Lyophilised *Micrococcus lysodeikticus* cells were purchased from Sigma Chemical Co. Ltd. (Poole, Dorset, U.K.).

2.1.2 Culture media

Nutrient agar and nutrient broth II (NB) were obtained from Oxoid (Unipath, Basingstoke, U.K.). Tryptic soya agar and broth were both purchased from Difco (West Molesey, Surrey, U.K.). Terrific broth (TB) (Tartoff and Hobbs, 1987) used for the growth of *E. coli* JM83 was composed of KH₂PO₄, 2.3 g/L; K₂HPO₄, 3.78 g/L; bactotryptone, 12 g/L; yeast extract, 24 g/L and glycerol 4 mL/L. High biomass media (HBM) for the growth of *E. coli* JM107 strain had the following composition: glycerol, 20 g/L; (NH₄)₂SO₄, 7 g/L; NaH₂PO₄·2H₂O, 6.24 g/L; yeast extract, 40 g/L; antifoam solution, 1 mL/L. The pH was adjusted to 7 with 1 M NaOH. Yeast extract came from Difco (West Molesey, Surrey, U.K.) and bactotryptone from Oxoid (Unipath, Basingstoke, U.K.). Ampicillin (di-sodium salt), kanamycin and isopropyl β -D-thiogalacto-pyranoside (IPTG) were purchased from Sigma Chemicals (Poole, Dorset, U.K.).

2.1.3 Chemicals

The materials, 3-aminopropyltriethoxysilane, glutaraldehyde (Grade I), 1,4-butanediol diglycidyl ether, iminodiacetic acid (disodium salt), ethanolamine, potato starch S-2630, iodine and potassium iodide were obtained from Sigma Chemical Co. Ltd. (Poole, Dorset, U.K.). Imidazole was purchased from Aldrich Chemicals (Gillingham, Dorset, U.K.) and Coomassie Protein Plus protein assay reagent from Pierce and Warriner Ltd. (Cheshire, U.K.). Sodium borohydride, copper (II) chloride, zinc chloride and nickel chloride and all other chemicals, of AnalaR grade, were supplied by BDH Chemicals (Poole, Dorset, U.K.).

Chelating Sepharose 6B, IgG Sepharose 6 Fast Flow, prepacked 5 mL HiTrap Chelating Sepharose HP columns and PD-10 columns prepacked with Sephadex G-25 M were purchased from Pharmacia Biotech (St. Albans, Herts., U.K.).

2.1.4 Proteins

α -chymotrypsinogen A from bovine pancreas (E.C.3.4.21.1, type II, C4879), tuna heart cytochrome *c* (E.C.1.9.3.1, type XI, C2011), horse heart cytochrome *c* (E.C.1.9.3.1, type VI, C7752), *Candida krusei* cytochrome *c* (E.C.1.9.3.1, type VII, C4381), bovine haemoglobin (H2500) and hen egg white lysozyme (E.C.3.3.1.17, grade I, L6876) were from Sigma Chemical Co. Ltd. (Poole, Dorset, U.K.) and were used without further purification.

2.2 Magnetic Support Particle Preparation

2.2.1 Preparation of iron oxide particles

Superparamagnetic metal oxide particles were prepared by mixing a solution of iron (II) (Fe^{2+}) and iron (III) (Fe^{3+}) salts with base to form precipitates which were silane coated according to Advanced Magnetics Patent (Josephson, 1987). A solution (700 mL) of 0.5 M FeCl_2 and 0.25 M FeCl_3 was filtered through a 0.45 μm cellulose nitrate membrane. A 5 M NaOH solution was equilibrated in a waterbath (Julabo 12B, Julabo Labortechnik GmbH, Germany) to 60°C. 100 mL distilled water in a 500 mL beaker was placed under an overhead mixer fitted with a stainless steel paddle. While mixing on the lowest speed setting, 200 mL 0.5 M $\text{Fe}^{2+}/0.25$ M Fe^{3+} iron chloride solution and 200 mL 5 M NaOH were added simultaneously. A black precipitate was formed immediately and mixing was continued for 4 minutes. The particles (~ 10-11 g) were allowed to settle under gravity

and the supernatant was aspirated using a peristaltic pump (100 rpm Watson-Marlow, Cornwall, England.). The particles (which occupied a settled volume of ~ 200 mL) were transferred to a 2 L beaker, resuspended by stirring with a glass rod and brought to the 2 L mark with distilled water. The particles were allowed to settle under a weak magnetic field (~ 0.01 T (Tesla)) by placing on a magnetic stirrer at setting 1. This procedure was repeated 2-3 times until the pH of the supernatant had dropped to 7. The particles were resuspended to 1 L in 0.2 M NaCl and allowed to settle. This wash step was repeated. The particles were then resuspended to 1 L with methanol and allowed to settle. This wash step was repeated 3 times. The particles which settled more slowly in methanol were preferentially separated on a platform 0.3 T magnet. The particles, finally suspended in 250 mL methanol, were stored at 4°C.

2.2.2 Silane coating

10 mL 3-APTES (p-aminophenyltrimethoxy-silane) was added to approximately 10 g ferric oxide particles in 250 mL methanol and mixed for 3 minutes at 3000 rpm using a PT RR6000 Kinematica AG homogeniser (Polytron, Switzerland). 5 mL glacial acetic acid was added and the particles were homogenised for 11.6K rpm for 10 minutes and 4.65K rpm for 2 hours. 200 mL glycerol was added and the suspension was heated in a fume cupboard under nitrogen to a temperature of 160°C in a 500 mL round bottomed flask, fitted with a glass stirrer. After allowing to cool, the particles were washed 3 times, as before, in 2 L distilled water.

2.2.3 Polyglutaraldehyde grafting

2.2.3.1 *BioMag® particles*

Amine-terminated iron oxide particles (BioMag®, PerSeptive Biosystems, U.S.A., supplied by Metachem Diagnostics, Piddington, U.K.) were grafted with a layer of polyglutaraldehyde according to a variation of the procedure described by Halling and Dunnill, (1979). Amine terminated BioMag® particle suspension (50 mg/mL) was vortex-mixed and 500 µL (25 mg) was pipetted into a clean pH stat vessel containing 24.5 mL of 2.04% (v/v) glutaraldehyde solution giving a final glutaraldehyde concentration of 2% (v/v). The pH was rapidly adjusted to 11 by the addition of 0.5 M sodium hydroxide using an autoburette titration instrument (Radiometer, Copenhagen, Denmark) and held there for a period of 60 minutes. The reaction mixture was transferred to a clean 50 mL falcon tube and the modified support was recovered by a magnetic separation unit comprising tube racks fitted with side-pull permanent neodymium bar magnets (PerSeptive Biosystems, U.S.A). The supernatant was then

aspirated off and the support particles were washed 10 times with water, twice with 1 M sodium chloride and twice more with water, by cycles of resuspension, vortex-mixing and magnetic recovery using successively decreasing wash volumes. The polyglutaraldehyde-coated particles were finally suspended in distilled water to a concentration of ~ 25 mg/mL, and stored at 4°C.

* Note that later on BioMag® chelator particle preparations were carried out at a higher particle concentration of 37.5 mg/step volume.

2.2.3.2 *In-house particles*

The polyglutaraldehyde coating of in-house silane-coated ferric oxide particles (section 2.2.1 and 2.2.2) was scaled up as follows. 50 mL 70% aqueous glutaraldehyde (2% final concentration) and water, to a final volume of 1.75 L, were added to approx. 10 g silane coated iron oxide particles (particle concentration ~ 5.7 mg/mL) which were mixed using an overhead mixer (Citenco F.H.P motor, Borehamwood, Herts, U.K.) fitted with a stainless steel spiral paddle. The pH was adjusted to 11 with 1 M NaOH and maintained there for 1 hour in a fume cupboard. The polyglutaraldehyde coated particles were allowed to settle and the supernatant was pumped away. The particles were washed four times with distilled water followed by 2 washes with 1 M NaCl (2 L volumes) and stored at 4°C.

2.2.4. Reduction of surface carbonyl groups

Four different routes were investigated for the introduction of epoxide groups onto the exterior polymer coating of the BioMag® polyglutaraldehyde-coated supports. Three of these involved a common reduction step involving sodium borohydride to convert the aldehyde bearing surface to an alkoxide intermediate. The alkoxide was then hydrolysed under three different sets of conditions to liberate the hydroxyl groups, and hence^{provide} a support surface suitable for epoxide activation.

Polyglutaraldehyde-coated supports (~ 25 mg/mL) were recovered from suspension by magnetic separation and resuspended in absolute ethanol to a concentration of approximately 5 mg/mL in clean 50 mL falcon tubes, and mixed on a recipricol shaker at room temperature. Aliquots of an ice-cold solution (1.5 mL) containing 90 mg of sodium borohydride were added dropwise over a 5 minute period, to 5 mL portions of magnetic suspension while shaking continuously. The reaction suspensions were then mixed at room temperature for a further 40 minutes.

2.2.5. Alkoxide hydrolysis

Route 1 - Concentrated hydrochloric acid (1 mL) was added to 10 mL of ice cold water, mixed and then added very slowly to portions (~ 6.5 mL) of reaction mixture with great care. The acidified suspension was allowed to mix for a further two minutes at room temperature during which time some of the particles were observed to precipitate out of suspension.

Route 2 - 11 mL of ice cold dilute hydrochloric acid solution (1 mM, pH 3) was added slowly to ~ 6.5 mL of reaction mixture and the acidified suspension was then incubated at room temperature with shaking for a further 10 minutes.

Route 3 - The reaction mixture (~ 6.5 mL) was adjusted to a volume of 17.5 mL with ice cold water and mixed, before transferring to a 50°C waterbath for 3 hours.

The hydroxyl-terminated particles recovered from all 3 routes were washed 3 times with water, 3 times with 1 M sodium chloride and thrice more with water by cycles of resuspension, vortex-mixing and magnetic separation.

2.2.6. Epoxide activation

2.2.6.1 *BioMag® particles*

Approximately 25 mg quantities of hydroxyl-terminated supports (from *Routes 1, 2 & 3*) or polyglutaraldehyde coated (*Route 4* - 'direct epoxidation') particles were recovered from suspension and resuspended to 400 µL volume with water in sarstedt tubes. Aliquots (1070 µL) of a 70% solution of 1,4-butanedioldiglycidyl ether were added, followed by the addition of 30 µL of 5 M sodium hydroxide containing 1 mg of sodium borohydride (NaBH₄). Sodium borohydride is a relatively mild reducing agent which is specific for the carbonyl group in aldehydes and ketones (Chaiken and Brown, 1949). The reaction mixtures were agitated vigorously on a vibrax shaker (IKA VXRS17, Janke & Kunkel GmbH, Germany) for 6 hours at room temperature. The final reactant concentrations were - 50% 1,4-butanediol diglycidyl ether, 0.1 M NaOH, and 0.67 mg/mL NaBH₄.

The epoxy-activated supports were recovered magnetically, washed extensively (x 8) with water, and twice with 20 mM sodium phosphate buffer, pH 6.8 containing 1M sodium chloride. Epoxy-activated supports were stored at 4°C in the phosphate buffer, pH 6.8.

2.2.6.2 *In-house particles*

For the scaled up in-house magnetic particle preparation, the optimal final 1,4-butanediol diglycidyl ether concentration of 45% was used (section 3.7). Approx. 10 g (200 mL settled volume by gravity) polyglutaraldehyde particles were transferred to a 500 mL Duran bottle. The particles were washed three times with distilled water. The supernatant was removed by separation on 0.3 T platform magnet and the particles were resuspended to 135 mL with distilled water. 275 mL 70% 1,4-butanediol diglycidyl ether was added followed by 4 mL 10 M NaOH and 4 mL 60 mg/mL NaBH₄ to a final volume of 400 mL and particle concentration 25 mg/mL. The suspension was mixed vigorously and shaken by rotated inversion (REA X2 Heidolph, Germany), for 6 hours at room temperature. The particles were washed four times with distilled water (500 mL per wash).

2.2.7. Iminodiacetic acid coupling

2.2.7.1 *BioMag® particles*

Iminodiacetic acid (IDA) coupling was performed according to an adapted method from Porath (1975) and Porath and Olin (1983). Epoxy-activated supports (~ 25 mg) were recovered from suspension by magnetic separation and resuspended to 600 µL volumes with distilled water. Aliquots (400 µL) of 30% iminodiacetic acid (IDA) in 2 M sodium carbonate were added to each tube (final concentration of 12% IDA), followed by 10 µL of solution containing 0.6 mg NaBH₄. The tube contents were vortex-mixed and incubated in a waterbath at 60°C for about 24 hours with gentle shaking. The IDA-coupled supports were washed twice with water, twice with 20 mM sodium phosphate buffer, pH 6.8 containing 1 M NaCl and finally resuspended to a particle concentration of approximately 25 mg/mL in 20 mM phosphate; 1 M NaCl, pH 6.8 solution and placed at 4°C.

IDA-coupled particles were magnetically retrieved from solution and washed twice with water, once with 0.1 M acetate buffer, pH 3.8 and again with water until the washings were neutral, before suspending in 1 M ethanolamine and incubating at 4°C for 48 hours in order to block excess unreacted epoxide groups. The 'blocked' support preparations were then washed 3 times with water to remove excess ethanolamine and finally resuspended in 20 mM sodium phosphate buffer, pH 6.8, containing 1 M NaCl, and stored at 4°C.

2.2.7.2 *In-house particles*

The in-house scaled up preparation of magnetic chelator particles were IDA coupled using an optimal final concentration of 30% IDA (section 3.7) at a particle concentration 37.5 mg/mL. The particles were washed (x 1) with 2 M Na₂CO₃. The magnetically separated support was brought to 264 mL with 30% IDA in 2 M Na₂CO₃ and 2.65 mL 60 mg/mL NaBH₄ was added. The suspension was mixed well and left to shake at 60°C in a waterbath (Clifden) for 24 hours.

The IDA coupled supports were washed twice with distilled water and unreacted epoxide groups were blocked by mixing with 267 mL 1 M ethanolamine and leaving at 4°C over 48 hours. The 'blocked' supports were then washed (x 3) with distilled water and stored at 4°C.

2.2.8. Metal ion charging

2.2.8.1 *BioMag® particles*

Magnetic chelator supports were charged with the metal ions Cu²⁺, Zn²⁺ or Ni²⁺ just before use. 'Blocked' supports were separated magnetically from storage buffer which was aspirated off and the support was washed by resuspension in 0.1 M acetate buffer, pH 3.8, containing 1 M sodium chloride (or 0.5 M NaCl in later experiments). Support particles (1-10 mg) were charged with metal ions, by separation and resuspension in 1.5 mL of 0.1 M acetate, pH 3.8; 1 M NaCl containing either 5 mg/mL CuCl₂·6H₂O, ZnCl₂·6H₂O or NiCl₂·6H₂O and incubated on a vibrax shaker for 1 hour. The charged supports were then washed sequentially, twice with 0.1 M acetate buffer, pH 3.8; 1 M NaCl, to remove excess unbound metal ions, and water, and then equilibrated with 20 mM sodium phosphate, pH 6.8; 1M NaCl, ready for use. Control 'uncharged' supports were subjected to identical procedures using buffers lacking 'added' metal ions.

2.2.8.2 *In-house particles*

The IDA coupled and 'blocked' magnetic chelator supports were washed (x 3) with 0.1 M sodium acetate buffer pH 3.8 containing 0.5 M NaCl. The supports settled much more rapidly and completely, leaving a clear supernatant, in the presence of salts. Approx. 2.5 g of support was magnetically separated and resuspended in 100 mL 5 mg/mL CuCl₂ in 0.1 M acetate, 0.5 M NaCl, pH 3.8 and mixed by rotated inversion for 1 hour at room temperature. The Cu²⁺-charged supports were washed (x 3) with 0.1 M sodium acetate, 0.5 M NaCl, pH 3.8 buffer and (x 4) with 0.02 M sodium phosphate, 0.5 M NaCl, pH 7.2 buffer.

2.3 Magnetic Support Particle Characterisation

2.3.1 Determination of amine group density

2.3.1.1 TNBS assay

Reactive amino groups were determined by the assay involving TNBS (2,4,6-trinitrobenzene sulphonic acid) as described by Dean et al. (1970). TNBS is thought to react by nucleophilic substitution with free NH_2 groups on the support surface to produce an immobilised trinitrophenyl derivative, which when hydrolysed produces picric acid which is released into solution (Habeeb, 1966).

The amine compound to be tested (silanized BioMag[®]) was suspended in 0.1 M sodium tetraborate pH 9.3 to a volume of 1 mL. 25 μL of 30 mM TNBS was added, mixed well, and allowed to mix on a vibrax shaker at room temperature for 30 minutes. Following magnetic separation the absorbance of the aspirated supernatant was read at 420 nm (Beckman DU 64 spectrophotometer, Beckman Instruments, High Wycombe, U.K.). A standard curve was constructed with known concentrations of L-alanine and a reagent blank consisted of the TNBS solution mixed with 1 mL of 0.1 M sodium tetraborate.

2.3.1.2 SPDP assay

The assay method used was an adaptation of the method described by Carlsson et al. (1978). Amine terminated magnetic particles were treated with an excess of SPDP (N-succinimidyl 3-[2-pyridyldithio] propionate) in a buffer/solvent mixture to convert all amino groups to 2-pyridyldithiopropionamide functions. Treatment with excess dithiothreitol (DTT) reduces the included disulphide bond and releases pyridine-2-thione into solution as a chromophore and its concentration was measured spectrophotometrically.

20 μL (1 mg) amine-terminated particles were washed with 20 mM sodium phosphate buffer, pH 6.8 and the volume was adjusted to 1 mL with the same buffer. 0.3 mL of 20 mM SPDP solution (in 99.5% ethanol) was added dropwise and left for 30 minutes shaking at room temperature. Excess reagent was removed by washing with buffer. The volume was adjusted to 1 mL with buffer and 0.1 mL of 50 mM DTT was added. The mixture was shaken for a few minutes to release the pyridine-2-thione. The support was magnetically separated and the absorbance at 340 nm of the aspirated supernatant was measured against a buffer blank. Pyridine-2-thione has ϵ_{max} of 8080 at 340 nm.

2.3.2 Determination of epoxide group density

Reactive epoxide groups were determined by a procedure adapted from the methods described by Sundberg and Porath (1974) for use with agarose supports. The reaction involves the oxirane ring and sodium thiosulphate resulting in the release of OH^- which can be followed by titration with hydrochloric acid in a pH-stat.

A sample of epoxide activated support (approximately 1 mg) was resuspended to 1 mL with distilled water and transferred to a purpose built pH titration vessel designed for small sample volumes. The pH was adjusted to 7. 1 ml of 2 M sodium thiosulphate pH 7 was added to the stirred epoxy-activated preparations and the pH was kept constant until the reaction was complete (typically 15-40 minutes) by the addition of 0.01 M HCl using a pH-stat autoburette (Radiometer, Copenhagen, Denmark). The amount of oxirane present in solution was calculated from the amount of HCl needed in order to maintain neutrality.

2.3.3 Determination of ligand group density

Iminodiacetic acid (IDA) densities on supports were determined by inference from measurements of immobilised metal ion (M^{2+}) concentrations. Hochuli et al. (1987) and others have shown that there is a 1:1 stoichiometry for the binding of M^{2+} to immobilised IDA when M^{2+} is in excess. Metal ion concentration was measured by atomic absorption spectrophotometry using the appropriate lamps.

The sample of support was washed twice with 1 mL 0.1 M EDTA which strips the support of metal ions by chelation. The support was magnetically separated and the supernatant was diluted as appropriate and aspirated into the flame. Copper was determined at 320.4 nm and zinc at 213.9 nm using single element lamps, operated at 10 mA and 16 mA currents respectively, with an air-acetylene flame in a atomic absorption spectrophotometer AA3100 (Perkin Elmer, Seer Green, U.K.). Metal ion concentration in parts per million (ppm) was determined from an absorption curve of samples of known concentration (1 ppm \equiv 1 $\mu\text{g}/\text{mL}$).

2.3.4 Quantitative support measurement

An estimated quantity of magnetic support was completely hydrolysed by dissolution in 1 mL of concentrated hydrochloric acid. The ferrous/ferric ion content was measured by atomic absorption spectrophotometry as described in section 2.3.3 above. Iron ions

absorb at 248.3 nm at a current setting of 16 mA. In addition dry weight measurements of supports were determined on an analytical balance after 24 hour desiccation in a 100° C oven.

An equal volume of suspended support samples were quantitatively determined (in quadruplicate) by atomic absorption spectrophotometry (AAS) and by dry weight measurement. Support quantity determined by dry weight was found to be 1.15 times lower than by atomic absorption analysis. Support quantities were routinely determined by AAS but quoted as dry weight equivalents by dividing by a factor of 1.15.

2.3.5 Measurement of pH stability

2.3.5.1 *Potassium thiocyanate test*

This test determined the pH stability of the supports by measuring the effect of pH on ferric ion (Fe^{3+}) liberation from amine-terminated iron oxide supports. It was adapted from the method used by Munro (1976). The test was employed over a pH range of 0 (1 M HCl) to 14 (1 M NaOH). To 50 μL (2.5 mg) of amine-terminated BioMag® suspension was added 25 μL of pH test solution (two sets). One set was stationary and the other was shaken on a vibrax shaker at room temperature for 24 hours. The particles were separated magnetically, the supernatant was aspirated and 50 μL were mixed with 50 μL of 1 M potassium thiocyanate. The appearance of a colour (pink to brick red in intensity) indicated Fe^{3+} ion leakage, which was measured spectrophotometrically at 480 nm (1 cm light path). Molar concentrations of liberated ferric ion were calculated against a standard curve of ferric chloride solutions of known concentration. The test is sensitive to ferric ion concentrations as low as 10^{-4} M.

2.3.5.2 *Effect of successive coating and coupling chemistries*

The effect of coating and coupling reactions on the pH stability or corrosion resistance of supports at the various stages in the preparation of magnetic chelator supports was tested, i.e., from the core particle → amine terminated particle → polyglutaraldehyde coated particle → epoxy-activated particle → IDA coupled particle.

Known quantities of magnetic support particles (~ 2.5 mg/test) were subjected to a range of HCl concentrations, 10 M, 1 M, 0.1 M, 0.01 M and 0.001 M, corresponding to pH values of 0, 1, 2, and 3, for 9 time intervals ranging between 1-360 minutes. The magnetic particle preparations were mixed vigorously with the acid solution and shaken for a given time period. Following magnetic separation the supernatant was assayed for

ferric ion content by atomic absorption spectroscopy at 248.3 nm (section 2.3.3). Ferric ion concentration in solution was expressed as a percentage of the total used per test.

2.4 Magnetic Particle Performance Analysis

2.4.1 Experiment to optimise ligand density

Polyglutaraldehyde-coated amine-terminated BioMag[®] support was directly epoxy-activated under reducing alkaline conditions (*Route 4*) as described in section 2.2.6.1, but using a range of 1, 4-butanediol diglycidyl ether concentrations. The epoxy activated supports were then coupled with iminodiacetic acid (IDA) at various concentrations and excess epoxide groups were blocked with ethanolamine before charging the immobilised chelate groups with Cu²⁺ ions and testing their specific adsorption capacity towards *C. krusei* cytochrome *c*.

2.4.1.1 Effect of varying oxirane concentration

Six identical test samples of polyglutaraldehyde-coated support (~ 10 mg/test) were epoxy-activated (section 2.2.6.1) using six percentage (final) 1, 4-butanediol diglycidyl ether concentrations; 0, 30, 40, 50, 57.6 and 60.5%. ~ 2 mg magnetically separated sample from each of the tests were assayed to determine the active epoxide group density (section 2.3.2) and subsequently the support was quantitatively determined (section 2.3.4). The remainder test samples were IDA coupled, blocked (section 2.2.7) and charged with copper ions (section 2.2.8.1), so that the immobilized copper density and by inference the IDA ligand density could be determined (section 2.3.3).

2.4.1.2 Effect of varying IDA concentration

Epoxide activated (50% 1, 4-butanediol diglycidyl ether) magnetic support, suspended in 1 M Na₂CO₃ was divided into 7 test samples (~ 4 mg/test). The test samples (150 µL) were mixed with 10 µL 60 mg/mL NaBH₄ and appropriate volumes of 1 M Na₂CO₃ and 30% IDA in 1 M Na₂CO₃ to give a range of % (final) IDA concentrations of 0, 5, 7.5, 10, 15, 20 and 30% in 1 mL final volume. The support was incubated for 24 hours at 60° C and blocked as normal (section 2.2.7). The test samples were charged (section 2.2.8) with Cu²⁺ ions, stripped and the IDA ligand density ρ_{IDA} determined (section 2.3.3). In addition, the capacity of the charged supports for *C. krusei* cytochrome *c* was determined. Support and protein were mixed together in a ratio of 2:1 and allowed to bind overnight, shaking at 6°C. The support was magnetically separated and washed x 4 with 0.02 M sodium phosphate, 0.5 M NaCl buffer, pH 7.2 and the bound protein was eluted in two washes with 0.1 M sodium acetate, 0.5 M NaCl buffer, pH 3.8.

2.4.2 Adsorption-desorption studies of native metal-binding proteins by magnetic chelator supports

A set of native haem proteins with variable numbers of surface exposed histidine residues were separated by and eluted from magnetic chelator supports immobilised with metal ions.

Magnetic chelator supports (~ 2 mg), prepared by preparative *Routes 1-4* (sections 2.2.4, 2.2.5 and 2.2.6) were washed with 0.1 M sodium acetate, 1 M NaCl, pH 3.8 buffer and divided into two parts (~ 1 mg). One part was charged with Cu^{2+} , Zn^{2+} or Ni^{2+} ions as appropriate (section 2.2.8) and the other was left as a control, lacking immobilised metal ions. The test and control support samples, prepared by *Routes 1-4* (i.e., *Route 1*; pH 0 hydrolysis, *Route 2*; pH 3 hydrolysis, *Route 3*; 50°C hydrolysis, and *Route 4*; direct epoxidation) were equilibrated by washing in binding buffer, 0.02 M sodium phosphate, 1 M NaCl, pH 6.8. The protein solutions were prepared in binding buffer and allowed to interact, at a 1:1 weight ratio of protein to support, for 1 hour, shaking at room temperature. The supports were magnetically separated, the supernatant was aspirated and the support was washed first with binding buffer (0.02 M sodium phosphate, 1 M NaCl, pH 6.8) to remove unbound or loosely bound protein. The bound protein was pH eluted by successive washes with buffers of decreasing pH (0.1 M sodium acetate, 1 M NaCl buffer at pH 6, pH 4.8 and pH 3.8). A final wash with 0.1 M imidazole, 1 M NaCl displaced any remaining protein. An extinction coefficient was determined for each of the haem proteins which absorb maximally at 420 nm. The A_{420} of the supernatant washes were read spectrophotometrically, and by using the appropriate extinction coefficient, the protein concentration was calculated (section 2.7.1). The total protein recovered per test was calculated by summing the protein content of all the supernatant washes. The protein bound per test was calculated by subtracting the unbound protein from the total protein recovered. The protein bound after each successive wash was calculated by subtracting the protein in each wash from the bound protein. The amount of protein bound was expressed per mg (calculated by dry weight measurements) of support (section 2.3.4).

2.4.3 Experiment to compare protein adsorption-desorption profiles of magnetic chelator and chelating Sepharose 6B supports.

3 mL of chelating Sepharose 6B (Pharmacia) slurry was washed and separated in batch mode by mixing by inversion and centrifuging at 10,000 rpm for 10 minutes (Beckman

CS6 centrifuge, Beckman Instruments, High Wycombe, U.K.). The support was charged with Cu^{2+} ions (section 2.2.8) and suspended in 3.8 mL volume (containing 2.1 mL wet Sepharose 6B as Sepharose 6B exists initially as a 70% slurry). Magnetic chelating support was similarly washed and charged with Cu^{2+} ions by vortex mixing and magnetic separation. 100 μL of the charged slurry suspension (55 μL wet Sepharose is the equivalent packed-bed volume) and a volume containing 5.65 mg magnetic support were transferred (x 2) into two separate 2 mL Sarstedt tubes. One of the tubes of each set was washed twice with 0.05 M EDTA, 1 M NaCl to remove Cu^{2+} and serve as an uncharged control. Both the charged test and the uncharged control were washed twice with equilibration/wash buffer (0.02 M sodium phosphate, 1 M NaCl, pH 6.8) and both sets were performed in duplicate. 1 mL of protein solution at excess concentration (10 mg/mL) was allowed to mix with the support samples for two hours at room temperature with shaking. The supports were washed and shaken between washes, for 1 hour (x 1), 30 minutes (x 4) and 10 minutes (x 1) to remove all unbound and loosely bound protein. Bound protein was eluted by lowering the pH with two 0.1 M sodium acetate, 1 M NaCl, pH 3.8 buffer washes of 30 and 15 minutes followed by two 10 minute washes with 100 mM imidazole. The protein content of the washes was calculated by measuring their A_{280} (extinction coefficient of *C. krusei* cytochrome *c* = 19,864) and by Bradford assay (section 2.7.1).

2.4.4 Determination of adsorption isotherms for native metal-binding proteins on magnetic chelator supports.

All protein solutions (1 mg/mL) were prepared in binding/equilibration buffer (0.1 M sodium phosphate, 1 M NaCl, pH 7) at room temperature. About 1 mg of magnetic chelator support, either charged with Cu^{2+} or Zn^{2+} ions or left uncharged as a control (section 2.2.8), were combined with 1.5 mL of each protein solution at a different concentration (0, 5, 10, 20, 30, 40, 50, 100, 200, and 300 μg). The support/protein mixtures were incubated at 6°C overnight (~ 15 hours) on a vibrax shaker. The supports were magnetically separated and washed x 4 with equilibration buffer to remove unbound and loosely bound protein. The first supernatant and subsequent washes were analysed (Bradford assay, section 2.7.1) for protein content. The amounts of bound protein were then calculated by difference and the adsorption isotherms plotted where possible.

2.4.5 Experiment to investigate the effect of magnetic support recycle for re-use

Magnetic chelator support charged with Cu^{2+} ions was cycled 3 times through charging, binding, washing, elution, cleaning and metal ion stripping process steps. The effect of recycling via these steps and support re-use on chelating ligand density, protein adsorption capacity and iron core leaching was monitored.

About 10 mg of magnetic chelator support was equilibrated (x 4 washes) with 0.1 M sodium acetate, 1 M NaCl, pH 3.8 buffer, and charged (x 1) with 5 mg/mL CuCl_2 in the same buffer. Free unchelated Cu^{2+} ions were washed away (x 3) with the acetate buffer, followed by (x 3) washes with 0.1 M sodium phosphate, 1 M NaCl, pH 7. The support was allowed to bind with about 340 mg (in excess) *C. krusei* cytochrome *c* protein dissolved in 0.1 M sodium phosphate, 1 M NaCl, pH 7 overnight and shaking at 6°C. The support was washed (x 4) with the phosphate buffer at pH 7 and the bound fraction was eluted by washing (x 2) with the acetate buffer at pH 3.8. The support was then stripped of metal ions by washing (x 2) with 0.1 M EDTA, 1 M NaCl solution and cleaned by washing (x 3) with 0.1 M NaOH. This series of process steps was repeated head-to-tail on the same support sample 3 times. The process was repeated on an equal quantity of uncharged support which served as a control. 1.8 mL wash volume was used. For each cycle Cu^{2+} ion concentration was measured (section 2.3.3) to determine chelating ligand density and protein adsorption capacity was determined by measurement of the concentration of protein bound (Bradford assay, section 2.7.1). In addition, the amount of $\text{Fe}^{2+}/\text{Fe}^{3+}$ leaching from the magnetic ferric oxide support core at successive cycles was determined by atomic absorption spectrophotometric analysis of the washes at 248.3 nm using a single element iron lamp (as described in section 2.3.3).

2.4.6 Recovery of recombinant metal-binding protein expressed in *E. coli*

2.4.6.1 Extracellular histidine-tailed single chain antibody fragment from culture medium

A recombinant penta-histidine tailed single chain antibody fragment incorporating a hinge region (ScFv hinge(his)₅), expressed in *E. coli* XL1 blue cells (Martin, 1995), was cultured as described in section 2.5.2. Culture supernatant containing ScFv hinge(his)₅ was dialysed against 20 mM sodium phosphate buffer, 1 M NaCl, pH 8 (3 mg total protein/mL). About 1.5 mg samples of magnetic chelator support were charged separately with Cu^{2+} , Ni^{2+} and Zn^{2+} metal ions (section 2.2.8) and one was left

uncharged to act as a control. The supports were equilibrated with 20 mM sodium phosphate buffer, 1 M NaCl, pH 8 and mixed with 1 mL dialysed culture supernatant for 1 hour at room temperature on a vibrax shaker. The support was magnetically separated and the supernatant (unbound fraction) was retained. The bound fraction was eluted by washing (x 4) the support with 300 μ L 0.1 M EDTA, 1 M NaCl solution. The unbound (0.9 mL) and pooled bound (1.1 mL) fractions were TCA precipitated (section 2.7.3.1) and analysed by SDS-polyacrylamide gel electrophoresis and Western blotting (sections 2.7.4 and 2.7.5).

2.4.6.2 Intracellular histidine-tailed T4 lysozyme from crude cell extract

E. coli cells (JM107 strain, pQR752) expressing a recombinant cysteine-free T4 lysozyme, tagged at its C-terminus with a metal-binding tail sequence, were cultured (1 L) as described in section 2.5.3 on nutrient broth media. The harvested cells were disrupted by sonication (section 2.5.5.3) in 50 mM Tris-HCl, pH 7, centrifuged to remove cell debris and dialysed against 20 mM sodium phosphate, 0.5 M NaCl, pH 7.2. Recombinant T4 lysozyme was purified from the extract on a Zn²⁺ or Cu²⁺-IDA immobilised metal affinity chromatography (IMAC) HiTrap™ column (section 2.6.1.2). Fractions were analysed for total protein (section 2.7.1) and lysozyme activity (section 2.7.2.1). Eluted fractions of purified recombinant T4 lysozyme, with highest activity, were pooled.

75 μ L x 3 of the crude cell extract (5 mg protein/mL) was adjusted to 1.5 mL with binding buffer (20 mM sodium phosphate, 0.5 M NaCl, pH 7.2) after mixing with ~ 2 mg of Cu²⁺-charged (x 2/test) and uncharged (x 1/test) magnetic chelator supports. Binding took place at 6°C overnight (~ 15 hours) on a vibrax shaker. The supports were recovered by magnetic separation, washed twice with 20 mM sodium phosphate, 0.5 M NaCl, pH 7.2, to remove loosely-bound material and then treated with two successive washes of elution buffer (0.1 M sodium acetate, 0.5 M NaCl, pH 3.8). The liquid-phase samples (1.5 mL volumes) were analysed for lysozyme activity, protein content and composition (sections 2.7.1, 2.7.2.1 and 2.7.4).

2.4.7 Recovery of native and recombinant metal-binding proteins from crude *E.coli* homogenate

2.4.7.1 Recovery of haemoglobin from solution spiked with whole cells and media.

The effect on the binding capacity of magnetic chelator supports for haemoglobin, a native metal-binding high affinity protein, was determined in the presence of whole *E. coli* cells and media components.

Wild type *E. coli* JM107 strain was grown (50 mL) as described in section 2.5.3 until an OD₆₀₀ 4.56 was reached after 6 hours (1.9 g/L dry cell weight). About 3.4 mg quantities of Cu²⁺-charged and uncharged (section 2.2.8) magnetic chelator support were equilibrated in 1 mL of 20 mM sodium phosphate, 0.5 M NaCl, pH 7.2 buffer. The support samples were magnetically separated and mixed respectively (6 charged and 6 uncharged) with 0.25 mL (1 mg) bovine haemoglobin dissolved in 20 mM sodium phosphate, 0.5 M NaCl, pH 7.2 and with 0.75 mL of the solutions described in Table 2.1.

Table 2.1 Solutions spiked with *E.coli* cells, cell debris and media components.

Sample no.	Sample composition	Dry cell weight (mg)
1.	20 mM sodium phosphate, 0.5 M NaCl, pH 7.2 buffer	0
2.	1 mL 20 mM sodium phosphate, 0.5 M NaCl, pH 7.2 buffer containing cell equivalent of 1 mL cell culture	1.425
3.	1 mL cell culture containing cell equivalent of 2 mL cell culture	2.85
4.	1 mL cell culture	1.425
5.	0.5 mL cell culture / 0.5 mL media (sterile)	0.712
6.	1 mL media (sterile)	0

The media used was high biomass media (section 2.1). Binding took place overnight, shaking at 4°C. The supports were washed (x 3) with 20 mM sodium phosphate, 0.5 M NaCl, pH 7.2 buffer, once with 0.1 M sodium phosphate, 0.5 M NaCl, pH 3.8 buffer and twice with 0.1 M EDTA, 0.5 M NaCl solution. An extinction coefficient for haemoglobin

was determined and protein analysis of the first supernatant and the supernatant washes was performed by measuring A_{420} .

2.4.7.2 Recovery of recombinant T4 lysozyme from crude extract in the presence of cells and cell debris

T4 lysozyme-his was expressed as before by culturing *E. coli* JM107 pQR752 (section 2.5.3). Aliquots of culture containing known concentration of cells were resuspended in 20 mM sodium phosphate, 0.5 M NaCl, pH 7.2 buffer prior to disruption by sonication (section 2.5.5.3) to release intracellular protein. 1 mL samples, some containing cells and some with the cells removed, at two cell concentrations, were mixed with Cu^{2+} -charged magnetic chelator supports and with an uncharged control set. Binding took place overnight, shaking at 6°C. Following aspiration of the supernatant, the supports were washed (x 4) with 0.02 M sodium phosphate, 0.5 M NaCl, pH 7.2 buffer and eluted (x 3) with the same buffer at pH 3.8 and by two washes with 0.1 M imidazole. The collected liquid fractions were assayed for protein content and lysozyme activity. The cell concentrations were determined by estimation of dry cell weight (section 2.5.4.2).

2.4.8 Magnetic particle separation technology using a high gradient magnetic separation device

Magnetic chelator support particles (0.5 g) were prepared as described in section 2.2. 1 L culture of *E. coli* JM107 pQR752 producing T4 lysozyme-his was harvested following 3 hours induction. The cells were resuspended to 250 mL with 0.02 M phosphate buffer, 0.5 M NaCl, pH 7.2, divided into 4 lots, disrupted by sonication and pooled (section 2.5.6.3). ~ 0.5 g Cu^{2+} -charged support was magnetically separated and resuspended with 245 mL T4 lysozyme-his producing *E. coli* cell homogenate. The suspension was mixed by tumbling overnight at 4°C on a REAX 2 Heidolph (Germany).

The high gradient magnetic separation device consisted of a variable field bipole electromagnet (Tesla Engineering Ltd., Storrington, England, U.K.) controlled via a 20 V D.C. transformer (Drake Transformers Ltd., Wickford, England, U.K.). The maximum flux density in the air-filled space (4 cm gap x 11 cm width x 30 cm length) when operated at 625 A is 1.5 Tesla. The space between the magnetic poles can accommodate a cylindrical canister of maximum volume 3.4 L (3.8 cm diameter x 30 cm length).

The high gradient magnetic filter material was a ferromagnetic stainless steel wool, #434, of thickness 0.2-0.25 mm which was kindly donated by J. A. Kostuch, ECC International, England, U.K. (supplier: International Steel Wool Corporation, Ohio,

U.S.A.). The steel wool was treated (by P. Pannu, of this department) with perfluorooctyl triethoxysilane and coated with polyvinyl alcohol in order to protect against corrosion (Theodossiou, 1993) and to minimise any non-specific adsorption. The coated wool was randomly but tightly packed into a perspex 20 cm³ canister which includes a top and bottom distribution plate with 4 mm pore size. The electromagnet was set at 0.4 T with the aid of a portable gaussmeter 700 (Trilec Instruments Ltd., Wiltshire, England, U.K.) which was used to measure the magnetic flux density in the space where the canister rests between the two magnetic poles.

With the magnetic field set at 0.4 T (143 mA and 3.1 V), the high gradient magnetic filter was loaded with Cu²⁺-charged magnetic chelator support / cell homogenate mix (1.11 mg support / mL) which had been contacted with mixing for 12 hr at 4°C. The magnetic support/cell homogenate suspension (in phosphate buffer) was pumped against gravity into the packed canister at 10.5 mL/min using a peristaltic pump (Watson and Marlow Ltd., Falmouth, England, U.K.) using tubing of 6 mm bore size. Fractions were collected at two minute intervals by a Pharmacia LKB 2211 Superrac fraction collector. After approximately 3/4 of the loading suspension had been pumped through the canister, support began to break through the filter matrix and wash out of the canister. In response to this the magnetic field was increased to 0.5 Tesla. However, breakthrough continued and after a further 1.5 column volumes of feed, loading was stopped, at which point 130 mL had been pumped into the canister.

The filter matrix was flushed through by washing with 0.02 M phosphate buffer, 0.5 M NaCl, pH 7.2 at successive flowrates of 10.5, 20 and 30 mL/min (~ 25 column volumes). The matrix was then washed with elution buffer, 0.1 M sodium acetate, 0.5 M NaCl, pH 3.8 at 10.5 mL/min and fractions were collected at a rate of 1 fraction per 30 sec (4.5 column volumes). The magnetic field was turned off and the filter matrix was flushed with acetate buffer at high flowrate (90 mL/min) for 7 column volumes. The matrix was removed from the canister and magnetic support was dissociated and dislodged from the matrix by vibration and vigorous shaking with aliquots of elution buffer (14.5 column volumes).

Collected fractions were assayed for total protein (section 2.7.1) and lysozyme activity (section 2.7.2.1) and OD₆₀₀ was measured (section 2.5.5.1). The support IDA ligand density (section 2.3.3) and the amount of support recovered (section 2.3.4) was also determined.

2.5 Fermentation

2.5.1 *E. coli* HB101 expressing ZZ-his fusion protein

A six residue affinity peptide, containing a His-X-His sequence, was polymerised head to tail four times and fused to a synthetic IgG-binding domain, designated ZZ, based on staphylococcal protein A. Ljungquist et al. (1989) observed a relatively strong interaction for the fusion protein to a Zn²⁺-charged immobilised metal affinity column. *Escherichia coli* HB101 pEZTZ expressing the ZZ-His4 fusion protein was received as a gift from M. Uhlén, Royal Institute of Technology, Stockholm, Sweden.

2.5.1.1 Shake flask cultivation

A starter culture of *E. coli* HB101 harbouring pEZTZ-His4 plasmid (taken from a Tryptic Soya agar (Difco) plate containing ampicillin at 100 mg/L) was grown overnight in a 50 mL conical flask in a reciprocal shaking incubator (200 rpm) in 5 mL of Tryptic Soya Broth (Difco) (30 g/L) supplemented with yeast extract (5 g/L) and ampicillin (100 mg/L) at 37°C. The main culture, 200 mL in a 2 L flask, was inoculated (5% v/v) and grown under the same conditions and harvested during exponential growth.

Cells were harvested by centrifuging at 8000 rpm for 20 minutes (Beckman J2 M1). The ZZ-derived protein was released from the periplasmic space by osmotic shock essentially as described by Nossal and Heppel, (1966) (section 2.5.5.1). The periplasmic fractions were first purified using IgG affinity chromatography, followed by immobilised metal affinity chromatography on a zinc-charged Sepharose column according to Ljungquist and co-workers (1989) (section 2.6).

2.5.2 *E. coli* XL1-blue expressing histidine-tailed single chain antibody fragment

Single-chain antibody fragments which were originally derived from the anti-cancer antibody B72.3, were genetically altered in order to facilitate their purification by immobilised metal affinity chromatography (Martin, 1995). A recombinant pentahistidine tailed single chain antibody fragment incorporating a hinge region (ScFv hinge(his)₅) which is expressed in *E. coli* XL1 blue cells was kindly provided by S. Martin of this department.

2.5.2.1 Shake flask cultivation

E. coli XL1-blue pSM encoding for ScFv hinge(his)₅ was taken from a -70°C stock on to a Luria-Bertrani (LB) agar plate supplemented with kanamycin (30 mg/L) and incubated at 30°C over 4 days. An overnight starter culture in LB broth at 30°C was used to inoculate (2% v/v) 200 mL of the same media supplemented with kanamycin (30 mg/L), which was grown in a shaking incubator at 37°C and 200 rpm for about 5-8 hours until an OD₆₀₀ ~ 0.8 was reached. The culture was induced with IPTG (0.05 mM) and allowed to grow overnight, for a further ~ 18 hours, at a reduced temperature of 30°C. The cells lyse following induction and release the recombinant antibody fragments to the medium. The culture was spun down at 8000 rpm for 30 minutes (Beckman J2 M1). The supernatant was retained, aliquoted and stored at -20°C.

2.5.3 *E. coli* JM107 expressing histidine-tailed T4 lysozyme

E. coli K12 JM107 pQR752 encoding for ampicillin resistance and cysteine-free bacteriophage T4 lysozyme was genetically modified to carry a poly-histidine tail sequence at its C-terminus (Sloane et al., submitted) and was kindly provided by R. P. Sloane, Department of Biochemistry and Molecular Biology, University College London.

2.5.3.1 Shake flask cultivation

A loopful of *E. coli* JM107 pQ752 cells taken from a -70°C glycerol stock were streaked on a nutrient agar plate supplemented with ampicillin at 100 mg/L. The plate was incubated at 30°C for two to three days. A single colony was transferred to a universal bottle containing 5 mL of media supplemented with ampicillin, which was incubated at 37°C or 28°C, (optimised conditions), with agitation at 200 rpm on an orbital shaker for about 10 hours. This seed culture in exponential growth phase provided an inoculum (1% or 5% v/v) for the main culture, 50 mL in a 250mL unbaffled conical flask or 250 mL in 2 L unbaffled flask, which was grown with antibiotic present under the same conditions of temperature and agitation. At mid-exponential growth the culture was induced with IPTG (1 mM) and typically harvested 3 hours later.

2.5.3.1 Pilot scale cultivation

Stirred tank batch cultivations were carried out successively in a 14 L Chemap, 42 L LH and a 7 L LH 2000 Series fermenter (Incelltech LH-SGI, Reading, Berkshire, U.K.) with 3000 Series instrumentation. Main culture media was sterilized in situ after which the pH was adjusted and maintained at 7.0 with 2 M H₂SO₄ and 4 M NaOH. The dissolved oxygen tension (DOT) and pH were monitored by Ingold electrodes (Ingold, Switzerland) linked to the i3000 series instrumentation. Cultivation parameters and gas

exhaust composition were logged using Real Time Data Acquisition Software (RT-DAS). Seed culture preparation was according to directions for shake flask cultivation with appropriately scaled sub-culture volumes. A 5% (v/v) inoculum was used. All liquid cultures were supplemented with 100 mg/L ampicillin to maintain plasmid stability.

2.5.3.1.1 Centrifugation

Shake flask fermentations were harvested by centrifugation (Beckman J2 M1, JA 10 rotor) at 6,000 rpm for 20 minutes at 4°C. Smaller scale 1 mL samples were sedimented by centrifuging for 10 minutes at 13,000 rpm in a minifuge (M 11 Beckman). Bioreactor fermentations at 7, 14 and 42 L scale were harvested in a Sharples 1P tubular bowl centrifuge. This centrifuge operates at a speed of 45,000 rpm which is achieved by an air driven turbine, operating at a pressure of 2 barg. (max).

2.5.4 *E. coli* JM83 expressing α -amylase

E. coli JM83 containing the plasmid pQR187 which encodes for *Streptomyces thermoviolaceus* CUB74 α -amylase and kanamycin resistance (provided by J. J. Pierce of this department) was maintained at -70°C. Cells were reactivated by growing on nutrient agar plates containing 1% potato starch and 20 μ g/mL kanamycin. A loop full of cells was resuspended in 50 mL terrific broth containing 10 μ g/mL kanamycin and grown for 8 h at 37°C and 200 rpm in a reciprocating incubator. The main cultures containing the same media were then inoculated with 1% of the starter and grown for a further 18 h at 37°C and 200 rpm to a final OD₆₀₀ 11.6

2.5.5 Analytical methods

2.5.5.1 Optical cell density

Cell growth and biomass accumulation were monitored hourly by optical cell density readings at 600 nm against a blank of sterile medium. The spectrophotometer (DU 64, Beckman) was calibrated to zero absorbance with 1/4 Ringers thiosulphate solution and all samples read were diluted 1:10 with the same solution.

2.5.5.2 Dry cell weight

Dry cell weight was measured by harvesting 1 mL of cells in a 1.5 mL pre-dried and pre-weighed eppendorf tube and drying the pellet at 100°C for 24 hours or until a constant weight was obtained.

2.5.5.3 Cell count and plasmid stability

Viable cell count was performed on nutrient agar plates. Plasmid stability was studied and expressed as the percentage of colony forming units (cfu) on plates with antibiotic (e.g., ampicillin) to plates without antibiotic. Plasmid stability was measured by the 'plate ratio' technique (Hopkins et al., 1987). 10 μ L x 3 of diluted (in 1/4 strength thiosulphate Ringers solution) fermentation broth was plated onto both non-selective nutrient agar and selective (containing 100 μ g/mL ampicillin) agar. After incubation at 30°C for 48 hours the number of colonies were counted and the stability, as the percentage of plasmid-containing cells was calculated.

2.5.6 Cell disruption

2.5.6.1 Osmotic shock

A method for the osmotic shock of cells in exponential phase was developed by Nossal and Heppel, (1966). The method involved suspending bacterial cells first in sucrose-EDTA solution, and then in 5 x 10⁻⁴ M MgCl₂.

About 1 g wet weight cells were suspended in 40 mL 0.033 M Tris, pH 7.1 at room temperature. 40 mL of 40% sucrose solution was added with rapid stirring followed by 0.1 M Na₂EDTA, pH 7.1 to give a concentration of 1 x 10⁻⁴ M. The mixture was shaken vigorously for 10 minutes and centrifuged for 15 minutes at 8500 rpm at 4°C (Beckman J2 M1). The drained pellet was rapidly dispersed in 80 mL of ice cold MgCl₂ 5 x 10⁻⁴ M. The suspension was stirred gently on ice for 10 minutes and centrifuged as before. The supernatant containing the released protein was retained, aliquoted and stored at -20°C.

2.5.6.2 Osmotic shock with lysozyme

Cell periplasmic lysis was also carried out according to a modification of the the method developed by French (1993). Pelleted cells (1 mL culture) were resuspended in a volume of lysis buffer (20% (w/v) sucrose, 0.001 M EDTA and hen egg white lysozyme at 500 μ g/mL), 40% of the initial culture volume (400 μ L). The mixture was incubated for 20 minutes at room temperature. An equal volume (400 μ L) of ice cold reverse osmosis grade water was added to the suspension which was left for a further 10 minutes. The mixture was then harvested at 10,000 rpm in a minifuge for 10 minutes and the supernatant containing the released periplasmic protein was decanted and retained.

2.5.6.3 Sonication

Following centrifugation the cell pellet of a 1 mL sample of culture (small scale) or of a 1 L culture (larger scale) was resuspended in an appropriate (minimum) volume (i.e., 0.5

mL (small scale) or ~ 20 mL (larger scale)) of buffer, 10 mM Tris, pH 7 or 20 mM phosphate, 0.5 M NaCl, pH 7.2. The cell suspension was subjected to 3 - 15 x 30 second pulses of 8 amplitude microns in a Soniprep 150 MSE sonication device (MSE Scientific Instruments Ltd., Sussex, U.K.). The sample was kept cool on ice. The cell debris was separated by centrifugation either at 13,000 rpm in a minifuge for small scale samples or at 14,000 rpm for 10 minutes in Beckman J2 M1, JA 17 rotor for larger samples. The supernatant of the disrupted cells was analysed for protein content and enzyme activity.

2.5.6.4 Homogenisation

A Gaulin Micron Lab 40 (APV Gaulin GmbH) small scale (max. volume 40 mL) high pressure homogeniser was used. The system cooled by coils of passing glycol has an operating pressure range of 100 to 1600 bar. The product cylinder was filled to within 0.5 cm of its maximum capacity and the cell suspension was passed one or more times at a single pressure. The product cylinder was unloaded after each pass, rinsed and refilled with a new sample or with the same sample for repeated passes.

2.5.7 Concentration

2.5.7.1 Sucrose dehydration

Following immobilised metal affinity chromatographic pH elution, the eluted fractions of recombinant T4 lysozyme-his were pooled, transferred to dialysis tubing (12-14 kD cut off) and concentrated by dehydration in the presence of excess sucrose at 4°C. The dialysis tubing was packed on all sides with dry sucrose, which resulted in hydration of the sucrose and concentration of the protein solution. The sucrose coating was changed hourly (x 4). Finally the sample was dialysed for 15 h at 6°C against lysis buffer (20% (w/v) sucrose, 0.001 M EDTA, pH 7), ready to effect periplasmic release from *E. coli* cells.

2.6 Column Affinity Chromatography

2.6.1 Immobilised metal affinity chromatography

2.6.1.1 Chelating Sepharose 6B

Native haem proteins (from the cytochrome *c* and albumin family groups) with various numbers of surface accessible histidines were separated by immobilised metal affinity chromatography (IMAC) on chelating Sepharose 6B support (Pharmacia) in a packed C10/10 column (Pharmacia) as described by Hemden et al. (1989).

Iminodiacetic acid (IDA) chelating Sepharose 6B, supplied as a suspension in 20% ethanol, was washed thoroughly on a sintered glass filter with 10 column volumes of distilled water (50 mL). 7 mL of a 75% slurry suspension gives a bed volume of 5 mL. The washed slurry was packed in a column (Pharmacia C10/10) via a packing reservoir under a flowrate of 0.25 mL/minute using a Beckman 'System Gold' low pressure FPC system. The column was washed with two column volumes of distilled water and five column volumes of 20 mM sodium phosphate buffer, pH 6.8, containing 1 M NaCl. It was charged with five column volumes of 5 mg/mL of metal chloride in 0.1 M sodium acetate buffer, 1 M NaCl, pH 3.8. Unbound metal ions were washed out with five column volumes of acetate buffer. The column was finally equilibrated with (five column volumes) of phosphate buffer. The buffers were degassed by filtration through a cellulose nitrate membrane (0.2 µm) under vacuum prior to use.

A sample mixture (5 mL) of native haem metal-binding proteins (typically containing 1 mg of each protein) equilibrated in 20 mM sodium phosphate, 1 M NaCl, pH 7.2 buffer was applied to the column via a superloop. On-line A_{280} protein measurement of the flowthrough was monitored by the Beckman 'System Gold'. The column was washed with phosphate equilibration buffer to flush through unbound and loosely bound material. The extent of this step depends on the strength of the protein binding interaction. Elution commenced by passing 0.1 M sodium acetate, 1 M NaCl, pH 6 through for three column volumes followed by a descending pH gradient from pH 7 to pH 3.5 over 20 column volumes. 0.1 M sodium acetate, 1 M NaCl, pH 3.8 was passed through for three column volumes and finally the column was washed with distilled water. In order to separate native metal-binding albumin proteins elution was performed, in addition to the elution conditions described, with 0.1 M sodium acetate, 1 M NaCl, pH 4.8, followed by an imidazole gradient (1-15 mM) in phosphate buffer, pH 7.2. The eluted peak fractions (2 mL) were collected in 11 x 16 tubes using a fraction collector (Pharmacia LKB frac 100). Further analysis of eluted fractions by the Bradford protein assay (section 2.7.1) and SDS-polyacrylamide gel electrophoresis (section 2.7.3) was carried out.

2.6.1.2 *HiTrap™ chelating column*

A 5 mL HiTrap™ chelating column (Pharmacia) was used, which was packed with Chelating Sepharose High Performance support matrix, capable of a maximum flowrate of 20 mL/min. The column was washed with 15 mL distilled water which was passed through using a 20 mL syringe. 2.5 mL of 0.1 M metal chloride solution was used to charge the column. Unbound metal ion was washed out with 15 mL of distilled water. The sample to be loaded was clarified by centrifugation and its composition was adjusted to the pH and ionic strength of the start buffer by overnight dialysis. The column was

equilibrated with 5 column volumes of start buffer (0.02 M Na₂HPO₄, 0.5 M NaCl, pH 7.2). The sample was applied at a flowrate of 2 mL/min by a peristaltic pump (Pharmacia) and fractions were collected by an LKB frac 100 (Pharmacia) and retained for further analysis. About 5 column volumes of wash buffer were applied until no material appeared in the effluent. Elution was effected by a step gradient at decreasing pH with 0.02 M Na₂HPO₄, 0.5 M NaCl, pH 3.5 at a lower flowrate of 1mL/min to promote higher resolution. The volume of elution buffer required depended on the strength of the protein-metal interaction.

2.6.2 IgG affinity chromatography

Purification of a two domain protein A fusion protein conjugate (ZZ-his) on IgG Sepharose was carried out according to the method described by Ljungquist et al. (1989). IgG Sepharose 6 Fast Flow (Pharmacia) was supplied in 50 mM potassium phosphate, pH 7.2; 1.0 mM magnesium chloride and 20% ethanol. 2.5 mL of this suspension was packed in a Pharmacia C10/10 column to give a bed volume of 2.0 mL. The gel was washed with 10 bed volumes of tris-saline Tween buffer (TSTa) (50 mM tris, pH 7.6, 150 mM NaCl and 0.05% Tween 20) to remove traces of ethanol. The column was operated by gravity feed. The column was equilibrated with 3 bed volumes each of (a) 0.5 M acetic acid, pH 3.4, (b) TSTa, (c) 0.5 M acetic acid, pH 3.4 and (d) TSTa until the pH of the eluent was neutral. The pH of the sample was adjusted to neutral and then applied to the column. The gel was washed with 10 bed volumes of TSTa and 2 bed volumes of TSTb (25 mM tris, pH 7.4; 200 mM NaCl and 0.05% Tween 20) supplemented with 10 mM EDTA. The column was equilibrated with 5 mM ammonium acetate, pH 5.0 and elution was performed with 0.2 M acetic acid, pH 3.3 (pH adjusted using ammonium acetate). Eluted fractions were collected and retained for further analysis. After use the column was re-equilibrated with TSTa until pH of the effluent was around 7.0 and the gel was stored in this buffer.

2.6.3 Antigen (mucin) affinity chromatography

The purification of single chain antibody fragments carrying a hinged penta-histidine tail was achieved by using mucin-Sepharose affinity chromatography.

2.6.3.1 Coupling of mucin to Sepharose

Mucin (N-Acyl-neuraminic acid glycoprotein) was dissolved on a roller rig at 30 mg/mL in coupling buffer (0.1 M NaHCO₃, 0.5 M NaCl pH 8.3, 0.1 M Tris-HCl pH 8). The A₂₈₀ was read. 2 g cyanogen bromide activated Sepharose (Pharmacia) was dissolved in 1

mM HCl (1 g \equiv 3.5 mL swollen gel). The Sepharose was washed on a scintered glass funnel with 400 mL of 1 mM HCl to remove additives. The Sepharose was allowed to dry on the funnel and scooped out and added to the dissolved mucin. The mixture was rotated on a roller rig overnight at 4°C. Excess ligand was removed using a scintered glass funnel and the Sepharose was washed using 400 mL of coupling buffer. Any remaining active groups were blocked by first washing through with 0.1 M Tris-HCl, pH 8 and then incubating on a roller rig with 100 mL of Tris-HCl either for two hours at room temperature or overnight at 4°C. The product was washed with three cycles of alternating pH each consisting of a 400 mL wash of 0.1 M sodium acetate, 0.5 M NaCl, pH 4 buffer followed by 0.1 M Tris-HCl, 0.5 M NaCl, pH 8 buffer. The support was washed with 35 mL (5 times volume) of phosphate buffered saline (PBS), 0.1 M citric acid (not pH adjusted to 2), 2 M sodium thiocyanate and finally PBS in order to remove any contaminants.

2.6.3.2 Purification on mucin-Sepharose

The mucin coupled support was packed in a Pharmacia C10/10 column to give a bed volume of 7 mL. Using the Beckman 'System Gold' low pressure FPC system, the column was equilibrated with 5 column volumes of PBS/azide (0.05%). The sample was loaded at a flow-rate of 2-3 column volumes per hour (0.3 mL/min). The column was then washed with PBS/azide until the A_{280} trace was < 0.05 . Elution took place with 0.1 M citric acid and the A_{280} was read by an on-line UV detector. The pH of the collected fractions was brought to neutral by the addition of a few drops of 1 M Tris base and fractions with protein were pooled and retained for further analysis. The column was washed with 2 M sodium thiocyanate until the baseline was constant.

2.6.4 Gel filtration

A PD 10 gel filtration column (Pharmacia) was employed. These are gravity operated polypropylene syringe-like columns which contain Sephadex G-25 for rapid desalting and buffer exchange. Each PD-10 column contains approx. 8.5 mL of Sephadex G-25 media with a bed height of 5 cm.

The top and bottom cap were removed and the end of the column tip was cut. The column was equilibrated with approximately 2.5 mL of 0.02 M Na_2HPO_4 , 0.5 M NaCl, pH 7.2. Up to 2.5 mL sample was loaded and the buffer exchanged sample was eluted using up to 3.5 mL of the phosphate buffer.

2.7 Protein Analysis

2.7.1 Determination of protein concentration

The total protein concentration in a sample was measured spectrophotometrically using Coomassie Plus Protein Assay Reagent (Pierce and Warriner Ltd., Cheshire, U.K.). The reagent is based on the assay devised by Bradford (1976) but the modified solution has enhanced linearity and sensitivity to low protein concentrations (Sedmak et al., 1977). Protein content was also determined using the microtitre adaptation of the Bradford assay (Biorad, New York, U.S.A.).

The concentration of haeme proteins were also spectrophotometrically estimated at 420nm, using calculated molar extinction coefficients of 56100, 45100, and 44500 L/mole/cm for tuna heart (MW 12,170), horse heart and *C. krusei* (MW 12,600) cytochrome *c* proteins respectively, and 57700 L/mole/cm for bovine haemoglobin.

2.7.2 Enzyme assays

2.7.2.1 Lysozyme assay

Lysozyme activity was determined by measuring the lytic activity against *Micrococcus lysodeikticus* cells based on the method used by Locquet et al. (1968). One unit of activity is defined as a change in absorbance of 0.001 per minute at 450 nm and 4°C in a 1 mL reaction mixture (1 cm light path). 100 µL of sample was mixed with 900µL of a 0.25 mg/mL suspension of *M. lysodeikticus* cells in 67 mM phosphate buffer pH 6.2 and the decreasing turbidity was monitored spectrophotometrically (Beckman DU 70 'TimeDrive' option) over 1 minute. A standard activity curve was constructed using known concentrations of hen egg white lysozyme.

2.7.2.2 α -Amylase assay

α -Amylase activity was measured using a modification of the method of Blachin-Roland and Masson (1989) adapted for use on a microtitre plate. The substrate used was 0.5% soluble starch in 15 mM Na₂PO₄ buffer (pH 5.8). The iodine stop reagent was prepared fresh by diluting 200 µL of stock solution (2.2% iodine (I₂)/ 4.4% potassium iodide (KI)) into 100 mL of 2% KI solution. An appropriate dilution of the lysed fraction was made up to 150 µL using 15 mM Na₂PO₄ buffer in a microtitre plate and pre-incubated at 50°C. At the beginning of the assay 150 µL of pre-incubated starch solution was added to the sample wells, and at various time intervals thereafter 15 µL of the reaction mixture was pipetted into 300 µL of iodine/KI stop solution on a separate microtitre

plate. At the end of the assay the absorbance was measured at 620 nm using a Dynatech MR7000 plate reader (Billingshurst, West Sussex, U.K.). The amylase activity is calculated by taking the gradient of the graph, dividing by the volume of the sample and adjusting the modified volume to give the full scale assay equivalent. This gives activity in terms of absorbency Units/mL/min where one absorbency unit is equivalent to the hydrolysis of 14.3 μg of soluble starch per minute at 50°C.

2.7.3 Preparation of samples for electrophoresis

2.7.3.1 *Trichloroacetic acid precipitation*

Trichloroacetic acid (TCA) protein precipitation concentrates protein in addition to cleaning up protein samples by the removal of nucleic acids and lipids, prior to their separation by reducing SDS-PAGE.

1. The sample volume was adjusted to 1 mL with buffer or distilled water in a 1.5 mL eppendorf tube. 333 μL of 100% TCA solution was added to give a final concentration of 25% TCA, mixed by inversion and incubated at 4°C for a minimum of two hours.
2. The precipitated proteins were obtained by centrifugation at 13,500 rpm for 7 minutes (Beckman Microfuge II) for small amounts of protein or at 6,500 rpm for large amounts (a visible precipitate). The supernatant was decanted carefully and discarded.
3. 1 mL acetone/hydrochloric acid (5 mM) solution was added, followed by a vortex mixing to break up the pellet.
4. The mixture was centrifuged and the supernatant decanted as in step 2. 1 mL acetone was added, vortexed, centrifuged and decanted again as in step 2.
5. The pellets were dried in a speed vacuum dessicator (Savant Speed Vac, sc 100) for 15 minutes. They were stored dry at -20°C or dissolved in sample buffer for gel analysis.

2.7.3.2 *Sample preparation*

Protein samples were either run untreated or if protein concentrations were low they were TCA precipitated first (described in section 2.7.3.1). TCA precipitated samples were dissolved in an appropriate volume (20-50 μL) of reducing sample buffer (Table 2.3). Unprecipitated samples were mixed 1:1 with sample buffer. Immediately before loading, the samples were reduced by boiling them in water for 3 minutes. They were briefly centrifuged to collect condensation on the sides of the tubes and to sediment any solid material.

2.7.4 Polyacrylamide gel electrophoresis

Discontinuous sodium dodecyl sulphate polyacrylamide gel electrophoresis (SDS-PAGE) was performed as described by Laemmli (1970). A discontinuous gel consists of a resolving or separating gel (lower) and a stacking gel (upper). The stacking gel acts to concentrate large sample volumes resulting in better band resolution. Polyacrylamide gels are made by polymerising acrylamide in the presence of a crosslinker N,N' -methylene-bis-acrylamide. The porosity of the gel is adjusted by either varying the total acrylamide concentration, or by altering the monomer:crosslinker concentration. The proteins to be analysed are denatured by the anionic detergent, SDS, which confers on them negative charge. The proteins are reduced by β -mercaptoethanol in the sample buffer, thus there is no secondary structure to affect the rate of migration and separation is wholly dependent on protein molecular weight (Shapiro et al., 1967).

2.7.4.1 Preparation of denaturing gels

All gel electrophoresis was carried out using Atto gel electrophoresis systems (Genetic Research Instrumentation).

1. A set of glass plates were cleaned with ethanol and assembled by fitting a rubber gasket, clamping at either side and standing in an upright position.
2. The resolving gel was prepared according to the formulation in Table 2.2 using all the stock solutions except 10% APS and TEMED. The solution was mixed gently by inversion and 0.5 μ m syringe filtered before addition of last two stock solutions. The solution was mixed gently by inversion and poured straight away (using a Pasteur pipette) into the assembled gel sandwich to fill 2/3 of the interplate space. Distilled water was carefully overlaid on top to ensure a level gel and to prevent air bubbles forming. The gel was left to polymerise for ~ 40 minutes. Then the water was drained off with filter paper.
3. The stacking gel was prepared according to the formulation in Table 2.2 in the same manner as the resolving gel. After pouring the gel, a 12-toothed comb was inserted between the two plates, in the top of the stacking gel and at a slight angle to prevent entrapment of air bubbles.
4. When the stacking gel was polymerised (after about 30 minutes) the comb was pulled out gently and the wells were washed with running buffer to remove any unpolymerised gel fragments.

Table 2.2 Gel formulations for discontinuous SDS-PAGE.

	Resolving gel	Stacking gel
Gel Solutions	12%	4%
Acrylamide/bis (30%) ^(a) (mL)	4.00	0.65
1.5 M Tris-HCl pH 8.8 ^(b) (mL)	2.50	–
0.5 M Tris-HCl pH 6.8 ^(c) (mL)	–	1.25
10% SDS (mL)	0.10	0.05
10% Ammonium persulphate ^(d) (mL)	0.05	0.025
TEMED ^(e) (mL)	0.005	0.005
Distilled water (mL)	3.35	3.05
Total volume (mL)	10.005	5.03

^(a) Acrylamide/Bis (30%): 29.2 g acrylamide and 0.8 g bisacrylamide were dissolved and brought to 100 mL with distilled water. The solution was stored at 4°C in the dark.

^{(b), (c), (e)} Stored at 4°C

^(d) 10% ammonium persulphate was prepared freshly with distilled water immediately before casting the gel.

^(e) TEMED: N, N, N', N'-tetramethylethylenediamine.

2.7.4.2 Loading and running gels

The clamps and rubber gasket were removed and the gel was slotted in position in the electrophoresis tank. The upper and lower reservoir were filled with running buffer (1 x) (Table 2.3). The prepared samples (10-20 µL) were loaded into the wells with a micropipette fitted with gel loading tips (Anachem). Molecular weight markers in the 12.3-78 kD range (Electran, BDH) were reconstituted in sample loading buffer to a concentration of 1 mg/mL and stored in 20 µL aliquots at -20°C. They were heat-treated and loaded in the same manner as the protein samples. The lid, connected to a power unit (Gibco, BRL-400L) was fitted to the electrophoresis box (Atta, GRI Ltd.) and a constant current of 15 mA per gel (400 Volts) was applied until the samples reached the resolving gel and then the current was raised to 20 mA per gel. The running time was 2-3 hours, after which, the bromophenol blue tracking dye had reached the bottom reservoir.

Table 2.3 SDS-polyacrylamide gel stock solutions.

Sample buffer	8 mL solution containing: (stored at -20°C)	0.5 M Tris-HCl, pH 6.8 (1.0 mL) Glycerol (0.8 mL) 10% SDS (1.6 mL) 2-6-Mercaptoethanol (0.4 mL) Bromophenol blue (0.004 g) Distilled water (4.2 mL)
Running buffer pH 8.3 (5x stock)	1 L solution containing: (stored at 4°C)	Tris base (15 g) Glycine (72 g) Sodium dodecyl sulphate (5 g)
Fixing solution	1L solution containing: (stored at room temp)	Glacial acetic acid (70 mL) Methanol (400 mL) Distilled water (530 mL)
Staining solution	1 L solution containing: (stored at room temp)	Methanol (417 mL) Acetic acid (167 mL) Coomassie blue G-250 (1 g) Distilled water (417 mL)
Destaining solution	1 L solution containing: (stored at room temp)	Methanol (333 mL) Acetic acid (100 mL) Distilled water (567 mL)

2.7.4.3 Gel staining and destaining

On completion of electrophoresis, the gel was removed and the stacking gel was cut away. The resolving gel was placed in fixing solution and gently shaken for 1-2 hours on a rocking platform (Luckham 4RT, Denley Instruments Ltd., England, U.K.) and then placed in a staining solution for a minimum of one hour (Table 2.3). The gel was destained with destaining solution and stored in a 20% methanol solution.

2.7.4.4 Gel documentation

Photographed gels were scanned at 560 nm using Beckman DU 70 spectrophotometer in gel scan mode, fitted with a gel slits accessory.

2.7.5 Western blotting

Polypeptides in a sample were separated using gel electrophoresis (Section 2.7.4) and immobilised onto a solid support. When current is applied to the polyacrylamide gel the proteins are transferred, and covalently bind, to nitrocellulose paper. When bound to the surface of the membrane, the proteins become extremely sensitive to immunodetection techniques.

2.7.5.1 Horizontal semi-dry electroblotting

The protein samples were electrophoresed on a denaturing, reducing polyacrylamide gel, but not fixed or stained. Rainbow markers (Amersham), with a molecular weight range of 14.3-200 kD, were used since these are transferred onto nitrocellulose and appear as differently coloured bands.

1. The gel was equilibrated in transfer buffer (Table 2.4) for 15 minutes. Pieces of filter paper (Whatman 3MM) and a piece of 0.45 μm nitrocellulose paper were cut to size (1-2 cm larger than the gel in each dimension), and soaked in transfer buffer for a minute.
2. Three pieces of filter paper, followed by the sheet of nitrocellulose were carefully laid onto the base of a BioRad electrobloter. Any air bubbles, which could interfere with electrophoresis, were removed. The gel was positioned, right way up, on the nitrocellulose, again taking care not to trap bubbles.
3. The lid of the electrobloter unit was closed and the power supply (BioRad 200/2.0) was set to a voltage of ~ 20 V, and a constant current of 0.8 A. Electrotransfer of the proteins took 30 minutes.

Table 2.4 Western Blot stock solutions.

Transfer buffer pH 8.8	1 L solution containing:	Tris (5.82 g) Glycine (2.93 g) 10%SDS (3.7 mL) Methanol (200 mL)
Blocking buffer	2 L solution containing:	Phosphate buffered saline (18.9 g) Casein (20 g) 0.1% Tween (2 mL)
Wash buffer	1 L solution containing:	Phosphate buffered saline (9.45 g) 0.1% Tween (1 mL)

2.7.5.2 Immunodetection of immobilised protein

1. The nitrocellulose membrane was 'blocked' by gently shaking in blocking buffer (Table 2.4) for 1 hour. The protein, casein, binds to the nitrocellulose and inhibits non-specific binding of the detecting antibody.
2. The membrane was placed on a glass plate in a humid incubating chamber, in order to keep the membrane moist. The chamber consisted of wet paper inside an air-tight plastic box. 5 μ L rabbit monoclonal antibody in 2.5 mL of blocking buffer was pipetted evenly over the nitrocellulose membrane which was incubated at room temperature for 45 minutes.
3. The membrane was washed with blocking buffer in a separate box 3 times for 10 minutes each.
4. A revealing antibody was used which was conjugated to horseradish peroxidase (HRP). This enzyme catalyses a colour-generating reaction which enables detection and staining of the monoclonal antibody. The membrane was treated with 5 μ L donkey anti-rabbit polyclonal IgG (H and L)-HRP in 5 mL blocking buffer as in step 2.
5. The blot was then washed with blocking buffer 3 times for 10 minutes each and with wash buffer (Table 2.4) for 10 minutes.
6. The blot was stained using diaminobenzidine (DAB). One 10 mg DAB tablet was dissolved freshly in 50mL PBS and 500 μ L of a 80 mg/mL nickel chloride solution was added dropwise.

7. The mixture was then filtered with Whatman no. 3 filter paper and, just prior to use a 10 μL drop of hydrogen peroxide solution was added. This was pipetted over the membrane which was allowed to develop a blue/black colour for 3-5 minutes for a strong antibody and 15-20 minutes for a weak antibody.

CHAPTER 3

MAGNETIC SUPPORT DEVELOPMENT AND CHARACTERISATION

3.1 Aim

The aim was to develop a stable, non-porous magnetic support particle, functionalised with metal chelating ligands, capable of immobilising first series transition metal ions and zinc ions with a specific interaction affinity for metal-binding proteins. A micron-sized magnetic support was required which had a low settling rate but was susceptible to rapid and facile separation under the influence of a magnetic field. Optimisation of the activation and coupling procedures and characterisation of the support in terms of its stability and functional group density at each stage in the derivatisation process was sought. A further aim was to elucidate the mechanisms of protein retention and in doing so determine the support capacity for specifically adsorbed protein. The establishment of optimal handling conditions, including binding, washing and elution process parameters was also a priority.

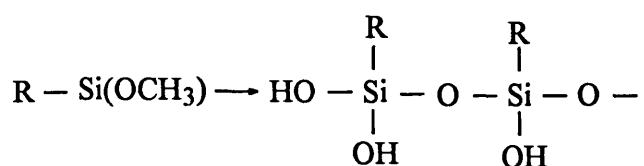
3.2 Introduction

The starting material selected for the preparation of magnetic chelators was an amine-terminated non-porous superparamagnetic iron oxide (BioMag[®], PerSeptive Biosystems, Framingham, Mass, U.S.A.) with a particle size of 0.5-1.5 μm diameter, density of $\sim 2.5 \text{ g/cm}^3$ and available surface area of between 100 and 150 m^2/g (Josephson, 1987). These iron oxide core particles comprise clusters of superparamagnetic crystals of dimensions roughly 300 \AA or less. Superparamagnetism is the magnetic behaviour which is characterised by responsiveness to a magnetic field without resultant permanent magnetization. The property is lost when the crystal size is increased much beyond 300 \AA (e.g. $> 500 \text{\AA}$) and the material then becomes ferromagnetic. In the absence of an externally applied magnetic field, because they are small and only weakly magnetic, they can be dispersed very easily as slow settling suspensions possessing extremely high surface areas. Magnetic separation times of less than about ten minutes can be achieved by contacting a vessel containing a dispersion of the particles with a pole face of a permanent magnet no larger in volume than the volume of the vessel, where the magnetic separation time is defined to be the time for the turbidity of the dispersion to fall by 95%

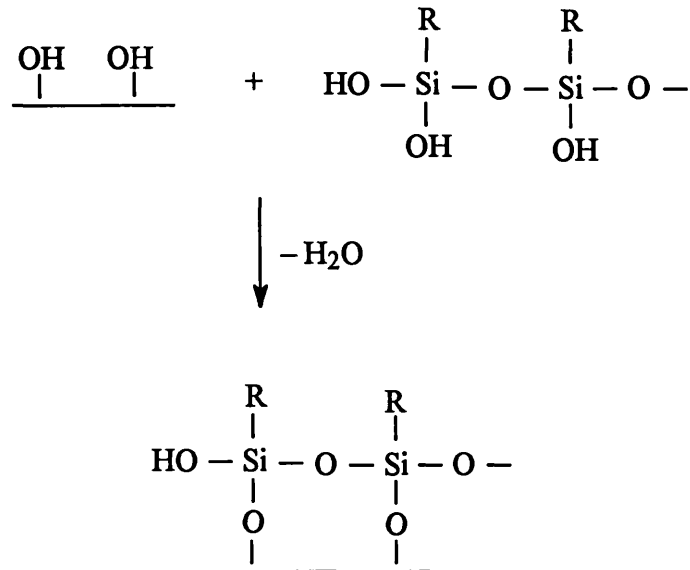
(Josephson, 1987). Once a field is applied they become magnetic, agglomerating readily due to inter-particle forces and are separated easily.

The BioMag[®] iron oxide core particles were surrounded by a stable silane coat. Silane coupling agents form metal siloxane bonds (M–O–Si) where M is the metal and Si is the coupling agent, silica (Plueddemanns, 1991), and this bond retains composite properties through harsh environments (Wang and Jones, 1993). Silanisation procedures carried out in the past employed air and / or oven drying in the dehydration step. When applied to silanisation of magnetic carrier particles, such dehydration methods allowed the silanised surfaces of the particles to contact each other, which tended to result in interparticle bonding, including, e.g., cross-linking between particles by siloxane formation, van der Waals interactions or physical adhesion between adjacent particles. This interparticle bonding yielded covalently or physically bonded aggregates of silanised carrier particles of considerably larger diameter (> 10 μm) than individual carrier particles of diameter range 1.5-10 μm (Hersh and Yaverbaum, 1976).

In the silanisation procedure followed according to the BioMag[®] patent (Josephson, 1987), silane (3-aminopropyl trimethoxysilane) was deposited on the metal oxide core from acidic organic solution. The silanisation reaction occurred in two steps. First, a trimethoxysilane was placed in an organic solvent (methanol), water and an acid (glacial acetic acid). It condensed to form silane polymers;



Secondly, these polymers associated with the metal oxide, perhaps by forming a covalent bond with surface OH groups through dehydration:



Adsorption of silane polymers to the metal oxide is also possible. However, good silane coats are only observed when there is evidence of chemical rather than purely secondary bonding between the silane primer and the metal oxide surface (Gettings and Kinlock, 1977). Good bonding across an interface requires maximal initial formation of M–O–Si, a minimum equilibrium concentration of water at the interface and polymer structures that hold silanols at the interface. The reaction of metal-siloxane bonds with water is of major importance for the stability of the metal-silane interface; the reaction below must not proceed too far to the right.



Adsorptive or covalent binding of the silane polymer to the metal oxide was accomplished by heating the silane polymer and metal oxide in the presence of a wetting agent miscible in both the organic solvent and water. Glycerol, with a boiling temperature of about 290°C, is a suitable wetting agent. Heating to about 160°-170°C in the presence of glycerol served two purposes. It insured the evaporation of water, the organic solvent (methanol) and any excess silane monomer. Moreover, the presence of glycerol prevented the aggregation or clumping and potential cross-linking of particles, that is an inherent problem of other silanisation techniques when dehydration is brought about by heating to dryness.

The presence of silane on iron oxide particles was indicated by the observation that after treatment with 6N hydrochloric acid, the iron oxide was dissolved and a white, amorphous residue was left which is not present if the unsilanised iron oxide is similarly digested. These results suggest that the acid insoluble residue was silane, though no direct evidence in the form of a test on the residue was presented (Josephson, 1987).

The starting point for work with non-porous magnetic supports was begun in the 1970s, in this department, where Robinson et al. (1973) were the first to develop a non-porous magnetic support for immobilised enzymes. The majority of published work on magnetic supports since then concerns their use with immobilised enzymes and in cell sorting applications. Comparatively little has been published on the application of magnetic affinity adsorbents in protein purifications and most of these have involved porous support structures (Dunnill and Lilly, 1974; Ennis and Wisdom, 1991; Mosbach and Andersson, 1977; Whitesides et al., 1983).

Two decades on, in this department, silane-coated BioMag[®] iron oxide particles were stabilised by grafting on a layer of polyglutaraldehyde as described by Halling and Dunnill (1979a). The subsequent chemical reactions that were adapted and developed to produce metal chelating ligands on magnetic supports, were based on the work carried out by Porath et al. (1975) and others who chemically derivatised agarose to invent the technique known as immobilised metal affinity chromatography (section 1.3)

3.3 Choice of Preparative Route

In the first step, common to all routes, glutaraldehyde was polymerised as a layer onto the surface of the amine-terminated particles. At alkaline pH glutaraldehyde is known to polymerise to a product containing free carbonyl groups (Monsan et al., 1975). Kawahara et al. (1992) suggested that a dilute (2-7%) aqueous solution of monomeric glutaraldehyde is converted to the polymeric form by the action of amino groups and the newly formed polyglutaraldehyde is involved in cross-linking reactions. The polyglutaraldehyde graft serves primarily by providing a stably coated mineral support and secondly as a facile means of coupling biological ligands through simple organic chemistry to the support. It may also offer some degree of corrosion protection by creating a diffusional barrier to H⁺ and OH⁻ transport.

From the polyglutaraldehyde-coated structure, which provides an aldehyde-bearing surface suitable for further activation, four different procedures were explored to introduce epoxide groups onto the outer surface of the coated particles, as described in

section 2.2 and shown schematically in Figure 3.1. *Routes 1, 2, and 3* involved a prior common reduction step (step III) involving NaBH_4 , to the alkoxide intermediate, but differed subsequently in the conditions employed to liberate the hydroxyl moieties, by hydrolysis, of the alkoxide intermediate (step IV). In *route 4* steps III and IV were bypassed and the polyglutaraldehyde-coated support (from step II) was epoxidated directly under reducing alkaline conditions (step V), without prior conversion of the carbonyl surface functions into free hydroxyls.

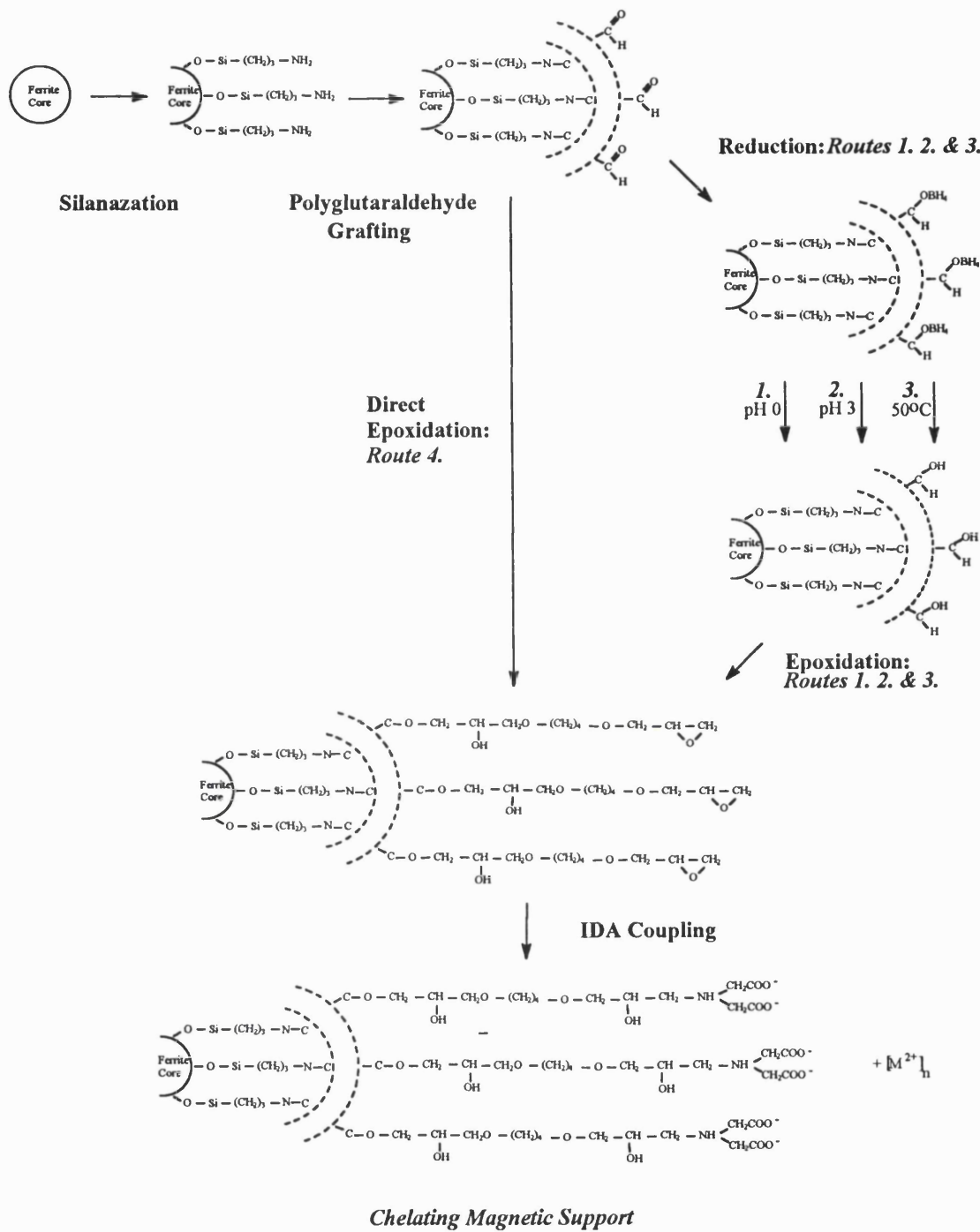


Figure 3.1 Scheme for preparation of non-porous magnetic chelator supports.

3.3.1 Comparison of preparative routes

In the first method (*route 1*) standard hydrolysis conditions (Harwood and Moody, 1990) were used but it was clear from visual observation that rapid corrosion of the support cores was taking place. It appeared that extreme acid conditions resulted in

attack of the iron oxide core by H^+ ions, leading to partial dissolution of the particles. Clearly milder hydrolysis conditions were required. The pH stability of polyglutaraldehyde-coated particles was therefore investigated and will be discussed in section 3.5.1. Efficient coupling of IDA to epoxy-activated surfaces generally involves long incubation times at elevated temperatures (50–60°C) and it was therefore necessary to show that the polyglutaraldehyde-coated structure would not fail under such conditions. In routes 2 and 3, hydrolysis of the alkoxide was carried out at 50°C (neutral pH) and at pH 3 (room temperature), respectively. Under these conditions no evidence of particle corrosion was detected.

The four preparations were epoxy-activated by means of a bifunctional oxirane. Epoxide activation chemistry was preferred over methods involving cyanuric chloride. Recent work in our laboratories and elsewhere has demonstrated that significant improvements in both stability and capacity of metal chelate supports are achieved using epichlorohydrin (Pitfield, 1992) and 1,4-butanediol diglycidyl ether (Morgan et al., in press) in place of cyanuric chloride. Bisoxiranes serve the dual function of introducing reactive oxirane groups onto the support surface and of stabilising the support by simultaneous cross-linking (Sundberg and Porath, 1974). In addition, the use of bisoxirane (1,4-butanediol diglycidyl ether) allows the attachment of metal chelating groups (iminodiacetic acid (IDA)) to the matrix via long hydrophilic spacers which reduce the risk of steric hindrance. The oxirane density of epoxy-activated supports from all four routes were measured prior to coupling with IDA and charging with Cu^{2+} ions (section 2.3.2). The active surfaces were then tested for their adsorptive properties in batch mode using proteins with known binding characteristics with Cu^{2+} -IDA systems (section 2.4.2).

A set of native haem proteins bearing variable numbers of surface accessible histidine residues were tested with the Cu^{2+} -charged magnetic chelator supports (Table 3.1). The affinities of these proteins for commercial metal charged IDA adsorbents are well documented (Hemden et al., 1989; Todd et al., 1994) and their binding behaviours can be attributed principally to the number, geometry and accessibility of their surface exposed histidine residues. It was thought that tuna cytochrome *c* had no accessible histidine residues (Hemden et al. 1989) and so it was used in initial experiments as a control protein. However, it was demonstrated (section 3.4) and subsequently found (Todd et al., 1994) to have a partially accessible histidine. A control protein with no accessible histidine residues (α -chymotrypsinogen) was not tested here but was introduced later on.

Table 3.1 Properties of selected proteins. Interaction strength is gauged towards Cu²⁺-IDA, where (-) represents no binding; (+) represents the weakest; and (+++++) the strongest binding. In the third column of data the figures in parentheses represent the % accessibility of the imidazole side-chain at that position in the amino acid sequence. The original sources of information are indicated by the superscripted letters in square parentheses (see key below).

Proteins species	Interaction strength	No. of surface histidines	Sequence position and % accessibility [c]	Other residues	possible
Bovine α -chymotrypsinogen	- [a]	0 [a]			
Tuna heart cytochrome <i>c</i>	- [b] / + [c]	1 [c]	26 (11%)	Trp 33 [c]	
Horse heart cytochrome <i>c</i>	+ [b] / ++ [c]	2 [c]	26 (11%) 33 (17%)		
<i>Candida krusei</i> cytochrome <i>c</i>	+++ [b,c]	3 [c]	26 (11%) 33 (17%) 39 (71%)	Cys 102 [c]	
Bovine haemoglobin	+++++ [d,e]	20 [d,e]			

[a] Sulkowski, 1987

[b] Hemden et al., 1989

[c] Todd et al., 1989

[d] Van Dam et al., 1989

[e] Wuenschell et al., 1990

3.3.2 Preparative route evaluation

All four support preparations exhibited selective binding of native haem proteins indicating the presence of surface attached IDA functions. The binding of haem proteins to the magnetic chelator supports was primarily mediated through bound Cu^{2+} ions because much lower amounts of adsorption to 'uncharged' supports were observed. The results of these experiments are summarised in Table 3.2. There is a clear relationship between the number of surface exposed histidines on a protein (Table 3.1) and the capacity of the Cu^{2+} -charged supports to bind them (Table 3.2), under the saturating conditions ($> 800 \mu\text{g protein/mL}$) of the test. Increasing the numbers of surface histidines was accompanied by increased capacities. The binding capacity of Cu^{2+} -IDA linked supports is evidently related to the intermediate epoxide density prior to coupling (Table 3.2). The support prepared by direct reductive epoxidation (*route 4*) possessed by far the highest epoxide density ($\sim 3000 \mu\text{moles/g}$) and also the highest capacities for selective adsorption of haem proteins (e.g. 89 and 105 mg protein/g for *C. krusei* cytochrome *c* and haemoglobin respectively). The results indicate that the binding capacity of the four support preparations decreased in the following order: *route 4* (direct epoxidation) $>$ *route 3* (50°C hydrolysis) $>$ *route 2* (pH 3 hydrolysis) $>$ *route 1* (pH 0 (zero) hydrolysis). The degree of success of the support preparations correlates with increasingly mild reaction conditions employed in their preparation. Examination of the results for non-specific binding suggests perhaps that supports prepared by *routes 3* and *4* show lower levels of non-specific binding than supports prepared by acid hydrolysis routes (*1* and *2*). Nevertheless the levels of non-specific binding were significant (it is shown further on (section 3.10) that it can be extinguished completely by raising the IDA ligand density on supports beyond $\sim 30 \mu\text{moles/g}$). The direct epoxidation route was selected for further development because this method gave the highest intermediate epoxide densities and specific binding capacities together with low non-specific binding, and also the additional advantages of being the easiest and quickest.

Table 3.2 Comparison of routes for the preparation of magnetic chelator particles.

	Ligand	Route 1	Route 2	Route 3	Route 4
Epoxide density ($\mu\text{moles/g}$) ^(a)	Oxirane	50	253	468	2969
Binding capacity: (mg/g) ^(b)					
Horse cytochrome <i>c</i>	Cu ²⁺ -IDA	nd	29.0	35.4	nd
	IDA	nd	19.7	21.7	nd
<i>C. krusei</i> cytochrome <i>c</i>	Cu ²⁺ -IDA	nd	70.7	nd	88.9
	IDA	nd	13.3	nd	13.0
Bovine haemoglobin	Cu ²⁺ -IDA	47.5	70.9	76.2	105.0
	IDA	15.5	13.3	20.8	15.1

^(a) Accurate measurements of immobilised Cu²⁺ densities were not possible at this time.

^(b) Binding experiments were performed using saturating levels of protein (~ 800 $\mu\text{g/mL}$).

3.4 Adsorption Profiles of Haem Proteins on Magnetic Chelator Supports Charged with Various Metal Ions

An important factor influencing selectivity in the recovery of proteins by immobilised metal affinity interactions is the choice of metal ion (section 1.3.2). Magnetic chelator supports prepared by *routes 2* (pH 3 hydrolysis) and *4* (direct epoxidation) were deemed successful in terms of maintenance of particle core integrity and protein binding capacity (section 3.3.2). They were selected for further testing (section 2.4.2) to compare the effect of zinc and the first row transition metal ions, copper and nickel, on the binding profiles of two native haem metal-binding proteins, namely, tuna heart cytochrome *c* (1 histidine), and *C. krusei* cytochrome *c* (3 histidines).

Estimation of chelated metal ion content by measuring spectrophotometrically at the maximum absorption wavelength in the case of the coloured metal ions was limited by the small quantities of adsorbent being handled and by the very low extinction coefficient

of Cu^{2+} at 800 nm. It has been shown by Hochuli and co-workers (1987) and others, that there is a 1:1 stoichiometry for the binding of Cu^{2+} ions to immobilised IDA when Cu^{2+} is supplied in excess. Atomic adsorption spectroscopy was therefore successfully used at a later stage to determine chelated metal ion density and by inference ligand density.

C. krusei cytochrome *c* demonstrated the highest binding affinity for Cu^{2+} -charged support, less the values for non-specific binding, (*route 4* - 63.8 mg/g; *route 2* - 52.34 mg/g) (Table 3.3). The subtracted values for non-specific binding (i.e., protein bound in the absence of metal ions) varied according to the preparation (~ 13-16 mg/g for Cu and Zn-charged and ~ 42 mg/g for Ni-charged supports). There was some specific binding of *C. krusei* cytochrome *c* to both preparations charged with Zn^{2+} ions but Zn^{2+} -charged *route 2* preparation does not demonstrate binding above background levels.

It was assumed that tuna heart cytochrome *c* had no accessible histidine residues because it was not retained by Cu^{2+} -charged chelating Sepharose in IMAC studies (Hemden et al., 1989). In fact, it does carry a partially accessible histidine residue, His 26 (Dickenson and Timkovich, 1975), which caused it to bind to Cu^{2+} -charged (22.0 mg/g) and to a lesser extent Ni^{2+} -charged magnetic chelator supports prepared by *route 4* (direct epoxidation). More recently Todd et al. (1994) have demonstrated that its binding to a Cu^{2+} -IDA-TSK gel is consistent with attachment via one histidine.

Both haem proteins demonstrated higher specific binding to magnetic chelator supports prepared by *route 4* compared to *route 2*. This is consistent with previous findings (section 3.3.2) that magnetic chelator supports prepared by direct reductive epoxidation of the polyglutaraldehyde coat demonstrate specific binding of more native 'his' proteins. This preparative route was followed in all further studies. In addition the highest specific binding affinity was found with supports charged with copper ions.

Table 3.3 Effect of metal ion species on binding of native 'his' proteins on magnetic chelator supports. Support preparations, *route 2* (pH 3 hydrolysis) and *route 4* (direct epoxidation), were charged respectively with Cu^{2+} , Ni^{2+} and Zn^{2+} metal ions and were tested with (a) tuna heart cytochrome *c* and (b) *C. krusei* cytochrome *c* and expressed as mg protein bound per g of support less non-specifically adsorbed protein in the absence of metal ions.

Protein bound	<i>Route 2</i>			<i>Route 4</i>		
	Cu^{2+} - charged	Ni^{2+} - charged	Zn^{2+} - charged	Cu^{2+} - charged	Ni^{2+} - charged	Zn^{2+} - charged
Tuna cytochrome <i>c</i> (mg/g support)	10.7	0.0	0.0	22.0	5.2	0.0
<i>C. krusei</i> cytochrome <i>c</i> (mg/g support)	52.3	0.0	10.8	63.8	2.1	3.5

3.5 Support Characterisation

3.5.1 pH stability

There was a need to determine early on in the handling of iron oxide particles a 'safe' pH range to work within, in terms of the extremes of acid and alkali on support integrity. The effect of pH on the liberation of Fe^{3+} ions from amine terminated BioMag[®] was investigated using the relatively insensitive potassium thiocyanate test (section 2.3.5.1). The results were expressed as a percentage of the amount of iron oxide particles used. Shaking the samples had little effect on the results.

Very acidic pH conditions have a dramatic effect upon the iron oxide particles and this is illustrated in Figure 3.2. The particles were resistant to corrosive attack above pH 2.5 but could not tolerate anything below this. Strong alkaline conditions did not appear to compromise particle stability but this was not unexpected in view of the fact that alkaline corrosion products (Fe^{2+} and Fe^{3+} ions) are not soluble under alkaline conditions and are therefore not detectable using this assay.

Corrosion can take place under acidic and alkaline conditions. Corrosion in, for example, NaOH takes place by oxidation/reduction which leads to secondary corrosion products that precipitate at the particle surface. According to Oelkrug et al. (1992) the chemical reactions responsible for multi-step precipitation are as follows. First, Fe(II) goes to Fe(III) in two steps; $\text{Fe} \Rightarrow \text{Fe}(\text{OH})_2 \Rightarrow \text{FeOOH}$. Then Fe(III) goes to Fe(II) in a dissolution/precipitation reaction resulting in $\text{FeOOH} \Rightarrow (\text{FeOOH})^-_{\text{aqueous}} \Rightarrow [\text{Fe}(\text{OH})_2]_{\text{crystallite}}$. With increasing contact in alkaline solution, the dominant changes at a metal surface are the appearance of small precipitated particles of roughly 200-500 nm in diameter. The 200 nm particles are ~ 15 nm high and look like low flat islands uniformly clustered. With increasing oxidation/reduction cycles the particles grow. Further crystallisation occurs at existing particles to leave most of the surface coated.

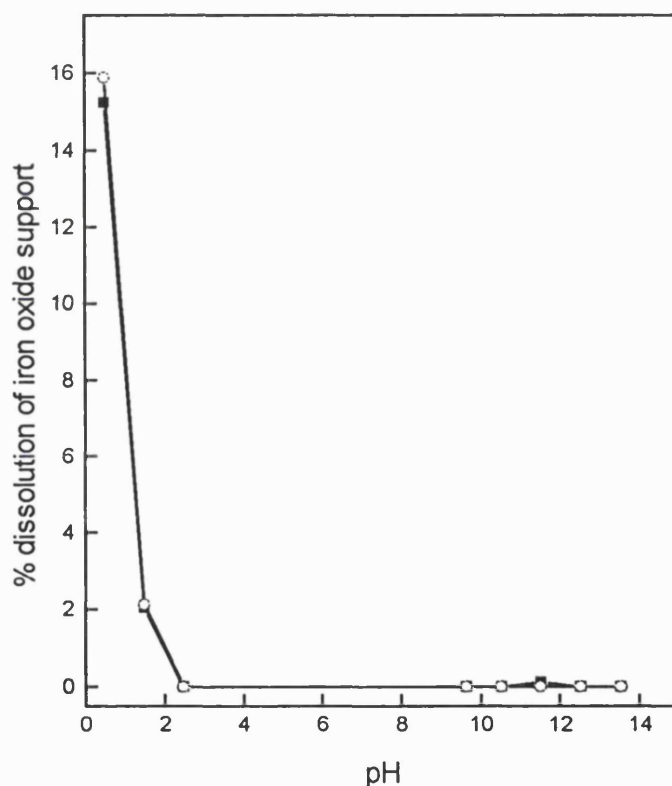


Figure 3.2 Effect of pH on the destruction of amine terminated iron oxide magnetic particles. Shaken (■) and un-shaken (○).

3.5.1.1 Effect of successive coating and coupling chemistries on corrosion resistance

An accelerated acid corrosion test was used to investigate the corrosion resistance of magnetic particles after each step in the preparation of magnetic chelator supports and thereby demonstrate the effect of successive coating and coupling chemistries on the support stability.

The stages of support preparation tested were as follows: iron oxide core particle (starting material) → amine terminated iron oxide → polyglutaraldehyde-coated particle → epoxide-activated particle → IDA coupled particle.

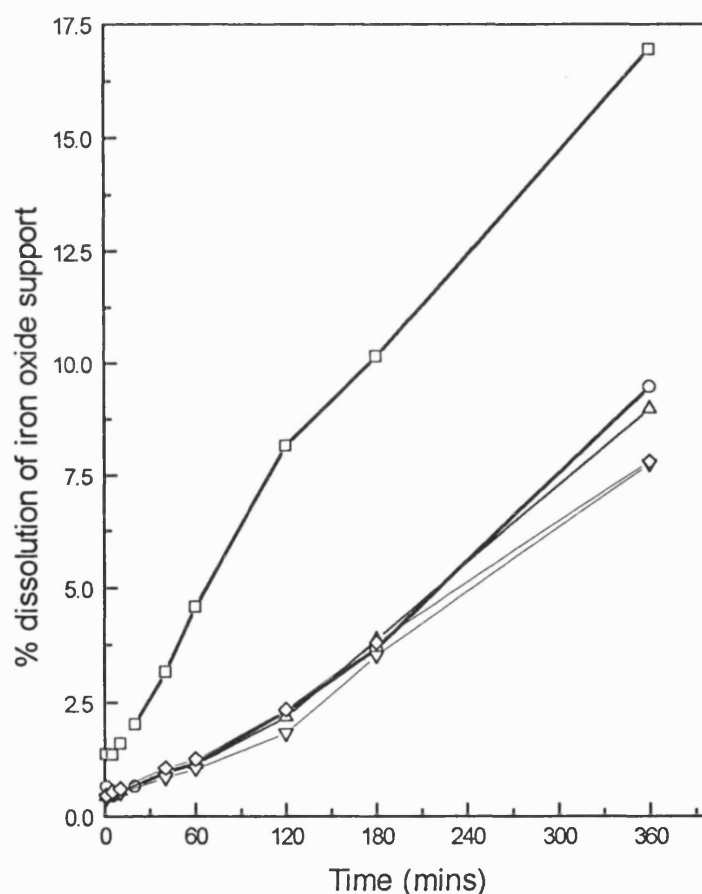


Figure 3.3 The effect of magnetic support preparation process coating and coupling reactions on the acid corrosion resistance of the iron oxide core particles exposed to 1 M HCL (pH 0). Iron oxide core (□), silane coated (amine-terminated) (○), polyglutaraldehyde coated (△), epoxide activated (◇) and iminodiacetic acid coupled (▽).

Successive treatments of the iron oxide core appear to reinforce a protective diffusion barrier which is demonstrated by increased resistance of the particles to acid corrosion. It is probable that the increasing degrees of cross-linking and depth of coat, increase the time for H^+ to get through to the metal oxide surface. The strongest line of defence against acid attack was conferred by the amine-terminated siloxane coat - the iron oxide particle before this appearing very vulnerable. Studies of hydrolysed γ -aminopropyl triethoxysilane interaction with inorganic surfaces concluded that a thick, dense poly-(aminosiloxane) coating was formed on the surface (Wang and Jones, 1993). This appears to offer the core particle considerable protection from acid attack. The protection afforded by successive treatments was not as dramatic but becomes more pronounced after prolonged exposure to 1 M HCl (6 hours). There was quite a significant jump in corrosion resistance from the polyglutaraldehyde to the epoxide-activated support at the longer test times and this could be due to a cross-linking of neighbouring epoxide groups. After 1 hour in the presence of 1 M HCl just 1% of IDA-coupled support has corroded compared to 1.2% amine-terminated and 4.6% uncoated ferric oxide. The preparation process conferred an apparent 4.5 fold increase in corrosion resistance to the chelator support in these accelerated corrosion tests. The factor decreased to 2-fold after exposure to acid for 6 hours.

3.5.2 Functional group density

An important aspect of support characterisation was the determination of functional group densities at each of the key stages in the preparation of magnetic chelator supports. Thus, the effect of the efficiency of derivatisation on ligand density and ultimately support binding capacity could be identified and optimised. Existing assay methods were developed to measure primary amino group, epoxide group and immobilised metal ion densities (sections 2.3.1 to 2.3.3) which were routinely employed to monitor batch to batch variations in preparations. Optimisation of the latter two are discussed in section 3.10.

3.5.2.1 Primary amino group determination

Silane coated, amine-terminated BioMag[®] iron oxide particles were quoted by the manufacturers to have an amine group density of $\sim 240 \mu\text{moles/g}$. This figure was determined using a ninhydrin-based assay (Advanced Magnetics Inc., personal communication) and represents the total immobilised amine content, including the unreactive or inaccessible amine groups. The TNBS and SPDP assay methods determine free or reactive amine groups and present a more realistic measurement of useful amino group density. The silane coated particles were assayed using these two methods (section

2.3.1). The assays were performed in triplicate on different batch particle preparations and a functional amine group density of 93-100 $\mu\text{moles/g}$ was recorded. Polyglutaraldehyde-coated amine-terminated particles were assayed and amine content was found to be negligible ($\sim 1.4 \mu\text{moles/g}$) confirming the efficient coating and therefore blocking of the silane groups. Based on these figures the polyglutaraldehyde graft coated about 98.5% of the silane coated (amine-terminated) particle, thus lashing the silane layer in place and forming a second defensive layer around the iron oxide core.

3.5.3 Magnetic support recycle for re-use

Support/buffer compatibility and the effects of re-using non-porous magnetic chelator support particles were investigated as described in section 2.4.5. Support matrices are generally expected to suffer decreased performance with re-use and age, the ligand density being the most important indicator of support efficiency. Support robustness and chemical stability were characterised by monitoring the liquid supernatant washes for metal ion leakage from the core particle over 3 successive cycles under accelerated ageing conditions. An extreme regime for equilibration, stripping and cleaning was devised in order to present a real challenge to the iron oxide supports. The series of process steps per cycle were divided into 3 phases. The first was 'preparation' (i.e., equilibration with 0.1 M acetate buffer, pH 3.8, charging with CuCl_2 solution and washing with 0.1 M acetate buffer, pH 3.8), the second was 'testing' (i.e., equilibration with 0.1 M phosphate buffer pH 7.0, binding with protein solution in the same buffer, washing with 0.1 M phosphate buffer pH 7.0 and eluting with 0.1 M acetate buffer, pH 3.8) and the third was 'regeneration' (stripping with 0.1 M EDTA and cleaning with 0.1 M NaOH). Fe ions, as a percentage (w/w) of total Fe support content at the start of cycle 1, are plotted for the 3 process phases (Figure 3.4).

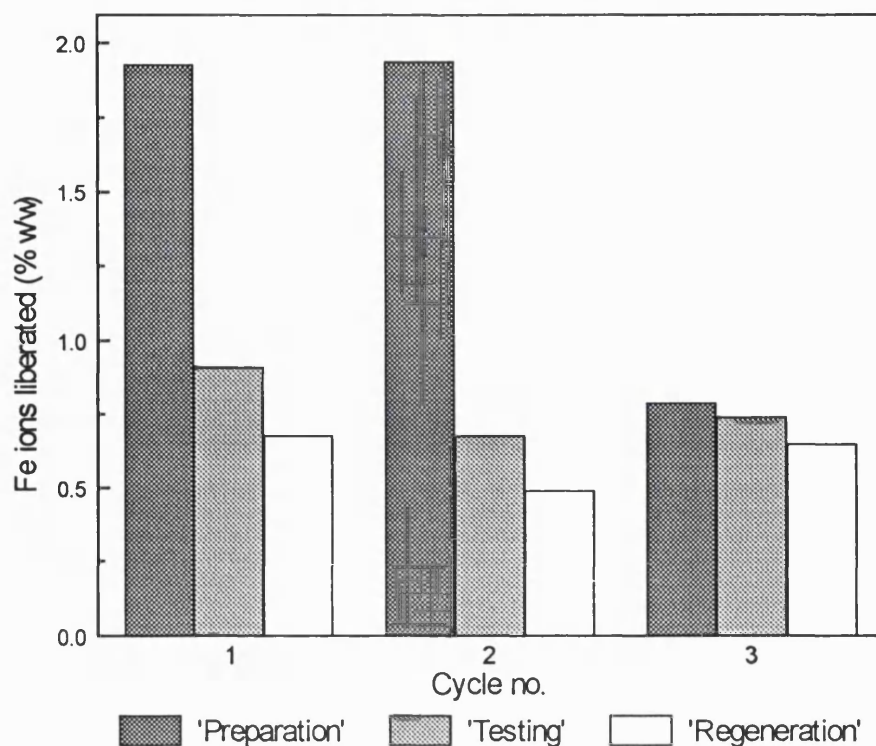


Figure 3.4 Effect of recycle, over 3 successive cycles, on magnetic support integrity. Leaching of iron during preparation (i.e., equilibration, charging and washing), testing (i.e., equilibration and washing) and regeneration (stripping and cleaning) was monitored by atomic absorption spectrophotometry.

Low levels of Fe ion leaching occur over 3 successive cycles with 3.52% lost in the first cycle, 3.23% lost in the second and 2.33% lost in the third (9.1% lost in total over 3 cycles). Fe ion leakage values (% w/w) expressed per unit volume (mL) indicate the effect of buffer type on the extent of leakage occurring (Figure 3.4). In relative terms the 'preparation' phase which comprises exclusively of washes with 0.1 M acetate buffer, pH 3.8 has the highest levels of Fe ion leakage. The 'testing' phase (less than one third acetate pH 3.8 buffer, the remainder phosphate pH 7 buffer), by comparison, displays lower leakage, but leakage levels are raised again in the 'regeneration' phase of EDTA and NaOH washes. It appears that the magnetic support is particularly vulnerable when exposed to the low pH acetate buffer and to a lesser extent to what would have been thought of as severe EDTA and NaOH (section 3.5.1) solutions. The low pH (3.8) buffer probably has a mild corrosive effect on the magnetic support. 0.1 M phosphate buffer,

1M NaCl pH 7 was tested for its suitability as a storage buffer for magnetic support and over a period of 1 month only 0.018% of the Fe leached into the bulk phase.

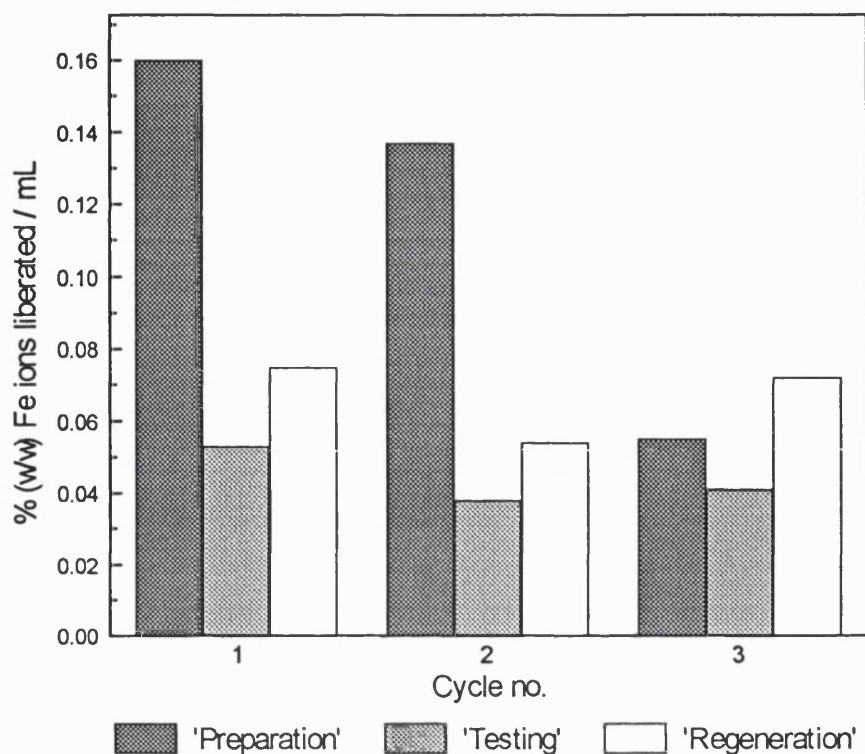


Figure 3.5 Effect of 'preparation', 'testing' and 'regeneration' phases (i.e., buffer composition) on Fe ion liberation (% total w/w) per unit volume (mL).

A drop in immobilised Cu^{2+} ligand density ($\mu\text{moles/g}$ support) occurs over the 3 cycles (20% reduction overall) (Figure 3.6) and support protein binding capacity mirrors this. This is substantially greater than the degree of damage to the core particle which suggests that the coat is being compromised. Thus, prolonged support use with recycle under these conditions leads to low levels of Fe ion leaching, a drop in ligand density and protein binding capacity and a slight increase in non-specific protein adsorption to uncharged support. Phosphate buffer (0.1 M) at neutral pH is a suitable solution for short and long-term magnetic support storage.

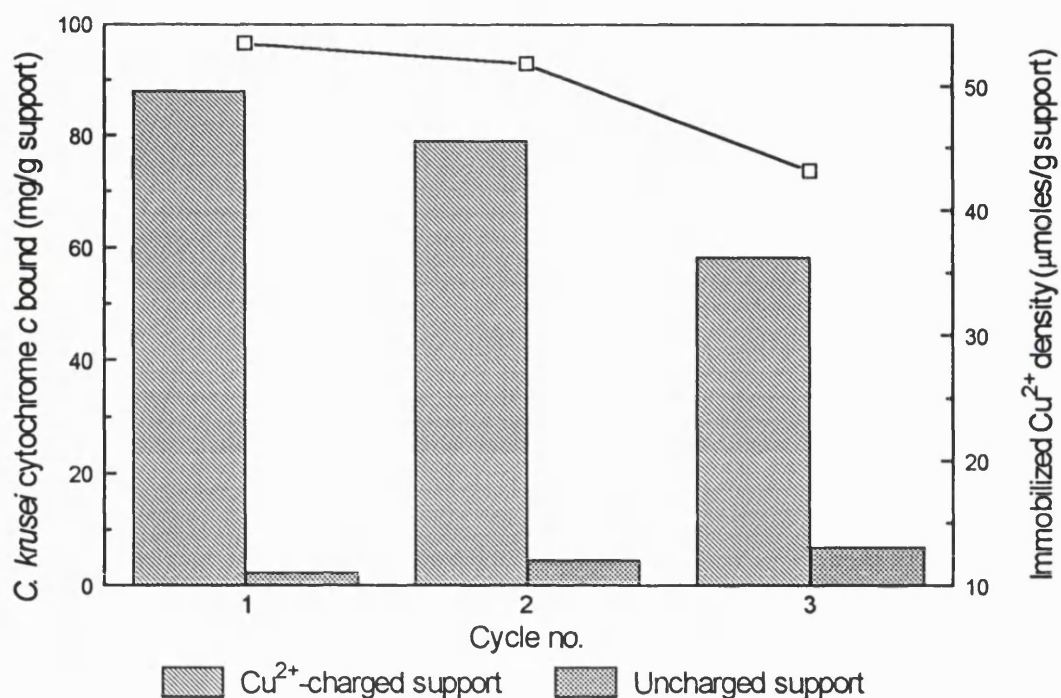


Figure 3.6 Effect of support recycle over 3 successive cycles on immobilised Cu²⁺ (ligand) density (□) and protein binding capacity.

Future work will need to investigate more thoroughly iron oxide support core stability, i.e., iron core leaching over 10 cycles of re-use. In the 'accelerating ageing' recycle experiments described in this section the support was stripped with EDTA and then recharged with metal ion between each cycle. It should not be necessary to strip the support of metal ions after use with a strong chelating agent such as EDTA which can only serve to threaten the iron core. Future work should investigate the effective ligand density over successive cycles without stripping and re-charging the support each time.

3.5.3.1 Particle aggregation

In all experiments, supports were carefully scrutinised for evidence of particle aggregation resulting effectively in larger particles with reduced surface area and accompanied by increased settling rates. There was little visible or experimental evidence for agglomeration, due to polyglutaraldehyde coating, epoxidation or coupling reactions. Furthermore, repeated exposure of particle preparations to magnetic fields of 0.1-0.3 Tesla did not result in particle aggregation. In contrast, Halling and Dunnill (1979a) found that aggregation of sub-micron (but ferromagnetic) particles of manganese zinc ferrite and larger (3-7 µm) nickel carbonyl process powder, did occur. Aggregation of sub-micron particles was principally caused by polyglutaraldehyde-coating, whereas

aggregation of nickel powder was primarily due to magnetic attractive forces rather than coating.

3.6 Comparison of Magnetic Chelator Supports with Chelating Sepharose 6B

A direct comparative evaluation of the binding capacity of magnetic chelator and chelating Sepharose 6B supports for the native metal-binding 'his' protein *C. krusei* cytochrome *c* was carried out in batch mode. The batch binding experiment was performed as detailed in section 2.4.3 and elution was effected by a step fall in pH and finally by displacement with imidazole. The results are shown in Table 3.4.

The capacity of magnetic chelator supports compares favourably with the more conventional and commonly used chelating Sepharose 6B supports. The maximum adsorbed under saturating batch binding conditions when expressed per unit volume or weight (see Table 3.4) is shown to be 12% greater for the chelator magnetic supports. Any non-specific or background binding was eliminated for both support types by extensive washing prior to elution of the bound fraction.

Table 3.4 Comparison of batch binding capacities of chelating magnetic and Sepharose 6B supports.

	Chelating Sepharose 6B		Magnetic chelator support	
	mg bound/mL bed volume ^(a)	mg bound/g of bed volume ^(b)	mg bound/mL batch volume ^(c)	mg bound/g dry weight ^(d)
<i>C. krusei</i> cytochrome <i>c</i> bound	32.62	31.98	37.14	36.46

^(a) Protein bound per unit volume of Sepharose 6B in a packed column.

^(b) Protein bound per unit weight of Sepharose 6B in a packed column (1.02 g/mL).

^(c) Protein bound per unit settled volume of magnetic support (1.11 g/mL).

^(d) Protein bound per unit dry weight of magnetic support.

The density of Sepharose 6B in a packed bed (1.02 g/cm^3) was determined by subtracting the weight of the column un-packed from the column packed to a known bed volume. The working density of the magnetic supports (1.11 g/mL) seems low for a non-porous support with such a high surface area ($100\text{-}150 \text{ m}^2/\text{g}$). This may be explained by the particle conformation which is comprised of clusters of 300 \AA crystals suspended in a liquid medium. Very fine particles are incapable of dense packing and entrain water (Josephson, 1987) and this would explain why the magnetic particles exist as a 'wet cake' with a lot of associated liquid when they are separated on a magnet and the liquid phase has been removed.

The amount of protein eluted by pH 3.8 and imidazole washes, expressed as a percentage of the total recovered, imply a higher binding affinity of *C. krusei* cytochrome *c* for magnetic chelator supports (Figure 3.7). The first 0.1 M acetate pH 3.8 buffer wash elutes 47% of the bound protein from the magnetic support and 68% from the Sepharose 6B support, hence the protein is more tightly bound and more difficult to elute from the magnetic chelator support. 53% and 32% respectively is dissociated by washing with 0.1 M imidazole solution. Therefore complete desorption would be expected by eluting with imidazole buffer alone. The high binding affinity that exists between the magnetic chelator and the metal-binding protein is desirable to ensure strong interaction and successful recovery in a batch process where a high partition coefficient (very close to 1) and association constant are necessary.

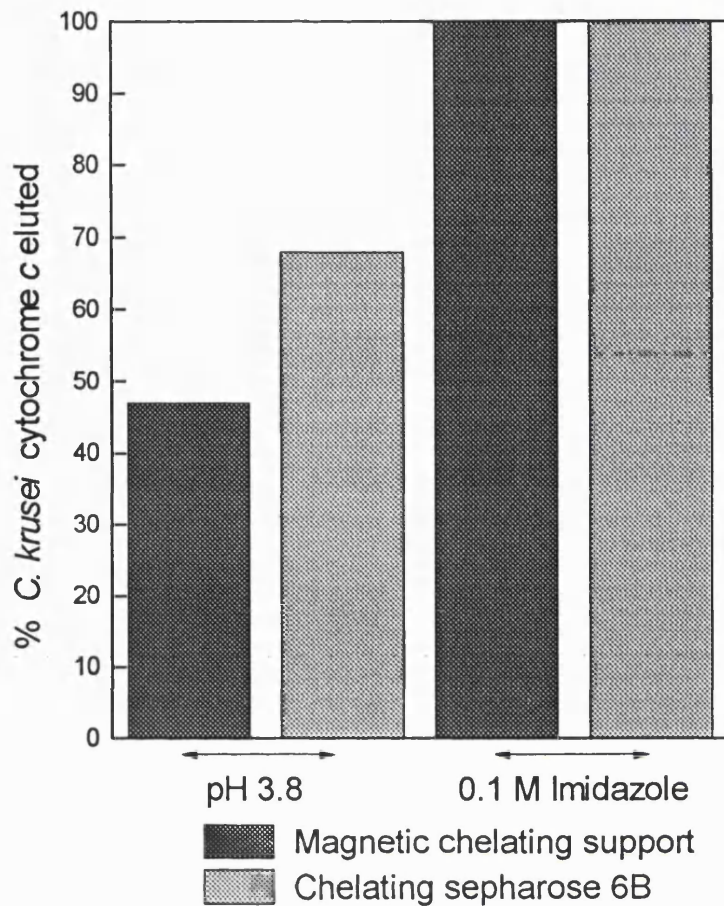


Figure 3.7 Comparison of elution pattern of *C. krusei* cytochrome *c* from chelating magnetic and chelating Sepharose 6B supports, expressed as a percentage of total eluted in one wash with pH 3.8 or 0.1 M imidazole. Magnetic chelating support (dark grey bar) and chelating Sepharose 6B (light grey bar).

3.7 Separation of Native Metal-binding Proteins

The protein binding characteristics, that is, maximum protein capacity and dissociation constant, of Cu^{2+} -charged magnetic chelator supports were tested using a range of commercial haem proteins. The test proteins used (Table 3.1) were selected for their varied affinity for M^{2+} -IDA surfaces, resulting from the nature of their surface exposed amino acid side chains; primarily the number and geometry of accessible histidines (Hemden et al., 1989; Porath et al., 1975; Porath and Olin, 1983). The resolution profiles of three haem proteins, tuna (one histidine), horse (two histidines) and *C. krusei* cytochrome *c* (three histidines), separated by immobilised metal affinity chromatography

on a Cu^{2+} -charged Chelating Sepharose column are illustrated in Figure 3.8. Increased strength of binding (in the presence of 1 M NaCl) correlated with increased numbers of surface accessible histidine residues which required decreasing pH to effect protein elution. Tuna cytochrome *c* eluted in the flowthrough and horse and *C. krusei* cytochromes *c* at eluted at pH 6.0 and 3.8 respectively in accordance with the findings of Hemden et al. (1989). They claimed that the frequency of accessible histidine residues were as follows: tuna (0 histidines), horse (1 histidine) and *C. krusei* (2 histidines), which would have explained the non-interaction of tuna cytochrome *c*. However, this is not the case and is demonstrated and discussed further in sections 3.4 and 3.8.

α -Chymotrypsinogen A, which has a low affinity for metal chelates, was used as an indicator of non-specific binding (Sulkowski, 1987). The expected order of binding to Cu^{2+} -IDA is, in order of increasing affinity: α -chymotrypsinogen, tuna heart cytochrome *c*, horse heart cytochrome *c*, *C. krusei* cytochrome *c* and bovine haemoglobin.

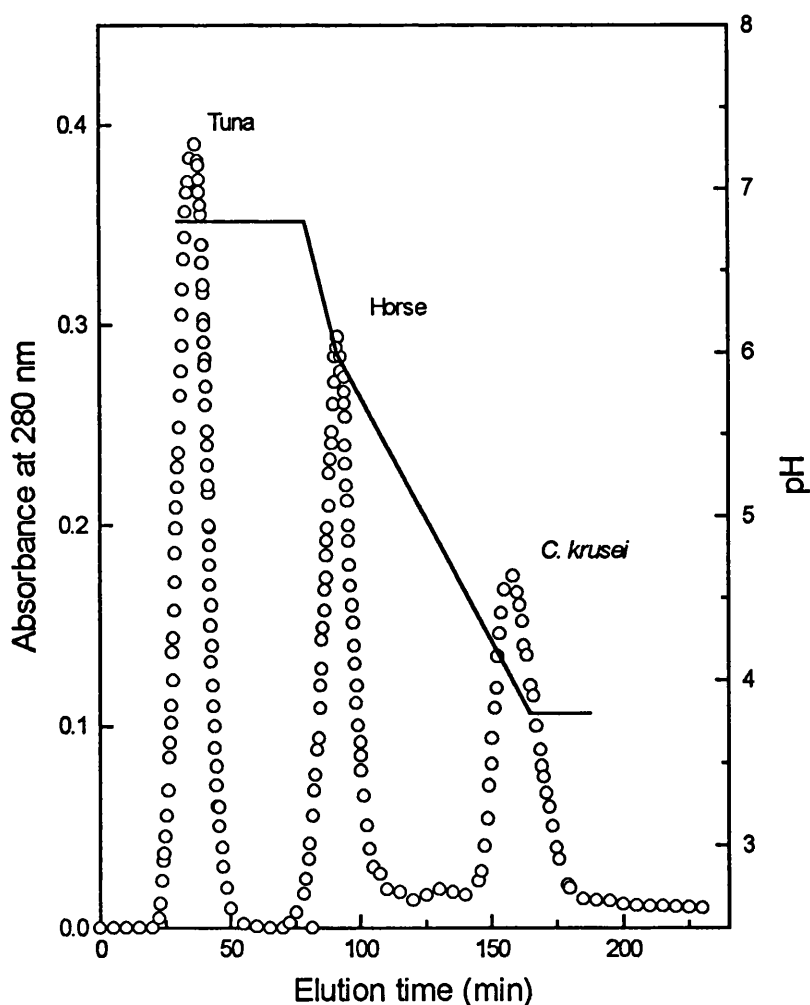


Figure 3.8 Resolution of cytochromes *c* on IDA- Cu^{2+} -charged Chelating Sepharose column. Elution by pH gradient.

3.8 Adsorption Isotherms

Adsorption isotherms of the native haem proteins were measured at near neutrality at which pH surface histidines are unprotonated and free to coordinate bound metal ions (Todd et al., 1994). Equilibrium was achieved very quickly for *C. krusei* cytochrome *c* and haemoglobin binding to Cu²⁺-charged magnetic chelators but 15 h contact was routinely employed to ensure that equilibrium was attained for all test proteins and supports under investigation.

Equilibrium binding studies (Hutchens et al., 1988) have shown that a simple Langmuir-type model may not adequately describe protein binding to immobilised metal affinity supports. According to the Langmuir model, adsorption is characterised by a single binding energy and a maximum adsorption capacity corresponding to monolayer surface coverage. Binding heterogeneity as evidenced by non-linear Scatchard plots (Scatchard, 1949) is often observed for tightly binding proteins (Hutchens et al., 1988; Hutchens and Yip, 1990). Scatchard plots for the haem proteins (Figure 3.9) demonstrated that only tuna cytochrome *c* gave a linear fit implying a single class of interaction site which could be described by the simple Langmuir model (eqn. 3.1). The proteins with more than one surface histidine clearly exhibited more complex binding behaviour synonymous with at least two different types of binding affinities. The bi-Langmuir model (eqn. 3.2) adequately describes the equilibrium binding data for these proteins. Simple Langmuir binding is described by eqn. 3.1, where Q is the amount of protein adsorbed per g of support and C is the liquid-phase protein concentration at equilibrium. This model is fully described by two constants, a dissociation constant K_d and the maximum capacity for adsorbed protein, Q_{max} .

$$Q = \frac{Q_{max} \cdot K_d C}{1 + K_d C} \quad \text{Eqn. 3.1}$$

In the bi-Langmuir model (eqn. 3.2), two types of binding sites, tight and weak, are each respectively described by a binding constant, $K_{d,A}$ and $K_{d,B}$.

$$Q = \frac{Q_{max A} K_{d,A} C}{1 + K_{d,A} C} + \frac{Q_{max B} K_{d,B} C}{1 + K_{d,B} C} \quad \text{Eqn. 3.2}$$

The maximum capacities at these two sites are correspondingly, $Q_{max A}$ and $Q_{max B}$ and the overall Q_{max} equals the sum of the two capacities.

Figure 3.10 shows equilibrium adsorption isotherms for proteins on magnetic chelator supports with ligand densities of 35 $\mu\text{mol/g}$ and Table 3.5 shows the Langmuir constants derived from the data in Figure 3.10.

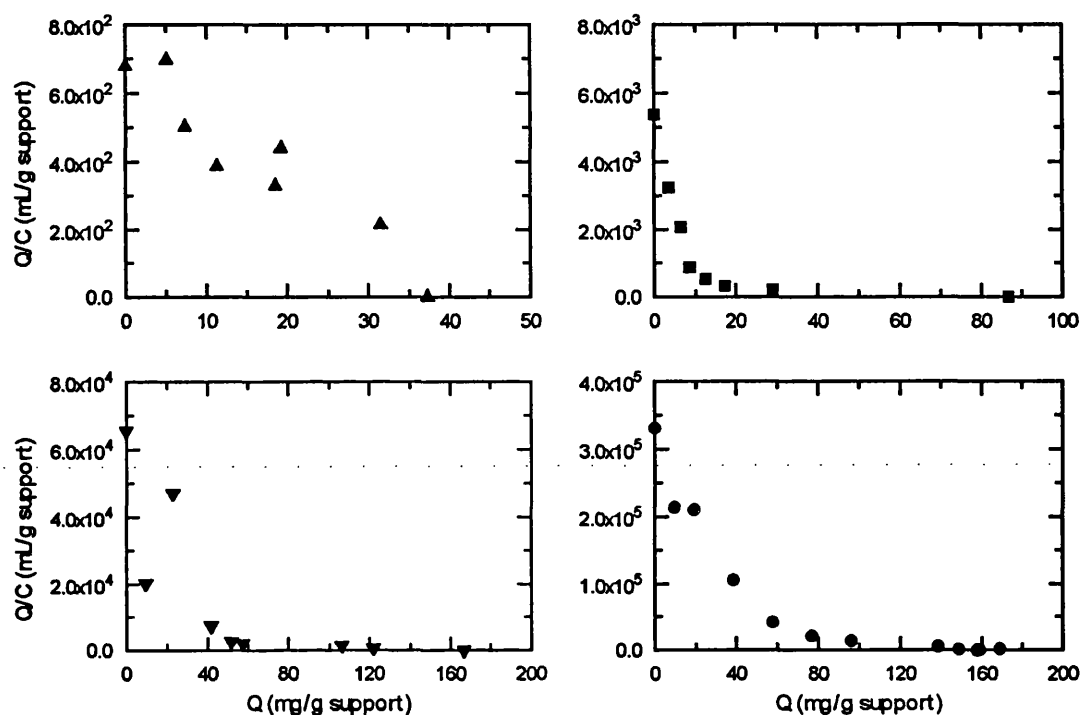


Figure 3.9 Scatchard plots of tuna cytochrome *c* (▲), horse cytochrome *c* (■), *C. krusei* cytochrome *c* (▼) and bovine haemoglobin (●) equilibrium binding data.

α -Chymotrypsinogen, selected as a probe for non-specific binding, failed to bind in both the presence and absence of copper ions, as expected. The binding of haem proteins with surface exposed histidines on the other hand, was specifically mediated through immobilised metal ions. Very low levels of binding occurred for all test proteins regardless of their numbers of surface histidines in the absence of copper ions. For Cu^{2+} -charged supports the number of surface exposed histidines greatly influences the binding strength and capacity for the individual proteins.

Adsorption of proteins with multiple and strongly interacting surface histidine residues, namely *C. krusei* cytochrome *c* and especially haemoglobin, was very strong (first binding constants, K_{dA} of $\sim 4 \times 10^{-8}$ M for *C. krusei* and $\sim 2 \times 10^{-9}$ M for haemoglobin) and of high capacity (Q_{max} values of ~ 168 mg *C. krusei* cytochrome *c* and ~ 158 mg haemoglobin per g of support). The other haem proteins, tuna cytochrome *c* with a single

partially exposed histidine at position 26, and horse cytochrome *c*, with the same histidine at position 26 and an additional partially accessible histidine residue at position 33, superficially displayed very similar equilibrium binding profiles (Figure 3.10) though clear differences are observed in Scatchard plots. A linear fit for tuna cytochrome *c* and a curve for horse cytochrome *c* indicate dissimilar binding profiles and imply a single site of interaction for the former and more than one for the latter (Figure 3.9). The maximum capacity of Cu²⁺-charged magnetic chelator particles for *C. krusei* cytochrome *c* was roughly twice that of the horse cytochrome *c* and four times that of tuna cytochrome *c*. According to Todd and co-workers (1994) this increased capacity for tightly bound proteins either reflects heterogenous numbers of binding sites with differing affinities, or increased compaction of bound protein molecules through simultaneous multi-site interaction compared to low affinity single binding sites. They also suggested that the protein binding constant depends on the availability of copper sites and that binding is significantly weaker at low surface concentrations of copper that presumably cannot support multiple site interactions.

Strictly speaking the tightness of binding is reflected by the initial slope of the isotherm (i.e. $Q_{\max.A}/K_{d.A}$). The initial slope of the isotherm for haemoglobin was roughly 5 times that of *C. krusei* cytochrome *c*, which in turn was 50 and 500 times larger than those of horse and tuna cytochromes *c* respectively (Table 3.5). These results are in good agreement with the expected order of binding strength observed for these proteins (Table 3.1) with commercial Cu²⁺-IDA derivatized TSK (Todd et al., 1994) and Sepharose gels (Hemdan et al., 1989).

No binding of tuna and horse cytochromes *c* to Zn²⁺-charged supports was noted and only very weak low capacity binding (< 30 mg/g support) was observed with *C. krusei* cytochrome *c*. These findings were also reported by Hemden and co-workers (1989) for the same proteins on Zn²⁺-IDA Sepharose. Haemoglobin bound to Zn²⁺-charged supports, but this too was at very low levels (< 50 mg/g support) compared with, for example, the binding to Cu²⁺-charged supports.

Table 3.5 Langmuir binding parameters for native proteins to magnetic chelator supports. Adsorption isotherms of proteins have been fitted to the Langmuir and bi-Langmuir models.

Protein species	$Q_{\max A}$ (mg/g support)	K_{dA} (M)	$Q_{\max B}$ (mg/g support)	K_{dB} (M)	Tightness of binding, Q_{\max}/K_d (mL/g support)
Tuna cytochrome <i>c</i>	37.29	5.00×10^{-6}			6.78×10^2
Horse cytochrome <i>c</i>	8.43	1.27×10^{-7}	78.34	3.30×10^{-5}	5.32×10^3
<i>C. krusei</i> cytochrome <i>c</i>	34.15	4.15×10^{-8}	132.71	6.79×10^{-6}	6.53×10^4
Bovine haemoglobin	41.76	1.97×10^{-9}	116.06	1.10×10^{-7}	3.31×10^5

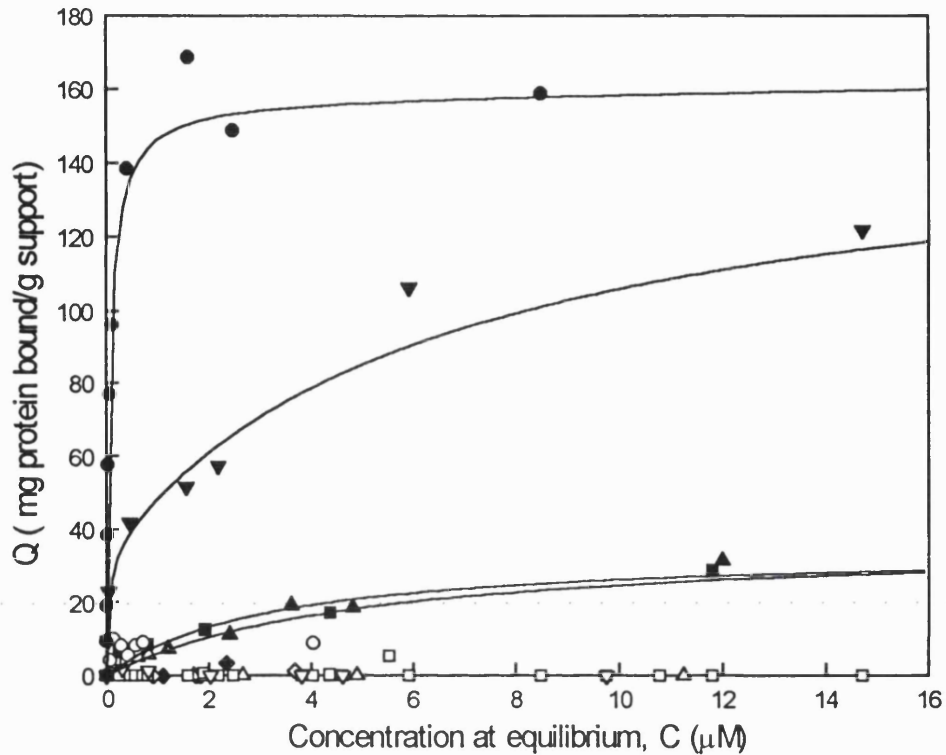


Figure 3.10 Equilibrium binding isotherms for native proteins on IDA-Cu²⁺ magnetic chelator supports. The solid line through the data for tuna cytochrome *c* represent the fit of Langmuir isotherms (eqn. 3.1). Solid lines through the data for *C. krusei* and horse cytochromes *c* and haemoglobin represents the fit of the bi-Langmuir model (eqn. 3.2). Bovine α -chymotrypsinogen (\blacklozenge, \diamond), tuna cytochrome *c* ($\blacktriangle, \triangle$), horse cytochrome *c* (\blacksquare, \square), *C. krusei* cytochrome *c* ($\blacktriangledown, \triangledown$), bovine haemoglobin (\bullet, \circ). Cu²⁺-charged IDA (filled symbols); uncharged IDA (open symbols). The IDA-ligand density of the magnetic chelator supports used was 30 $\mu\text{moles/g}$.

3.9 Desorption of Haem Proteins

The batch desorption of native haem proteins bound to Cu^{2+} -charged magnetic chelator support is illustrated in Figure 3.11. Protein-loaded supports were incubated with one wash of each buffer (increasing elution strength from left to right) and the amount of protein released expressed as percentages of the total bound (section 2.4.2). An IDA-ligand density of $28 \mu\text{moles/g}$ was measured. The ligand density of support preparations influences the ease of elution and this is discussed further in section 3.11. In accordance with the isotherm data presented above in section 3.8, tuna and horse cytochromes *c* showed very similar elution patterns indicating similar strengths of interaction with this support. Substantial elution of both proteins could be achieved in one wash of acetate, pH 4.8 (~ 35% and 27% respectively) rising to 75% (tuna) and 83% (horse) with one wash of acetate, pH 3.8. Essentially complete desorption of these cytochromes *c* could be achieved using one wash of 100 mM imidazole. *C. krusei* cytochrome *c* and especially haemoglobin exhibited much tighter binding than the other cytochromes *c* - only 29% of the *C. krusei* cytochrome *c* was eluted with one wash at pH 3.8, while eluted haemoglobin was barely detectable (3%) in the liquid-phase under these conditions.

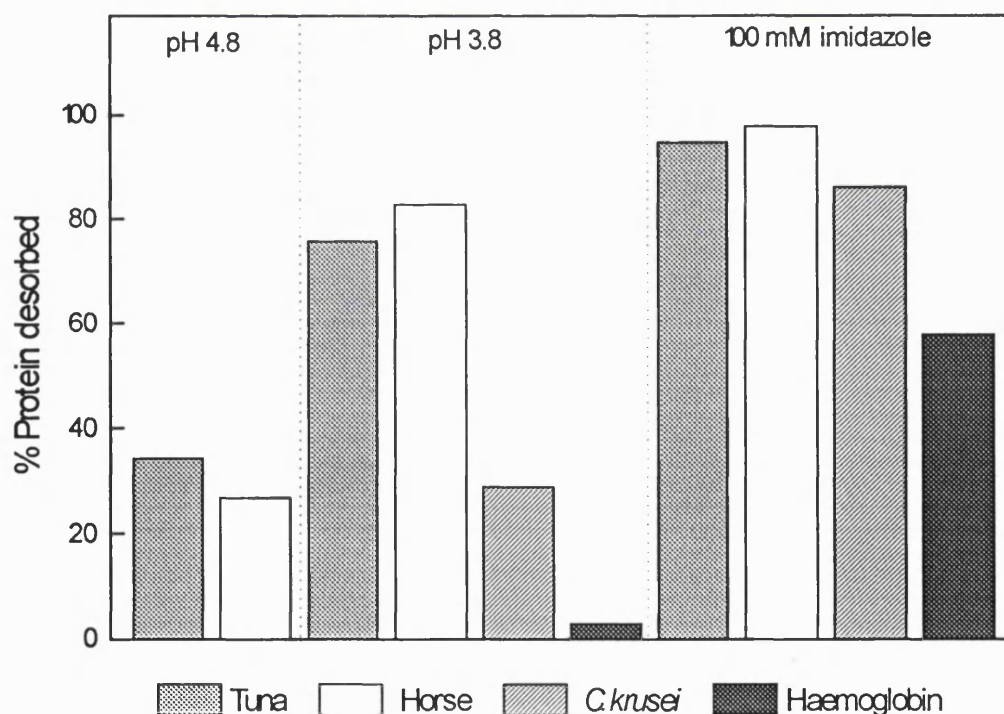


Figure 3.11 Batch desorption of haem proteins from 'loaded' Cu^{2+} -charged magnetic chelator supports.

Single washes with 100 mM imidazole however could effect efficient desorption of *C. krusei* cytochrome *c* (86%) and even haemoglobin (nearly 60%). Virtually complete desorption of *C. krusei* cytochrome *c* from Cu²⁺-charged magnetic supports was demonstrated with two successive washes, while complete recovery of haemoglobin required three successive washes.

3.10 Optimisation of Supports

Previous findings have shown (section 3.3.2) that clear relationships exist between the intermediate epoxide density, the ligand density and the protein binding capacity. Optimisation experiments were undertaken to improve, in the first instance, epoxide group densities, followed by iminodiacetic acid (IDA) ligand densities with the overall aim of increasing protein binding capacity. Polyglutaraldehyde-coated particles were epoxy-activated, IDA coupled and screened for their ability to bind *C. krusei* cytochrome *c*, under saturating conditions - systematically varying first the concentration of 1,4-butanediol diglycidyl ether (Figure 3.12) and then of IDA (Figure 3.13).

Epoxide activation, which is the stage in the preparative process after polyglutaraldehyde coating, fulfils the dual role of providing a highly active oxirane group for coupling of IDA, as well as acting as a spacer molecule (10 carbon atom chain) to minimise steric hindrance effects and thus provide room for IDA molecules to bind. A final concentration of 50% 1,4-butanediol diglycidyl ether was used in the initial magnetic chelator studies. To optimise the epoxide group densities the supports were activated with a range of final percentage concentrations of 1,4-butanediol diglycidyl ether (section 2.4.1.1). The results are shown in Figure 3.12.

The optimum concentration of 1,4 butanediol diglycidyl ether was found to be about 40-45%. At higher concentrations (> 50%), inter-molecular cross-linking of epoxide molecules may account for the sharp drop in surface oxirane density that is observed (Morgan et al., in press) (Figure 3.12). Supports prepared under these conditions (40% epoxide and 12% IDA) possessed high surface oxirane (7000 $\mu\text{moles/g}$), affinity ligand densities ($\sim 32.5 \mu\text{moles Cu}^{2+}/\text{g}$) and protein binding capacities (> 127 mg *C. krusei* cytochrome *c/g* support) and such figures were consistently recorded in tests of this type.

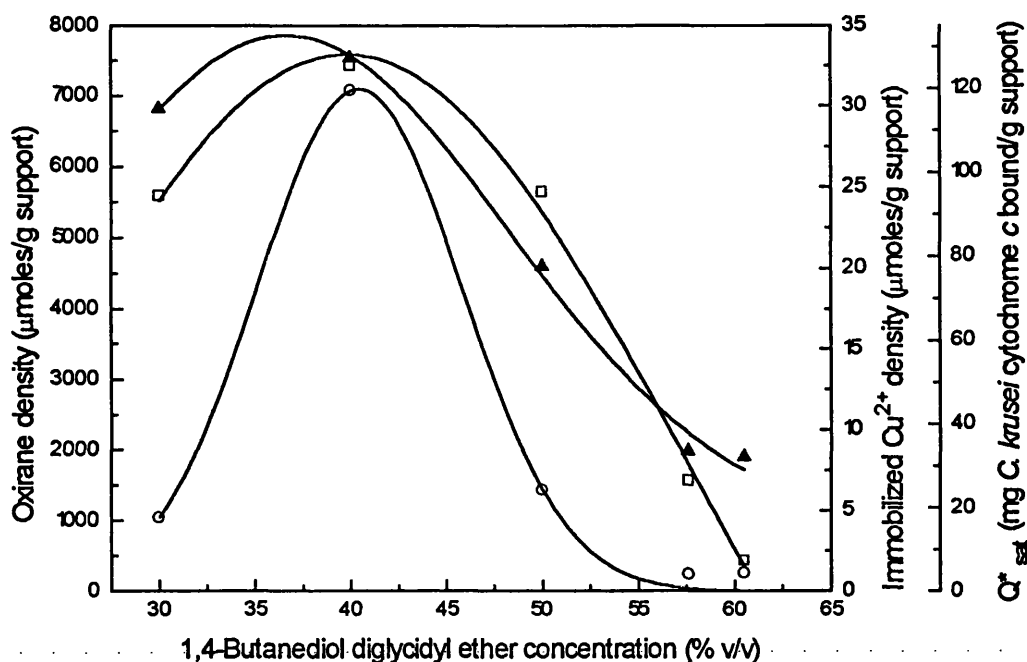


Figure 3.12 Effect of 1,4-butanediol diglycidyl ether concentration on surface oxirane density, ligand density and specific protein binding capacity. Epoxy-activated supports were coupled using 12% (w/v) IDA and protein binding capacities were measured using *C. krusei* cytochrome *c* at ~ 800 μg/mL. Surface oxirane (O), immobilised Cu²⁺ (□) and binding capacity (▼).

Comparison of the oxirane and Cu²⁺ densities shows roughly two orders of magnitude difference. The possible explanations for this are that the great majority of oxiranes may be buried within the surface polymer coat or that neighbouring epoxides crosslink with each other, or a combination of both. The net effect would be a reduction in the number of epoxide functions accessible to react with IDA.

Further substantial increases in ligand density were discovered by raising the IDA concentration during coupling (Figure 3.13). Ligand densities in excess of 60 μmoles/g were achieved by activating polyglutaraldehyde supports with 1,4-butanediol diglycidyl ether and coupling them with IDA at a concentration of 30% (w/v) (Figure 3.13). A saturation curve begins to plateau above 12% IDA at which stage maximum protein binding capacity has also been reached. Figure 3.14 illustrates the effect of immobilised Cu²⁺ density on the binding of *C. krusei* cytochrome *c*. Specific binding, due solely to immobilised Cu²⁺ ions (Q^*_{Cu}), was calculated by subtracting values for binding to

uncharged supports from those to charged supports. The relationship is roughly sigmoidal, maximal levels of binding ~ 200 mg/g support were achieved at 30-40 μ moles/g.

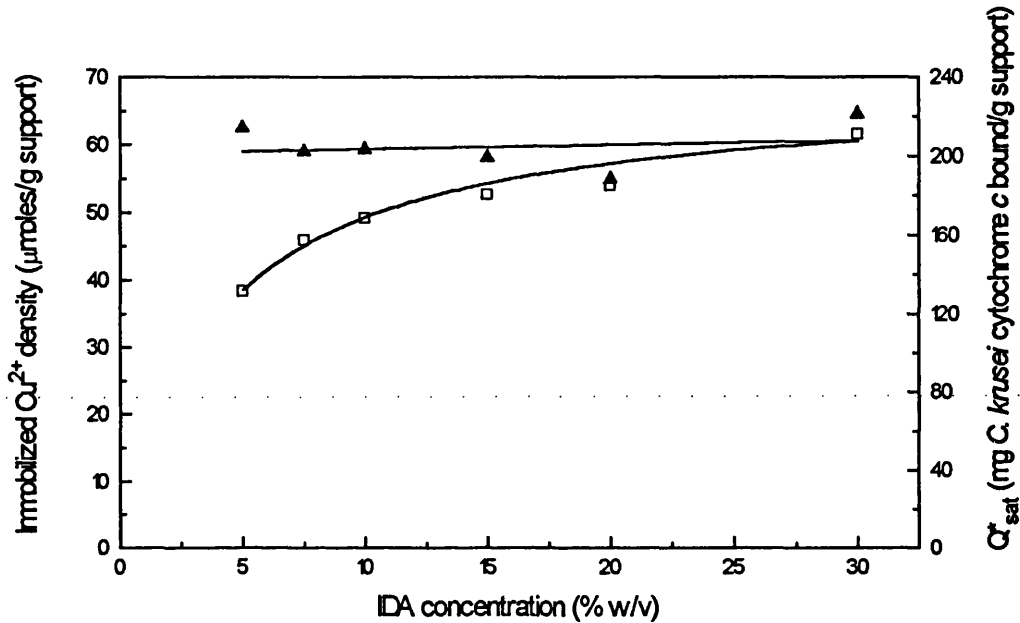


Figure 3.13 Effect of IDA concentration on the immobilised Cu^{2+} (ligand) density and protein binding capacity of charged magnetic chelator supports. Supports were epoxy-activated using 50% 1,4-butanediol diglycidyl ether and coupled with IDA at various concentrations. Protein binding capacity was measured using *C. krusei* cytochrome *c* at ~ 1 mg/mL. Immobilised Cu^{2+} (\square), binding capacity (\blacktriangle).

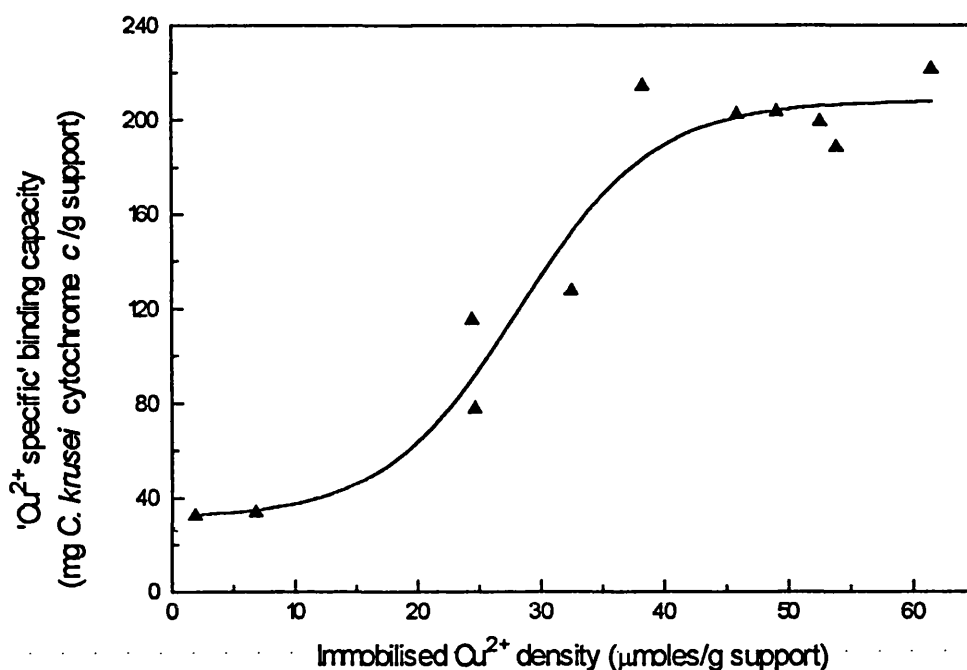


Figure 3.14 Relationship between Q_{Cu}^* , the 'Cu²⁺ specific' binding capacity and the immobilised Cu²⁺ ligand density for magnetic chelator supports.

Although maximum protein capacity has been reached, the benefit of supports prepared with high ligand densities became apparent when it was found that the background non-specific binding of cytochromes *c* could be prevented completely by raising the IDA ligand density above 30 µmoles/g (Figure 3.14). This ligand density is equivalent to a calculated spacing, between successive IDA functions, of 36 Å - roughly the same as the molecular dimensions of cytochrome *c* (34 Å). Direct interaction with the base matrix is the probable cause of non-specific binding of proteins on supports with relatively low IDA substitution (< 30 µmoles/g). Typical figures for the amounts of protein that can be covalently attached to amine-terminated BioMag[®] particles are 200-300 mg/g (Josephson, 1987). In view of this, it is interesting that the capacities of Cu²⁺-charged magnetic chelator supports, following coating, epoxidation and coupling steps are still at these levels (e.g. maximum Q_{sat} values of 221 mg *C. krusei* cytochrome *c* and 229 mg of haemoglobin per g of support).

3.11 Effect of Ligand Density on Protein Binding

The similarity in behaviour for tuna and horse cytochromes *c* 'binding to' and 'desorbing from' charged magnetic chelator particles (Figures 3.10 and 3.11), using supports with Cu^{2+} densities below 30 $\mu\text{moles/g}$, was somewhat surprising in view of the results published by Hemdan and co-workers (1989) together with our own observations on the interaction of tuna, horse and *C. krusei* cytochromes *c* with Cu^{2+} -IDA Sepharose (Figure 3.8). Although binding to metal chelates is dominated by histidine residues, the contribution of other residues (especially Cys and Trp) cannot be ruled out. For example, the bulky sidechain of Trp33 in tuna cytochrome *c* (see Table 3.1) may contribute to a similar extent to the 11% exposed imidazole side chain of His33 in horse cytochrome *c*. However, recent work (Todd et al., 1994) together with my own findings (Figure 3.15) indicate that this behaviour is dependent on the Cu^{2+} -ligand density of the support.

Batch adsorption experiments with test proteins and many support preparations, differing in their surface IDA density, allowed further characterisation of the surface binding properties of the supports to be made. Figure 3.15 shows the effects that increasing ligand density had on the binding of haem proteins to charged and uncharged magnetic chelator particles. Capacities are expressed as effective monolayer surface areas covered per g of support. Specific surface areas (m^2/g) were calculated using cited molecular dimensions (Louie and Brayer, 1990; Stryer, 1988), and experimentally determined binding capacities (Q_{sat}). The assumptions made were that no change in molecular footprint occurs on binding to the support surface and that loose cubic packing is adopted. For the tightly-binding haemoglobin and *C. krusei* cytochrome *c*, Cu^{2+} -IDA densities below $\sim 10 \mu\text{moles/g}$ elicited only very low levels of binding ($< 20 \text{m}^2/\text{g}$). By 15-20 $\mu\text{moles/g}$ however binding coverage rose steeply for both proteins (slopes of $\sim 3.2 \text{m}^2/\mu\text{moles}$ of Cu^{2+} for haemoglobin and $\sim 3.3 \text{m}^2/\mu\text{moles}$ of Cu^{2+} for *C. krusei* cytochrome *c*) with further increase in density of Cu^{2+} ions. Limiting coverages of $\sim 60 \text{m}^2/\text{g}$ ($\equiv 212 \text{mg/g}$) and $\sim 115 \text{m}^2/\text{g}$ ($\equiv 209 \text{mg/g}$) were achieved at Cu^{2+} densities of $> 30 \mu\text{moles/g}$ and $> 40 \mu\text{moles/g}$ for haemoglobin and *C. krusei* cytochrome *c* respectively.

The binding of tuna and horse cytochromes *c*, was very different to that of *C. krusei* cytochrome *c* and haemoglobin. Up to Cu^{2+} ligand densities of 28-30 $\mu\text{moles/g}$ both cytochromes *c* bound at low levels of $\sim 20 \text{m}^2/\text{g}$. However on increasing the ligand density beyond this point the behaviour of the two proteins differed considerably. The surface coverage increased quite steeply for horse cytochrome *c* in a roughly linear

fashion (slope of $\sim 1.75 \text{ m}^2/\mu\text{moles Cu}^{2+}$) and limiting coverage (for packing of cytochromes *c*, $\sim 115 \text{ m}^2/\text{g}$) was approached at $\sim 80 \mu\text{moles}$ of Cu^{2+} per g of support.

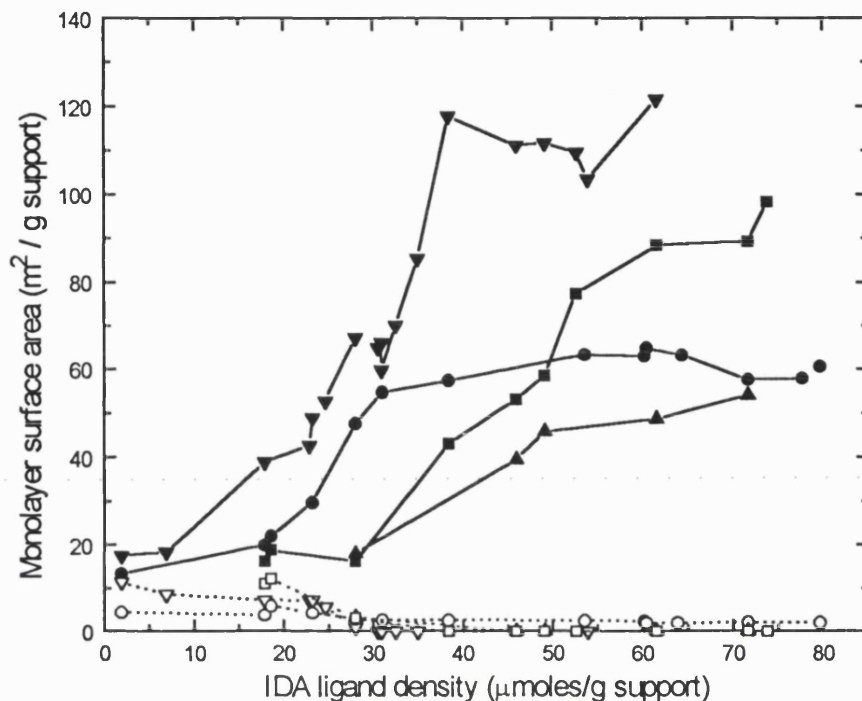


Figure 3.15 Effect of IDA ligand density on the binding of haem proteins to magnetic chelators supports. Binding is expressed as effective monolayer surface areas calculated using the molecular dimensions of the proteins (cytochromes *c* - 34\AA diameter sphere, haemoglobin tetramer - 55\AA diameter sphere) assuming 'cubic' packing, and the measured binding capacity figures per g support. (Maximum binding levels of 221 mg/g for *C. krusei* cytochrome *c* and 229 mg/g for haemoglobin to Cu^{2+} -charged particles are equivalent to monolayer surface areas of $\sim 122 \text{ m}^2/\text{g}$ and $\sim 65 \text{ m}^2/\text{g}$ respectively. Tuna cytochrome *c* ($\blacktriangle, \triangle$); horse cytochrome *c* (\blacksquare, \square); *C. krusei* cytochrome *c* ($\blacktriangledown, \triangledown$); and bovine haemoglobin (\bullet, \circ). Cu^{2+} -charged IDA (filled symbols); uncharged IDA (open symbols).

The effect of increasing density (from 30 to $72 \mu\text{moles Cu}^{2+}/\text{g}$) on the binding of tuna cytochrome *c* was less dramatic (slope of $\sim 0.7 \text{ m}^2/\mu\text{moles Cu}^{2+}$) and limiting coverage was not reached. These findings are in good agreement with recent work (Johnson and Arnold, 1995; Todd et al., 1994).

Although protein molecules interacting with solid surfaces generally undergo some conformational changes (Gekko and Hasegawa, 1986; Kondo et al., 1993), monolayer surface areas of the magnetic chelator particles were based on the assumption that the molecular dimensions would not change on binding. For cytochromes *c* there is strong indirect evidence to support this assumption. Arnold's group employed the Tempkin model (Johnson and Arnold, 1995) to describe reversible binding of cytochromes *c* to Cu²⁺-IDA-TSK gel. The model describes a physically relevant parameter, Q_o (the protein surface capacity per unit binding energy) that is consistent with estimates of cytochrome *c* limiting coverage based on its crystal structure (Louie and Brayer, 1990; Stryer 1988). The footprint of the haemoglobin tetramer on the other hand is likely to change quite considerably. Changes in shape or compressibility of globular proteins (Gekko and Hasegawa, 1986; Kondo et al., 1993) increase with increasing molecular flexibility - ranging from 0 (no change - the "hardest") through to 11×10^{-12} cm²/dyn (largest changes - the "softest"). Haemoglobin has an adiabatic compressibility of 10.9×10^{-12} cm²/dyn at 25°C (Gekko and Hasegawa, 1986; Kondo et al., 1993) and is therefore classified as a very soft protein. By contrast cytochrome *c* is one of the hardest proteins examined to date, having an adiabatic compressibility, measured under identical conditions, of 0.066×10^{-12} cm²/dyn (Gekko and Hasegawa, 1986). The haemoglobin tetramer is a 55Å sphere, while its subunit dimensions are 45Å x 35Å x 25Å (Stryer, 1988). The increase in measured surface area that one might expect purely on the basis of dissociation of the haemoglobin tetramer (and no further gross changes in dimensions) into its subunits, is of the order of ~1.2 - ~2.1 fold. (An increase in surface area of ~1.2 is calculated when an intact haemoglobin tetramer (55Å x 55Å) dissociates into four subunits - which bind to the support surface via their '25Å x 35Å' faces. Increases in surface area of ~1.5 or ~2.1 are calculated if binding is via the '45Å x 25Å' or '35Å x 45Å' faces of the subunits respectively.)

When haemoglobin was chromatographed on normal Cu²⁺-IDA Sepharose columns (where the Cu²⁺ density is ~ 20 µmoles/mL of adsorbent) elution using descending pH gradients, imidazole and even EDTA failed to displace the protein in any form. Its removal from the column was only achieved using sanitization with 0.2 M NaOH. (Good chromatographic results with haemoglobin on Cu²⁺-IDA gels can be achieved using IDA supports charged to very low Cu²⁺ density with limiting concentrations of Cu²⁺ ions (F.H. Arnold, personal communication)).

Given these findings it is entirely plausible that the haemoglobin tetramer dissociates on binding, perhaps 'driven' by the sheer number and strength of up to 20 (maximum

possible) interactions per molecule. Therefore estimation of the useful surface areas available on magnetic chelators using cytochromes *c* as a probe are likely to be more reliable than those obtained using haemoglobin.

3.11.1 Effect of ligand density on non-specific binding

In addition to the advantages of high capacity and interaction strength, increasing the ligand density beyond 30 $\mu\text{moles/g}$ is accompanied by substantial reductions in the levels of non-specific background binding (*i.e.* that to uncharged IDA) of all proteins tested (Figure 3.15). Moreover non-specific binding of cytochromes *c* is effectively eradicated with high density supports ($> 30 \mu\text{moles/g}$). This ligand density is equivalent to a calculated spacing, between successive IDA functions, of 36 Å -roughly the same as the molecular dimensions of cytochrome *c* (34 Å) (Todd et al., 1994). Direct interaction with the base matrix is the probable cause of non-specific binding of proteins on supports with relatively low IDA substitution ($< 30 \mu\text{moles/g}$). It is probable that the introduction of polar groups onto the surface of epoxy-activated polyglutaraldehyde-coated particles covers up previously exposed areas of the 'sticky' base matrix. In support of this, non-specific (and possibly covalent) binding of for example, *C. krusei* cytochrome *c*, to bare polyglutaraldehyde-coated and 'blocked' epoxy-activated supports, occurs at significant levels (60 and 15 mg/g respectively).

3.11.2 Comparison with commercial supports

Arnold's group employed the bi-Langmuir (Todd et al., 1994) and Tempkin (Johnson and Arnold, 1995; F.H. Arnold, personal communication) models to describe the binding of *S. cerevisiae* iso-1-cytochrome *c* histidine variants and native cytochromes *c* (tuna and horse) to densely covered Cu^{2+} -IDA-TSK gel. When charged to maximum capacity under saturating conditions, multi-site binding was observed with this support for horse cytochrome *c* (two partially accessible histidines). However, when the same support was charged with limiting levels of Cu^{2+} (*e.g.* $< 50\%$) this multisite binding was lost and simple Langmuir models could adequately account for binding (Todd et al., 1994). Furthermore the binding profile for horse cytochrome *c* was very similar to that observed for tuna cytochrome *c* with only one partially accessible histidine (and therefore incapable of multisite binding). The surface areas of Sepharose and TSK supports are not known, but the ligand densities and maximum binding capacities of IDA-linked TSK (Todd et al., 1994) and Sepharose supports are very similar (*e.g.* Cu^{2+} densities of 18.5 and 20 $\mu\text{moles/mL}$ of support; Q_{max} of ~ 30 and 32.6 mg of *C. krusei* cytochrome *c* per

mL of support). (The Cu^{2+} ligand density, and Q_{max} for *C. krusei* cytochrome *c* binding to Cu^{2+} -IDA Sepharose were determined experimentally (section 3.6)). It is not surprising that these supports exhibit similar binding characteristics towards the cytochromes *c* but there are notable differences. For example, Cu^{2+} -IDA-TSK appears to be more strongly interacting than Cu^{2+} -IDA-Sepharose. Tuna cytochrome *c* does not bind to Cu^{2+} -charged IDA Sepharose supports but does bind to the Cu^{2+} -IDA TSK gel and also to Cu^{2+} -charged magnetic chelator particles. In their behaviour towards the haem proteins the magnetic chelator supports would appear to more closely resemble the TSK. Factors other than purely 'ligand density' are likely to be responsible for the differences in binding behaviour of these Cu^{2+} -IDA-linked adsorbents (e.g. uniform or clustered ligands; orientation of the ligand, steric hindrances and the nature of the base matrix). Not surprisingly, the immobilised ligands were more effectively utilised on the non-porous particles than on either commercial porous support. Macromolecules binding to a non-porous support do not face the problems typically associated with porous supports (e.g., transmission through pores and internal diffusion limitation).

3.12 Conclusions

The preparation of micron-sized non-porous magnetic metal chelator adsorbents derivatized with the chelating agent, iminodiacetic acid, have been prepared for the selective recovery of proteins by metal chelate affinity adsorption. Four preparative routes employing epoxide activation chemistries were investigated to introduce IDA onto the surface of polyglutaraldehyde-coated particles. The presence of surface bound IDA was demonstrated by the selective binding of Cu^{2+} and by the behaviour of Cu^{2+} charged and uncharged supports towards native haem proteins known to bind commercially available Cu^{2+} -IDA adsorbents. The simplest and most direct procedure was developed further.

Supports prepared by this method were optimised with respect to ligand density and specific binding capacity. These coating and derivatization methods result in supports with a high level of substitution and low non-specific binding while retaining a high effective surface area for binding of the target protein (>200mg/g). Furthermore, the resulting magnetic chelator supports possess excellent long term storage stability.

Densely-substituted magnetic chelator supports are preferred because in addition to the strong interaction strengths and high capacities that they present, non-specific binding is minimised. Also a densely-derivatised support allows greater flexibility for the separation

of different proteins, because a desired Cu^{2+} density can be tailored simply by charging supports with limiting concentrations of metal ions (Todd et al., 1994).

By testing the magnetic supports with a range of native histidine-bearing proteins, the mechanism and factors affecting protein retention were elucidated. Maximum binding capacities and corresponding dissociation constants were calculated and were found to critically reflect the number of accessible histidine residues. Equilibrium binding of multiple histidine proteins is tighter than expected because it probably involves simultaneous interactions with more than one immobilised metal ion.

CHAPTER 4

SEPARATION OF PREDERIVATISED METAL-BINDING PROTEINS

4.1 Aim

The main aim was to demonstrate efficient and selective recovery of a recombinant histidine-tailed protein by affinity separation on magnetic chelator supports from a crude homogenate environment containing suspended solids, many other proteins and small molecular competitors. An initial aim was to screen a selection of polyhistidine proteins using immobilised metal affinity chromatography to identify the best candidate/system. Following this, batch binding (and desorption) experiments were designed to investigate the effect of different components of crude homogenate on the strength and capacity of binding and the possible mechanisms behind this. All of these investigations were designed in order to gain an understanding of a magnetic affinity separation system which may be applied at large scale using high gradient magnetic separation.

4.2 Screening of Prederivatised Recombinant Proteins by IMAC

Genetic modification of the protein of interest by addition of an affinity 'tag' or 'tail' provides a means of identifying and specifically recovering the target protein (section 1.4). The recovery of three different polyhistidine-tailed recombinant proteins using immobilised metal affinity chromatography and magnetic chelator supports was explored.

4.2.1 ZZ Histidine fusion protein

A gene fragment encoding a histidine containing peptide, His-Gly-His, was polymerised at gene level to a multiplicity of four and fused to a synthetic IgG-binding protein, designated ZZ, based on staphylococcal protein A (Ljungquist et al., 1989). The fusion protein was kindly provided by M. Uhlén, Royal Institute of Technology, Stockholm, Sweden. Ljungquist and co-workers (1989) purified the ZZ fusion protein using IgG affinity chromatography following its release from the periplasmic space by an osmotic shock procedure (Nossal and Heppel, 1966). It was then retained by immobilised metal affinity chromatography on Zn²⁺-charged IDA Sepharose and eluted at pH 5.0 ± 0.2 using a step pH gradient.

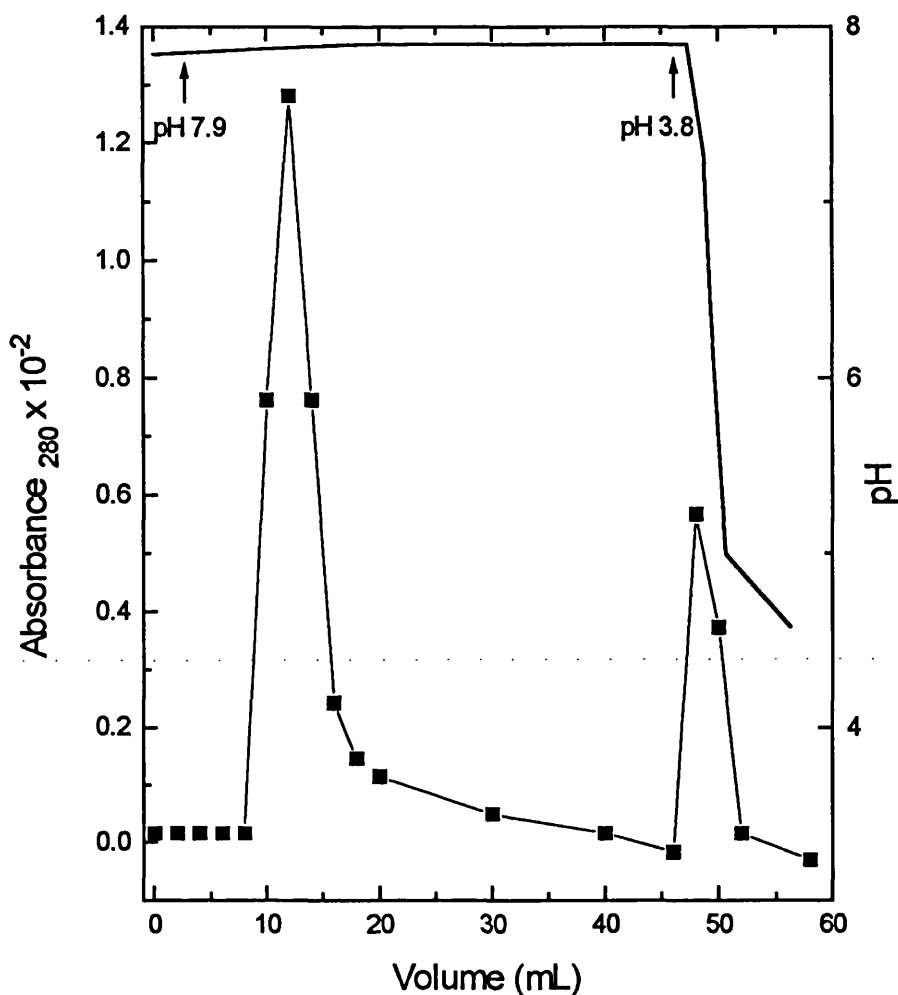


Figure 4.1 Immobilised metal affinity chromatography of recombinant ZZ-His4 fusion protein on a Zn²⁺-IDA Sepharose 6B column. Protein A₂₈₀ (■) and pH(—). Degraded ZZ portion of the fusion protein elutes in the flowthrough.

The protein was expressed and the purification repeated as described by Ljungquist et al., (1989) (sections 2.5.1, 2.5.5.1, 2.6.2 and 2.6.1.1). The IgG affinity purified ZZ-His4 (18.3 kD) protein was analyzed by gel electrophoresis in 14% SDS-polyacrylamide gels. A single protein band of ~ 18 kD was visible in the first acetate eluted fraction. However, as noted by Ljungquist et al., (1989) the ZZ-derived protein stained poorly with Coomassie stain and the band diffused and disappeared from the gel over 24 h. In addition, it was not possible to determine protein concentration by Coomassie assay and so the absorbance at 280 nm was monitored. The IgG purified ZZ-His4 was chromatographed on a IMAC Zn²⁺-IDA column. ZZ-His4 was eluted using a step pH gradient between pH 7.5-5.0 (Figures 4.1 and 4.2).

The first larger peak, which occurred in the flowthrough, corresponded to a protein of ~15 kD in size. This is probably the proteolytically degraded ZZ portion (15.7 kD) of the full-length fusion protein, which, without the histidine tail was not retained by Zn²⁺-IDA (Figures 4.1 and 4.2). Confirmation by Western blotting and/or end tail sequence analysis was not attempted but would confirm the identity of the 15 kD species. Ljungquist and co-workers (1989) also reported proteolytic degradation of the ZZ-His8 fusion protein which was evidenced by two bands corresponding to proteins of smaller sizes.

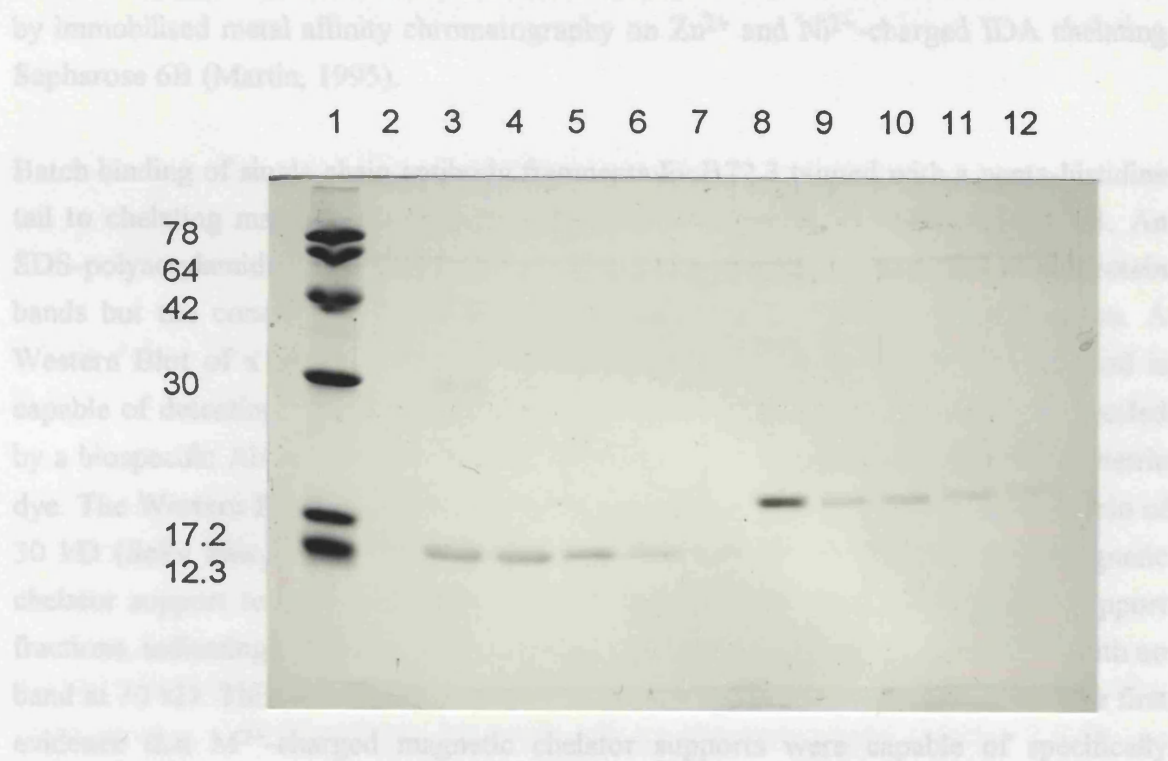


Figure 4.2 Recovery of ZZ-His4 by Zn²⁺-IDA Sepharose 6B IMAC. *lane 1*, molecular weight markers; *lanes 2-7*, flowthrough peak of degraded ZZ IgG binding protein; *lanes 8-12*, pH eluted (~ pH 5.0) ZZ-His4 peak.

Direct recovery of ZZ-His4 from the periplasmic fraction using IMAC was not reported by Ljungquist et al. (1989) and my attempts to achieve this in these laboratories were unsuccessful. The many problems associated with this recombinant protein such as the fact that it was not possible to separate using IMAC unless it had been pre-purified by IgG affinity chromatography, its lack of stability, and its low reaction sensitivity to Coomassie stain, argued that this system was not suitable for further development and consequently experiments to test magnetic affinity supports were not undertaken.

4.2.2 Histidine-tailed single chain antibody fragment

Recombinant penta-histidine tailed single chain antibody fragments incorporating a hinge region from the parent antibody (ScFv_{hingehis₅}) (Martin, 1995), were expressed in *E. coli* (section 2.5.2) and excreted to the medium. As is typical in the production of antibody fragments the titre was low, about 4.5 mg/L culture medium (4.5 g/L total protein). Successful purification to single band purity has been achieved in this laboratory by immobilised metal affinity chromatography on Zn²⁺ and Ni²⁺-charged IDA chelating Sepharose 6B (Martin, 1995).

Batch binding of single chain antibody fragments Fv B72.3 tagged with a penta-histidine tail to chelating magnetic support was carried out as described in section 2.4.6.1. An SDS-polyacrylamide gel, stained with Coomassie blue, revealed many unbound protein bands but the concentration was too low to detect protein in the bound fraction. A Western Blot of a replica gel was run (section 2.7.5). This more sensitive method is capable of detecting nanogram quantities of protein, and antibody present was revealed by a biospecific Ab-Ab complex, where the second antibody is tagged by a colorimetric dye. The Western Blot (Figure 4.3) revealed a single band corresponding to a protein of 30 kD (ScFv his₅) in the bound fraction of Cu²⁺, Ni²⁺ and Zn²⁺-charged magnetic chelator support tests. The band was more intense for Cu²⁺ and Zn²⁺-charged support fractions, indicating a higher protein capacity. The control (uncharged) was clean with no band at 30 kD. This preliminary result, at an early stage in the project, provided the first evidence that M²⁺-charged magnetic chelator supports were capable of specifically recovering recombinant histidine-tailed protein from extracellular suspensions.

4.3 Recovery

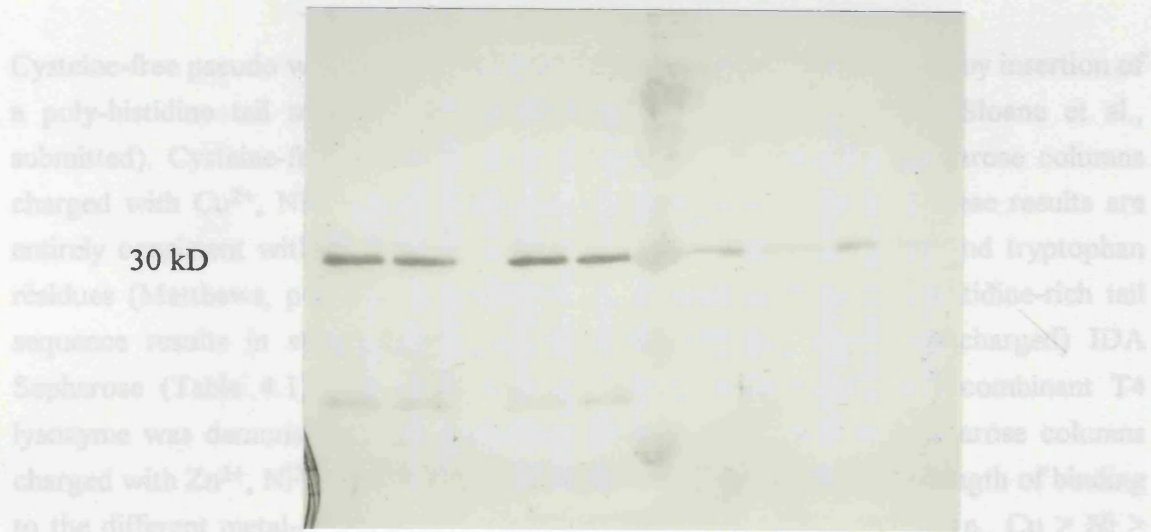


Figure 4.3 Western blot of batch binding of ScFvhinge(his)₅ with magnetic chelator supports. *Lanes 1, 2, 4 & 5*, unbound fractions of Cu²⁺, Ni²⁺ and Zn²⁺-charged and un-charged supports; *lane 6*, molecular weight markers ('rainbow' coloured); *lanes 7, 8, 9, 10*, bound fractions of Cu²⁺, Ni²⁺ and Zn²⁺-charged and un-charged supports.

Attempts to improve the expression level of ScFvhinge(his)₅ were largely unsuccessful. Purification of ScFvhinge(his)₅ by mucin affinity chromatography (section 2.6.3) was performed with the aim to provide sufficient protein to test with magnetic chelator supports but this method was not pursued because of the insufficient antibody titres achievable. A major problem in working with this protein was its low expression level in the supernatant (~ 4.5 mg/L). In addition the concentration was difficult to ascertain by gel scanning because of the presence of native *E. coli* proteins with similar molecular weights and no method for easily assaying the ScFvhinge(his)₅ was available. For these reasons, research activity with this system was abandoned at this stage.

4.2.3 Histidine-tailed T4 lysozyme

A cysteine-free T4 lysozyme tagged at its C-terminus with a metal-binding tail sequence, N-His-Gln-(His)₃-C, was successfully separated from crude cell extract and from crude homogenate at high yield and purity using Cu²⁺-IDA magnetic supports (see below, section 4.3).

4.3 Recovery of Histidine-tailed T4 Lysozyme

Cysteine-free pseudo wild type T4 lysozyme has been genetically modified by insertion of a poly-histidine tail sequence (N-His-Gln-His₃-C) at the C-terminus (Sloane et al., submitted). Cysteine-free T4 lysozyme does not bind to chelating Sepharose columns charged with Cu²⁺, Ni²⁺ or Zn²⁺ ions (Sloane et al., submitted) and these results are entirely consistent with the structural data on accessibility of histidine and tryptophan residues (Matthews, personal communication). The introduction of a histidine-rich tail sequence results in strong binding to metal-charged (but not to un-charged) IDA Sepharose (Table 4.1). Successful recovery and purification of the recombinant T4 lysozyme was demonstrated by immobilised metal affinity on IDA Sepharose columns charged with Zn²⁺, Ni²⁺ and Cu²⁺ ions (Sloane et al., submitted). The strength of binding to the different metal-charged supports varied in a predictable manner, i.e., Cu > Ni > Zn.

4.3.1 Recovery from *E.coli* cell extract

Cu²⁺-charged magnetic chelator supports were chosen for the recovery of recombinant T4 lysozyme from crude *E. coli* extracts. High density Cu²⁺-charged (53 μmoles/g) and un-charged supports were contacted with *E. coli* cell-free cell extract containing the target protein, separated magnetically and washed sequentially with buffers of increasing stringency to elute first, entrained or weakly-bound materials and contaminating *E. coli* proteins and then, the recombinant T4 lysozyme (section 2.4.6.2). The results are presented in Figure 4.4 (a) and (b) and in Table 4.1.

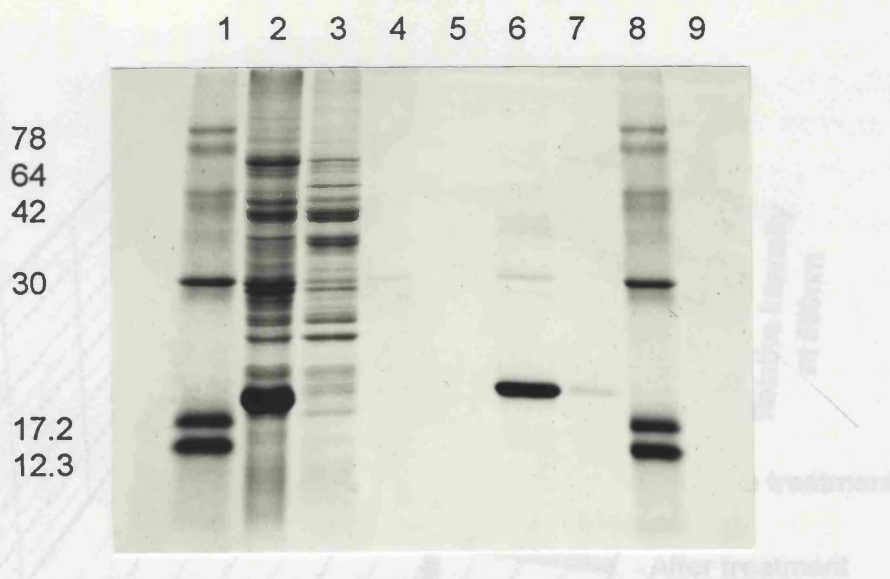


Figure 4.4 (a) Direct recovery of recombinant T4 lysozyme from crude *E. coli* cell extracts on magnetic chelator supports. SDS-PAGE analysis of unbound and bound (desorbed) samples. *Lane 1*, molecular weight markers; *lanes 2 & 3*, unbound protein from IDA and Cu^{2+} -IDA magnetic chelators; *lanes 4 & 5*, protein desorbed from Cu^{2+} -charged magnetic supports by first and second washes of phosphate buffer, pH 7.2 respectively; *lanes 6 & 7*, protein desorbed from Cu^{2+} -charged magnetic supports by first and second washes of 0.1 M acetate buffer, pH 3.8.

After the binding step 3.4-7.8% (densitometric and enzyme activity measurements respectively) of the T4 lysozyme-his remained in the bulk phase. Contacting the loaded Cu^{2+} -charged particles with two successive washes of phosphate equilibrium buffer removed only a very small amount of the firmly bound enzyme (7.6% in the first and 5.3% in the second wash) and small amounts of weakly binding or entrained material (Table 4.1), indicating that the enzyme was bound very firmly and that there was little evidence for non-specific binding. Furthermore, recombinant T4 lysozyme failed to bind 'un-charged' supports confirming that binding is specifically mediated through immobilised Cu^{2+} ions. Complete desorption of the residual bound enzyme was achieved with only two washes of 0.1 M acetate pH 3.8 and ~80% of the recovered activity was removed in the first wash. The purity of eluted T4 lysozyme-his was found to be 94%, as determined by scanning densitometry of Coomassie blue stained gels. The total recovery of initial target enzyme present in crude extract was 79-84% (as measured by activity and gel densitometry respectively) with a purification factor of ~4.3.

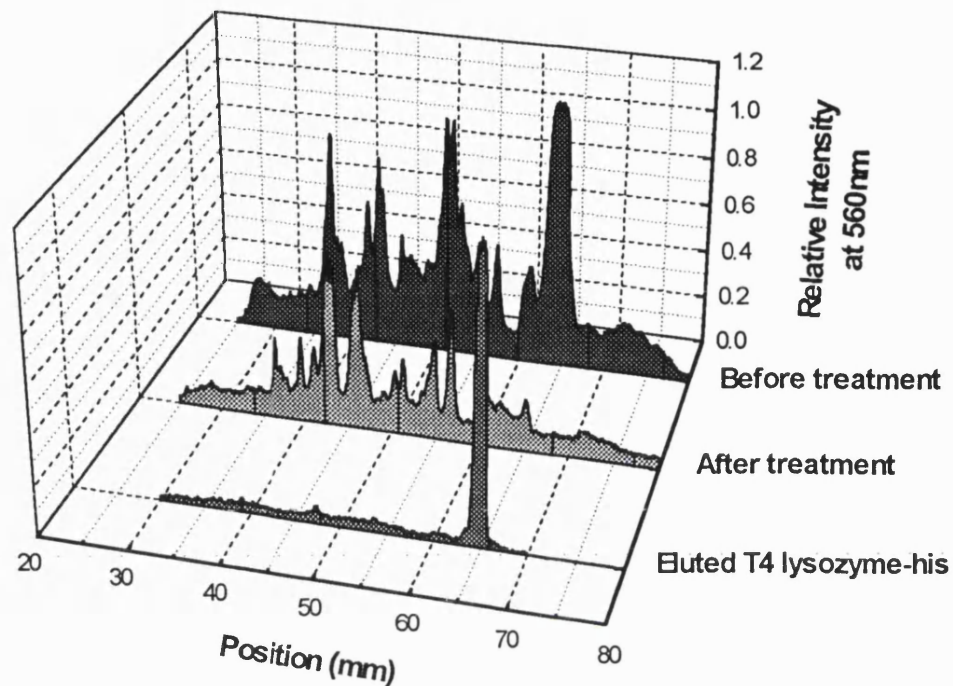


Figure 4.4 (b) Graphic reproduction of SDS-PAGE analysis showing the recovery of recombinant T4 lysozyme-his from crude *E. coli* cell-free extract.

After the binding step 3.4-7.8% (densitometric and enzyme activity measurements respectively) of the T4 lysozyme-his remained in the bulk phase. Contacting the loaded Cu^{2+} -charged particles with two successive washes of phosphate equilibrium buffer removed only a very small amount of the firmly bound enzyme (7.6% in the first and 5.3% in the second wash) and small amounts of weakly binding or entrained material (Table 4.1), indicating that the enzyme was bound very firmly and that there was little evidence for non-specific binding. Furthermore, recombinant T4 lysozyme failed to bind 'un-charged' supports confirming that binding is specifically mediated through immobilised Cu^{2+} ions. Complete desorption of the residual bound enzyme was achieved with only two washes of 0.1 M acetate pH 3.8 and ~ 80% of the recovered activity was removed in the first wash. The purity of eluted T4 lysozyme-his was found to be 94%, as determined by scanning densitometry of Coomassie blue stained gels. The total recovery of initial target enzyme present in crude extract was 79-84% (as measured by activity and gel densitometry respectively) with a purification factor of ~ 4.5.

Table 4.1 Recovery of recombinant T4 lysozyme from crude *E. coli* cell extract by Cu²⁺-charged magnetic chelator supports.

Step	Variable	% Initial material	% Remaining in supernatant	% Lost in:		% Recovered by:		% Enzyme and protein recovery	% Purity	Purification factor
				wash 1	wash 2	elution 1	elution 2			
Crude extract	Activity	100						100	21.1	1
	Protein	100						100		
Binding	Activity		7.8							
	Protein		77.0							
Washing	Activity			7.6	5.3					
	Protein			4.3	0.9					
Elution	Activity					50.0	29.3	79.3	94.0	4.5
	Protein					13.0	4.8	17.8		

Chapter 4 Separation of Prederivatised Recombinant Proteins

The results of a more conventional two-step procedure, i.e., clarification by centrifugation followed by chromatography on Cu²⁺-IDA are included in Table 4.2 for comparison. Approximately 3-5% of the enzyme is lost within the sedimented material after centrifugation (R. Sloane, personal communication). The overall recovery of T4 lysozyme-his for the combined centrifugation and chromatography steps is > 90% with a 3.8 fold purification factor but the purity of the pooled peak activity is less than 82%. While 'cutting' the peak fraction may improve the purity of the the T4 lysozyme-his, this could only be achieved with some loss of yield. A further disadvantage of chromatography on Cu²⁺-IDA was that the T4 lysozyme was eluted in a large volume whereas that eluted from Cu²⁺-charged magnetic chelators was in a much more concentrated form.

Table 4.2 Recovery of recombinant T4 lysozyme from *E. coli* extracts - comparison of magnetic purification with a two-step conventional chromatographic procedure.

Purification step	% Yield	% Purity ^[a]	Purification factor
Crude extract	100	21.1	1
Magnetic IMA separation	79.3	94.0	4.45 ^[a] -4.60 ^[b]

Purification step	% Yield	% Purity ^[a]	Purification factor
Crude extract	100	21.1	1
Clarified extract	95.9	22.5	1.05
IMAC on HiTrap™ column	91.1	81.5	3.72 ^[b] -3.86 ^[a]

Values obtained by densitometry of Coomassie blue-stained gels [a] and from enzyme and protein assays [b].

The affinity interaction of the metal-binding protein for magnetic chelator supports was strong enough to ensure efficient capture the T4 lysozyme-his from contaminant cellular proteins and other components at near neutral pH and to withstand several washing steps prior to elution. In many affinity interactions a dissociation constant of > 10⁻⁶ M is observed which is often not sufficiently low to ensure complete adsorption and protein

retention during washing steps. Unlike *C. krusei* cytochrome *c*, the recombinant metal-binding T4 lysozyme binds to Zn^{2+} and Ni^{2+} -charged Sepharose supports in addition to Cu^{2+} charged adsorbents. Recombinant T4 lysozyme is eluted after *C. krusei* cytochrome *c* on Cu^{2+} -IDA agarose (pH 3.6) suggesting that it possesses an interaction strength intermediate between that of *C. krusei* and haemoglobin. A histidine-tail of at least this strength is necessary to make a batch adsorption process viable and the effective dissociation constant is probably of the order of 10^{-7} M.

4.3.2 Recovery from *E.coli* cell homogenate

A major objective of this work was to achieve a high yield, high purity, batch separation of recombinant T4 lysozyme from a homogenised cell suspension containing unbroken cells, broken cell debris and unwanted protein by non-porous foulant resistant magnetic supports.

4.3.2.1 Process optimisation

The effect of media components and cellular material on support behaviour and adsorption efficiency was investigated in preliminary experiments. Cu^{2+} -charged magnetic supports were challenged with recovery of haemoglobin from a range of different solutions. Binding solutions of bovine haemoglobin were spiked with various combinations of *E. coli* cells and media components, (both fresh and spent) before contacting with Cu^{2+} -charged magnetic chelator supports (section 2.4.7.1). The results are illustrated in Figure 4.5 and the haemoglobin challenging solution compositions are described in Table 4.3.

The control test (sample 1) of haemoglobin in phosphate buffer with no cells present, had a binding capacity of 132 mg/g support which was taken to represent a binding efficiency of 100% in these tests. In the presence of cellular biomass produced by 1 mL of culture, resuspended in 1 mL of phosphate buffer (sample 2), a binding efficiency of 90% was achieved (117 mg/g). The initial ligand density (measured before the experiment) was 43 μ moles/g support and the level of non-specific adsorption was low at about 10.5 mg/g support. A drop in adsorption capacity of only 10%, due to the presence of whole *E. coli* cells, is a measure of the relative resistance of non-porous magnetic supports to fouling by cellular materials. However the efficiency of binding was dramatically and detrimentally affected by the presence of media components (high biomass media) and the amount of haemoglobin adsorbed per g of support dropped steadily as the proportion of growth media in the suspension increased (Figure 4.5).

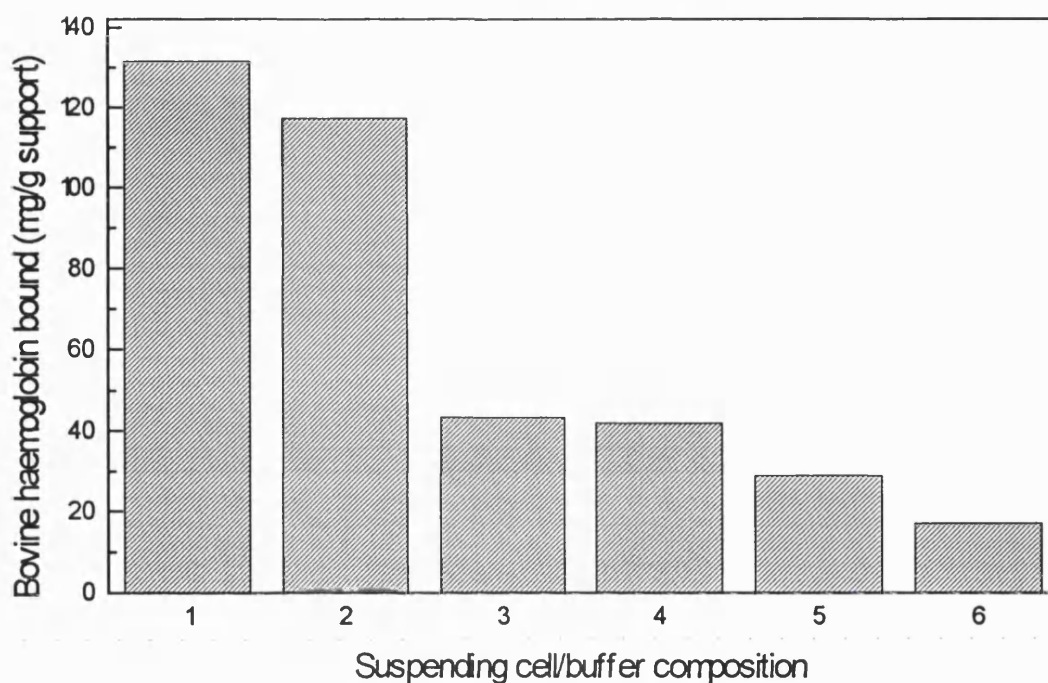


Figure 4.5 The effect of various suspension concentrations of cells / media and buffer composition on the the adsorption efficiency of Cu^{2+} -charged magnetic chelator supports for bovine haemoglobin. See table 4.3 for guide to suspending cell/buffer composition.

Table 4.3 Composition of solutions used to test the effect of cells, media components and buffer on the adsorption efficiency of magnetic chelator supports for bovine haemoglobin.

Sample	Suspension composition	Dry cell weight (mg)
1	20 mM sodium phosphate, 0.5 M NaCl, pH 7.2 buffer	0
2	1 mL 20 mM sodium phosphate, 0.5 M NaCl, pH 7.2 buffer containing cell equivalent of 1 mL cell culture	1.425
3	1 mL cell culture containing cell equivalent of 2 mL cell culture	2.850
4	1 mL cell culture	1.425
5	0.5 mL cell culture / 0.5 mL media (sterile)	0.712
6	1 mL media (sterile)	0

Clearly in future work care must be taken to wash cells thoroughly free of media before homogenisation. Binding efficiency was at its lowest, 13%, in the presence of un-used sterile media without cells. It is probable that components in the media such as amino acids, proteins or metal binding agents block or strip metal ions from the support, leaving it unable to adsorb the target protein. The effect is strongest in un-used media. Cells resuspended in phosphate buffer of neutral pH, spiked into a solution of haemoglobin had a relatively minor negative effect on the binding capacity of magnetic chelator supports. Phosphate buffer was chosen for its compatibility both physiologically and with magnetic supports.

4.3.2.2 Recovery of recombinant T4 lysozyme

The affinity and adsorption capacity of magnetic chelator supports for recombinant T4 lysozyme in a suspension of crude *E. coli* homogenate containing whole cells, cell debris, cellular material and contaminant protein was investigated. As a result of the previous experiment's findings (section 4.3.2.1) cells were resuspended in phosphate buffer prior to cell disruption by sonication (section 2.4.7.2). Cu^{2+} -charged (and un-charged control) magnetic supports were contacted with the released protein in the presence and absence of crude cell extract at two different cell concentrations (9.41 and 18.82 mg) as measured by dry cell weight. The higher cell concentration releases double the amount of protein and T4 lysozyme-his saturation capacity was reached at ~ 180 mg/g support (ligand density 67 $\mu\text{moles/g}$) in both the crude and clarified extract (Figure 4.6). Such a high capacity value following recovery from crude and clarified extract indicated that support performance was not adversely affected by foulants in the suspension. However, twice the amount of non-specific binding occurred in the crude extract (34 mg/g).

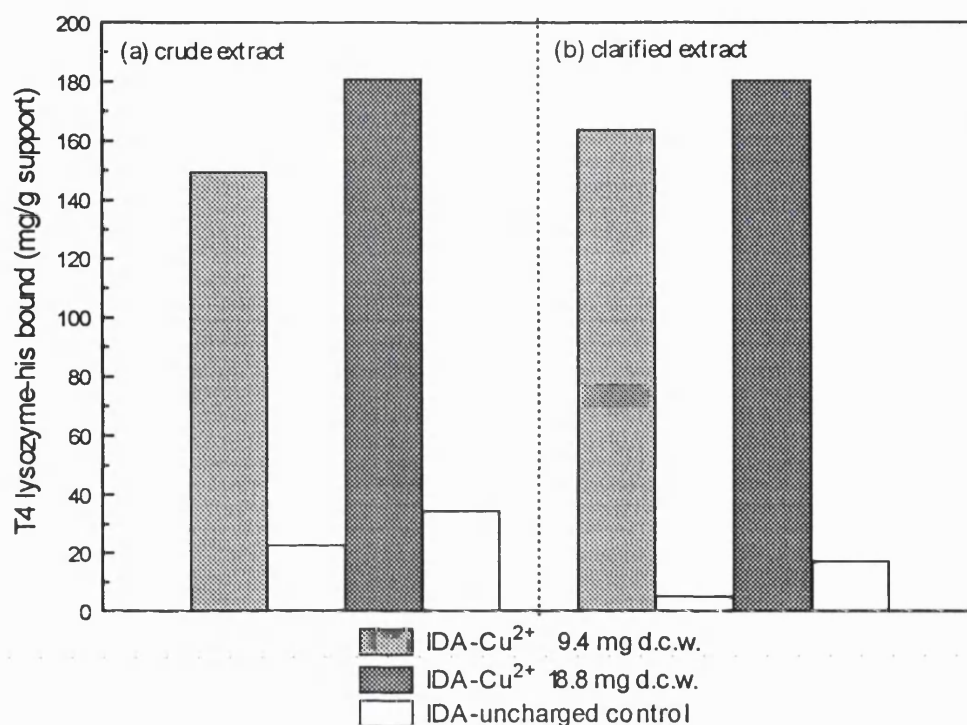


Figure 4.6 Magnetic affinity recovery of recombinant T4 lysozyme-his from (a) crude extract in the presence of cells and (b) clarified extract with the cells and cell debris removed, at two different biomass concentrations, 9.4 mg and 18.8 mg dry cell weight.

Figures 4.7 and 4.8 show SDS-PAGE evidence of Cu²⁺-charged magnetic chelator support recovery of T4 lysozyme-his from clarified extract (cell free) and from crude extract respectively. There is little apparent difference between the washed and eluted protein profiles in the presence and absence of cell homogenate. Complete desorption of T4 lysozyme-his in two washes with 0.1 M acetate buffer, pH 3.8 was reported in section 4.3.1. However, in this case elution was carried out using three washes of 0.02 M phosphate buffer, pH 3.8 followed by two washes of 100 mM imidazole. The imidazole washes were responsible for displacing about 65% of the bound protein. 0.02 M phosphate buffer has low buffering ability at pH 3.8 and it is likely that the pH drifted above this to a value insufficiently low enough to displace the bound polyhistidine T4 lysozyme. Enzyme activity, as measured by the lysozyme assay (section 2.7.2.1), was reduced by 80% in crude cell extract. Components of the crude homogenate could block enzyme action, but interference with the assay method, which is based on turbidometric difference, may not be ruled out. However, the activity of enzyme desorbed from the crude homogenate test (by phosphate buffer pH 3.8 washes), was relatively unaffected, as the cellular material was removed by washing steps prior to elution. It was not

possible to measure the activity recovered in the imidazole washes because imidazole interferes with the enzyme assay by spoiling the absorbancy readings.

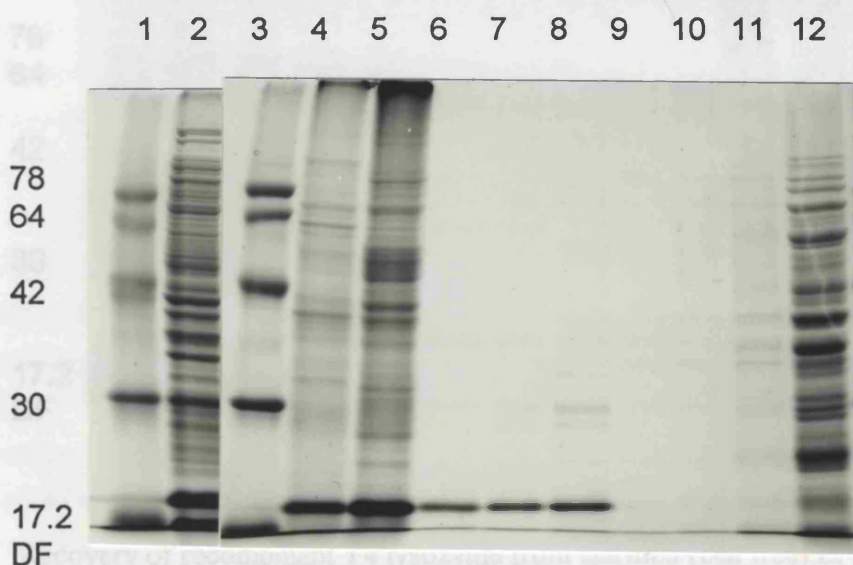


Figure 4.7 Recovery of recombinant T4 lysozyme from crude *E. coli* cell homogenate on Cu^{2+} -charged magnetic chelator supports. SDS-PAGE of unbound and bound (desorbed) samples. *Lanes 1 & 3*, molecular weight markers; *lane 2*, cell homogenate starting material; *lane 12*, unbound protein; *lanes 11, 10, & 9*, protein desorbed by washes of phosphate buffer, pH 7.2; *lanes 8, 7, & 6*, protein desorbed by washes of phosphate buffer pH 3.8, *lanes 5 & 4*, protein desorbed by washes of 0.1 M imidazole. Solids were sedimented by centrifugation prior to loading of gel.

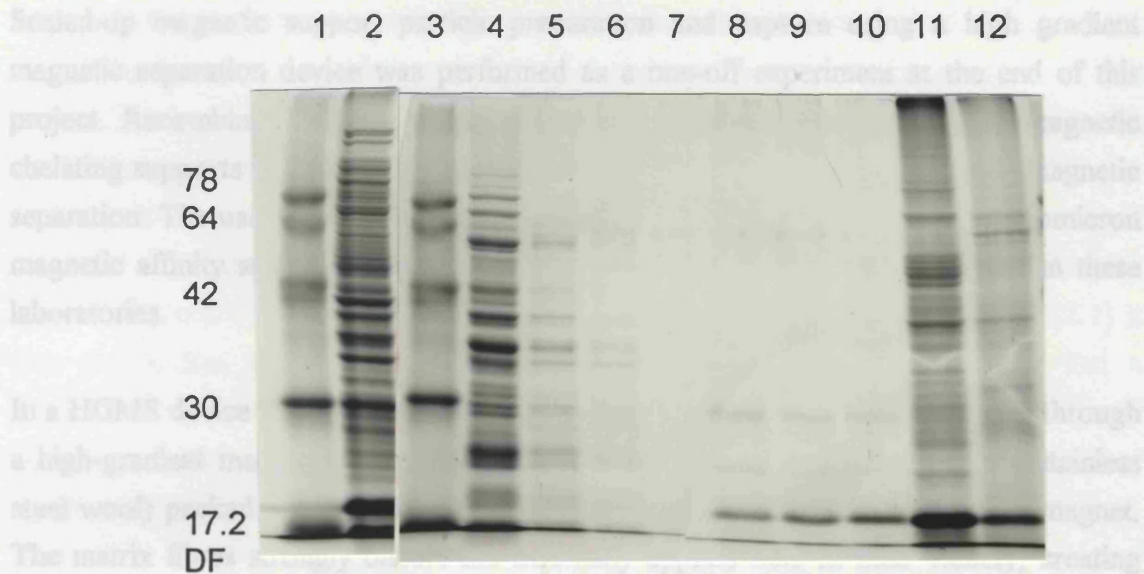


Figure 4.8 Recovery of recombinant T4 lysozyme from clarified (cell free) *E. coli* cell homogenate on Cu^{2+} -charged magnetic chelator supports. SDS-PAGE of unbound and bound (desorbed) samples. *Lanes 1 & 3*, molecular weight markers; *lane 2*, cell homogenate starting material; *lane 4*, unbound protein; *lanes 5, 6, & 7*, protein desorbed by washes of phosphate buffer, pH 7.2; *lanes 8, 9, & 10*, protein desorbed by washes of phosphate buffer pH 3.8, *lanes 11 & 12*, protein desorbed by washes of 0.1 M imidazole.

4.4 High Gradient Magnetic Affinity Separation

4.4.1 Introduction

The power and efficiency of magnetic separation is especially useful in large scale applications and is probably the only practical means whereby adsorbent particles of sub-micron dimensions can be recovered (Halling and Dunnill, 1980; Whitesides et al., 1983) from liquors containing biological particulates of roughly similar dimensions.

Magnetic separation had, until now, been carried out at bench scale (up to 2 mL test volumes) using a rack fitted with a permanent magnet. It is impossible, using only an externally applied field, to generate magnetic field gradients over large volumes (> several cm) and so in order to scale up the process, large scale magnetic particle capture was achieved by applying High Gradient Magnetic Separation (HGMS) technology (section 1.6).

Scaled-up magnetic support particle preparation and capture using a high gradient magnetic separation device was performed as a one-off experiment at the end of this project. Recombinant T4 lysozyme metal-binding protein was captured by magnetic chelating supports from crude cell homogenate and recovered by high gradient magnetic separation. The use and scale up of high gradient magnetic separation using submicron magnetic affinity supports is currently being investigated by numerous others in these laboratories.

In a HGMS device the suspension of magnetically responsive particles is passed through a high-gradient magnetic filter consisting of a ferromagnetic matrix (typically stainless steel wool) packed into a canister held between the poles of a powerful electromagnet. The matrix fibres strongly distort the externally applied field in their vicinity, creating strong local magnetic field gradients which attract and hold the magnetic particles within the canister while the external field is applied. The bulk of the trapped particles are released from the canister simply by flushing through when the field is switched off. Remaining particles held by residual magnetism in the steel wool are recovered by mechanical vibration. Since the ferromagnetic matrix typically occupies less than 5% of canister volume, the filter is a highly practical way to generate high magnetic field gradients across large volumes of space.

4.4.2 High gradient magnetic affinity separation of T4 lysozyme-his from *E. coli* cell homogenate

The conditions for the successful recovery at bench scale of T4 lysozyme-his (180 mg/g of Cu²⁺-charged magnetic support) from disrupted *E. coli* cells suspended in phosphate buffer, (as seen in the previous section 4.3.2.2), were mimicked where possible. A cell culture of similar OD₆₀₀ (4.5-5.0) was concentrated 4-fold to give a comparable cell concentration in the scaled-up high gradient magnetic separation.

Before commencing this work some preliminary magnetic particle capture experiments had been conducted by P. Pannu of this department. The high gradient magnetic filter was loaded with a suspension (130 mL) of Cu²⁺-charged magnetic chelator support and *E. coli* cell homogenate in phosphate buffer (section 2.4.8) (1.11 mg support/mL). Magnetic support particle breakthrough started to occur long before the matrix had reached saturation capacity. Despite increasing the magnetic field from 0.4 T to 0.5 T, breakthrough continued. There was visual evidence that the flow distribution was not even and that support was channelling through the matrix along the side of the canister.

Although the cannister was very tightly packed, the random arrangement of steel wool means that the evenness and reproducibility of packing is prone to inconsistencies.

The initial magnetic support ligand density was 35 $\mu\text{moles/g}$, but following contact with the cell homogenate and washing and elution steps, the ligand density dropped to 10.5 $\mu\text{moles/g}$. It is possible that the mix of very complex spent media components and disrupted cells may contain agents that compete with the IDA ligand and interact with the immobilised Cu^{2+} ions and pull them off the support. Previously (section 4.3.2.1) it was shown that the presence of the complex media (high biomass media) had a detrimental effect on support capacity, which was reduced by 87%. Future work will have to address this problem by washing cells prior to disruption to maximise removal of spent media components.

In spite of the low ligand density, 235 mg of protein was eluted using acetate elution buffer per g of support, 79% of which was eluted when the magnetised filter matrix was washed at 10.5 mL/min. A further 3.2% was flushed out at a flowrate of 90 mL/min with the magnetic field switched off (0 T) and 17.14% was washed off the support by vibrational washes.

Almost all (91.3%) of the insoluble cellular material was flushed through the ferromagnetic matrix in the load flowthrough and wash fractions as indicated by optical density measurements. The remaining 8.7% was recovered in the final vibrational washes which dissociated the support from the filter matrix.

4.9 Conclusions

Non-porous magnetic chelator supports charged with Cu^{2+} ions were used to recover recombinant polyhistidine-tailed T4 lysozyme from crude cell-free *E. coli* extract and from disrupted *E. coli* cell homogenate. The selective recovery of recombinant polyhistidine-tailed T4 lysozyme by magnetic chelator adsorbents illustrates the potential application of this process as a generic method of protein purification. The target protein was adsorbed strongly and affinity separated at high capacity (180 mg/g) from a crude suspension of cell debris and other proteins. These foulant resistant, high capacity, affinity supports may be employed directly in batch separation of metal-binding protein from crude liquors at an early stage in the downstream process, thus reducing costs and improving yield.

Process optimisation work found that culture media components interfered with protein recovery from the crude cell suspension by interfering with and blocking support action.

Chapter 4 Separation of Prederivatised Recombinant Proteins

Cell resuspension in phosphate buffer at neutral pH prior to homogenisation, resulted in equal recovery efficiency in the presence and absence of broken cells.

An initial experiment to recover T4 lysozyme-his from crude cell homogenate using 'in house' Cu^{2+} -charged magnetic chelator supports and high gradient magnetic separation provided promising results (235 mg protein was eluted using acetate buffer per g of support). This work is on-going in these laboratories.

CHAPTER 5

FERMENTATION AND EXPRESSION OF RECOMBINANT T4 LYSOZYME

5.1 Aim

The overall aim of fermentation studies on *Escherichia coli* JM107 pQR752 producing recombinant bacteriophage T4 lysozyme was to optimise the growth and protein productivity and use this knowledge to produce the recombinant protein at scale for downstream purification by magnetic chelator adsorbents.

5.2 Introduction

Pseudo wild-type cysteine-free T4 lysozyme, kindly provided by Brian Matthews, University of Oregon, U.S.A., was modified by site-directed mutagenesis (Rhona Sloane, Department of Biochemistry and Molecular Biology, University College London) to carry a poly-histidine tail at its C-terminus. Workers in Matthew's lab observed that standard batch cultivation of T4 lysozyme wild type on Luria Bertrani medium resulted in lysis about 1.5 hours after induction. T4 lysozyme is not specifically secreted to the periplasm and although its expression should not be lethal, leakage occurred leading to lysis of the entire culture (Matthews, personal communication).

5.3 *E. coli* Fermentation on Nutrient Broth

5.3.1 Shake flask cultivation

Cultivation in 2 L conical flasks (250 mL volume) of nutrient broth growth media was performed in the first instance according to a set of partially optimised parameters. A log phase 1% (v/v) inoculum was used (section 2.5.3.1). After 3 hours at 37°C and 200 rpm ($OD_{600} \sim 0.8$) the culture, in mid-exponential growth, was induced with IPTG (1 mM) and harvested two hours later. Growth ceases one hour after induction as can be seen from the OD_{600} (Figure 5.1) and the viable cell count drops from 5.6×10^8 to 1.0×10^7 cfu/mL. The rate of recombinant T4 lysozyme (T4 lysozyme-his) synthesis is highest in the first hour but by two hours 62% has leaked to the medium.

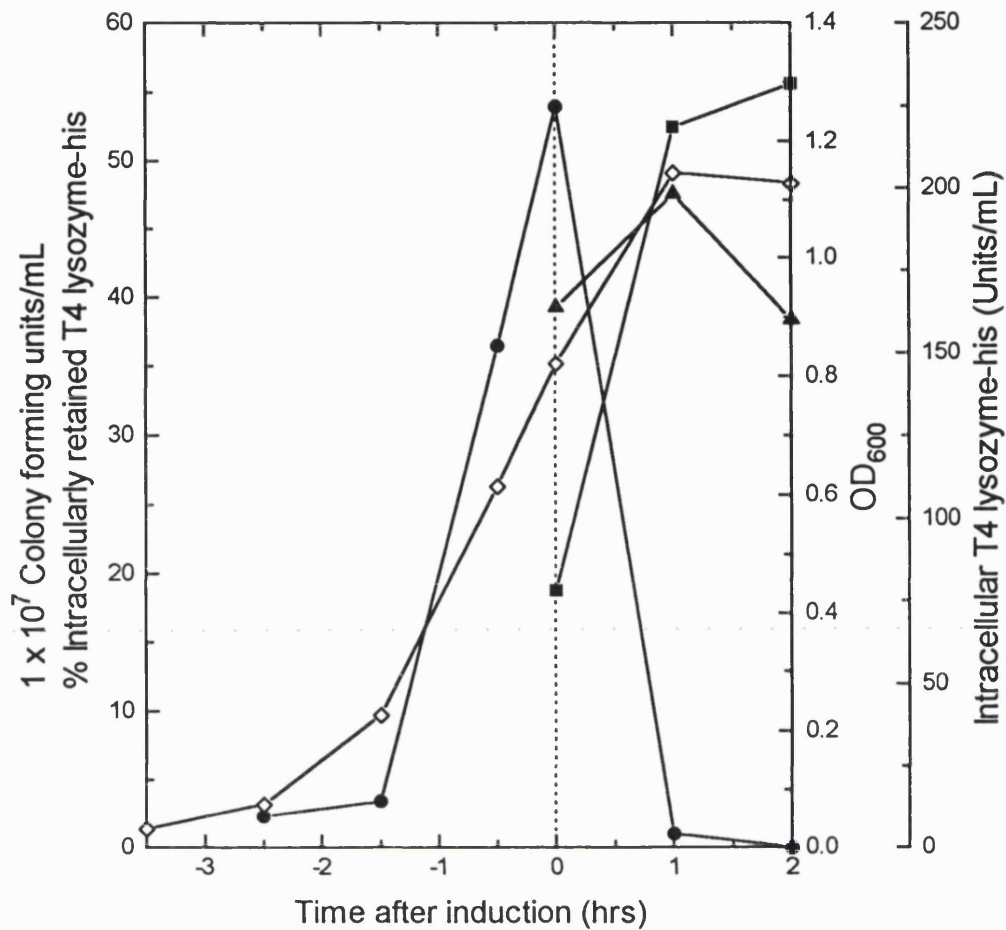


Figure 5.1 Shake flask fermentation of *E. coli* pQR752 producing recombinant T4 lysozyme (T4 lysozyme-his). Profiles of OD₆₀₀ (◇), colony forming units/mL (●), intracellular T4 lysozyme-his activity (Units/mL) following IPTG induction (■) and percentage T4 lysozyme-his retained intracellularly (▲).

5.3.2 Bioreactor cultivation

Scaled up cultivations of *E. coli* pQR752 were performed in a 14 L and 42 L bioreactor on nutrient broth media and at 37°C. The experimental aim was to scale up growth from shake flasks and in doing so obtain information on the growth characteristics and important scale up parameters affecting this recombinant protein producing organism.

5.3.2.1 14 L fermentation

The seed culture was used to inoculate (5% v/v) a 14 L (8.4 L working volume) Chemap bioreactor vessel of the same media and antibiotic composition (section 2.5.3.1). Agitation was set at 500 rpm, aeration at 4 L/min or 0.48 volumes per vessel volume per minute (vvm), temperature at 37°C and pH at 7. Temperature and pH were kept constant throughout.

After 5.0 hr (OD_{600} 1.79) the culture, in late exponential phase, was induced with 1 mM IPTG and harvested 2.5 hr later (OD_{600} 2.17). Following induction there was no further increase in optical density as cell growth levelled out and carbon evolution rate (CER) and oxygen uptake rate (OUR) declined (Figure 5.2). On line measurements indicate that the cells had already entered stationary phase when they were induced. A sample was taken to monitor T4 lysozyme-his production hourly before and half hourly after induction.

Levels of T4 lysozyme-his, as measured by activity, present in the cells and media in the 5 hours of growth before induction are almost negligible and samples run on an SDS-polyacrylamide gel confirmed this. After induction most of the T4 lysozyme-his produced is retained within the cell for the first hour. At 1.5 hr 75% is retained intracellularly, but by 2-2.5 hr there is 40-50% leakage of the enzyme to the medium (Figure 5.3). Hence, build-up of T4 lysozyme-his within the cytoplasm has resulted in leakage and eventually cell lysis. The fact that the cells had stopped growing when induced, possibly due to nutrient deficiency, suggests that they were prone to lyse. Added to that was the increased metabolic burden forced by the synthesis and build up of T4 lysozyme-his. Lysis means rupture of the cell wall and death of the cell and therefore ceased synthesis of T4 lysozyme-his. Purification of the target protein which is distributed 50:50 intra and extracellularly is undesirable from a process perspective. Further cell disruption may be necessary to release the remaining cell associated protein and it must now be purified from a dilute suspension of cell debris and contaminating media components.

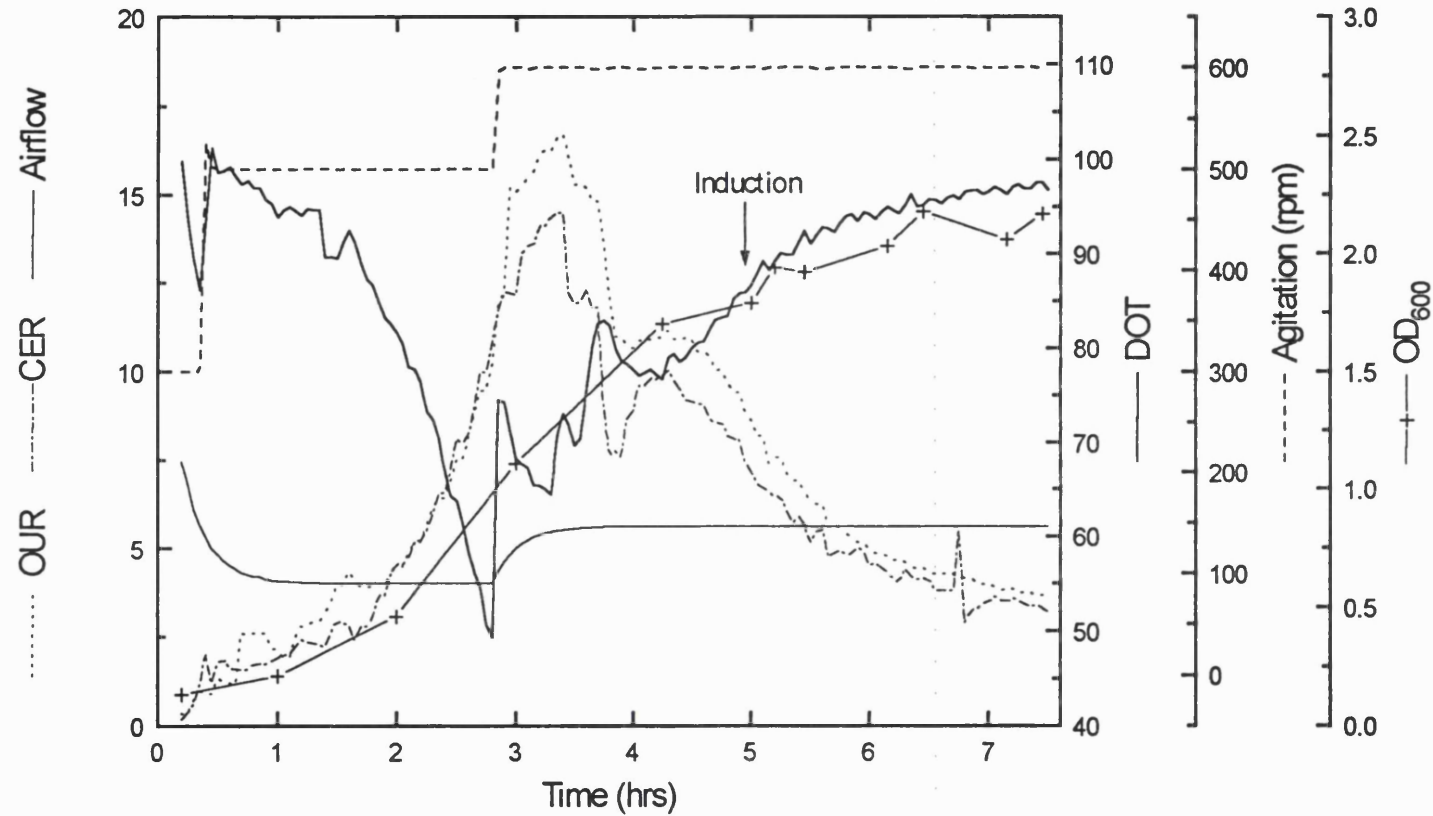


Figure 5.2 Real-time on-line data plot of 14 L (8.4 L ww) *E. coli* pQR752 fermentation on nutrient broth media. On-line variables and optical cell density: oxygen uptake rate (OUR); carbon evolution rate (CER); airflow (L/min); percentage dissolved oxygen tension (DOT); agitation (rpm) and OD₆₀₀. IPTG induction took place after 5 hours growth at OD₆₀₀ 1.79 as indicated by the arrow.

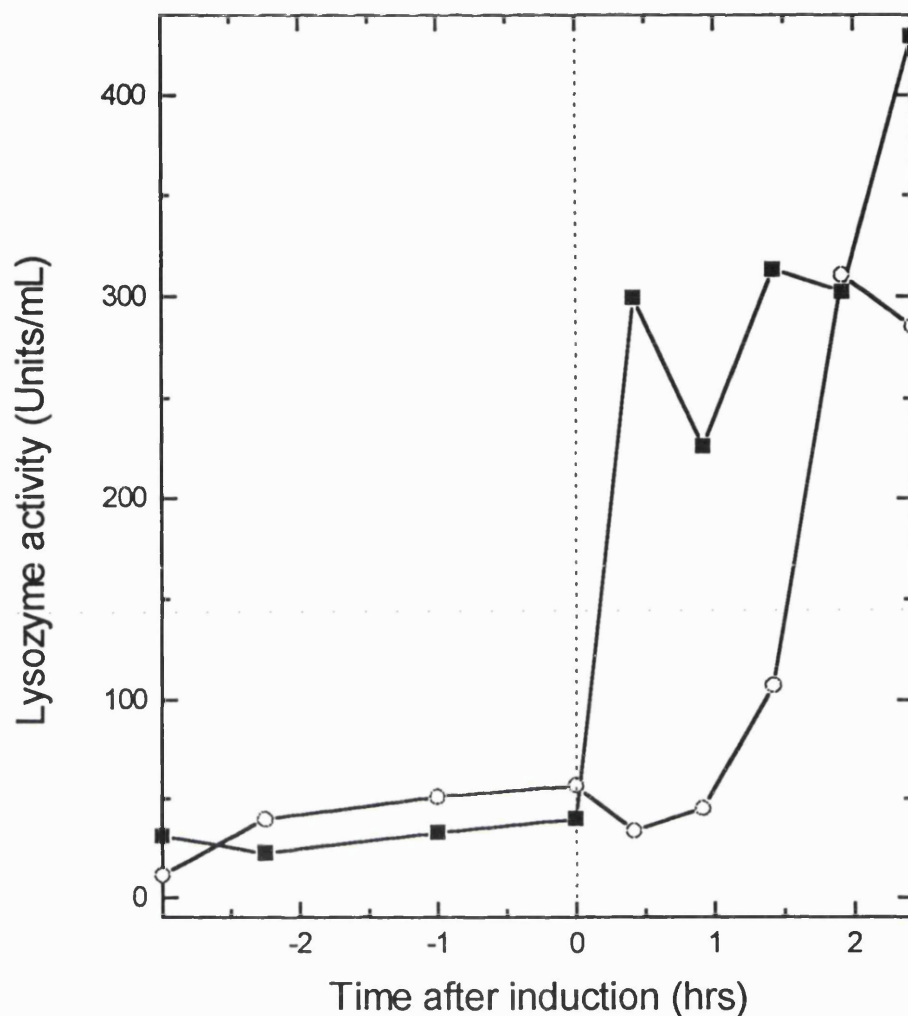


Figure 5.3 Cellular distribution of T4 lysozyme-his following a 14 L fermentation. Intra (■) and extracellular (○) distribution before and after induction from a 14 L (8.4 L ww) fermentation of *E.coli* pQR752 grown on nutrient broth. Time zero induction is indicated by a dotted line. 40-50% T4 lysozyme-his has leaked to the medium at 2-2.5 hr after induction.

5.3.2.2 42 L fermentation

A 42 L batch fermentation (25 L working volume) was carried out in a LH series 42 L bioreactor under the same conditions as the 14 L Chemap fermentation. After 4.75 hrs (OD_{600} 1.87) the culture was induced with 1 mM IPTG and harvested 1.75 hr later. The cells of 1.7 g/L final dry cell weight, were separated in a 1P tubular bowl centrifuge. The cell paste was retained and stored at -20°C .

The culture appeared to be in late log phase (OD_{600} 1.87) at the point of induction but on-line CER and OUR data suggest growth had stopped before this (Figure 5.4). Cell lysis occurred, repeating the pattern seen in the previous 14 L Chemap fermentation. At one hour after induction 75% of T4 lysozyme-his produced was retained within the cell, but by 1.75 hr 50% had leaked to the medium (Figure 5.5). The rate of lysozyme synthesis in both fermentation runs was also about the same: 14 L Chemap; 302 Units/mL and 42 L LH; 378 Units/mL were retained intracellularly, after 1.92 and 1.83 hr respectively. The slightly higher rate in the 42 L LH is probably due to accelerated growth due to faster agitation which was raised to 800 rpm after 2.5 hr growth (maximum agitation in 14 L Chemap was 600 from $t = 3.5$ hr), and airflow of 0.76 vvm as compared to 0.59 vvm in the 14 L Chemap.

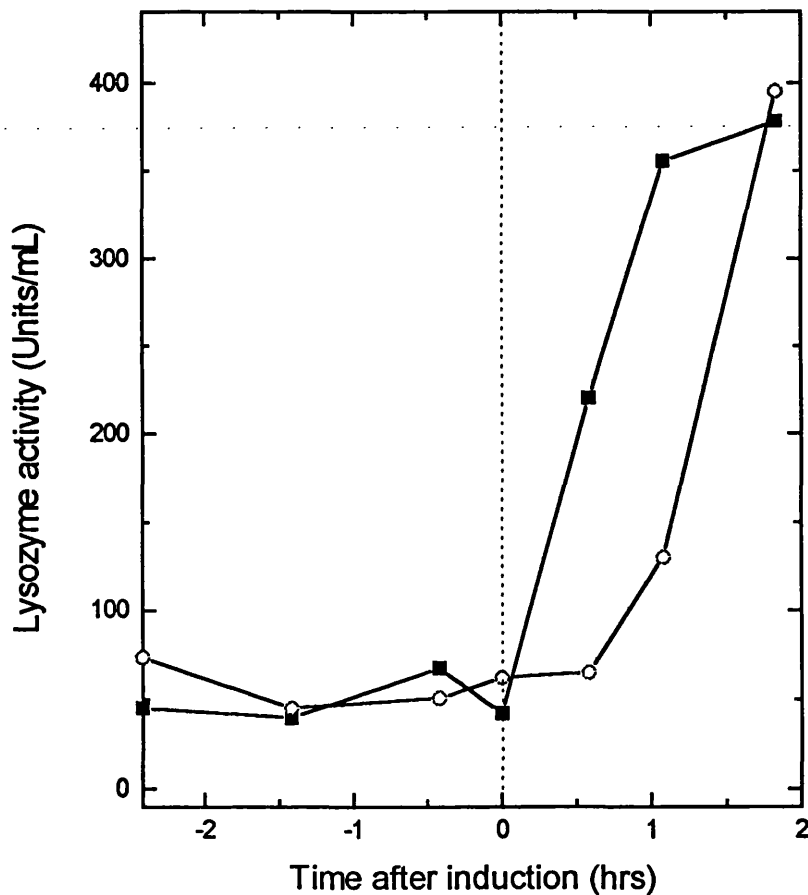


Figure 5.5 Distribution of T4 lysozyme-his following a 42 L fermentation. intra (■) and extracellular (○) distribution before and after induction from a 42 L (25 L wv) fermentation of *E.coli* pQR752 grown on nutrient broth. Time zero induction is indicated by a dotted line. 50% T4 lysozyme-his has leaked to the medium by 1.75 hours after induction.

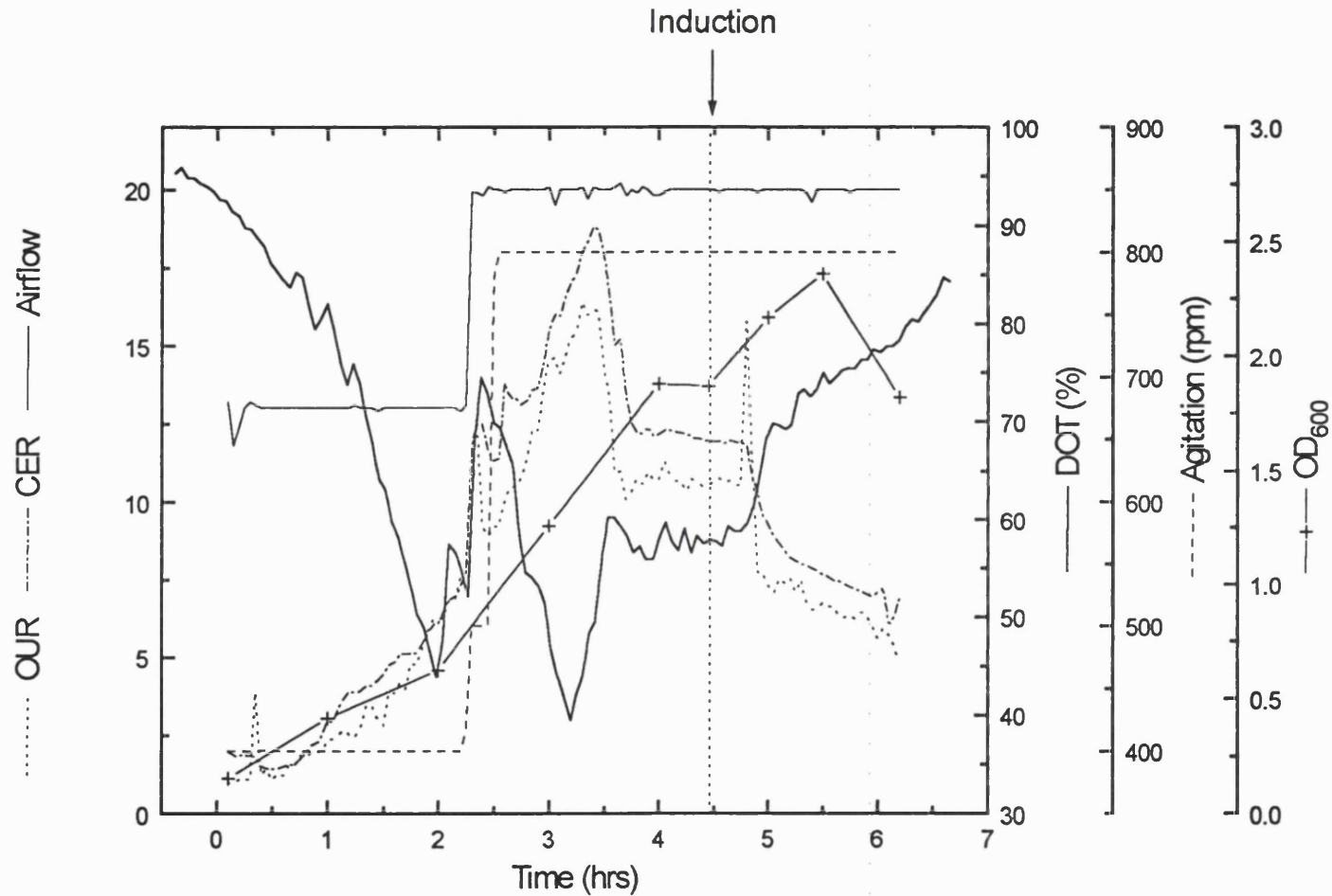


Figure 5.4 Real-time on-line data plot of 42 L (25 L wv) *E. coli* pQR752 fermentation on nutrient broth media. On-line variables and optical cell density: oxygen uptake rate (OUR); carbon evolution rate (CER); airflow (L/min); percentage dissolved oxygen tension (DOT); agitation (rpm) and OD₆₀₀. IPTG induction took place after 4.5 hours growth at OD₆₀₀ 1.87 as indicated by the arrow and dotted vertical line.

After induction OUR and CER start to decline as cells lyse and die. The viable cell count drops from 1.6×10^9 colony forming units or cfu/mL at induction to 0.4×10^9 cfu/mL at harvest and plasmid stability decreases from 100% to 34% over the same period with > 50% decline in plasmid stability within half an hour of induction (Figure 5.6).

The growth rate slows after induction and oxygen uptake and carbon evolution rates decline. The reduction in growth rate can be ascribed to the metabolic burden resulting from plasmid relating activities (Ryan and Parulekar, 1991). The addition of IPTG to wild type *E. coli* has been shown to alter metabolism and protein pattern and its addition retards cellular growth at all stages of the growth curve (Sakamoto et al., 1994).

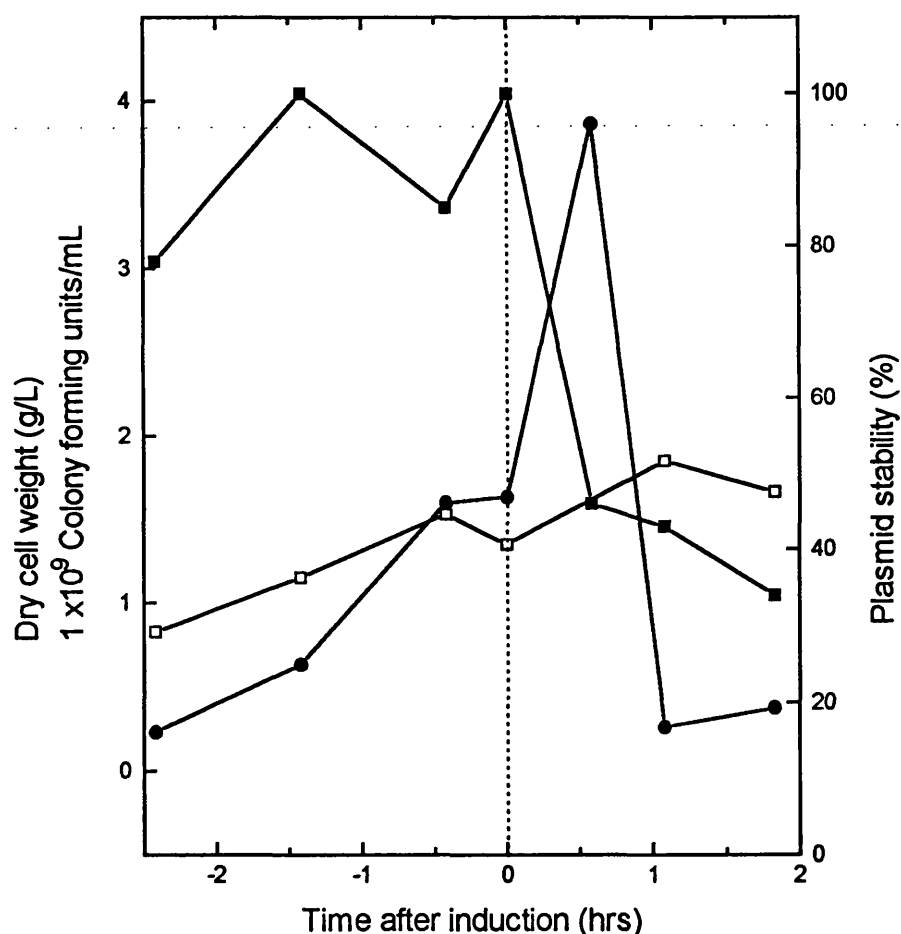


Figure 5.6 Off-line measurements of 42 L *E. coli* pQR752 fermentation grown on nutrient broth. Dry cell weight (g/L) (□), colony forming units (cfu/mL) (●) and plasmid stability (%) (■) over the time course before and after induction.

5.3.2.3 Discussion

In both 14 L and 42 L fermentations the highest rate of T4 lysozyme-his production was seen in the first hour following induction which then levelled out. This coincides with leakage of the lysozyme to the medium; 25% is leaked 1.0 to 1.5 hours and 50% 2.0 to 2.5 hours after induction. Plasmid stability dropped from 100% to 43% after 1.0 hour and to 34% by ~ 2.0 hours.

The peptidoglycan layer provides a framework for attachment of DNA prior to its replication and segregation (Hendrickson et al., 1982). Membranes of plasmid-containing cells are thought to become very leaky and fragile and this may result partly from the attachment of a large number of plasmids to the outer cell membrane. This is manifested by a growth rate differential between plasmid free and plasmid bearing cells (plasmid stability) as the plasmid bearing cells are destroyed and leak the protein contents to the medium. The decline in the production rate of product after 1 hour (after induction) can be explained in part by the depletion of amino acids from the medium (Strandberg et al., 1991). The intracellular accumulation of product could also have a negative effect on the cells and cause them to lyse.

The enzymatic nature of the heterologous protein product itself, T4 lysozyme, may exacerbate cell leakage by its lytic action on the already vulnerable cell membrane. Specific action of the enzyme on the peptidoglycan layer would be expected to rapidly result in complete lysis. Accumulation of target protein has been shown to be limited at least in part by the build up of toxic waste products during induction (MacDonald and Neway, 1990).

Plasmid stability can have a strong influence on product formation. Selective pressure may be exerted by the presence of an ampicillin resistant plasmid but Jung et al. (1988) report that ampicillin at 100 mg/L is degraded in less than 30 minutes by secreted β -lactamase in the medium.

Batch mode fermentation on nutrient broth media under these conditions is limiting in terms of biomass concentration reached, cell integrity and plasmid stability on induction with IPTG, leading to low productivity. A significant improvement which will be seen further on was achieved by changing the media composition and the growth temperature.

5.4 Optimisation of Cell Growth and Recombinant Protein Production

5.4.1 Introduction

The effect of media composition and temperature on growth of *E. coli* JM107 pQR752 was investigated. The aim was to compare the effect of complex media compositions (containing high concentrations of organic nitrogen) on cell growth, cell density and T4 lysozyme-his titres. A high level of organic nitrogen, mainly in the form of yeast extract, has been shown to enhance gene expression during the induction period (Tsai et al., 1987).

The effect of reducing the growth temperature from 37°C to 28°C on T4 lysozyme-his production and cell integrity following induction was explored. Evidence suggests that formation of soluble recombinant proteins in *E. coli* is favored by lower growth temperature (23-30°C). This was observed for several *E. coli* strains and for different plasmid constructions (Scheimn and Noteborn, 1988).

The effect of varying the concentration of the analogue IPTG inducer and phase of growth at time of induction was investigated. The reduction in IPTG concentration necessary to induce gene expression would be desirable in terms of cost.

5.4.2 Effect of media composition and temperature

Experiments were carried out in 250 mL flasks in 50 mL media and in duplicate. An overnight culture, grown on the respective media types, provided an inoculum (1% v/v) and two sets of cells, at 28°C and at 37°C, were cultured separately in nutrient broth (NB), terrific broth (TB) and high biomass medium (HBM) (section 2.5.3). OD₆₀₀, dry cell weight, viable cell count and plasmid stability were monitored. The cultures were not induced in the first instance.

As was seen previously, nutrient broth could only sustain active growth until an optical density of about 1.0 was reached. After 9 hours growth TB and HBM cultures at 37°C appeared to be in late exponential growth phase, whereas TB and HBM grown at 28°C were still growing actively and linearly (Figure 5.7). This suggests that conditions for improved growth could be more favorable at the lower temperature. This is borne out by higher biomass concentrations at 28°C as measured by dry cell weight (Table 5.1). At t (time) = 9 hr the number of cfu/mL were higher for the cultures at 28°C. The cultures

Table 5.1 Effect of media type and temperature on growth of *E. coli* JM107 pQR752. Measured dry cell weight (g/L), colony forming units per mL (CFU/mL) and plasmid stability (%) for culture grown in TB (terrific broth) and HBM (high biomass medium) at (28°C and 37°C) after 9 and 26 hours growth.

	Growth time t = 9 hours				Growth time t = 26 hours			
	TB (28°C)	HBM (28°C)	TB (37°C)	HBM (37°C)	TB (28°C)	HBM (28°C)	TB (37°C)	HBM (37°C)
Dry cell weight (g/L)	6.0	3.0	1.4	1.5	–	–	–	–
Colony forming units per mL (cfu/mL)	11 x10 ⁹	8.3 x10 ⁹	4.6 x10 ⁹	3.0 x10 ⁹	1.6 x10 ¹⁰	9.3 x10 ⁹	8.0 x10 ⁹	2.7 x10 ⁹
Plasmid stability (%)	69	85	0	90	83	100	0	55

were grown overnight and at $t = 26$ the number of cells retaining the ampicillin resistant plasmid were 10 fold greater for the cultures at the lower temperature. TB (37°C) completely lost the plasmid and the plasmid stability of HBM (37°C) dropped from 90% at $t = 9$ to 55% at $t = 26$, whereas TB (28°C) and HBM (28°C) had a plasmid stability of 83 and 100% respectively.

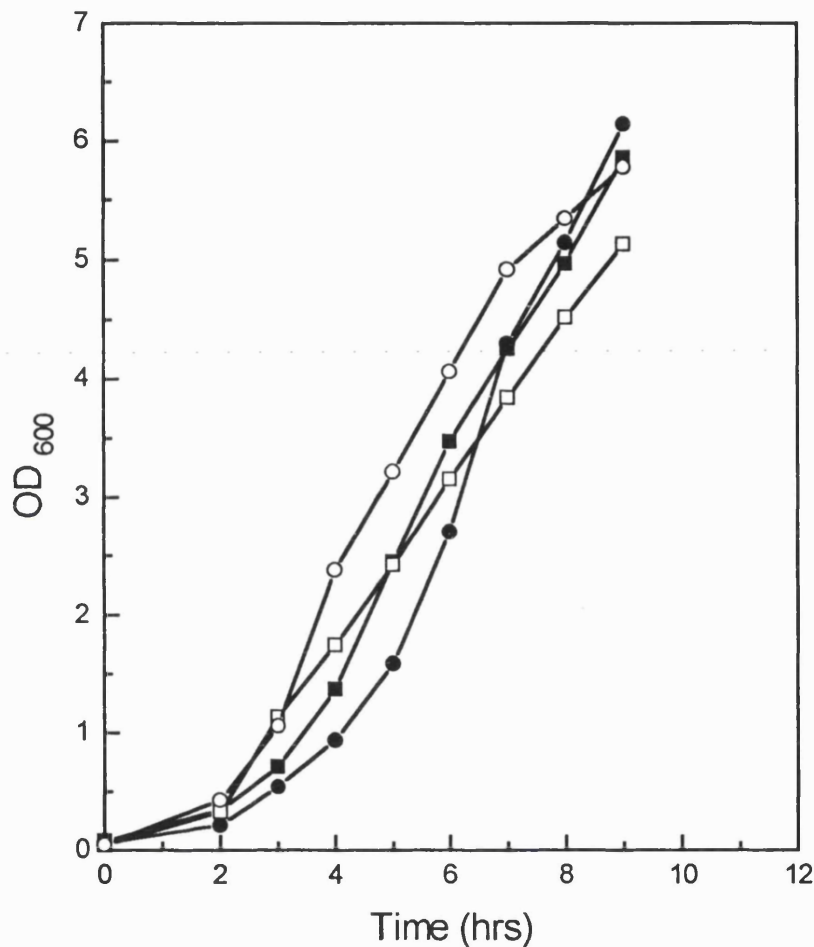


Figure 5.7 Growth curves of *E. coli* pQR752 grown on two different complex media types and at two different temperatures - not induced. High Biomass Medium (HBM) at 28°C (●) and 37°C (○) and Terrific Broth (TB), at 28°C (■) and 37°C (□).

Reduced metabolic stress on the organism due to the lower temperature appears to result in prolific and stable growth as seen by increased biomass and retention of ampicillin resistance. It follows that these cultures should produce more T4 lysozyme-his which was subsequently confirmed, see below.

The experiment was repeated to test the effect of temperature (37°C and 28°C) and media type (HBM, TB and as a control NB) on growth and T4 lysozyme-his production. Also this time the cultures were induced with 1 mM IPTG.

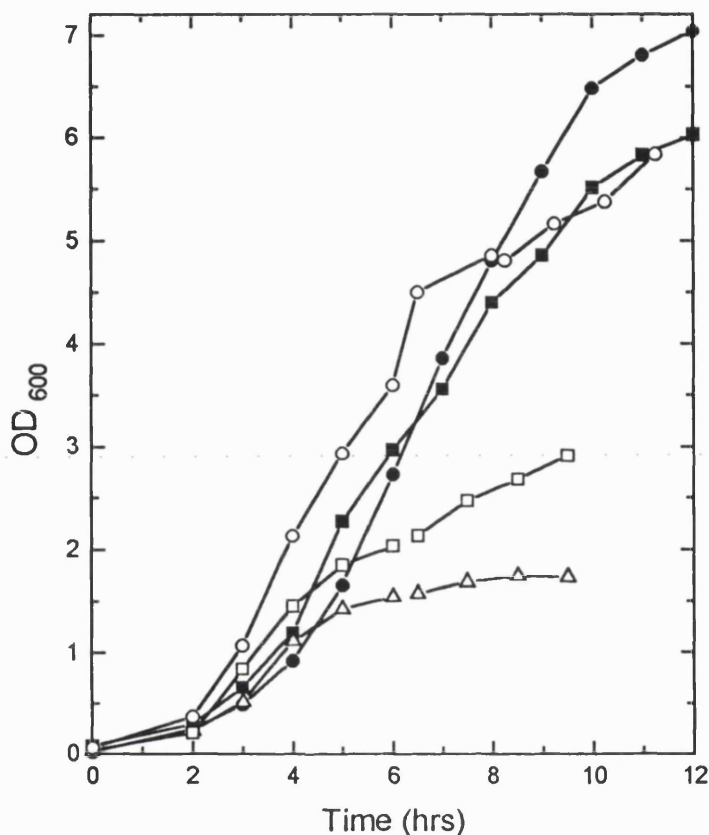


Figure 5.8 Growth curves of *E. coli* pQR752 producing T4 lysozyme-his grown on two different complex media types and at two different temperatures. High Biomass Medium (HBM) at 28°C (●) and 37°C (○), Terrific Broth (TB) at 28°C (■) and 37°C (□), and Nutrient Broth (NB) at 37°C (△). Each culture was induced with IPTG 3 hours before harvest (the last OD₆₀₀ reading).

NB and TB at 37°C were induced after 6.5 hr growth at OD₆₀₀ 1.57 and 2.13 respectively as the growth rate began to slow down. Similarly HBM at 37°C was induced at 8.5 hr (OD₆₀₀ 4.81). At 28°C HBM and TB (NB culture failed to grow) were still growing exponentially when they were induced at t = 9, OD₆₀₀ 4.86 and 5.17 respectively (Figure 5.8). Following induction NB (37°C) and to a lesser extent TB (37°C) cultures stopped growing. HBM (37°C), TB (28°C) and HBM (28°C) continued

growing but the growth rate gradually slowed down. HBM (28°C) reached the highest OD₆₀₀ of 7.04 after 3 hours induction.

Samples taken at hourly intervals following induction were assayed for lysozyme activity. After 3 hours induction, HBM (28°C) which had the highest biomass concentration, produced the most T4 lysozyme-his (702 Units/mL, 1003 Units/mg) and over the 3 hour induction period 90-94% was retained within the cell (Figure 5.9 and Table 5.1)). In contrast, HBM at 37°C produced 3 times less, (260 Units/mL, 413 Units/mg). In addition a lower percentage of T4 lysozyme-his was retained within the cell (65-85%) compared to the HBM at 28°C. T4 lysozyme-his was also produced by TB cultures in greater quantities at the lower temperature, i.e., 539 Units/mL at 28°C compared to 466 Units/mL at 37°C. About 87% was recovered in the cell at the lower temperature but only 60% at 37°C. NB culture, grown only at 37°C, had at t = 1 induction, 99% of T4 lysozyme-his produced present within the cell, which corresponded to 499 Units/mL with a high specific activity of 1847 Units/mg. After 1 hour cells grown on nutrient broth and at 37°C lyse and leak recombinant T4 lysozyme to the medium where 64% and 54% were found at t = 2 and t = 3 after induction.

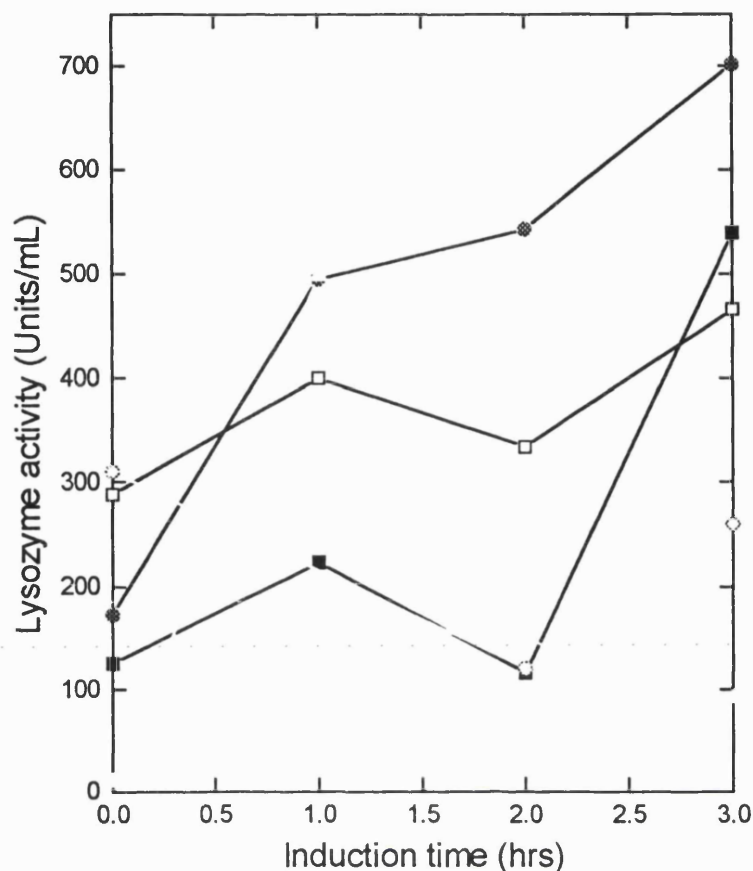


Figure 5.9 Activity of intracellular T4 lysozyme-his produced by *E. coli* pQ752 grown on High Biomass Medium. T4 lysozyme-his retained intracellularly at $t = 0, 1, 2$ and 3 hours after induction when *E. coli* pQ752 is grown on High Biomass Medium (HBM) at 28°C (●) and 37°C (○), Terrific Broth (TB) at 28°C (■) and 37°C (□), and Nutrient Broth (NB) at 37°C (Δ).

5.4.2.1 Discussion

In summary, the recombinant *E. coli* organism cultivated on high biomass medium at 28°C achieved the highest biomass (3-fold increase on the 37°C culture) and produced the highest T4 lysozyme-his concentration. In addition about 90-94% of the lysozyme was intracellularly retained.

Exponential growth continued for longer at the lower temperature with concomitant higher biomass production. On induction the cultures at the lower temperature kept growing, albeit more slowly, in contrast to the cultures at the higher temperature which levelled off straight away. It is well known that cultivation temperature substantially influences the specific rates of cellular growth (Shiloach and Bauer, 1975; Kapralek et

al., 1991). The positive effect seen by lowering the growth temperature might be as a result of the extension of culture time in conditions that retained high productivity of the cells (Sakamoto et al., 1994).

Media composition can be separated into three broad classes: complex, semi-complex and defined. Large scale commercial production normally uses complex media in a batch or fed-batch mode of operation (Namdev et al., 1993). Complex media usually support high specific growth rates compared to defined media. This is due to the presence of biosynthetic intermediates and growth factors which the cell no longer needs to synthesize, thus decreasing the metabolic burden. All three media types tested were complex. The yeast extract concentration of terrific broth was 24 g/L and of high biomass medium was 40 g/L (there was no yeast extract in nutrient broth). Yeast extract is thought to affect regulatory processes concerning the initiation of transcription and translation and also synthesis of certain proteins (Xiaoli et al., 1990). Yeast extract supplemented media gave the highest biomass stimulation per unit of component added compared with supplementation with various amounts of amino acids, vitamins, minerals, purines/pyrimidines, tryptone, casamino acids, casein peptone or gelatin peptone. Sakamoto et al. (1994) found that productivity increased 3-fold when yeast extract was supplied and that an increase from 5 to 20 g/L enhanced productivity 5.5-fold. The evidence found in the literature supports the much enhanced productivity and cell integrity of cells grown on HBM with a yeast extract concentration of 40 g/L. Because nutrient depletion is no longer a problem, healthier and therefore stronger cell walls may form which are less prone to leak cellular protein following induction. A cessation of T4 lysozyme-his leakage halts the rapid destruction and lysis of cells seen formerly with cultivation on nutrient broth at 37°C.

Plasmid stability was enhanced by a lower growth temperature and by growth on a high yeast extract concentration. High biomass medium grown at the lower temperature supported an increasing number of viable cells into stationary phase and plasmid stability was maintained. Kuowei et al. (1994) also found that decreasing the cultivation temperature resulted in an increase in plasmid stability.

5.4.3 Effect of induction conditions and IPTG concentration

Cultivations were carried out under the optimised conditions of growth on high biomass medium at 28°C. A set of identical cultures, in log phase of growth and at an OD₆₀₀ of about 4.0 (8 hr growth) were IPTG induced. A range of IPTG concentrations (final

concentration) were added; 1 mM, 100 μ M, 10 μ M 1 μ M and 0 μ M IPTG and the cultures were grown for a further 3 hours.

Quantitative protein and lysozyme activity was monitored intra and extracellularly at $t = 0$ and at $t = 1, 2$ and 3 hours following induction. Induction has the effect of slowing cell growth as the cells switch to production of T4 lysozyme-his (Figure 5.10).

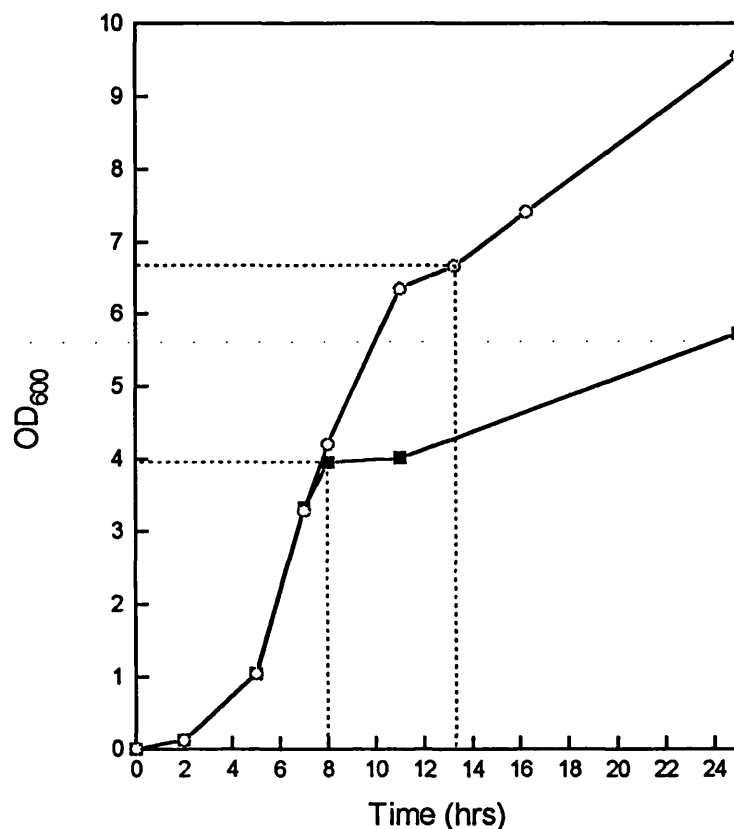


Figure 5.10 Growth curves of *E. coli* pQR752, IPTG induced at mid-log and late-log phase of growth. IPTG (1 mM) induction in mid-log (■) and late log (○) growth phase. Cultivation was on High Biomass Medium and at 28°C. The dotted lines indicate when induction took place.

Figure 5.11 shows that 1 mM IPTG final concentration resulted in the highest levels of T4 lysozyme-his activity (906 Units/mL) in the cell. T4 lysozyme-his production increases almost linearly in the three hours following induction, but there was no further increase and activity levels remained constant within the cell as can be seen at $t = 14$ h, 920 U/mL. A minimum of 1 mM IPTG (final concentration) is necessary to induce the promoter fully to produce T4 lysozyme-his. It is possible that higher concentrations could result in more efficient induction but cost limitations require a satisfactory

minimum concentration to be found. Lower concentrations are not sufficient to initiate induction properly.

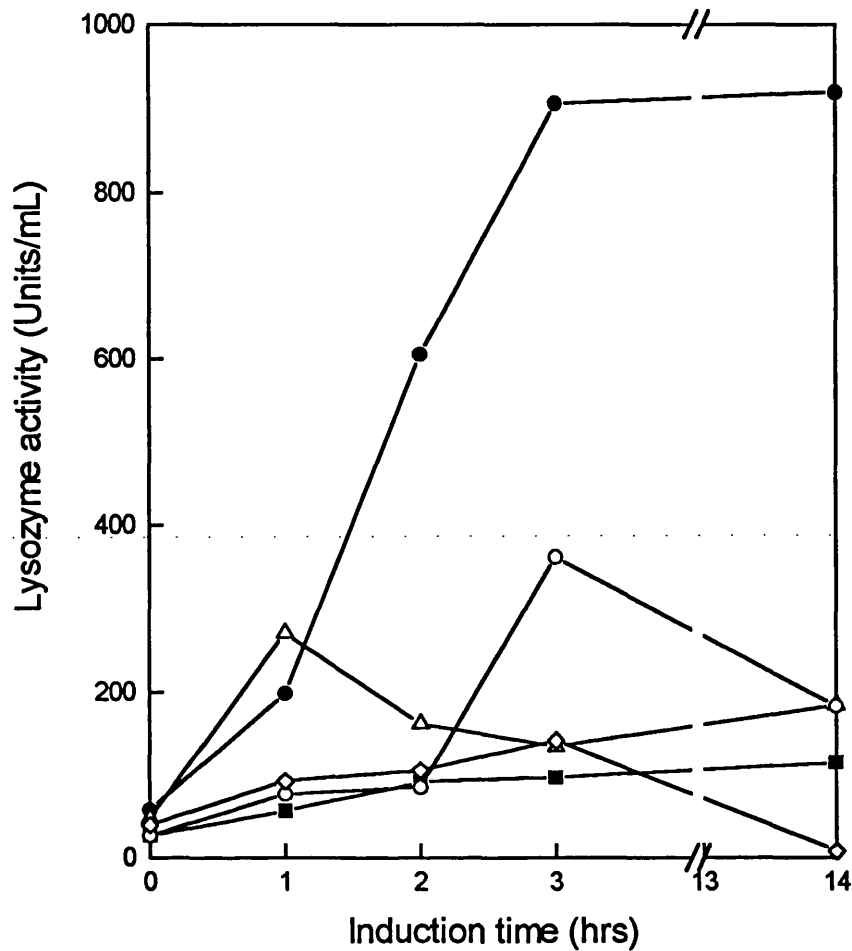


Figure 5.11 Lysozyme activity (intracellular) as a result of mid-log phase IPTG induction of *E. coli* pQR752 producing T4 lysozyme-his. 1000 μM (●), 100 μM (Δ), 10 μM (\circ), 1 μM (\diamond) and no IPTG (\blacksquare).

Tracking of lysozyme activity revealed little or no leakage of T4 lysozyme-his from the cell and no external accumulation over a three hour period (Figure 5.12). After 14 hours in the induced state the extracellular level of T4 lysozyme-his did rise slightly, indicating a certain degree of leakage from the 25 hr old cell. The leakage was insufficient to cause lysis of the cells. In fact, levels of T4 lysozyme-his in the medium are close to background levels in the un-induced culture.

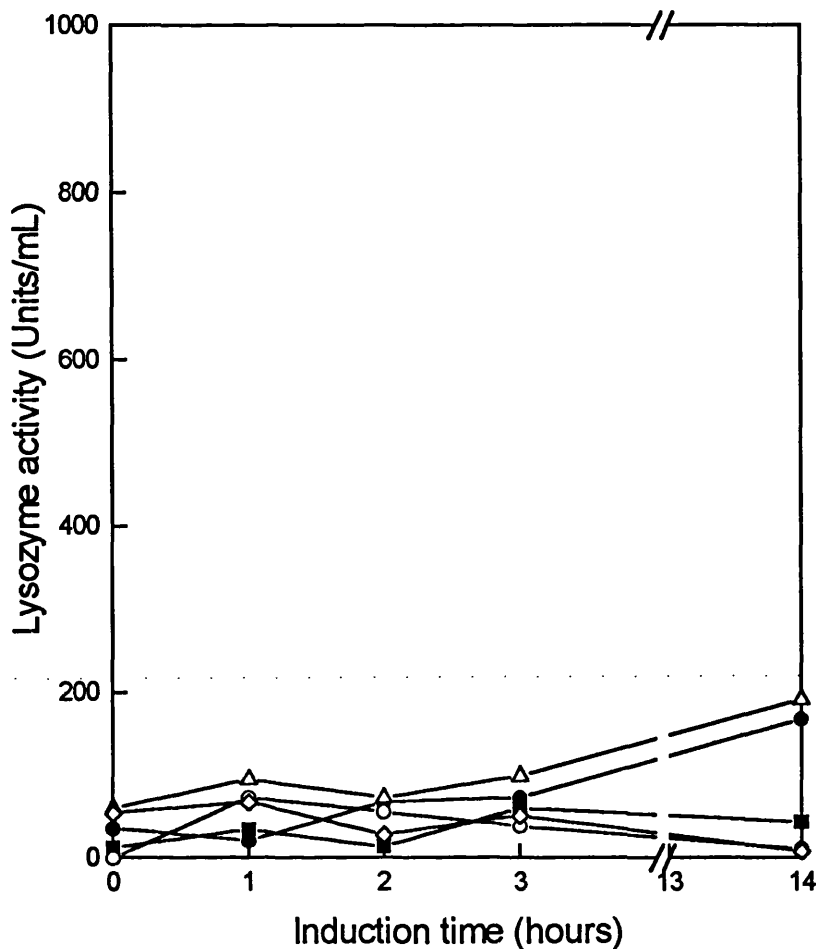


Figure 5.12 Lysozyme activity (extracellular) as a result of mid-log phase IPTG induction of *E. coli* pQR752 producing T4 lysozyme0-his. 1000 μM (●), 100 μM (Δ), 10 μM (○), 1 μM (◇) and no IPTG (■).

The same experimental procedure of varying the final concentration of IPTG was repeated except that the set of cultures were induced at late log phase i.e., $\text{OD}_{600} \sim 7.0$ (13 hours growth) (Figure 5.10) and the IPTG final concentrations were slightly different at 1 mM, 200 μM , 100 μM , 20 μM and 0 μM . The cells were entering stationary phase and 1 mM IPTG induction was met with limited success. There was no T4 lysozyme-his synthesised in the first hour following induction and production peaked (420 U/mL) after 2 hours but had dropped off by $t = 3$ (300 Units/mL) (Figure 5.13). Negligible T4 lysozyme-his leaked from the cell over the three hour induction period.

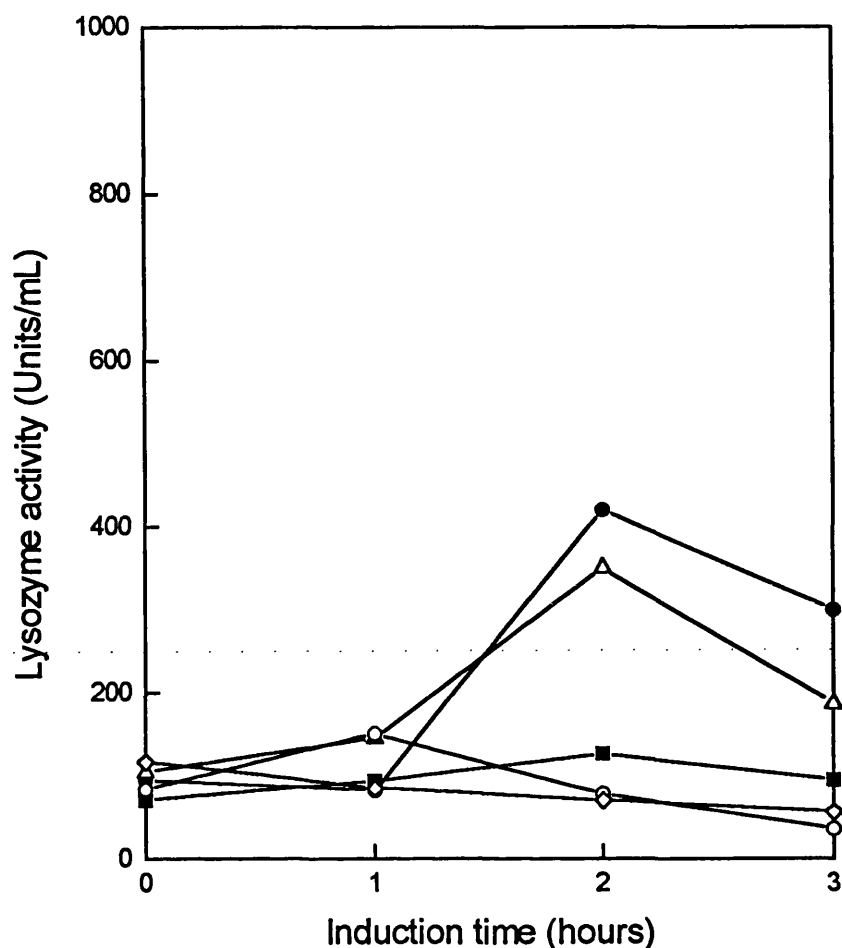


Figure 5.13 Lysozyme activity (intracellular) as a result of late log phase IPTG induction of *E. coli* pQR752 producing T4 lysozyme-his. 1000 μM (●), 100 μM (Δ), 10 μM (○), 1 μM (◇) and no IPTG (■).

Cells that have stopped growing actively (in stationary phase), nearing the end of their life cycle, do not have the resources or energy to fully initiate induction. Their response is slow and production peaks after 2 hours at less than half (46%) of the maximum potential.

5.4.3.1 Discussion

IPTG at 1.0 mM concentration is necessary for effective induction. The concentration of added inducer can influence gene expression as was seen by Wood and Peretti (1991) who observed a linear increase in β -galactosidase activity when the commonly used tac promoter inducer, IPTG, concentration was increased from 0.01 to 1.0 mM. Following induction there is an almost linear increase in intracellular T4 lysozyme-his concentration and 93% is retained intracellularly as was also seen previously (Section 5.4.2). In

addition, induction beyond 3 hours does not significantly augment lysozyme levels and by this time the cells become prone to minor leakage. Cells in mid-exponential phase of growth should be induced for optimal production of target protein as was also observed by Sakamoto et al. (1994). There is > 2-fold higher recovery of lysozyme activity from the mid-exponential cells. Therefore cells should be induced between OD₆₀₀ of 3-6 or after 3.75-10.5 hours growth in shake flasks.

5.5 *E. coli* Fermentation on High Biomass Medium

5.5.1 Bioreactor cultivation

7 L (5 L working volume) batch fermentations of *E. coli* JM107 pQR752 on high biomass medium (HBM) were carried out in a stirred tank 7 L LH2000 bioreactor (Incelltech LH-SGI, Reading, Berkshire, U.K.) at 28°C. The aeration rate was 2.5 L/min or 0.5 vvm and the pH was held constant at pH 7. Off-line optical cell density (OD₆₀₀), cell count and viability and dry cell weight were monitored throughout the fermentation. Total protein and recombinant T4 lysozyme-his activity were monitored at time zero induction and over the next three hours.

A preliminary run was carried out to determine the effect on the growth rate and parameter profile when scaling up from shake flask to 7 L bioreactor vessel. In this instance the culture was neither induced nor harvested.

The impellor speed was set at 400 rpm to start but because of depletion in the levels of dissolved oxygen due to uptake, the agitation was increased to 600 rpm after 4 hours and was raised by 200 rpm at further 2 hour intervals. At t = 9 the agitation was raised to an upper limit of 1200 rpm where it remained overnight. It appears that oxygen deprivation is a growth limiting factor on this complex media. Exponential growth continued until t = 9, OD₆₀₀ 10.78 when the culture became starved of oxygen (Figure 5.14).

At t = 7 (mid to late exponential phase) 6.3 x10⁹ colony forming units per mL (cfu/mL) were recorded. At t = 21 there were 5.3 x10¹⁰ cfu/mL (~ 10-fold increase) and 100% plasmid stability over the growth cycle. Dry cell weight was 6 g/L at late exponential phase (T = 9) and 10.4 g/L after 21 hours.

A second exponentially growing 6 hour culture of OD₆₀₀ 5.6 was induced with IPTG (1 mM) and was grown for a total of 23 hours before harvest. After 3 hours induction 85% of T4 lysozyme-his produced was retained within the cell (474 U/mL activity and 290

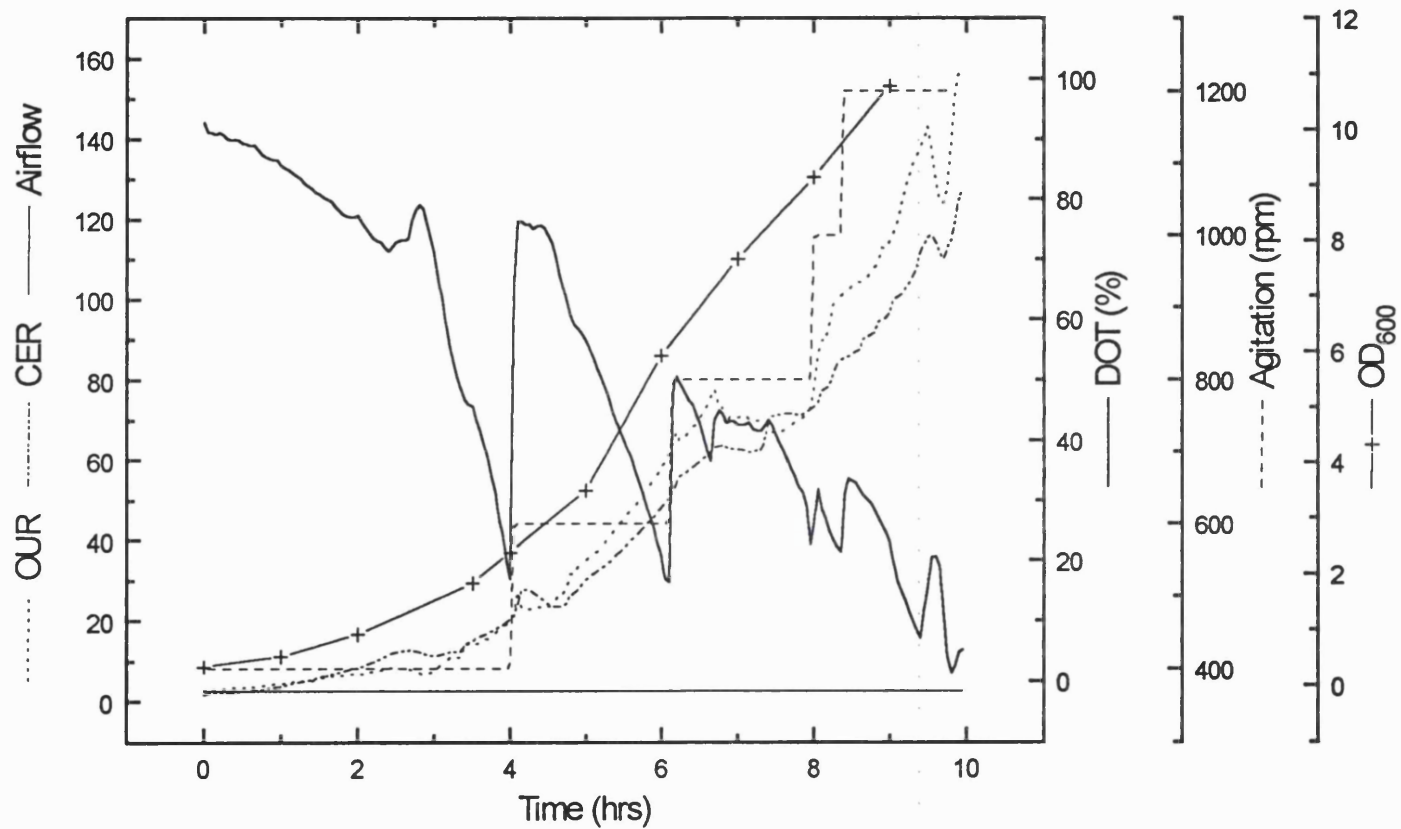


Figure 5.14 Real-time on-line data plot of 7 L (5 L ww) *E. coli* pQR752 fermentation on high biomass medium at 28°C. On-line variables and optical cell density: oxygen uptake rate (OUR); carbon evolution rate (CER); airflow (L/min); percentage dissolved oxygen tension (DOT); agitation (rpm) and OD₆₀₀. *The culture was not IPTG induced.*

Units/mg specific activity) (Figure 5.15). After 14 hours induction, intracellular T4 lysozyme-his activity reached 824 Units/mL, specific activity didn't really change (301 Units/mg), but the percentage retained within the cell dropped to 53% indicating cell lysis in stationary phase resulting in 50:50 distribution of T4 lysozyme-his between the cell and the medium.

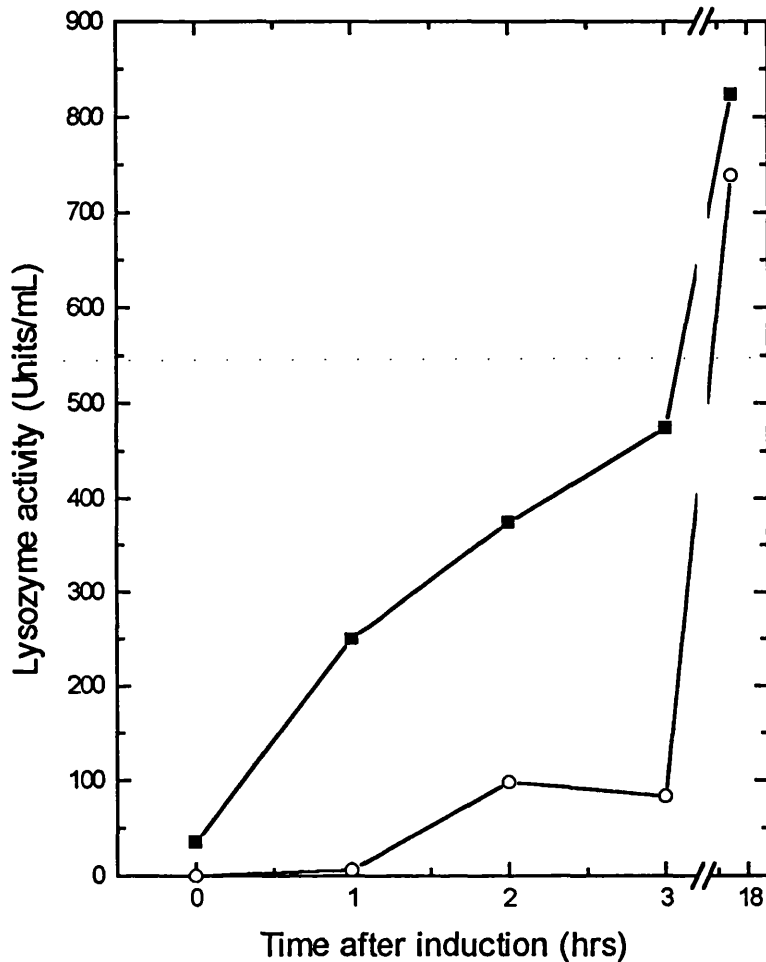


Figure 5.15 Cellular distribution of T4 lysozyme-his following 7 L fermentation on High Biomass Media. T4 lysozyme-his produced and distributed intra- (■) and extracellularly (○) following induction in 7 L *E. coli* pQR752 fermentation on High Biomass Medium at 28°C.

OD_{600} increases linearly in exponential growth phase until one hour after induction when the growth rate slows. The same pattern is seen with the dry cell weight (Figure 5.16). At the point of induction the concentration of cfu/mL was 5.5×10^9 and 81% plasmid

stability was recorded. Plasmid stability started to decrease following induction (plasmid stability was 66% at $t = 3$ induction). After 17 hours induction the cell count was 1.3×10^{10} cfu/mL and the plasmid stability about 0.42%. In effect the organism had lost the plasmid encoding for T4 lysozyme-his production as detected by ampicillin resistance. An explanation could be oxygen deprivation as the RT-DAS on-line data plot shows oxygen became limiting (DOT 40.9%) at $t = 9.17$, 3 hours after induction (Figure 5.17).

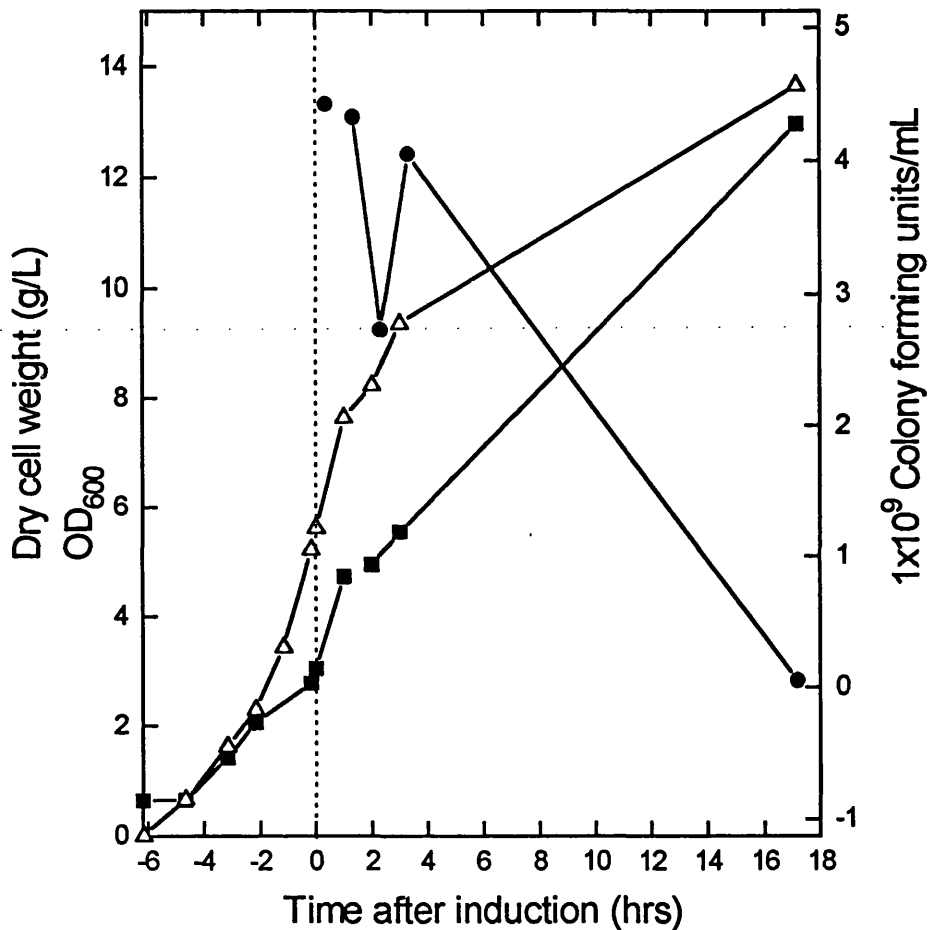


Figure 5.16 Growth of 7 L *E. coli* pQR752 fermentation (induced) on High Biomass Medium at 28°C. Dry cell weight (g/L) (■), optical cell density (OD₆₀₀) (Δ) and colony forming units per mL (cfu/mL) (●) are shown over time. The point of IPTG induction is represented by a dotted vertical line.

The concentration of T4 lysozyme-his found in the cell after 3 hours induction (474 U/mL activity and 290 Units/mg) is lower than expected, based on recoveries in shake flask experiments (702 Units/mL and 1003 Units/mg), although as before, > 85% was retained within the cell. The reason may be because the culture was induced too early in

exponential growth (OD_{600} 5.6). The un-induced 7 L fermentation was shown to grow exponentially until an OD_{600} 10.78 was reached and oxygen became limiting (Figure

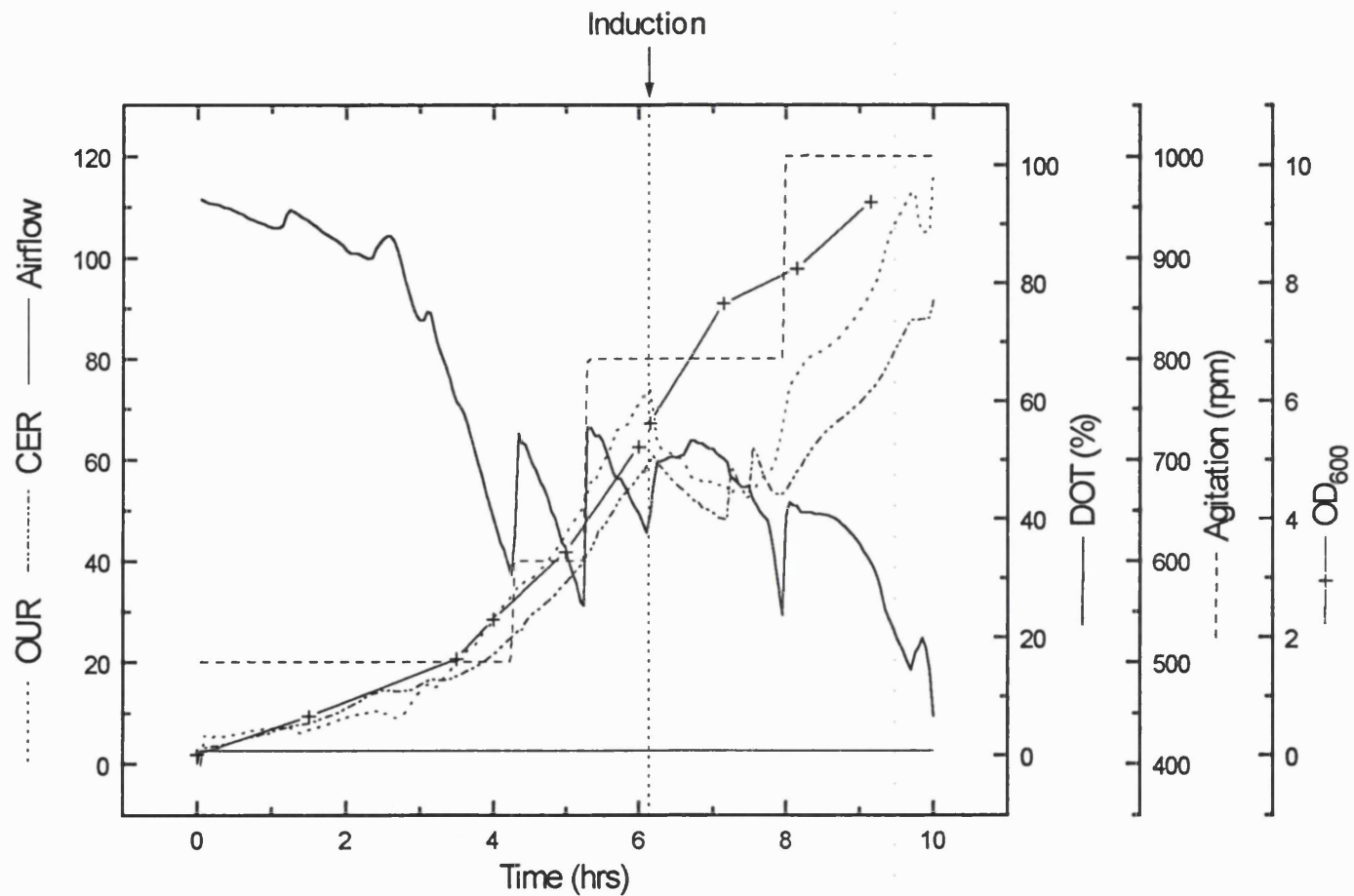


Figure 5.17 Real-time on-line data plot of 7 L (5 L wv) *E. coli* pQR752 fermentation on high biomass medium at 28°C. On-line variables and optical cell density: oxygen uptake rate (OUR); carbon evolution rate (CER); airflow (L/min); percentage dissolved oxygen tension (DOT); agitation (rpm) and OD₆₀₀. The culture was IPTG induced after 6 hours at OD₆₀₀ 5.6 as indicated by the dotted vertical line.

5.14). Shake flask experiments showed that optimum productivity was gained by inducing during mid-exponential growth. Rapidly dividing cells in early exponential growth are probably incapable of optimal recombinant protein synthesis. Evidence for this may be the continued production of T4 lysozyme-his by the more mature cells after 3 hours induction which is an aspect not found occurring in the shake flask experiments.

Plasmid stability can have a strong influence on product formation (Jung et al., 1988). A reduction in plasmid stability (66% after 3 hours induction) could also be attributed to induction taking place too early in the culture's growth. The metabolic burden placed on the young cells may force them, in response, to jettison the plasmid. It is probable that plasmid instability becomes more problematic in larger scale fermentations. The cells grow faster due to improved aeration and the ampicillin antibiotic, which confers segregational stability, gets used up more rapidly. Jung et al. (1988) report that when 100 mg/L of ampicillin was added to high density cultures it was degraded in less than 30 minutes by the secreted β -lactamase in the medium.

The on-line data plot indicates that the culture continued to grow actively with rising carbon evolution and oxygen uptake rate for 10 hours and $OD_{600} \sim 10$ was reached. The stirrer speed was increased by steps throughout to keep pace with oxygen demand and at $t = 10$ was 1000 rpm. Airflow was kept constant at 2.5 L/min. After $t = 10$ the culture was oxygen deprived and at $t = 23$ plasmid stability was 0.42%. Oxygen deprivation for longer than 0.5-1.5 hr can cause plasmid instability in *E. coli* (Namdev et al., 1993). Dissolved oxygen or nutritional status is thought to regulate replication of the plasmid. Amplification at the beginning of the slow growth phase depends on oxygen supply and that oxygen fluctuation in large-scale bioreactors may affect amplification of plasmids in *E. coli*. The dissolved oxygen concentration can rapidly become growth limiting at high cell concentration. This is usually a result of mass transfer limitations. The oxygen consumption will increase with both the growth rate as well as the high biomass concentration (Yee and Blanch, 1992).

In summary, *E. coli* JM107 pQR752 producing T4 lysozyme-his grows rapidly on high biomass medium and there is a danger that the culture could become oxygen limiting. If the fermentation had been harvested as expected at 3 hr following induction, plasmid stability would have been 66%, and 85% of T4 lysozyme-his produced would have been intracellularly retained. Future work should look to find the point in late exponential growth phase where induction would yield the highest titres of target protein. Plasmid stability could also be helped by controlling the rate of growth and determining the optimal point of induction.

5.5.2 High pressure homogenisation

The 23 hour old culture (OD_{600} 14), was harvested using a Sharples 1P tubular bowl centrifuge (section 2.5.3.1). This centrifuge operates at a speed of 45,000 rpm which is achieved by an air drive turbine, operating at a pressure of 2 bar (max.). 35.2 g/L wet weight of cells were collected and suspended in Tris buffer to give a 58.66% and a 29.33% cell suspension. Each cell suspension was passed through the homogeniser five times at 1200 bar and a sample was taken at each pass. The samples were kept on ice before being centrifuged at 13,500 rpm for 15 minutes. The supernatant was assayed for lysozyme activity and total protein content.

In both the 58% and 29% cell suspensions the highest levels of T4 lysozyme-his activity were found in the resuspended cell supernatant before any disruption. The stationary phase cells had lysed and already leaked 50% of the intracellular lysozyme. It is likely that further disruption occurred on resuspending the cells, accounting for the presence of lysozyme in the supernatant prior to homogenisation. Further cell breakage by five successive passes through the LAB 40 homogeniser at 1200 bar saw a dramatic drop in the free enzyme activity level for the 58% cell suspension. After the first pass activity dropped from 1247 Units/mL to 500 Units/mL and it remained constant at this value over the following four passes (Figure 5.18). The less concentrated cell suspension (29%) showed a gradual drop in the enzyme levels over the five passes, from 1009 Units/mL to 602 Units/mL.

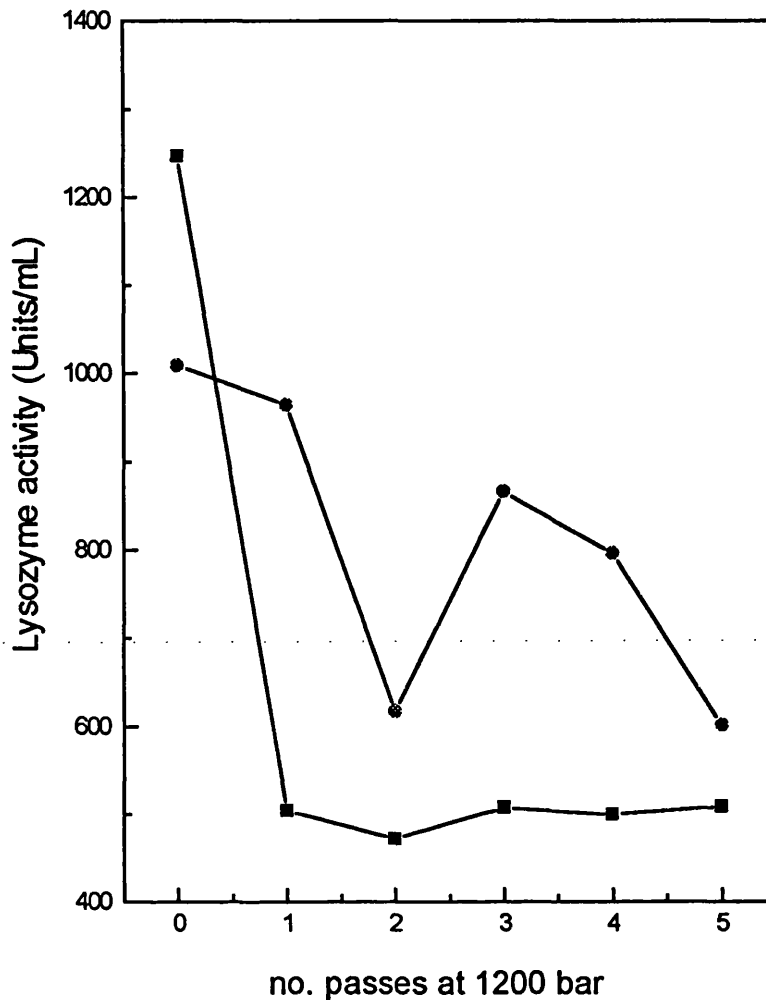


Figure 5.18 T4 lysozyme-his released by high pressure homogenisation of *E. coli* pQR752 cells (23 hr old). Lysozyme activity released at two cell suspension concentrations, 59% (■) and 29% (●).

These results suggest that the high pressure conditions (1200 bar) destroyed > 50% of the enzyme activity. Results from recombinant *E. coli* strains using a high pressure disrupter have shown that the lowest pressure required to break the cells is 4 kpsi and the highest is in excess of 35 kpsi; wild-type *E. coli* cells tend to break between 17 kpsi and 23 kpsi, depending on the growth conditions (Foster, 1995). Possibly the shear force of the first pass denatures the protein and damages the active site, so activity per unit mg of total protein plunges. For both cell suspension concentrations, the activities and specific activities drop dramatically after the first pass and level out over the subsequent 4 passes. The pattern of effect on specific activity is virtually the same for the 29% and 58% cell

suspensions but the damage is less pronounced for the less concentrated suspension, i.e., specific activities are > 2-fold higher (Figure 5.19).

This study of disruption of 23 hr old cells in stationary growth phase which had been induced for 17 hr was carried out as a preliminary investigation. Future work to find the optimal conditions (i.e., operating pressure and number of passes) for disruption and release of T4 lysozyme-his will need to be determined.

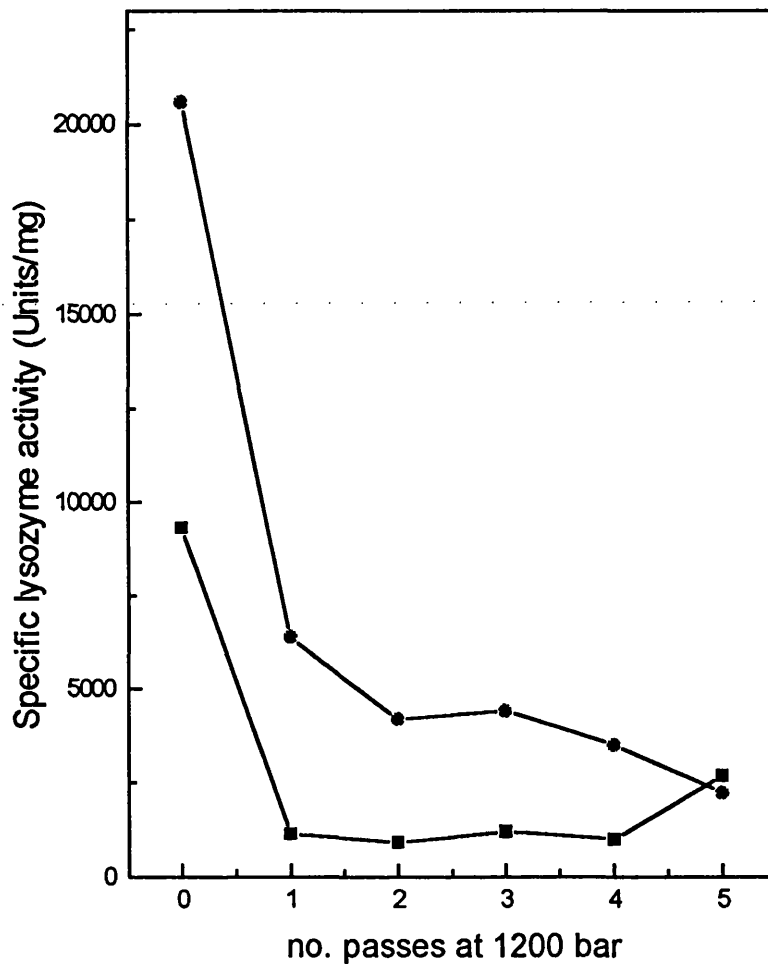


Figure 5.19 Specific activity of T4 lysozyme-his released by high pressure homogenisation. Release at of two different cell suspensions, 59% (■) and 29% (●) over 5 passes.

5.6 Conclusions

Problems of low biomass and leakage of T4 lysozyme-his to the medium when the strain was cultured on nutrient broth at 37°C were overcome by culturing on a yeast extract

rich medium at 28°C. This yielded high biomass concentrations and virtually eliminated leakage (85-95% T4 lysozyme-his was retained intracellularly after 3 hr induction). In this way problems of product leakage, premature cell lysis and large processing volumes were overcome. It was also found the cells should be induced during their exponential phase of growth for three hours before harvest with a minimum of 1 mM IPTG analogue inducer.

Shake flask culturing of cells in high biomass medium led to a ~ 4 fold increase in biomass and ~ 5.5 fold increase in a 7 L LH2000 Series fermenter. Intracellular accumulation of T4 lysozyme-his increased from 15-20% (shake flask) to 25-30% (fermenter) of the total cell protein. Up to 200 mg/L T4 lysozyme-his was produced in shake flasks and in excess of 400 mg/L was achieved in the fermenter as determined by scanning gel densitometry (Table 5.2).

Table 5.2 Effect of enriched culture media and temperature reduction on biomass, cell integrity and T4 lysozyme-his productivity.

	Shake Flask		Fermenter (7 L)
	Nutrient broth (37°C)	High biomass medium (28°C)	High biomass medium (28°C)
Harvest OD ₆₀₀	1.7	7.0	9.4
T4 lysozyme-his expression (% total protein) *	20	26	26
T4 lysozyme-his (mg/mL)	46	182	424
T4 lysozyme-his retained intracellularly (%)	50	94	85

* Determined by scanning densitometry of SDS polyacrylamide gel.

The high concentration of yeast extract (40 g/L) present in the medium is thought to lead to the formation of stronger cell walls which is borne out by increased retention of T4 lysozyme-his within the cell and higher sonication energy necessary to disrupt the cells. Enrichment of culture broth with yeast extract has been shown to increase production of biomass and recombinant protein in *E. coli* (Xiaoli et al., 1990). The presence of high levels of organic nitrogen in the form of yeast extract may result in increased product formation by protection of the recombinant protein from proteolytic degradation (Tsai et al., 1987); affect regulatory processes concerning the initiation of transcription and translation (Xiaoli et al., 1990) and aid enzyme stabilisation (Nancib et al., 1991). Higher levels of soluble recombinant protein can be obtained by lowering the culture growth temperature from 37°C to 30°C (Schein and Noteborn, 1988). There is no evidence for the formation of inclusion bodies or other insoluble aggregates within the cells grown and induced at 28°C in the high biomass medium.

CHAPTER 6

PERIPLASMIC LYSIS BY T4 LYSOZYME-HIS

6.1 Aim

The widespread use at scale of lysozyme, in periplasmic lysis and release, has been hampered by its high cost for single cycle use and its subsequent presence as a contaminant of the target protein. The aim of this work was to develop an enzymatic process to disrupt the peptidoglycan layer of the *E. coli* cell wall and release the contents of the periplasmic space using a re-usable poly-histidine tailed T4 phage lysozyme that is easily recovered in a single step by immobilised metal affinity separation.

6.2 Introduction

The gram negative bacterium, *Escherichia coli*, is the host of choice in many cases for the commercial production of recombinant proteins. However, few *E. coli* proteins are secreted into the extracellular medium (Müller et al., 1983) and the mechanisms for secretion are as yet poorly understood (Hirst and Welch, 1988). Cytoplasmic disruption techniques result in swamping of the target protein with contaminant intracellular material - hence the product must be separated from a complex mixture of contaminants. Genetic engineering of foreign or native signal sequences into recombinant proteins has allowed the expression of proteins into the periplasmic space of the bacteria. Periplasmic proteins normally represent only 4% of the total cell protein species (Nossal and Heppel, 1966), therefore, less extensive purification of recombinant proteins is required than for proteins located in the cytoplasm. The location of recombinant proteins in the periplasmic space has a number of further advantages over intracellular and extracellular release; they are often found to be in their native, biologically active form as the oxidative environment of the periplasm allows the correct folding due to disulphide bond formation (Pollit and Zalkin, 1983). Protein secretion into the periplasm of *E. coli* cells has been shown to confer stability (Talmadge and Gilbert, 1982) and only 7 out of 25 known cellular proteases are present in the periplasm which will reduce the incidence and risk of proteolytic digestion in comparison with the intracellular compartment (Swamy and Goldberg, 1982; Baneyx and Georgiou, 1991). Also periplasmic location reduces the volume that needs to be processed during downstream processing.

Periplasmic protein release can be brought about by chemical and enzymic lysis or by mechanical disruption. Mechanical disruption has several drawbacks including denaturation and inactivation of the target protein. Since cells have to be broken completely to obtain a high yield, all intracellular materials are released (Engler, 1985). Hence, the product must be separated from a complex mixture of contaminants. Alternatively, the commercial lytic enzyme, lysozyme, effects cell lysis by hydrolysing β -1,4 glycosidic linkages between alternating NAG-NAM (N-acetylmuramic acid - N-acetyl glucosamine) residues in the peptidoglycan layer of the cell wall (Neu and Heppel, 1965; Birdsell and Cota-Robles, 1967; Kaback, 1971). Its gentle and specific action offers the very attractive potential of differential protein release from the periplasmic space. However it has not been used widely for large scale intracellular product release due chiefly to the expense of using large amounts of the enzyme without any prospect of recycle.

This work describes a scheme for periplasmic protein release employing a 're-usable' recombinant histidine-tailed T4 lysozyme fusion protein which may be selectively recovered from the *E. coli* spheroplast/released protein mixture for re-use. Cysteine-free pseudo wild type T4 lysozyme has been genetically modified by insertion of a poly-histidine tail sequence (N-His-Gln-His₃-C) at the C-terminus. Successful recovery and purification of the recombinant T4 lysozyme (T4 lysozyme-his) was demonstrated by immobilised metal affinity on IDA Sepharose columns charged with Zn²⁺, Ni²⁺ and Cu²⁺ ions (Sloane et al., submitted). T4 bacteriophage and hen egg white lysozyme, both muramidases, have the same mode of lytic action. However, T4 lysozyme is ~250 times more active than hen egg white lysozyme on *E. coli* cells as a substrate (Tsugita et al., 1968) making it the ideal choice of enzyme for periplasmic processing of recombinant proteins in *E. coli*. Enzyme activity is not affected by the C-terminus attachment of the poly histidine-tail as it is located well away from the active site (Sloane et al., submitted).

6.3 Expression and Purification of T4 Lysozyme-his

Problems of low biomass and leakage of T4 lysozyme-his to the medium when the strain was cultured on nutrient broth at 37°C (Sloane et al., submitted) were overcome by culturing on a yeast extract rich medium at 28°C (section 5.4.2). This yielded high biomass concentrations and virtually eliminated leakage (85-95% T4 lysozyme-his was retained intracellularly after 3 h induction). 1 L culture was grown and induced as described in section 2.5.3.1 (wet cell weight 14.5 g/L). Harvested cells were sonicated (section 2.5.5.3). The supernatant was equilibrated in phosphate buffer and divided equally into two parts. One half was diluted to 21 mL with equilibration buffer prior to

its fractionation by immobilised metal affinity chromatography on a Cu^{2+} -charged HiTrap™ chelating column (section 2.6.1.2). T4 lysozyme-his, at 26% expression, was separated from the crude *E. coli* cell extract. The formation of a strong T4 lysozyme-his/ Cu^{2+} -Sephacrose complex resulted in peak elution at low pH (between 4.2-3.9) and over a large volume (107 mL). When 259 mg protein was loaded onto the 5 mL Cu^{2+} -charged chelating HiTrap™ column, 49.5 mg T4 lysozyme-his at 97% purity and a yield of 71% was obtained (Table 6.1 and Figure 6.1). A ten-fold concentration of pooled T4 lysozyme-his peak fractions (107 mL to 11 mL) was achieved by dehydration with sucrose followed by dialysis into lysis buffer (section 2.5.6.1).

Table 6.1 Purification of recombinant T4 lysozyme on Cu^{2+} -charged Chelating Sepharose HP.

Purification step	Volume (mL)	Total protein (mg)	Total activity (Units)	Specific activity (Units/mg)	Overall yield (%)	Purity (%)	Purification factor
Crude extract	21	258.50	13007	50	100	26	1
Cu^{2+} purified	11 ^(a)	49.50	8919	180	71	97	3.6 ^(b) -3.7 ^(c)

(a) Volume following 10-fold concentration.

(b) Calculated from specific activity.

(c) Calculated from scanning densitometry of SDS-polyacrylamide gel.

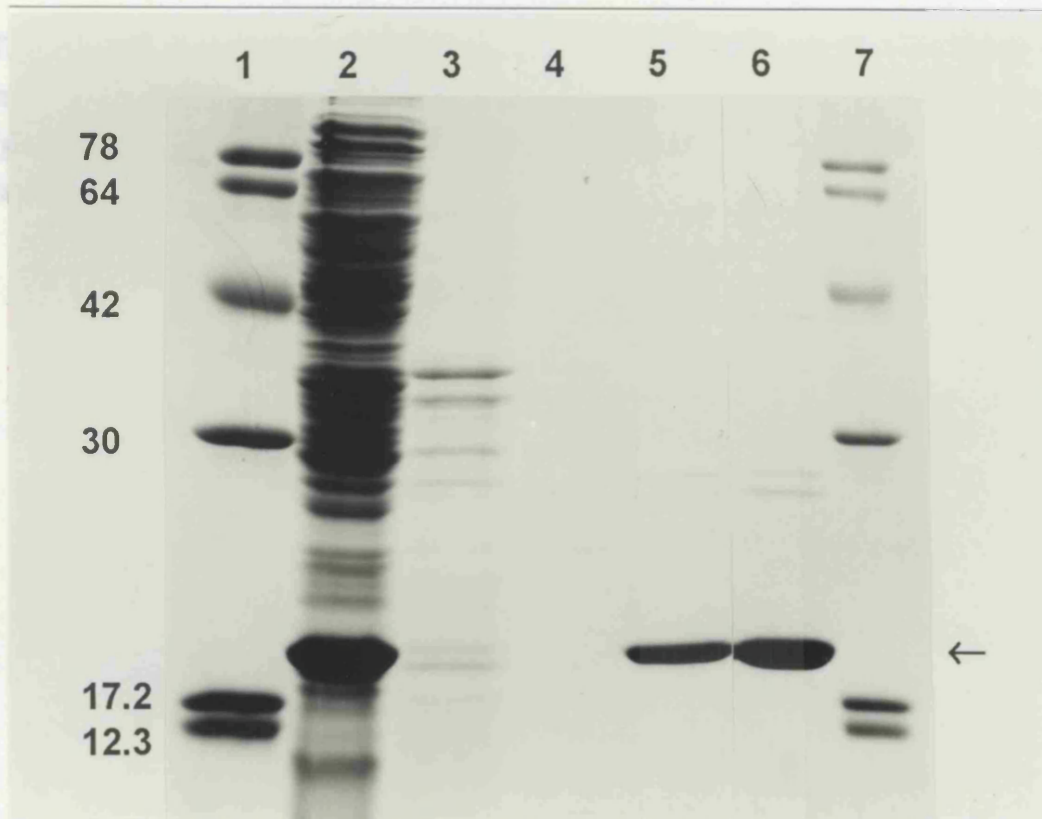


Figure 6.1 Immobilised metal affinity chromatographic recovery of recombinant T4 lysozyme on a Cu^{2+} -charged HiTrap™ column. An SDS polyacrylamide gel shows in *lanes 1&7*, molecular weight markers; *lane 2*, the loaded crude extract with T4 lysozyme-his expressed at 26%; *lane 3*, column flowthrough; *lane 4*, column wash; *lane 5*, eluted T4 lysozyme-his (pooled fractions); *lane 6*, T4 lysozyme-his concentrated.

6.4 Periplasmic Lysis

A culture of *E. coli* JM83 containing the plasmid pQR187 which encodes for *Streptomyces thermoviolaceus* CUB74 α -amylase was kindly provided by J. J. Pierce of this department (section 2.5.4). Cell lysis was carried out by a modified version of the method described by French (1993) which employed hen egg white lysozyme (section 2.5.6.2). T4 lysozyme-his purified by IMAC- Cu^{2+} and crude extract containing T4 lysozyme-his were tested separately.

Three T4 lysozyme-his concentrations in lysis buffer, 0.23, 1.5 and 2.75 mg, when contacted with a range of α -amylase producing *E. coli* cell concentrations caused periplasmic lysis and release of α -amylase (Figure 6.2). A control test with no lysozyme present displayed a low background level of α -amylase release. This is due to a degree

of lysis caused by the action of EDTA, present in the lysis buffer, on chelating metal ions on the cell surface and to the osmotic shock effect on the cells when transferred from a high sucrose concentration to a lower concentration when 1:2 diluted with cold distilled water.

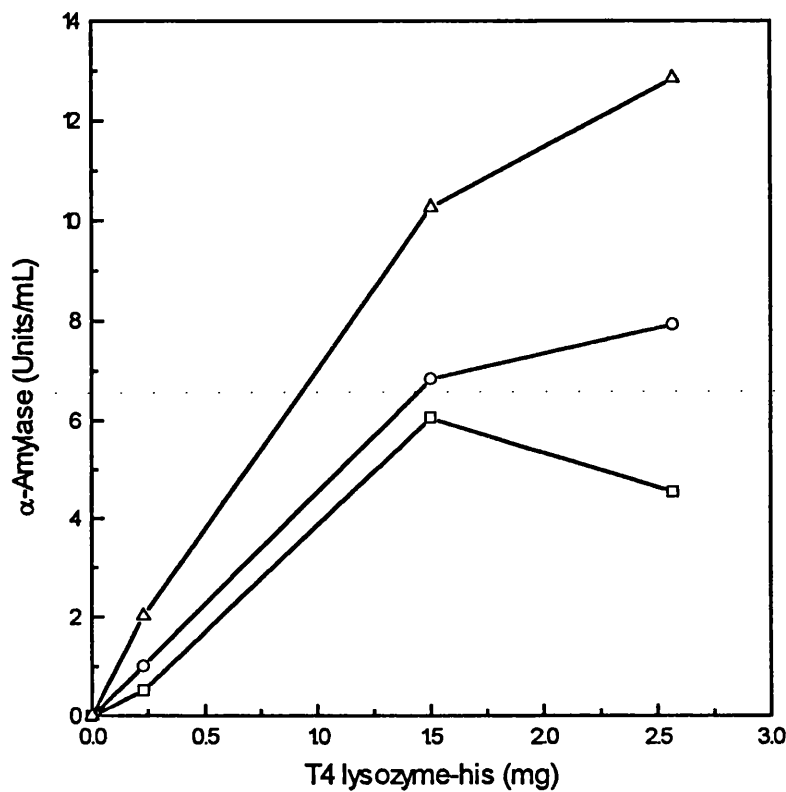


Figure 6.2 Release of α -amylase (activity Units/mL culture) from the periplasm by 0.23, 1.50 and 2.57 mg T4 lysozyme-his in lysis buffer at three increasing dry cell weight concentrations of 1.28 (\square), 2.55 (\circ) and 5.10 (Δ) mg/mL.

In an initial experiment, T4 lysozyme-his (0.23 mg) treated, cell-free lysed, cell extracts were pooled to provide sufficient material, dialysed against equilibration buffer and loaded on a Zn^{2+} -IMAC column. α -Amylase was collected in the flowthrough and T4 lysozyme-his was separated and eluted in a peak at pH 6.2-5.2. However, recovery was low, with only 19% of expected T4 lysozyme-his actually recovered. The disappearance of T4 lysozyme-his was found to be related to increasing cell concentration as measured by dry cell weight (Figure 6.3). T4 lysozyme-his recovered following centrifugation dropped steadily from 100% at 4.0×10^{-3} mg/mL to 14% at 4.0 mg/mL.

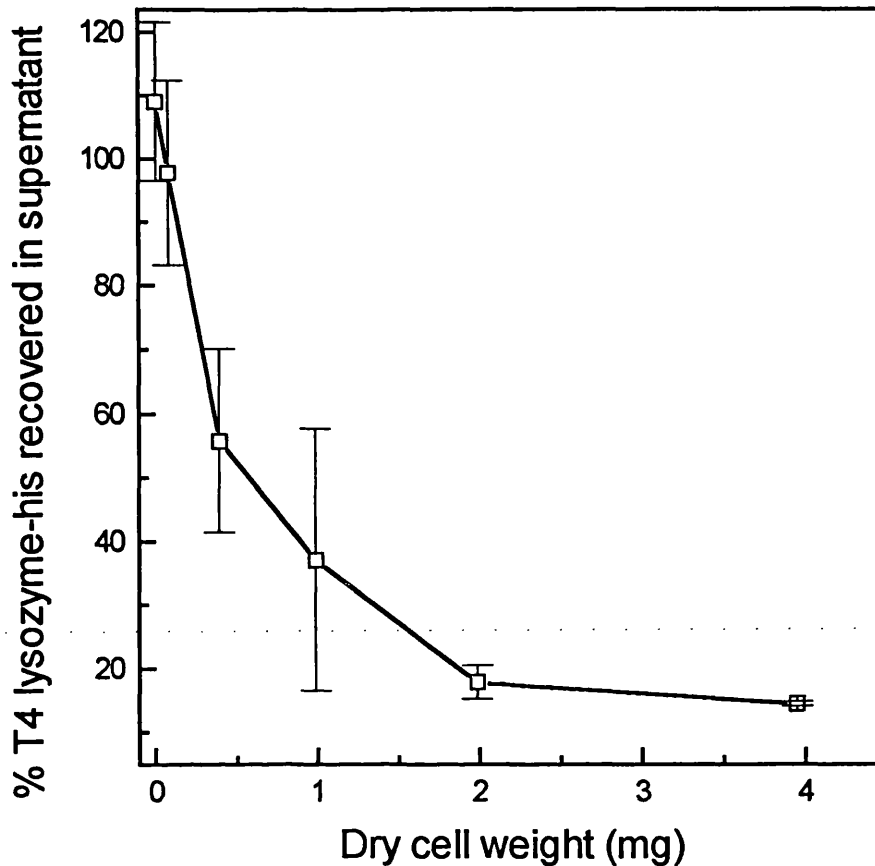


Figure 6.3 T4 lysozyme-his recovered (%) from lysed cell supernatant at increasing dry cell weight, at constant T4 lysozyme-his input concentration (0.23 mg).

There was an increase in the levels of α -amylase released from the periplasm with increasing dry cell weight concentration (Figure 6.2). Therefore, the disappearance of T4 lysozyme-his activity from the cell-free supernatant is not explained by deactivation or inhibition of the lytic enzyme. A more likely explanation is that T4 lysozyme-his is absorbed by the increase in the number of sites on the bacterial cell wall.

Lysozyme, with an iso-electric point of approximately 11 will be strongly positively charged at any pH of the medium at least up to pH 10.5. It can be assumed that the cell wall is negatively charged (Salton, 1964) even at neutral pH and thus the electrostatic forces will favour absorption of lysozyme by cells (Davies et al., 1969). Muraki et al. (1988) have argued that conditions of low pH and ionic strength lead to the creation of strong electrostatic forces between positively charged lysozyme and negatively charged cell wall. Hence, strong interaction would be expected in the lysis mixture at neutral pH

and relatively low ionic strength (the optimal conditions for catalytic activity). Also more T4 lysozyme-his would be adsorbed as the cell concentration is increased. It therefore appears that T4 lysozyme-his becomes immobilised to the peptidoglycan layer through electrostatic forces and although its action in lysing the cell wall is unaffected, its recovery can only be achieved by dissociation from the cell wall. According to Muraki et al. (1988) at high ionic strength and pH the electrostatic forces between enzyme and substrate will weaken and allow the two to dissociate. Figure 6.4 shows a schematic representation of the effects of change in ionic strength or pH on the electrostatic forces between positively charged lysozyme and negatively charged cells.

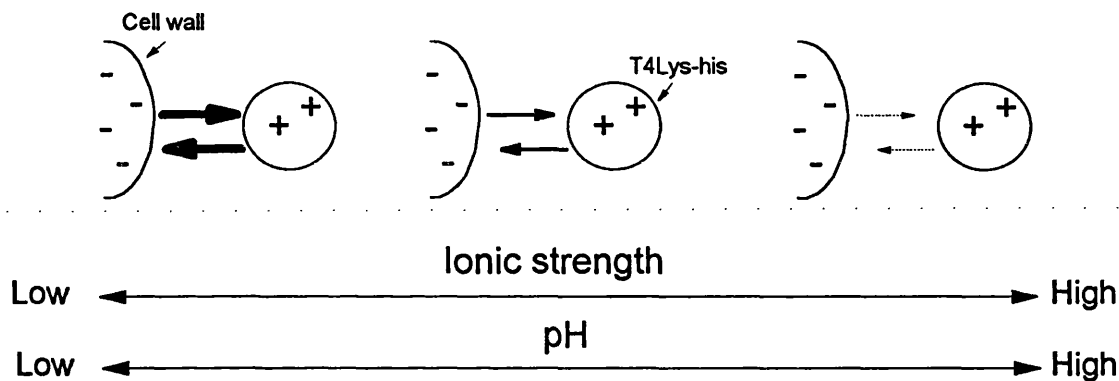


Figure 6.4 Schematic representation of the effect of ionic strength and pH on the electrostatic interaction between lysozyme and *M. lysodeikticus* cells (Muraki et al., 1988). The symbols + and - denote positive and negative charge respectively. The strength of electrostatic forces between enzyme and substrate are indicated by the thickness of the arrow.

In order to test this, the experiment was repeated to include two 1 mL washes of the lysed cell pellet with buffer of high ionic strength and pH (0.02 M phosphate, 0.5 M NaCl, pH 7.74). The inclusion of this step was successful in dissociating and releasing into solution a considerable amount of protein and T4 lysozyme-his (Table 6.2). Equal amounts of protein at comparable dry cell weights were recovered in the phosphate washes of cells treated with (a) T4 lysozyme-his (2.75 mg) in a crude protein cell extract mix and (b) purified T4 lysozyme-his (1.5 mg), suggesting a constant and saturated capacity of the lysed α -amylase containing cells for non-specific electrostatic adhesion of protein (Table 6.2). In the case of pure T4 lysozyme-his, a higher proportion of input protein (67-70% of 1.5 mg) was recovered in the washes compared to the crude enzyme preparation (7-10.5% of 9.9 mg). In the pure T4 lysozyme-his tests, lysozyme, as the only protein species present, evidently reacts electrostatically with the cells, resulting in

Chapter 6 Periplasmic Lysis

~73% disappearance of lysozyme, which is only released by washing. T4 lysozyme-his exists in a 1:5 ratio in the crude extract where other proteins compete for adhesion to the lysed cells resulting in ~29% of T4 lysozyme-his released by the high salt and pH washes.

Table 6.2 Recovery of recombinant T4 lysozyme-his from the cell-free lysis supernatant and from subsequent high pH and ionic strength phosphate buffer washes.

T4 lysozyme-his	Dry cell weight (mg/mL)	Protein in lysis supernatant (mg)	Protein in high salt / pH washes (mg)	T4 lysozyme-his in high salt / pH washes (%)
(a) in crude protein cell extract	1.28	8.36	0.65	27.65
	2.55	7.96	0.58	25.49
	5.10	7.53	0.89	33.64
(b) purified	1.28	0.29	0.64	67.63
	2.55	0.30	0.70	75.57
	5.10	0.37	0.87	76.14

(a) T4 lysozyme-his in crude extract and (b) purified T4 lysozyme-his in lysis buffer were used to periplasmically lyse various concentrations of α -amylase producing *E. coli* cells.

6.5 Post-lysis Recovery of T4 lysozyme-his

IMAC on Zn^{2+} -charged columns was chosen to recover T4 lysozyme-his from recombinant α -amylase and released periplasmic proteins. The strength of interaction is weaker on Zn^{2+} than Cu^{2+} (Hutchens and Yip, 1990; Beitle and Ataa, 1993) which means that T4 lysozyme-his elutes rapidly in a concentrated form without compromising purity and yield (Sloane et al., submitted). Released periplasmic protein fractions (pooled original supernatant and phosphate washes), spiked with pure T4 lysozyme-his and T4 lysozyme-his in crude extract, were buffer exchanged by gel filtration (section 2.6.4 to do) to remove EDTA and equilibrate in 0.02 M Na_2HPO_4 , 0.5 M NaCl, pH 7.2 buffer, prior to loading onto a Zn^{2+} -charged IMAC column (section 2.6.1.2). The periplasmic fractions including α -amylase which have no affinity for metal ions, eluted as expected in

the flowthrough. T4 lysozyme-his was retained by binding through immobilised metal ions and was eluted readily and in a small volume as a single peak, 99% pure, on a pH gradient between pH 6.0-5.2, (Figure 6.5 and 6.6). The four step post-lysis recovery of T4 lysozyme-his from the supernatant, phosphate washes, buffer exchange and IMAC- Zn^{2+} purification column, resulted in an overall yield of 87% with a purification factor of 5.2 (Table 6.3 and Figure 6.6).

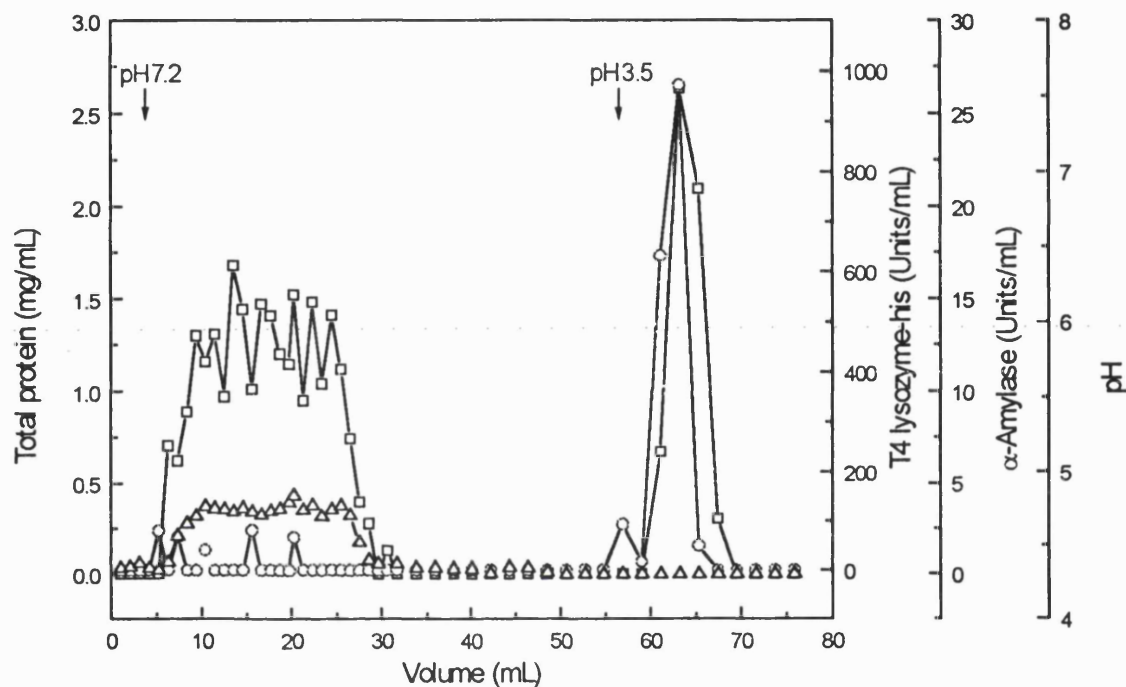


Figure 6.5 Chromatogram of IMAC- Zn^{2+} post-lysis recovery and purification of T4 lysozyme-his from released periplasmic protein. α -Amylase elutes in the flowthrough. Total protein (mg/mL) (\square), T4 lysozyme-his (Units/mL) (\circ), α -amylase (Units/mL) (Δ), pH (.....).

Table 6.3 Post-lysis recovery of recombinant T4 lysozyme-his from the released periplasmic protein.

Purification step	Volume (mL)	Total protein (mg)	T4 lysozyme (mg)	Overall yield (%)	Purity (%)	Purification factor
Lysed extract	15	41.42	13.76	100	19.23	—
Buffer exchange	19	38.39	12.75	92.67	19	—
Zn ²⁺ purified	8.4	11.99	11.99	87	99	5.15(c)

(c) Calculated from scanning densitometry of SDS-polyacrylamide gel.

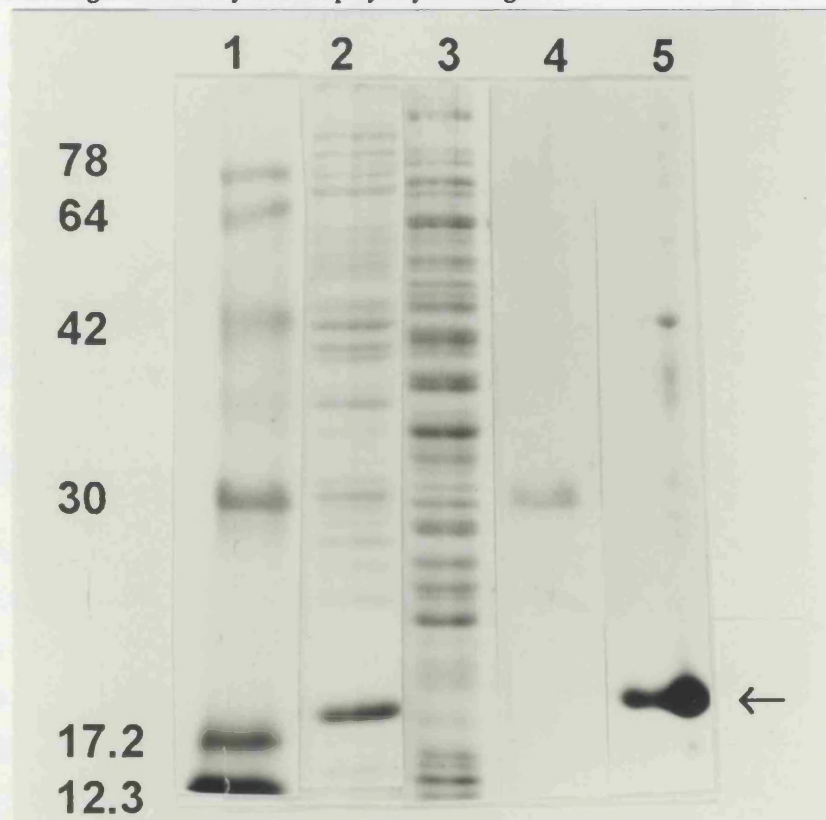


Figure 6.6 SDS-polyacrylamide gel showing post-lysis recovery of T4 lysozyme-his by IMAC-Zn²⁺. *Lane 1*, molecular weight markers; *lane 2*, periplasmically released protein spiked with T4 lysozyme-his; *lane 3*, column flowthrough; *lane 4*, column wash; *lane 5*, eluted T4 lysozyme-his.

6.6 Conclusion

In terms of processing and protein stability there are several advantages in expressing proteins secreted to the periplasmic space of *E. coli*. However, a major drawback has been the cost at large scale of single use lysis with a commercial lysozyme. Here, a process was described which achieved periplasmic lysis of *E. coli* cells, harbouring a periplasmically secreted recombinant α -amylase, by employing a re-usable poly histidine-tailed T4 bacteriophage lysozyme. The recombinant T4 lysozyme, recovered in a one-step purification by immobilised metal affinity chromatography (87% overall recovery and 99% purity), can be re-used, thus providing a more economical process for periplasmic release, with the added benefit of removal of lysozyme as a contaminant. Inclusion of a high pH and ionic strength buffer wash promoted dissociation of the recombinant T4 lysozyme from the lysed cell wall and dramatically enhanced recovery.

CHAPTER 7

CONCLUSIONS AND FUTURE WORK

7.1 Conclusions

Non-porous, micron-sized, magnetic iron oxide particles were functionalised with metal chelating iminodiacetic acid (IDA) ligands to produce a high capacity pseudoaffinity support. In magnetic affinity adsorption the covalently bound ligand binds to its target protein in solution and the resulting complex is removed from suspension by the application of a magnetic field. Magnetic chelator affinity interactions were carried out in free solution and their introduction at the start of the purification process rendered pre-treatment steps such as clarification and concentration unnecessary and in doing so reduce costs and increase yield.

The magnetic particles, although dense (2.5 g/cm^3), have a very low settling velocity due to their small size ($0.5\text{-}1.5 \text{ }\mu\text{m}$) and thermal fluctuations and consequently remain suspended in a gravitational field. They can however be quickly removed from suspension by the application of a magnetic field. Once the field is removed these 'superparamagnetic particles lose all magnetic memory, dissociate and mix independently in suspension with no aggregation taking place. Hence the particles may be re-used. Their small size also provides a large surface area which ensures a high protein binding capacity. Pseudoaffinity metal-chelating ligands are cheap and stable in contrast to classical biospecific ligands, e.g. antibodies, lectins. Further advantages include their ease of coupling to matrices at high density and their potential for use in the selective recovery of peptide pre-derivatized recombinant metal binding proteins.

Four preparative routes were investigated and one was selected for further development by virtue that it had the highest intermediate epoxide density and also the highest specific binding capacity. The preferred route involved (i) grafting a coat of polyglutaraldehyde onto the surface of amine-terminated particles followed by (ii) epoxy-activation of the aldehyde bearing surface under reducing conditions (iii) subsequent coupling of the chelating agent, iminodiacetic acid and (iv) final activation of the supports for use by charging with Cu^{2+} ions. The supports were assessed with respect to ligand density and specific protein binding capacity and their selectivity and interaction strength was assessed fully with a set of native proteins with known behaviour towards immobilised metal chelates.

The measurement of equilibrium adsorption isotherms revealed that binding of native proteins with surface exposed histidines was specifically mediated through immobilised metal ions and that increasing numbers of surface exposed histidines reflected increasing binding strength and capacity for the individual proteins. Langmuir and bi-Langmuir models were used to describe the adsorption isotherms in terms of a dissociation constant(s), K_d , and maximum capacity(ies) for adsorbed protein, Q_{max} , for bovine haemoglobin (20 histidines), *C. krusei* cytochrome *c* (3 histidines), horse cytochrome *c* (2 histidines) and tuna cytochrome *c* (1 histidine). α -Chymotrypsin (0 histidines), selected as a probe for non-specific binding, failed to bind both in the presence and absence of copper ions as expected. The first association constants (K_{a1}) for bovine haemoglobin and *C. krusei* cytochrome *c* are $1.97 \times 10^9 \text{ M}^{-1}$ and $4.15 \times 10^8 \text{ M}^{-1}$ respectively indicating the formation of strong and stable affinity complexes with Cu^{2+} -charged supports which for a single stage operation is high enough to ensure that after binding of target protein, and washing away of contaminating proteins, the desired protein can be eluted quantitatively. The corresponding Q_{max} values are 158 mg and 167 mg protein per g support.

A series of optimisation experiments revealed clear relationships between the intermediate epoxide density, the ligand density and the protein binding capacity. When the IDA concentration was raised to 15% (w/v) during coupling, Cu^{2+} -charged ligand densities as high as 60 $\mu\text{moles/g}$ were achieved. As the ligand density increases so do the interaction strengths and capacities. High IDA densities on uncharged supports are accompanied by a great reduction in non-specific binding. By increasing the density of IDA groups introduced onto the surface, the hydrophilic nature of the ligand may cover up patches of non-specific adsorbing ligands due to the base matrix molecules (such as polyglutaraldehyde and epoxide).

A native histidine-bearing protein, *C. krusei* cytochrome *c* (3 surface accessible histidines), binds to Cu^{2+} -IDA supports with a ligand density of 40 $\mu\text{moles/g}$ and a Q_{max} which is equivalent to a maximum effective surface area $> 100 \text{ m}^2$. The surface area was calculated using the protein molecular dimensions and assuming monolayer binding. The surface area of the amine-terminated iron oxide core particle has been estimated at between 100-140 m^2/g (Josephson, 1987) thus demonstrating that the subsequent coating and coupling steps in support preparation did not reduce the support's specific surface area. This also provided indirect evidence for lack of particle aggregation and suggested the formation of a very thin external coat since little effective surface area was sacrificed.

A recombinant bacteriophage T4 lysozyme carrying a polyhistidine tail at its C-terminus was purified in a single step to 94% purity from crude *E. coli* cell extract using IDA-Cu²⁺ magnetic chelator supports. By comparison, single step purification by Cu²⁺-charged IDA agarose supports achieved only 81% purity. Magnetic separation resulted in an overall yield of 82% achieved with a 4.5 fold purification factor.

Magnetic chelate recovery of recombinant T4 lysozyme from crude *E. coli* cell homogenate was achieved at levels close to those determined using pure haem proteins with $Q = 180$ mg/g support. The effect on support capacity caused by the presence of cells which were disrupted into phosphate buffer was minimal, thereby demonstrating that the Q of non-porous magnetic support is not affected by fouling components present in the cell homogenate.

Development and optimisation of T4 lysozyme producing recombinant *E. coli* fermentation conditions were carried out at bench and pilot scale. Leakage (50%) of recombinant T4 lysozyme to the medium following induction was virtually eliminated (90-95% retention after 3 hr induction) by culturing on a high concentration medium at a lower temperature of 28°C (from 37°C). This resulted in higher biomass concentration, recombinant T4 lysozyme productivity and intracellular yield. Productivity increased a further 9-fold on scale-up of the batch fermentation.

An enzymatic process to disrupt the peptidoglycan layer of an *E. coli* cell wall and release the contents of the periplasmic space was developed using poly-histidine tailed T4 phage lysozyme. The recombinant lysozyme was easily and quickly recovered in a single immobilised metal affinity chromatographic step (87% overall recovery and 99% purity) for re-use. Inclusion of a high pH and ionic strength buffer wash promoted dissociation of the recombinant T4 lysozyme from the lysed cell wall and dramatically enhanced recovery.

7.2 Future Work

Magnetic chelator support particles have been successfully demonstrated at bench scale to behave as stable, high capacity, high affinity supports which can be pulled out of solution by a low magnetic field allowing easy elution and recovery of the target protein. All magnetic chelator support particles referred to in this work have been prepared using a commercial silane coupled iron oxide core particle (BioMag[®], PerSeptive Biosystems, Framingham, Mass, U.S.A.) (with the exception of the supports used for HGMS, section 4.4). To allow scaled up magnetic affinity separation studies to begin in earnest and in

order to keep costs low, a search was conducted for a suitable, cheap and abundant supply of core magnetic particles. However, as none of the particles tested possessed the desirable characteristics of the BioMag[®] particles, we obtained the manufacturing BioMag[®] patents. Recent work in these laboratories has shown that the material described in the initial patents is not the same as that currently produced commercially. The commercial material is prepared using a different recipe which gives a truly superparamagnetic particle. The initial recipe cited in the patent yields particles which retain some partial ferromagnetic characteristics.

Currently in these laboratories, conditions for the reproducible manufacture of submicron superparamagnetic particles, by controlled precipitation of Fe²⁺ and Fe³⁺ ions, are being fine tuned. The particle size, crystal size and magnetic properties are influenced by the ratio of Fe²⁺/Fe³⁺ salts, the temperature at which the reaction takes place, the concentration of NaOH and the speed of mixing. The physical properties of the particles are being analysed (in conjunction with the Department of Physics, U.C.L.) by photon correlation spectroscopy (PCS), Mossbauer spectroscopy, X-ray diffraction (XRD) and vibrating sample magnetometry (VSM), to provide data on the particle size, crystal size, material and magnetic properties.

The most important property is thought to be the initial crystal size of the maghemite iron oxide (γ -Fe₂O₃) and not the particle size, which can be easily controlled by homogenisation. A 1 μ m particle made up of 300 Å crystals has 5 times the surface area of a 1 μ m particle composed of 500 Å crystals (O.R.T. Thomas, personal communication). Therefore, the high surface area displayed by the BioMag[®] particles is due to a 1 μ m particle composed of a cluster of 300 Å crystals.

Superparamagnetic, micron-sized particles composed of crystals of ~ 300 Å are currently being prepared and are both ideal and essential for successful process scale-up. Future work will involve their scaled-up preparation for affinity separations of recombinant proteins from crude homogenates using high gradient magnetic separation (HGMS).

Continuous improvements in the design and engineering of efficient magnetic separation systems will be sought. This will involve changes to the canister design, and the use of uniform trapping matrices to limit channelling effects that are commonly observed with random arrays of wire.

Magnetic chelator support use with recycle under accelerated ageing conditions resulted in Fe ion leaching and a drop in ligand density and protein binding capacity (section

3.5.3). Future work will need to investigate more thoroughly iron oxide support core stability, i.e., iron core leaching over 10 cycles of re-use and should also investigate the effective ligand density over successive cycles without stripping and re-charging the support each time.

Alternative 'perfluoroalkylsilane/PVA' coating methodologies may be employed in order to improve the corrosion resistant properties of magnetic chelator supports. The perfluoroalkylated polyvinyl alcohol coating, in these laboratories, of magnetic particles primed with perfluoroalkyl silanes in the preparation of biomimetic dye-linked supports demonstrated considerably enhanced corrosion resistance over polyglutaraldehyde-coated supports (Theodossiou, 1993), although ligand density and capacities achieved were lower with this support chemistry.

Bibliography

- Ahuja, S. K. (1976) *Colloid Interface Sci.* **57**, 438-445
- Albert, R. V., and Tien, C. (1985) *AICHE J.* **31**, 288
- Al-Hassan, Z., Ivanova, V., Dobрева, E., Penchev, I., Hristov, J., Rachev, R., and Petrov, R. (1991) *Journal of fermentation and bioengineering* **71**(2), 114-117
- Ambler, C. M. (1952) *Chem. Eng. Prog.* **48**(3), 150-158
- Andersson, L., and Sulkowski, E. (1992) *J. Chromatogr.* **604**, 13-17
- Andersson, L., Sulkowski, E., and Porath, J. (1991) *Bioseparation* **2**, 15-22
- Andrews, B. A., and Asenjo, J. A. (1987) *TIBTECH* **5**, 273-277
- Andrews, B. A., and Asenjo, J. A. (1989) in *Protein purification methods: a practical approach* (Harris, E. L. V., and Angal, S., eds), IRL press, Oxford
- Arnold, F. H. (1991) *Bio/Technology* **9**, 151-156
- Axelsson, H. A. C. (1985) in *Comprehensive Biotechnology*, Vol. 2 (Cooney, C. L., and Humphrey, A. E., eds), pp. 325-346, Pergammon Press, New York
- Baneyx, F., and Georgiou, G. (1991) *J. Bacteriol.* **173**, 2696-2703
- Bayer, E., and Wilchek, E. (1990) *J. Chromatogr.* **510**, 3-11
- Bean, C. P., and Livingstone, J. D. (1959) *J. Appl. Physics* **30**, 120S-129S
- Beitle, R. R., and Ataai, M. M. (1993) *Biotechnol. Prog.* **9**, 64-69
- Bell, D. J., Hoare, M., and Dunnill, P. (1983) *Adv. Biochem. Eng./Biotechnol.* **26**, 1-72
- Belter, P. A. (1985) in *Comprehensive Biotechnology*, Vol. 2 (Cooney, C. L., and Humphrey, A. E., eds), pp. 347-350, Pergamon Press, New York
- Belter, P. A., Cussler, E. L., and Hu, W. S., eds. (1988) *Bioseparations: Downstream Processing for Biotechnology*, John Wiley & Sons, New York
- Bennett, A. M. Integrity testing of the cell disrupter. Centre for applied microbiology and research report, Porton Down, Warwick: Constant Systems Ltd
- Berg, J. M. (1988) *Proc. Natl. Acad. Sci. USA* **85**, 99-102

- Berthold, H., Scanarini, M., Abney, C. C., Frorath, B., and Northemann, W. (1992) *Protein expression and purification* **3**, 50-56
- Bhattachacharjee, M., and Ali, E. (1992) *Anal. Biochem.* **201**, 233-236
- Birdsell, D. C., and Cota-Robles, E. H. (1967) *J. Bacteriol.* **93**, 427-437
- Birnbaum, S. S., and Larsson, P. O. (1982) *Appl. Biochem. Biotechnol.* **7**, 55-60
- Bisio, A. (1985) in *Scale-up of chemical processes* (Bisio, A., and Kabel, R. L., eds), John Wiley & Sons, New York
- Bitter, F. (1936) *Rev. Scient. Instrum.* **7** 479
- Bitter, F. (1940) *Rev. Scient. Instrum.* **11**, 373
- Bitton, C., and Mitchell, R. (1974) *Wat. Res.* **8**, 549
- Bjurstrom, E. (1985) *Chemical Engineer* **95**(4), 126
- Blachin-Roland, S., and Masson, J.-M. (1989) *Protein Eng.* **2**, 473-480
- Bleaney, B. I., and Bleaney, B. eds (1989) *Electricity and Magnetism*, Vol 2, Third edition, Oxford Science Publications.
- Bodeker, A. R., and Lenhoff, A. M. (1989) *Biotechnol. Prog.* **5**, 132-135
- Bollin, E. J., and Sulkowski, E. (1981) *J. Gen. Virol.* **52**, 227-233
- Bonnerjea, J., Oh, S., Hoare, M., and Dunnill, P. (1986) *Bio/Technology* **4**, 954-957
- Botros, H. G., and Vijayalakshmi, M. (1989) *J. Chromatogr.* **494**, 113-122
- Bradford, M. M. (1976) *Anal. Biochem.* **72**, 248-254
- Bramble, J. L. (1989) [Ph.D. Dissertation], University of Pennsylvania
- Breillatt, J. P., and Eveleigh, J. W. D. (1987): Bioaffinity and ion-exchange separations with liquid exchange supports. Eur. Patent EP 246 103, issued 19 Nov 1987.
- Briefs, K. G., and Kula, R.-M. (1992) *Chem. Engin. Sci.* **47**, 141-149
- Brummer, K. H., and Hemfort, H. (1988) in *Downstream Processes: Equipment and techniques* (Mizrahi, A., ed), Alan R. Liss, New York
- Buckmann, A. F., Morr, M., and Kula, M. R. (1987) *Biotechnol. Appl. Biochem.* **9**, 258-268

- Burns, M. A., and Graves, D. J. (1985) *Biotechnol. Prog.* **1**, 95 (N)
- Burns, M. A., and Graves, D. J. (1988) *Chem. Eng. Commun.* **67**, 315
- Burns, M. A., Kvesitadze, G. I., and Graves, D. J. (1985) *Biotechnol. Bioeng.* **27**, 137-145
- Chaberek, S., and Martell, A. E., eds. (1959) *Organic Sequestering Agents*, John Wiley & Sons,
- Chaiken, I. (1992) *Anal. Biochem.* **201**, 197-210
- Chaikin, S. W., and Brown, W. G. (1949) *ibid* **71**, 122-125
- Champluvier, B., and Kula, R.-M. (1992) *Bioseparation* **2**, 343-351
- Chaplin, M. F., and Kennedy, J. F. (1976) *Carbohydr. Res.* **50**, 267-274
- Charm, S. E., and Matteo, C. C. (1971) *Methods Enzymol.* **22**, 477-556
- Chen, J. P. (1990) *J. Ferment. Bioeng.* **70**, 199-209
- Chisti, J. A., and Moo-Young, M. (1986) *Enz. Microb. Technol.* **8**, 194-204
- Choquet, C. G., and Sprott, G. D. (1991) *J. Microbiol. Meths.* **13**, 161-169
- Clonis, Y. D., and Lowe, C. R. (1980) *Eur. J. Biochem.* **110**, 279-288
- Coakley, W. T., Brown, R. C., James, C. J., and Gould, R. K. (1974) *Biotechnol. Bioeng.* **16**, 659-673
- Cochrane, A. W., Chen, C.-H., Kramer, R., Tomchak, L., and Rosen, C. A. (1989) *Virology* **173**, 335-337
- Corradini, D., Rassi, Z. E., Horvath, C., Guerra, G., and Horne, W. (1988) *J. Chromatogr.* **458**, 1-11
- Coulet, P. R., Carlsson, J., and Porath, J. (1981) *Biotechnol. Bioeng.* **13**, 663-668
- Dalboge, H., Dahl, H.-H. M., Pederson, J., Hansen, J. W., and Christensen, T. (1987) *Bio/Technology* **5**, 161-164
- Darbyshire, J. (1981) in *Topics in fermentation and enzyme technology*, Vol. 5 (Wiseman, A., ed), pp. 147-476, Ellis Horwood, Chichester
- Datar, R. (1986) *Proc. Biochem.* **21**, 19-26
- Dauer, R. R., and Dunlop, E. H. (1991) *Biotechnol. Bioeng.* **37**, 1021-1028

- Davies, L. P., and Gerber, R. (1990) *IEEE Trans. Magnet.* **26**(5), 1867-1869
- Davies, R. C., Neuberger, A., and Witson, B. M. (1969) *Biochim. Biophys. Acta* **178**, 294-503
- Dean, P. D. G., Johnson, W., and Middle, F., eds. (1985) *Affinity Chromatography: a Practical Approach*, IRL Press, Oxford, U.K.
- Dekker, M., and Boom, R. (1995) *TIBTECH* **13**, 129-131
- Dekker, R. F. H. (1990) *Appl. Biochem. Biotechnol.* **23**, 25-39
- de Latour, C. (1973) *IEEE Trans. Magnet.* **9**(3), 314
- de Latour, C. (1974) *Magnetic fields in aqueous systems* [Ph.D. Dissertation], MIT, Boston
- Desarnaud, F., Marie, J., Larguier, R., Lombard, C., Jard, S., and Bonnafous, J.-C. (1992) *J. Chromatogr.* **603**, 95-104
- Doulah, M. S. (1977) *Biotechnol. Bioeng.* **19**, 649-660
- Dunnill, P., and Lilly, M. D. (1974) *Biotechnol. Bioeng.* **16**, 987-989
- Dyer, F. L., Martin, T. C., and Meadowcroft, W. H., eds. (1929) *Edison: His life and inventions*, Vol. 11, Harper & Brothers, New York
- Dykes, C. W., Bookless, A. B., Coomber, B. A., Noble, S. A., Humber, D. C., and Hobden, A. N. (1988) *Eur. J. Biochem.* **174**, 411-416
- Edy, V. G., Billiau, A., and De Sommer, P. (1977) *J. Biol. Chem.* **252**, 5934-5935
- Elmore, W. C. (1938) *Physical review* **54**, 1092
- Engler, C. R. (1979) *Disruption of microorganisms in high pressure flow devices* [Ph.D. Dissertation], University of Waterloo, Waterloo, Ontario, Canada
- Engler, C. R. (1985) in *Comprehensive biotechnology*, Vol. 2 (Moo-Young, M., ed), pp. 305-324, Pergamon Press, Oxford
- Ennis, M. P., and Wisdom, G. B. (1991) *Appl. Biochem. Biotechnol.* **30**, 155-164
- Ernst-Cabrerra, K., and Wilchek, M. (1988) *Trends. Anal. Chem.* **7**, 58
- Eveleigh, J. W. (1978) *J. Chromatogr.* **159**, 129-145
- Eyssa, Y. M., and Boom, R. W. (1976) *Int. J. Min. Proc.* **3**, 1-8

- Fausnaugh, J. L., Kennedt, L. A., and Regnier, F. E. (1984) *J. Chromatogr.* **317**, 141-155
- Finkelstein, A. V., Badretdinov, A. Y., and Ptitsyn, O. B. (1991) *Proteins: structure, function and genetics* **10**, 287-299
- Fischer, L., ed. (1980) *Gel filtration chromatography*, 2nd ed., Elsevier, Amsterdam
- Fish, N. M., and Lilly, M. D. (1984) *Bio/Technology* **10**, 62-627
- Foster, D. (1995) *Curr. Opin. Biotechnol.* **6**, 523-526
- Fountoulakis, M., Juranville, J.-F., Stuber, D., Weibwl, E. K., and Garotta, G. (1990) *J. Biol. Chem.* **265**, 13268-13275
- Fowell, S. L., and Chase, H. A. (1986) *J. Biotechnol.* **4**, 1-13
- Frantz, S. G. (1937) *Chemical and Metallurgical Engineering* **45**
- French, C. (1993) *Production and recovery of a recombinant α -amylase enzyme from Escherichia coli and Streptomyces lividans* [Ph.D. Dissertation], University College London
- Furlong, A. M., Thonsen, D. R., Marotti, K. R., Post, L. E., and Sharma, S. K. (1988) *Biotechnol. Appl. Biochem.* **10**, 454-464
- Gabler, F. R. (1985) in *Comprehensive Biotechnology*, Vol. 2 (Cooney, C. L., and Humphrey, A. E., eds), pp. 351-366, Pergamon Press, New York
- Gekko, K., and Hasegawa, H. (1986) *Biochemistry* **25**, 6563-6571
- Gelf, G., and Boudrant, J. (1974) *Biochim. Biophys. Acta* **334**, 467-470
- Gellf, G., and Boudrant, J. (1974) *Biochim. Biophys. Acta* **334**, 467-470
- Gentz, R., Certa, U., Takacs, B., Matile, H., Dobeli, H., Pink, R., Mackay, M., Bone, N., and Scaife, J. G. (1988) *EMBO J.* **7**, 225-230
- Gentz, R., Chen, C.-H., and Rosen, C. A. (1989) *Proc. Natl. Acad. Sci. USA* **86**, 821-824
- Gerber, F., and Biss, R. R., eds. (1982) *High gradient magnetic separation*, Elsevier Scientific, New York
- Germino, J., and Bastia, D. (1984) *Proc. Natl. Acad. Sci. USA* **81**, 4692-4696
- Gettings, M., and Kinloch, A. J. (1987) *J. Mater. Sci.* **12**, 2511

- Goeddel, D. V., Kleid, D. G., Bolivar, F., Heynecker, H. L., Yansura, D. G., Crea, R., Hirose, T., Kraszewski, A., Itakura, K., and Riggs, A. D. (1979) *Proc. Natl. Acad. Sci. USA* **76**, 106-110
- Goetz, V., and Graves, D. J. (1991) *Powder Technology* **64**, 81-92
- Goetz, V., Remaud, M., and Graves, D. J. (1991) *Biotechnol. Bioeng.* **37**, 614-626
- Goubron-Botros, H., Nanak, E., Nour, J. A., Birkenmeir, G., and Vijayalakshmi, M. A. (1992) *J. Chromatogr.* **597**, 357-364
- Goubron-Botros, H., and Vijayalakshmi, M. (1989) *J. Chromatogr.* **495**, 113-122
- Groman, E. V., Sullivan, J. A., Markinac, J. E., Neuringer, I. P., Finlay, C. A., Kenny, F. E., and Josephson, L. (1985) *BioTechniques* **4**, 156-160
- Groman, E. V., and Wilchek, M. (1987) *TIBTECH* **5**, 220-224
- Gupta, M. N., and Mattiasson, B. (1994) *Chemistry & Industry*, **9**, 673-675
- Gurd, F. R. N., and Wilcox, P. E. (1956) *Adv. Protein Chem.* **11**, 311-427
- Guzman, R., Torres, J. L., Carbonell, R. G., and Kilpatrick, P. K. (1989) *Biotechnol. Bioeng.* **33**, 1267-1276
- Habeeb, A. F. S. A. (1966) *Anal. Biochem.* **14**, 328-336
- Haekel, R., Hess, B., Lauterborn, W., and Wurster, K. (1968) *Hoppe-Seyler's Z. Physiol. Chem.* **349**, 699-714
- Halling, P. J., and Dunnill, P. (1979a) *Biotechnol. Bioeng.* **21**, 396-416
- Halling, P. J., and Dunnill, P. (1979b) *Eur. J. Appl. Microbiol. Biotechnol.* **6**, 195
- Halling, P. J., and Dunnill, P. (1980) *Enz. Microb. Technol.* **2**, 2-11
- Halwachs, W., Wandrey, C., and Schugerl, K. (1973) *Biotechnol. Bioeng.* **20**, 541-554
- Hammarberg, B., Nygren, P.-A., Holmgren, E., Elmblad, A., Moks, T., and Uhlén, M. (1989) *Proc. Natl. Acad. Sci. USA* **86**, 4367-4371
- Hammarberg, B., Nygren, P.-A., Holmgren, E., Elmblad, A., Tally, M., Hellman, U., Moks, T., and Uhlén, M. (1989) *Proc. Natl. Acad. Sci. USA* **86**, 4367-4371
- Hammond, P. M., Atkinson, T., Sherwood, R. F., and Scawen, M. D. (1991) *Pharm. Technol. Int.* (April), 24-30
- Harland, J. R., Oberteuffer, J. A., and Goldstein, D. J. (1976) *Chem. Eng. Prog.* (10), 79

- Harrison, S. T. L., Dennis, J. S., and Chase, H. A. (1991) *Bioseparation* **2**, 95-105
- Harwood, L. M., and Moody, C. J., eds. (1990) *Experimental Organic Chemistry - Principles and Practice*, Blackwell scientific publications, Oxford, U.K.
- Hatton, T. A. (1989) in *Surfactant-based separation* (Scameborn, J. F., and Harwell, J., eds), p. 55, Marcel Dekker, New York
- Hearon, J. Z. (1948) *J. natn. Cancer Inst.* **9**, 1
- Hemden, E. S., and Porath, J. (1985) *J. Chromatogr.* **323**, 265-272
- Hemden, E. S., Zhao, Y., Sulkowski, E., and Porath, J. (1989) *Proc. Natl. Acad. Sci. USA* **86**, 1811-1815
- Hendrickson, W. G., Kusano, T., Yamaki, H., Balakrishnan, R., King, M., Murchie, J., and Schaechter, M. (1982) *Cell* **30**, 915
- Herak, D. C., and Merrill, E. W. (1989) *Biotechnol. Bioeng.* **5**, 63-68
- Hersh, L. S., and Yaverbaum, S. (1975) *Clin. Chim. Acta* **63**, 69-72
- Hill, C. R., Thompson, L. G., and Kenny, A. C. (1989) in *Protein Purification Methods: a practical approach* (Harris, E. L. V., and Angal, S., eds), IRL Press, Oxford, UK
- Hirschbein, B. L., Brown, D. N., and Whitesides, G. M. (1982) *Chemtech*, 172-179
- Hirshbein, B. L., and Whitesides, G. M. (1982) *Appl. Biochem. Biotechnol.* **7**, 157
- Hirst, T. R., and Welch, R. A. (1988) *TIBS* **13**, 265-269
- Hochuli, E. (1990) in *Genetic Engineering*, Vol. 12 (Setlow, J. K., ed), pp. 87-98, Plenum Press, New York
- Hochuli, E., Bannwarth, W., Dobeli, H., Gentz, R., and Stuber, D. (1988) *Bio/Technology* **6**, 1321-1325
- Hochuli, E., Dobeli, H., and Schacher, A. (1987) *J. Chromatogr.* **411**, 177-184
- Holmes, M. A., and Matthews, B. W. (1982) *J. Mol. Biol.* **160**, 623-629
- Holmes, M. A., and Matthews, B. W. (1982) *J. Mol. Biol.* **160**, 623-639
- Hopp, T. P., Prickett, K. S., Price, V. L., Libby, R. T., March, C. J., Cerretti, D. P., Urdal, D. L., and Conlon, P. J. (1988) *Bio/Technology* **6**, 1204-1210

- Horisberger, M. (1976) *Biotechnol. Bioeng.* **18**, 1647-1651
- Horvath, C., and Lipsky, S. R. (1967) *J. Chromatogr. Sci.* **7**, 109
- Hsiung, H. M., Mayne, N. G., and Becker, G. W. (1986) *Bio/Technology* **4**, 991
- Hughes, D. E., Wimpenny, J. W. T., and Lloyd, D. (1971) in *Methods in Microbiology*, Vol. 5B (Norris, J. R., and Ribbons, D. W., eds), pp. 1-54, Academic, New York
- Hutchens, T. W. (1989) in *Protein purification: Principles, High Resolution Methods, and Applications* (Janson, J.-C., and Ryden, I, eds), VCH Publishers, New York
- Hutchens, T. W., and Yip, T. T. (1990) *J. Chromatogr.* **500**, 531-542
- Hutchens, T. W., and Yip, T.-T. (1991) *J. Inorg. Chem.* **42**, 105-118
- Hutchens, T. W., Yip, T. T., and Porath, J. (1988) *Anal. Biochem.* **170**, 168-182
- Inada, Y., Takahashi, K., Yoshimoto, T., Kodera, Y., Matsushima, A., and Saito, Y. (1988) *TIBTECH* **6**, 131-134
- Itakura, K., Hirose, T., Crea, R., Riggs, A. D., Heyneker, H. L., Bolivar, F., and Boyer, H. W. (1977) *Science* **198**, 1056-1063
- Itzhaki, R. F. (1972) *Anal. Biochem.* **50**, 569-574
- Iwata, H., Saito, K., Furusaki, S., Sugo, T., and Okamoto, J. (1991) *Biotechnol. Prog.* **7**, 412-418
- Janknecht, R., de Martynoff, G., Lou, J., Hipskind, R. A., Nordheim, A., and Stunnenberg, H. G. (1991) *Proc. Natl. Acad. Sci. USA* **88**, 8972-8976
- Janson, J.-C. (1982) in *Affinity chromatography and related techniques* (Grignau, T. C. J., Visser, J., and Nivard, R. J. F., eds), pp. 503-512, Elsevier scientific, Amsterdam
- Jhon, M. S., and Karis, T. E. (1989) in *Polymers in information storage technology* (Mittal, K. L., ed), pp. 229-310, Plenum Press, New York
- Johansson, G. (1987) in *Reactive dyes in protein and enzyme technology* (Clonis, Y., Atkinson, A., Bruton, S., and Lowe, C., eds), pp. 101-124, Macmillan Press, Basingstoke, UK
- Johansson, G., and Tjerneld, F. (1989) *J. Biotechnol.* **11**, 135-142
- Johnson, R. D., and Arnold, F. H. (1995) *Biochim. Biophys. Acta* **1247**, 293-297

- Jones, G. H. (1960) *Fifth International Processing Congress*, 717
- Josephson, L. (1987): Magnetic particles for use in separations. (to Advanced Magnetics, Inc.) Application: Cambridge, Mass. U.S.A. 749,692, 28 June 1985.
- Jung, G., Deneffe, P., Becquart, J., and Mayaux, J. F. (1988) *Ann. Inst. Pasteur/Microbiol.* **139**, 129-146
- Kaback, H. R. (1971) in *Methods in enzymology*, Vol. 22 (Colowick, S. P., and Kaplan, N. O., eds), pp. 99-120, Academic Press, New York
- Kaiser, R., and Miskolczy, G. (1970) *J. Appl. Physics* **41**, 1064-1072
- Kalpralek, F., Jecmen, P., Sedlacek, J., Fabry, M., and Zadrazil, S. (1991) *Biotechnol. Bioeng.* **37**, 71-79
- Karis, T. E., and Jhon, M. S. (1991) *Colloids and surfaces* **53**, 393-410
- Kay, G., and Lilly, M. D. (1970) *Biochim. Biophys. Acta* **198**, 276-285
- Kawahara, J., Ohmori, T., Ohkubo, T., Hattori, S., and Kawamura, M. (1992) *Anal. Biochem.* **201**, 94-98
- Kelley, B. D., and Hatton, T. A. (1991) *Bioseparation* **1**, 333-349
- Klapper, M. H. (1977) *Biochem. Biophys. Res. Comm.* **78**, 1018-1024
- Knorr, D., Shetty, K. J., and Kinsella, J. E. (1979) *Biotechnol. Bioeng.* **21**, 2011-2021
- Knott, J. A., Sullivan, C. A., and Weston, A. (1988) *Eur. J. Biochem.* **174**, 405-410
- Kohn, J., and Wilchek, M. (1982) *Biochem. Biophys. Res. Comm.* **107**, 878
- Kolm, H., Oberteuffer, J., and Kelland, D. (1975) *Sci. Am.*, 9
- Kondo, A., Oku, S., Murakami, F., and Higashitani, K. (1993) *Colloids and surfaces* **1**, 197-201
- Korinobu, S., and Uchiyama, S. (1982) *IEEE Trans. Magnet.* **18**(6), 1526-1528
- Kroner, K. H., Hustedt, H., and Kula, M.-R. (1984) *Proc. Biochem.* **19**, 170-179
- Kronick, P. L., Campell, G. M., and Joseph, K. (1978) *Science* **200**, 1074
- Kronick, P., and Gilpin, R. W. (1986) *Journal of biochemical and biophysical methods* **12**, 73-80
- Kruger, H. J., and Hammond, J. B. W. (1988) in *Methods in molecular biology*, Vol. III (Walker, J. M., ed), p. 363,,

- Kula, M.-R., and Shütte, H. (1987) *Biotechnol. Prog.* **3**, 31-42
- Kula, M., Shutte, H., Vogels, G., and Frank, A. (1990) *Food Biotechnol.* **4**, 169-183
- Kuowei, W., Jahng, D., and Wood, T. K. (1994) *Biotechnol. Prog.* **10**, 621-629
- Labrou, N., and Clonis, Y. D. (1994) *J. Biotech* **36**, 95-119
- Laemmli, U. (1970) *Nature* **227**, 680-685
- Lagbrou, N., and Clonis, Y. D. (1994) *J. Biotechnol.* **36**, 95-119
- Lannicelli, J. (1976) *IEEE Trans. Magnet.* **12**(5)
- Larsson, P. O., and Mosbach, K. (1979) *FEBS Lett.* **98**, 333-338
- Larsson, P. O., and Mosbach, K. (1979) *Biotechnol. Lett.* **1**, 501-509
- Lawver, J. E., and Hopstock, D. M. (1974) *Min. Sci. Eng.* **6**(3), 154
- Lebreton, J. P. (1977) *FEBS Lett.* **80**, 351-354
- LeCorre, S., Andrew, B. A., and Asenjo, J. A. (1985) *Enz. Microb. Technol.* **7**, 73-77
- Lee, S.-M. (1989) *J. Biotech* **11**, 103-118
189. LeGrice, S. F. J., and Leitch, G. (1990) *Eur. J. Biochem.* **187**, 307-314
- LeGrice, S. F. J., Naas, T., Wohlgensinger, B., and Schatz, O. (1991) *EMBO J.* **10**, 3905-3911
- Leitermann, W., Friedlander, F. J., Gerber, R., Hwang, J. Y., and Emory, B. B. (1984) *IEEE Trans. Magnet.* **MAG-20**(5), 1174-1176
- Leporati, E. (1986) *J. Chem. Soc. Dalton Trans.*, 199-203
- Lilius, G., Persson, M., Bulow, L., and Mosbach, K. (1991) *Eur. J. Biochem.* **198**, 499-504
- Lilly, M. D., and Dunnill, P. (1969) in *Fermentation Advances* (Perlman, L., ed), pp. 225-247, Academic, New York
- Ling, T. G. I., and Mattiasson, B. (1989) *Biotechnol. Bioeng.* **34**, 1321-1325
- Ljungquist, C., Breitholtz, A., Brink-Nilsson, H., Moks, T., Uhlén, M., and Nilsson, B. (1989) *Eur. J. Biochem.* **186**, 563-569
- Lochmuller, C. H., and Wigman, L. S. (1987) *J. Chem. Tech. Biotechnol.* **40**, 33-40

- Loetscher, P., Mottlau, L., and Hochuli, E. (1992) *J. Chromatogr.* **595**, 113-119
- Louie, G. V., and Brayer, G. D. (1990) *J. Mol. Biol.* **214**, 527-555
- Lowe, C. R. (1977) *Eur. J. Biochem.* **73**, 265-274
- Lowe, C. R. (1979) in *Laboratory techniques in biochemistry and molecular biology*, Vol. 7 II (Work, T. S., and Works, E., eds), pp. 269-522, Elsevier, Amsterdam, The Netherlands (N)
- Lowe, C. R., Burton, S. J., Burton, N. P., Stewart, D. J., Purvis, D. R., Pitfield, I., and Eapen, S. (1990) *J. Mol. Recog.* **3**, 117-122
- Lowe, C. R., Burton, S. J., Pearson, J., Clonis, Y. D., and Stead, C. V. (1986) *J. Chromatogr.* **376**, 121-130
- Lowe, C. R., and Dean, P. D. G., eds. (1974) *Affinity Chromatography*, John Wiley & Sons, London, U.K.
- Luong, J. H. T., Nguyen, A. L., and Male, K. B. (1987) *Bio/Technology* **5**, 564-567
- MacDonald, H. L., and Neway, J. O. (1990) *Appl. Environ. Microbiol.* **56**(3, March), 640-645
- Mackay, D., and Salusbury, T. (1988) *Chem. Eng.* **447**, 45-50
- Maisano, F., Testpro, S. A., and Grandi, G. (1989) *J. Chromatogr.* **472**, 422-427
- Mannweiler, K., and Hoare, M. (1992) *Bioproc. Engin.* **8**, 19-25
- Margel, S., Zisblat, S., and Rembaum, A. (1979) *J. Immunol. Meths.* **28**, 341-353
- Marston, F. A. O. (1986) *J. Biochem* **240**, 1-12
- Martin, S. E. V. (1995) [Ph.D. Dissertation], University College London
- Matsunaga, T., and Kamiya, S. (1987) *Appl. Microbiol. Biotechnol.* **26**, 328-332
- McLoughlin, S. B., and Lowe, C. R. (1988) *Rev. Prog. Coloration* **18**, 247-259
- Menz, E. T., Havelick, J., Groman, E. V., and Josephson, L. (1986) *Am. Biotech. Lab.* **4**, 46-51
- Milner, H. W., Lawrence, N. S., and French, C. S. (1950) *Science* **111**, 633
- Miltenyi, S., Muller, W., Weichel, W., and Radbruch, A. (1990) *Cytometry* **11**, 231-238
- Mita, K., Ichimura, S., and Zama, M. (1978) *Biopolymers* **17**, 2783-2798

- Moks, T., Abrahmsen, L., Holmgren, E., Billich, M., Olsson, A., Pohl, G., Sterky, C., Hultberg, H., Josephson, S., Holmgren, A., Jornvall, H., Uhlén, M., and Nilsson, B. (1987) *Biochemistry* **26**, 5239-5244
- Molday, R. S., and Mackenzie, D. (1982) *J. Immunol. Meths.* **52**, 353-367
- Molday, R. S., Yen, S. P. S., and Rembaum, A. (1977) *Nature* **268**, 437-438
- Monsan, P., Puso, G., and Mazarguil, H. (1975) *Biochimie* **57**, 1281
- Mosbach, K. (1983) in *Affinity chromatography and related techniques* (Chaiken, I. M., Wilchek, M., and Parikh, I., eds), pp. 209-222, Academic Press, New York
- Mosbach, K., and Andersson, L. (1977) *Nature* **270**, 259-261
- Muller, D., Hughes, C., and Goebel, W. (1983) *J. Bacteriol.* **153**, 846-851
- Munro, P. A. (1976) [Ph.D. Dissertation], University College London
- Munro, P. A., Dunnill, P., and Lilly, M. D. (1977) *Biotechnol. Bioeng.* **19**, 101-124
- Munro, P. A., Dunnill, P., and Lilly, M. D. (1981) *Biotechnol. Bioeng.* **23**, 677
- Muraki, K., Morikawa, M., Jigami, Y., and Tanaka, H. (1988) *Protein Eng.* **2**, 49-54
- Murkes, j. (1966) *Filtration & Separation* **3**, 112-114
- Muszynska, G., Zhao, Y.-J., and Porath, J. (1986) *J. Inorg. Biochem.* **26**, 127-135
- Naglak, T. J., Hettwer, D. J., and Wang, H. Y. (1989) in *Separation processes in biotechnology* (Asenjo, J. A., ed), Marcel Dekker, New York
- Namdev, P. K., Irwin, N., Thompson, B. G., and Gray, M. R. (1993) *Biotechnol. Bioeng.* **41**, 666-670
- Nancib, N., Branlant, C., and Boudrant, J. (1991) *J. Industr. Microbiol.* **8**, 165-170
- Neu, H. C., and Heppel, L. A. (1965) *J. Biol. Chem.* **240**, 3685
- Nielson, O. J., Costa-Giomi, P., Weinmann, R., Erslev, A. J., and Caro, J. (1988) *J. Immunol. Meths.* **111**, 1-9
- Nilsson, B., and Abrahmsen, L. (1990) in *Methods in Enzymology*, Vol. 185 (Goeddel, D. V., ed), pp. 144-161, Academic Press, San Diego
- Nilsson, B., Moks, T., Jansson, B., Abrahmsen, L., Elmblad, A., Holmgren, E., Henrichson, C., Jones, T. A., and Uhlén, M. (1987) *Protein Eng.* **1**, 107
- Nilsson, K., and Mosbach, K. (1980) *Eur. J. Biochem.* **112**, 397-402

- Nilsson, K., and Mosbach, K. (1981) *Biochem. Biophys. Res. Comm.* **102**, 449-457
- Nixon, L., Koval, C. A., Noble, R. D., and Slaff, G. S. (1992) *Chem. Mater.* **4**, 117-121
- Nossal, N. G., and Heppel, L. A. (1966) *J. Biol. Chem.* **241**, 3055-3062
- Nye, L., Forrest, G., Greenwood, H., Gardner, S., Jay, R., Roberts, J. R., and Landon, J. (1976) *Clin. Chim. Acta* **69**, 387-396
- Oberteuffer, J., and Wechsler, I. (1980) *AIME* **2**, 1178
- O'Carra, P., Barry, S., and Griffin, T. (1974) *Fed. Eur. Biochem. Soc. Lett.* **43**, 169-175
- Oder, R. R. (1976) *IEEE Trans. Mag.* **MAG-12(5)**, 428-435
- O'Shannessy, D. J. (1990) *J. Chromatogr.* **510**, 13
- Osterman, L. A., ed. (1986) *Methods of protein and nucleic acids research*, Vol. 3,,
- Ostlund, C. (1986) *Trends Biotechnol.* **4**, 288-293
- Parraga, G., Horvath, S. J., Eisen, A., Taylor, W. E., Hood, L., Young, E. T., and Klevit, R. E. (1988) *Science* **241**, 1489-1492
- Patel, P. N., Mahaia, M. A., and Cheryan, M. (1987) *J. Biotechnol.* **5**, 1-16
- Pepper, D. S. (1992) *Methods Mol. Biol.* **11**, 173-196
- Persson, M., Bergstrand, G. M., Bulow, L., and Mosbach, K. (1988) *Anal. Biochem.* **172**, 330-337
- Petrakis, L., Ahner, P. F., and Kiviat, F. E. (1981) *Sep. Sci. Technol.* **16(7)**, 745
- Pieters, B. R., and Bardeletti, G. (1992) *Enz. Microb. Technol.* **14**, 361-370
- Pitfield, I. (1992) [Ph.D. Dissertation], University of Cambridge
- Plueddemanns, E. P., ed. (1991) *Silane Coupling Agents*, Plenum Press, New York
- Pollak, A., Blumenfeld, H., Wax, M., Blaughn, R. L., and Whitesides, G. M. (1980) *J. Am. Chem. Soc.* **102**, 6324-6336
- Pollit, S., and Zalkin, H. (1983) *J. Bacteriol.* **153**, 27-32
- Porath, J. (1987) *Biopolymers* **26**, S193-S204
- Porath, J., Carlsson, J., Olsson, I., and Belfrage, G. (1975) *Nature* **258**, 598

- Porath, J., and Hansen, P. (1991) *J. Chromatogr.* **550**, 751-764
- Porath, J., and Olin, B. (1983) *Biochemistry* **22**, 1621
- Ratafia, M., and Keenan, J. (1986) *Am. Biotech. Lab.*, 40-47
- Regan, D. L., Dunnill, P., and Lilly, M. D. (1974) *Biotechnol. Bioeng.* **16**, 333-343
- Riley, D. J. (1987) [M.Sc. Thesis], University of Massachusetts
- Robinson, P. J., Dunnill, P., and Lilly, M. D. (1973) *Biotechnol. Bioeng.* **14**, 603-606
- Ryan, W., and Parulekar, S. J. (1991) *Biotechnol. Bioeng.* **37**, 430-444
- Sada, E., Katoh, S., and Terashima, M. (1980) *Biotechnol. Bioeng.* **22**, 243-246
- Sada, F., Katoh, S., and Terashima, M. (1981) *Biotechnol. Bioeng.* **23**, 1037-1044
- Sadana, A., and Raju, R. R. (1990) *BioPharm* **5**, 53-60
- Sakamoto, S., Terada, I., Iijima, M., Matsuzawa, H., and Ohta, T. (1994) *Appl. Microbiol. Biotechnol.* **42**, 569-574
- Salton, M. R. J., ed. (1964) *Proc. 3rd Int. Symp. Fleming's Lysozyme*, Milan
- Sambamurthy, K., and Vijaya, M. (1987) *Appl. Microbiol. Biotechnol.* **2**, 15-21
- Sandwick, R. K., and Schray, K. J. (1988) *J. Coll. Int. Sci.* **121**, 1-12
- Sassenfeld, H. M., and Brewer, S. J. (1984) *Bio/Technology* **2**, 76-81
- Sato, S. B., Sako, Y., Yamashina, S., and Ohnishi, S. (1986) *J. Biochem* **100**, 1481-1492
- Scatchard, G. (1949) *Ann. NY Acad. Sci.* **51**, 660-672
- Scawen, M. D., Atkinson, A., and Darbyshire, J. (1980) in *Applied Protein Chemistry* (Grant, R. A., ed), Applied science publications, New York
- Schein, C. H., and Noteborn, M. H. N. (1988) *Bio/Technology* **6**, 291-294
- Schneider, C., Newman, R. A., Sutherland, D. R., Asser, U., and Graves, M. F. (1982) *J. Biol. Chem.* **257**, 107-166
- Schutte, H., Kroner, K. H., Hustedt, H., and Kula, M.-R. (1983) *Enz. Microb. Technol.* **5**, 143-148

- Scopes, R. K., ed. (1994) *Protein Purification: Principles and Practice*, Third ed., Springer-Verlag, New York
- Sedmak, J. J. and Grossberg, S. E. (1977) *Anal. Biochem.* **79**, 544
- Selisker, M. Y., Herzog, D. P., Erber, R. D., Fleeker, J. R., and Itak, J. A. (1995) *J. Agric. Food Chem.* **43**, 544-547
- Setchell, C. H. (1985) *J. Chem. Tech. Biotechnol.* **35B**, 175-182
- Shiloach, J., and Bauer, S. (1975) *Biotechnol. Bioeng.* **17**, 227-239
- Shine, J., Fettes, I., Lan, N. C. Y., Roberts, J. L., and Baxter, J. D. (1980) *Nature* **285**, 456-461
- Siever, R. L., and Gernand, M. O. (1983): . USA Patent 4,367,153.
- Skerra, A., Pfitzinger, I., and Pluckthun, A. (1991) *Bio/Technology* **9**, 273-278
- Smith, J. C., Derbyshire, R. B., Cook, E., Dunthorne, L., Viney, J., Brewer, S. J., Sassenfeld, H. M., and Bell, L. D. (1984) *Gene* **32**, 321-327
- Smith, J. M. (1968) *Chem. Eng. Prog.* **64**(8), 78-82
- Smith, M. C., Furman, T. C., and Pidgeon, C. (1987) *Inorg. Chem.* **26**, 1965-1969
- Spalding, B. J. (1991) *Bio/Technology* **9**, 229-233
- Srinivasan, R., and Ruckenstein, E. (1980) *Sep. and Purif. Meth.* **9**(2), 267-370
- Strandberg, L., Kohler, K., and Enfors, S.-O. (1991) *Proc. Biochem.* **26**, 225-234
- Stryer, L., ed. (1988) *Biochemistry*, 3rd ed., W.H. Freeman & Co. Press, New York
- Sugimoto, T., Muramatsu, A., Sakata, K., and Shindo, D. (1993) *J. Coll. Int. Sci.* **158**, 420-428
- Suh, S.-S., and Arnold, F. (1990) *Biotechnol. Bioeng.* **35**, 682-690
- Suh, S.-S., Haymore, B. L., and Arnold, F. H. (1991) *Protein Eng.* **4**, 301-305
- Sulkowski, E. (1985) *Trends Biotechnol.* **3**, 1-7
- Sulkowski, E. (1987) in *Protein purification: micro to macro* (Burgess, R., ed), pp. 149-162, A.R. Liss Inc., New York
- Sulkowski, E. (1988) *Makromol. Chem. Macromol. Symp.* **17**, 335-348

- Sulkowski, E. (1989) *Bioessays* **10**, 170-175
- Sulkowski, E., Vastola, K., Oleszek, D., and Von Muenchhausen, W. (1982) *Anal. Chem. Symp. Ser.* **9**, 313
- Svoboda, J. (1994) *Minerals Engineering* **7**(5/6), 747-757
- Svoboda, J., and Ross, V. E. (1980) *Intl. J. Min. Proc.* **27**, 75
- Swamy, K. H. S., and Goldberg, A. L. (1982) *J. Bacteriol.* **149**, 1027-1033
- Szoka, P. R., Schreiber, A. B., Chan, H., and Murthy, J. (1986) *DNA* **5**, 11-15
- Taguchi, G., ed. (1986) *Introduction to Quality Engineering*, Asian Productivity Organisation, Tokyo
- Tahahara, M., Sagai, H., Inouye, S., and Inouye, M. (1986) *Bio/Technology* **6**, 195
- Talmadge, K., and Gilbert, W. (1982) *Proc. Natl. Acad. Sci. USA* **79**, 1830-1833
- Tamura, Y., Takahashi, K., Koder, Y., Saito, Y., and Inada, Y. (1986) *Biotechnol. Lett.* **8**, 877-880
- Tartoff, K. D., and Hobbs, C. A. (1978) *Focus* **9**, 12
- Terranova, B. E., and Burns, M. A. (1989) *Biotechnol. Progr.* **5**, 98
- Theodossiou, I. (1993) [M.Sc. Dissertation] University College London
- Todd, R. J., Van Dam, M. E., Caimiro, D., Haymore, B., and Arnold, F. H. (1991) *Proteins: structure, function and genetics* **10**, 156-161
- Todd, R. J., Van Dam, M. E., Casimiro, D., Haymore, B. L., and Arnold, F. H. (1991) *Proteins: structure, function and genetics* **10**, 156-161
- Torres, A. R., Dunn, B. E., and Edberg, S. C. (1984) *J. Chromatogr.* **316**, 125-132
- Torres, A. R., Peterson, E. A., Evans, W. H., Mage, M. G., and Wilson, S. M. (1979) *Biochim. Biophys. Acta* **576**, 385-392
- Trudel, M., Trepanier, P., and Payment, P. (1983) *Proc. Biochem.* **18**(1), 2-4
- Tsai, L. B., Mann, M., Morris, F., Rotgers, C., and Fenton, D. (1987) *J. Industr. Microbiol.* **2**, 181-187
- Tsugita, A., and Inouye, M. (1968) *J. Biol. Chem.* **243**, 391-397
- Tsung-Thing, H., and Jian-Jone, W. (1987) *Chem. Eng. Res. Des.* **65**, 237-242

- Turkova, J., ed. (1978) *Affinity Chromatography*, Elsevier Scientific, Amsterdam
- Uhlén, M., Moks, T., and Abrahmsen, L. (1988) *Biochem. Soc. Trans.* **16**(2), 111-112
- Uhlén, M., Nilson, B., Guss, B., Lindberg, M., Gatenbeck, S., and Philipson, L. (1983) *Gene* **23**, 369-378
- Ullman, A. (1984) *Gene* **29**, 27-31
- Vaccaro, D. E. (1990) *Am. Biotech. Lab.* **4**
- Van Dam, M. E., Wuenschell, G. S., and Arnold, F. H. (1989) *Biotechnol. Appl. Biochem.* **11**, 492-502
- van Leenputten, E., and Horisberger, M. (1974) *Biotechnol. Bioeng.* **16**, 385-396
- Wang, D. and Jones, F. R. (1993) *J. Mat. Sci.* **28**, 2481-2488
- Watson, J. H. P. (1973) *J. Appl. Physics* **44**, 4209
- Weber, D., and Bailon, P. (1990) *J. Chromatogr.* **510**, 59-69
- Werner, R. G., and Berthold, W. (1988) *Arzneimittel Forschung* **38**, 422-428
- Wheelwright, S. M. (1987) *Bio/Technology* **5**, 791-793
- Wheelwright, S. M., ed. (1991) *Protein engineering-design and scale-up of downstream processing*, Hanser, Munich
- White, M. D., and Marcus, D. (1988) in *Downstream processes: equipment and techniques* (Mizrahi, A., ed), Alan R. Liss, New York
- Whitesides, G. M., Kazlauskas, R. J., and Josephson, L. (1983) *TIBTECH* **1**, 144-148
- Wilkstrom, P., and Larsson, P. O. (1987) *J. Chromatogr.* **388**, 123-134
- Woll, J. M., Hatton, T. A., and Yarmush, M. L. (1989) *Biotechnol. Prog.* **5**, 57-62
- Wood, T. K., and Peretti, S. W. (1991) *Biotechnol. Bioeng.* **38**, 397-412
- Wuenschell, G. E., Naranjo, E., and Arnold, F. H. (1992) *Bioprocess Eng.* **5**, 199-202
- Wuenschell, G. E., Wen, E., Todd, R., Shnek, D., and Arnold, F. H. (1991) *J. Chromatogr.* **543**, 345-354
- Xiaoli, L., Robbins, J. W., and Taylor, K. B. (1990) *J. Industr. Microbiol.* **5**, 85-94
- Yee, L., and Blanch, H. W. (1992) *Bio/Technology* **10**, 1550-1556

Yip, T. T., Nakagawa, Y., and Porath, J. (1989) *Anal. Biochem.* **183**, 159-171

Yokoi, H., Yagishita, K., and Nakanishi, Y. (1990) *Bull. Chem. Soc. Jap.* **63**, 746-748

Zawistowska, U., Sangster, K., Zawistowski, J., Langstaff, J., and Friesen, A. D. (1988)
Cereal Chemistry **65**, 413-416

Zawistowska, U., Zawistowski, J., and Friesen, A. D. (1992) *Biotechnol. Appl.
Biochem.* **15**, 160-170